UNIVERSITY OF LIVERPOOL

Disposition of PEGylated Proteins

Thesis submitted in accordance with the requirements of the University of Liverpool for the degree of Doctor of Philosophy

George Terence Edge

November 2013

DECLARATION

This thesis is the result of my own work. The material contained within this thesis has not been presented, nor is currently being presented, either wholly or in part for any other degree or qualification.

George T. Edge

This research was carried out in the Department of Molecular and Clinical Pharmacology, Institute of Translational Medicine, University of Liverpool.

CONTENTS

ABSTRACT

Biologics are an increasing class of pharmaceuticals that possess many therapeutic benefits over typical, small-molecule drugs, such as; high specificity, reduced frequency of off-target effects, and the ability to mimic the body's own physiological system. Despite these advantages, biologics still suffer from limitations due in part to their inherent protein composition, including; rapid circulatory degradation, renal clearance, and immunogenicity. Consequently, methods to modify biologics have been sought that can ameliorate these limitations yet still maintain their efficacy. PEGylation, defined as the conjugation of polyethylene glycol (PEG) to biologics, is one such modification. The coupling of PEG increases the overall molecular weight (MW) of the biologic, resulting in reduced renal clearance, whilst simultaneously acting as a shield to protect against proteolytic degradation. Both of these effects extend the half-life of coupled biologics and improve their bioavailability. Furthermore, the extended residence times of PEGylated agents leads to an increase in efficacy in comparison to the non-PEGylated counterpart; since the therapeutic moiety has more opportunities to elicit a response. The shielding effect of PEG is also reported to reduce the immunogenicity of biologics through preventing immune recognition of antigenic epitopes present on the biologic's surface.

The benefits of PEGylation have been well validated and there are a number of PEGylated agents clinically available, with more in various stages of development. Despite this, however, there is still little known concerning the disposition, metabolism and biological fate of PEGylated proteins. Furthermore, whilst PEGylation can reduce the immunogenicity of a protein, this has not precluded the onset of a new immunogenicity raised against the PEG moiety itself, nor indeed has PEGylation been shown to universally reduce the immunogenicity of coupled proteins. Anti-drug antibodies (ADAs) and hypersensitivity reactions have been reported in both animal studies and patients receiving PEGylated agents. Furthermore, these adverse drug reactions (ADRs) occur against both the PEG and protein moieties of the conjugate. Consequently, there is a real need to understand the fundamental mechanics behind the metabolism, disposition and biological fate of PEGylated biologics, as well as defining the effect of PEGylation on the immune recognition, processing and presentation of the coupled protein.

The bioanalysis of PEGylated proteins is hindered by inherent difficulties associated with the PEG moiety. PEG is transparent, non-fluorescent, contains no ultra-violet (UV) chromophore, is polydisperse, and is not easily ionised; making analysis by spectroscopy and mass spectrometry difficult. The utility of radiolabeling is also limited due to issues arising from placement of the radiolabel within the conjugate. Consequently, alternative analytical tools are required for the comprehensive bioanalysis of PEGylated proteins.

In light of these issues the studies described in this thesis aimed to develop methodologies that can: 1) provide quantitative information concerning the biological fate and disposition of both the PEG and protein moieties of a PEGylated protein, and 2) define the effect of PEGylation on the processes involved in generating an immune response.

The first investigation in this thesis involved developing and optimising gel-based methodology and ^{1}H nuclear magnetic resonance (NMR) spectroscopy to monitor the kinetics, disposition and biological fate of a model PEGylated protein, ^{40K}PEG-insulin, in a rodent disposition study. Male Wistar rats were intravenously administered a single dose of ^{40K}PEG-insulin and maintained over a period of 28 days. Plasma and urine samples were collected almost daily and liver and kidneys harvested on days 14 and 28. ^{1}H NMR and gel-based analysis, incorporating western blotting for both PEG and insulin, and a barium iodide (BaI_2) stain for PEG, revealed that PEG persists in both biological tissues and fluids across 28 day days. However, the anti-insulin western blots revealed that the insulin moiety was either metabolically cleaved or sequentially degraded from PEG to the extent that no immunodetectable insulin was detected by day 7 in urine, or by day 14 in plasma, and could not be detected at all in liver and kidney tissue on days 14 and 28. However, an *in vitro* plasma stability study found the insulin moiety of ^{40K}PEG-insulin to be stable in plasma over 7 days, indicating that the loss of insulin signal observed *in vivo* must be occurring following cellular internalisation; potentially allowing for the liberated protein to be immunologically processed.

The second investigation in this thesis concerned the effect of PEGylation on *in vitro* cellular internalisation. A range of different PEG MWs were incubated with dendritic cells (DCs) – a model antigen presenting cell (APC) – and internalisation was assessed by flow cytometry and fluorescence microscopy. These data revealed that DC internalise PEG regardless of MW, suggesting that PEGylation, in terms of MW, may have little effect on

the internalisation of a PEGylated biologic by APC – over the clinically relevant PEG MW range used in this study.

Thirdly, the effect of PEGylation was assessed on the lysosomal and proteasomal pathways of antigen processing and presentation, events *en route* to producing an immune response which occur after cellular internalisation. Insulin was conjugated to a range of different MW PEGs and incubated with either lysosomes or proteasomes. PEG was shown to be stable to lysosomal proteolysis over a period of 7 days; however insulin was completely degraded within 2 hours. When coupled to PEG, the insulin moiety was again degraded completely within 2 hours regardless of PEG MW. No PEG MW effect was observed when analysing the peptide repertoires generated between the PEGylated insulin conjugates. Indeed, it was shown that PEGylation provides only local protection against lysosomal degradation at the site of attachment. However, when degraded by proteasomes a PEG MW-dependent effect was observed. Over 48 hours, insulin was nearly degraded to completion when conjugated to 20 kDa PEG. But when coupled to either 30 or 40 kDa PEG, only ~50% of the insulin moiety was degraded. When analysing the peptide repertoires, again PEG, regardless of MW, provided partial protection at the site of attachment. However, there was much more variation in the peptides generated between each PEGylated insulin.

In conclusion, the methods developed in this thesis represent facile, inexpensive analytical tools to comprehensively analyse the disposition, kinetics and biological fate of both the PEG and protein moieties of PEGylated proteins. Furthermore, the investigation presented in this thesis was the first of its kind to demonstrate that cleavage and/or degradation of a PEGylated protein can occur *in vivo*. Consequently, the methods described in this thesis could be easily used to provide a measure of the pharmacokinetics and tissue retention of PEGylated biologics in man. When analysing the effect of PEGylation on the processing of PEGylated proteins, there was shown to be little difference when processed via the lysosomal pathway of antigen processing. However, based on the peptide repertoires generated PEG did provide local protection against degradation at the site of attachment – suggesting that site-specific PEGylation, tailored for individual biologics, may provide a viable route to reduce the immunogenicity of the attached protein. Future investigation is warranted to further elucidate the potential effects of PEGylation on immunological events occurring downstream of lysosomal/proteasomal processing.

ACKNOWLEDGEMENTS

First and foremost I would like to thank my supervisors Dr Neil Kitteringham and Prof Kevin Park for their continued support, advice and guidance, for which I am truly grateful, as well as providing me with the opportunity to do this PhD.

I would also like to thank Dr Vicki Elliott, Jane Hamlett, Dr Roz Jenkins, Dr Caroline Earnshaw and Dr Anahi Santoyo Castelazo for their help and support throughout my PhD with all things proteomics. I am also indebted to Dr Jo Walsh, Dr Han Aw Yeang, Dr Junnat Hamdam, Lorna Kelly, Row Eakins, Phill Roberts, Pete Metcalfe and Dr Row Sison-Young for their kind friendship and expert technical assistance.

I would like to thank everyone who I have become friends with from the department; Jack Sharkey, Jon Lea, Tom Hammond, Phil Starkey Lewis, James Heslop, Monday Ogese, Carl Roberts, Hannah Aucott, Ali Rodrigues, Catherine Bell, Holly Bryan, Fiazia Yaseen, Pika Nithia-Jones, Eryi Wang, Ryan Nattrass, James Firman, Mike Wong, Rob Hornby, Richard Kia, Andrew Gibson, Andrew Sullivan, Luke Shelton, Laith Al-Huseini, Sam Williams, Amal Alami, Christina Churchman, Dammy Olayanju, Otuofu Mohammed Amali and Thilipan Thaventhiran. I'd also like to give a special thank you to Bhav Jagota.

A thank you also goes to my long-suffering friends Paul, Darren, Richard and Mike, who will be pleased, I'm sure, that they no longer have to listen to me "going on about the pegs!" On the plus side it also means no more jokes about how all I really do is hang up washing, and that I can finally get a proper job!

Finally, and most importantly, I'd like to thank my Mum and Dad, my brother James and the rest of my family, who have always been there for me. Without their love, support and belief in me, this Thesis would not have been possible.

PUBLICATIONS

Papers

Elliott, V.L.*, **Edge, G.T.***, Phelan, M.M., Lian, L.Y., Webster, R., Finn, R.F., Park, B.K. & Kitteringham, N.R. (2012) 'Evidence for metabolic cleavage of a PEGylated protein *in vivo* using multiple analytical methodologies.' *Molecular Pharmaceutics* **9** (5): 1291-1301.

*Joint first authorship

Edge, G.T., Elliott, V.L., Jenkins, R.E., Webster, R., Finn, R.F., Park, B.K. & Kitteringham, N.R. 'Effect of PEGylation on the antigen processing of PEGylated proteins.' *Manuscript in preparation.*

Abstracts

Edge, G.T., Elliott, V.L., Kitteringham, N.R., Phelan, M.M., Lian, L.Y., Webster, R., & Park, B.K. Analytical methodologies for determining the metabolism and disposition of PEGylated biopharmaceuticals. *The BTS Annual Congress 2011.*

Edge, G.T., Elliott, V.L., Kitteringham, N.R., Phelan, M.M., Lian, L.Y., Webster, R., & Park, B.K. Biological fate and immunogenicity of PEGylated proteins. *The BTS Annual Congress 2012.*

ABBREVIATIONS

ACN;	acetonitrile
ADA;	anti-drug antibodies
ADR;	adverse drug reaction
AMC;	7-amino-4-methylcoumarin
amu;	atomic mass units
APC;	antigen presenting cell
B_0;	magnetic field
BaI_2;	barium iodide
BCA;	bicinchoninic acid assay
BSA;	bovine serum albumin
$CaCl_2$;	calcium chloride
CLF;	crude lysosomal fraction
CLIP;	class II-associated invariant chain peptide
CO_2;	carbon dioxide
Ctrl;	control
D1;	relaxation delay
D_2O;	deuterium oxide
Da;	dalton
dATP;	deoxyadenosine triphosphate
DC;	dendritic cell
ddH_2O;	double-distilled water
DMEM;	Dulbecco's modified Eagle medium
DMSO;	dimethyl sulphoxide
DNA;	deoxyribonucleic acid
DTT;	dithiothreitol
E. coli;	Escherichia coli
ECL;	electrochemiluminescence
EFP;	combined command of ft, em and phase
ELISA;	enzyme-linked immunosorbent assay
Em;	emission

em;	exponential window function
EPO;	erythropoietin
EPR;	enhanced permeability and retention
Ex	excitation
FCS;	fetal calf serum
FDA;	Food and Drug Administrtion
FID;	free induction decay
FITC;	fluorescein isothiocyanate
FSC;	forward scatter
ft;	Fourier transform
g;	gram
GHz;	Gigahertz
GM-CSF;	granulocyte macrophage colony-stimulating factor
GS;	interactive adjustment of acquisition parameters
H_20;	water
HBSS;	Hank's Balanced Salt Solution
HCl;	hydrogen chloride
HEPES;	4-(3-hydroxyethyl)-1-piperazineethanesulfonic acid
HepG2;	human hepatocellular liver carcinoma cell
Hz;	Hertz
iDC;	immature DC
IFNγ;	interferon gamma
IgG;	immunoglobulin G
IgM;	immunoglobulin M
IL-2;	interleukin 2
IM;	intramuscular
IP;	intraperitoneal
IS;	internal standard
IU;	international unit
IV;	intravenous
JAK-STAT;	Janus kinase/signal transducers and activators of transcription
kDa;	kilodalton
kg;	kilogram

L^+;	enriched lysosomal fraction
LAMP1;	lysosomal-associated membrane protein 1
LC-ESI-MS/MS;	liquid chromatography electrospray ionisation MS/MS
LC-MS/MS;	liquid chromatography-tandem MS
LOD;	limit of detection
LOQ;	limit of quantification
LTT;	lymphocyte transformation test
M;	molar
mA;	milliamps
MALDI-ToF-MS;	Matrix assisted laser desorption ionisation time-of-flight MS
mDC;	mature DC
Methanol-d_4;	tetradeuteromethanol
mg;	milligram
$MgCl_{2;}$	magnesium chloride
MHC;	major histocompatability complex
MHz;	Megahertz
min;	minute
mL;	millilitre
mM;	millimolar
MS;	mass spectrometry
mS;	millisecond
MW;	molecular weight
MWCO;	molecular weight cut off
n.d.;	not determined
NaCl;	sodium chloride
nM;	nanomolar
NMR;	nuclear magnetic resonance
NS;	number of scans
O1;	frequency offset
PBMC;	peripheral blood mononuclear cell
PBS;	phosphate-buffered saline
PD;	pharmacodynamic
PDI;	polydispersity index
PEG;	polyethylene glycol
PEG-rHu BChE;	PEGylated recombinant human butylcholinesterase

PFA;	paraformaldehyde
PK;	pharmacokinetic
pK_a;	acid dissociation constant
ppm;	parts per million
PSN;	postnuclear supernatant
R^2;	coefficient of determination
RCF;	relative centrifugal force
rDNA;	recombinant DNA
RG;	receiver gain
rga;	receiver gain adjustment
rpm;	revolutions per minute
S/N;	signal-to-noise ratio
s;	seconds
SC;	subcutaneous
SCID;	severe combined immunodeficiency
SD;	standard deviation
SDS-PAGE;	sodium dodecyl sulphate-polyacrylamide gel electrophoresis
SEM;	standard error of the mean
SSC;	side scatter
$t_{½}$;	half-life
T_1;	spin-lattice relaxation
TAP	transporter associated with antigen processing
TCR;	T cell receptor
TD;	toxicodynamic
TFA;	trifluoroacetic acid
TNF-bp;	tumour necrosis factor binding protein
T_{null};	variable delay at which no signal is observed
TST;	tris-buffered saline
UV;	ultraviolet
v/v;	volume/volume
V;	volts
w/w;	weight/weight
µg;	microgram

µL;	microlitre
µM;	micromolar
µs;	microsecond

CHAPTER 1

General Introduction

CONTENTS

1.1 INTRODUCTION

Biologics, such as therapeutic proteins, peptides, antibodies and oligonucleotides, have great potential as drugs (Harris *et al.*, 2003). They bind with high affinity and specificity to their targets, resulting in high efficacy and reduced incidences of off-target effects (Leader *et al.*, 2008). Unfortunately, biologics also suffer from high rates of circulatory degradation, renal elimination and immunogenicity (Pasut *et al.*, 2007). PEGylation, the covalent attachment of polyethylene glycol (PEG), may be used to ameliorate these limitations (Roberts *et al.*, 2002). The coupling of PEG to proteins creates conjugates that possess improved pharmacokinetic (PK), pharmacodynamic (PD), physicochemical and immunological profiles in comparison to the unmodified protein (Veronese *et al.*, 2005). Furthermore, PEGylated conjugates also typically exhibit enhanced *in vivo* efficacy (Bailon *et al.*, 2009). The primary effects of PEGylation are reduced proteolytic degradation and renal clearance of the attached protein moiety; both of which act to extend the retention time of the drug (Fishburn, 2008). Smaller biologics typically benefit from reduced renal clearance due to the attachment of a large PEG moiety, whilst larger molecular weight biologics, such as antibodies, have their retention time primarily improved through reduced proteolytic degradation (Caliceti *et al.*, 2003). Other benefits resulting from PEGylation include: reduced immunogenicity; improved solubility of poorly soluble drugs; improved patient compliance, and enhanced stability over changes in pH and temperature (Fishburn, 2008). However, despite these beneficial properties, little is known regarding the metabolism, disposition and biological fate of PEGylated proteins (Knop *et al.*, 2010; Webster *et al.*, 2007; Webster *et al.*, 2009). This, in part, reflects the inherent difficulties associated with the bioanalysis of PEGylated macromolecules.

1.2 OVERVIEW AND HISTORY OF PROTEIN THERAPEUTICS

1.2.1 Proteins as Drugs

Proteins are biological molecules assembled from amino acids. They are an incredibly diverse set of macromolecules that are intimately involved in virtually all cellular functions of the human body; ranging from roles in catalysing biochemical reactions to defending the body against invading pathogens. There are estimated to be between 25,000 – 40,000 genes in the human genome, but the number of distinct proteins encoded by these genes may be much higher (Leader *et al.*, 2008). The ability of proteins to bind to their target molecule, or receptor, specifically, and elicit a response, is what makes proteins such suitable candidates for drug development; their high specificity and target affinity help reduce off-target effects and adverse drug reactions, as well as eliciting the appropriate therapeutic response (Pisal *et al.*, 2010). Indeed, proteins, as therapeutics, possess several other advantages over typical, small-molecule drugs. Proteins can specifically elicit a complex set of functions that small-molecule drugs are simply incapable of mimicking. Disease states often result from defective or mutated genes, or from disruption of normal cellular processes, which can be effectively combated by protein therapeutics; for example, through enzyme replacement therapy or the use of protein inhibitors to restore harmony to the disrupted pathway (Adair *et al.*, 2002). Human-derived protein therapies are generally better tolerated than those from animal or plant origin due to their recognition as “self” proteins by the patients’ immune system and therefore bypassing an immune-mediated response against the therapy, although immune responses can still be generated against human-derived protein therapeutics (Baker *et al.*, 2010; Leader *et al.*, 2008; Schellekens, 2003). This is particularly important given that the vast array of proteins endogenously produced by the human body can potentially be utilised by drug developers to manufacture novel therapeutics. In fact, the importance of our body’s naturally occurring proteins in treating disease has been recognised for thousands of years. It was recognised that body fluids, primarily blood, were important factors for health and

vitality; due to the actions of the various proteins they contain. Early civilisations, such as the ancient Chinese, promoted the drinking of blood and urine, to not only to aid in healing but also to improve strength and vitality (Materi *et al.*, 2007). However, it was not until nearly two thousand years later that research into the therapeutic benefits of proteins, though technically not yet discovered, truly began.

1.2.2 Blood Transfusions

The therapeutic benefits of blood, as previously mentioned, had been recognised for centuries. However, it was not until 1628 when William Harvey, a physician, published a paper detailing the continuous circulation of blood through the body, that the therapeutic potential of proteins present in the blood could begin to be harnessed (Barsoum *et al.*, 2002). This understanding provided the basis for future, albeit primitive, experimentation into blood transfusions for the treatment of wounds and other ailments. Indeed, the first recorded attempt at a blood transfusion for therapeutic purposes is believed to have occurred in 1492, after Pope Innocent VIII slipped into a stroke-induced coma; in this case, infusion occurred orally rather than intravenously (Sturgis, 1942)! Various efforts at blood transfusions were developed and refined over the following two centuries, culminating in the first successful blood transfusion between animals in 1665 in London by the physician Richard Lower (Brown, 2005). The first animal to human blood transfusion was performed by Professor Jean-Baptiste Denys in Paris in 1667, and replicated by Lower and Sir Edmund King five months later (Sturgis, 1942). However, fatal reactions to two of Denys' patients led to the eventual banning of blood transfusions in France and later in England (Sturgis, 1942). It wasn't until 1818 when Dr James Blundell, an obstetrician at Guy's Hospital in London, proposed that blood transfusions could be used to treat postpartum haemorrhaging that the first successful human to human blood transfusion occurred, and was simultaneously responsible for bringing blood transfusion back into medical practice

(Brown, 2005; Materi *et al.*, 2007). Blundell, acknowledging the previous work of John Henry Leacock in 1816 – who established that donor and recipient must be of the same species – extracted blood from a patient's husband and successfully transfused the blood into the patient; after which she recovered (Schmidt *et al.*, 2002). Blood transfusions continued to be used throughout the 19th century. Samuel Lane, a physician at St George's Hospital Medical School, aided by Blundell, performed the first blood transfusion to treat haemophilia, a disease resulting from deficiencies in blood-clotting proteins factors VIII and/or IX (Brown, 2005). It was not until 1901, however, that blood transfusions became safer following the publication of Karl Landsteiner's work elucidating the different blood groups. Landsteiner discovered 3 of the major blood groups (A, B and O), whilst the fourth blood group (AB) is credited to Jan Jansky in 1907 (Farr, 1979; Sturgis, 1942). Previously, transfusions occurring between donor and recipient of differing blood groups had led to agglutination of red blood cells due to the presence of antibodies against the donor blood cells, with often fatal consequences. Landsteiner's work allowed blood typing of both the donor and recipient, therefore preventing fatal reactions and allowing blood transfusions to occur safely (Farr, 1979). For this, Landsteiner was awarded the Nobel Prize in Physiology or Medicine in 1930 (Giangrande, 2000). The therapeutic utility of blood for the treatment of disease and other traumas had been well and truly recognised, which we know now to be due to the presence of proteins, such as factor VIII or albumin.

1.2.3 Vaccination

Proteins present in the blood are of course not the only body fluids/matter, which had been recognised to have therapeutic potential during the 18th and 19th centuries. Indeed, in 1796 the physician Edward Jenner developed an effective vaccine against smallpox, a disease which had ravaged mankind for thousands of years with its high mortality rate (Baxby, 1999; Brown, 2005; Materi *et al.*, 2007; Riedel, 2005). With it, the

concept of vaccination was borne; the ability to prevent the contraction of serious disease through vaccination has since saved countless lives (Stern *et al.*, 2005). Jenner knew that milkmaids who had contracted cowpox, a disease similar to smallpox but much milder and less virulent, were subsequently immune to smallpox (Bazin, 2003; Hilleman, 2000). He surmised that cowpox could be used as a prophylactic against smallpox and tested his hypothesis by inoculating an 8 year old boy, named James Phipps, with pus originating from the cowpox blisters of a milkmaid called Sarah Nelms. Phipps developed a slight temperature but otherwise no ill effects were observed. After 9 days Jenner inoculated Phipps with the pus from a smallpox lesion, however, no disease developed and Jenner concluded that Phipps had been immunised. After adding more successful cases to his study Jenner received worldwide acclaim and the use of smallpox vaccination spread rapidly, with great success (Baxby, 1999; Bazin, 2003; Lombard *et al.*, 2007; Materi *et al.*, 2007; Riedel, 2005).

During the 1870's the French biologist Louis Pasteur began extending the previous work of Jenner regarding smallpox vaccination. Whilst studying chicken cholera he observed that chickens inoculated with an old culture of chicken cholera germs did not die, as was the norm. He inoculated these chickens with fresh germ culture and found, as he had surmised, that the chickens had become immune to the germs in the fresh culture. Pasteur concluded that the chickens had used the older and subsequently weaker (attenuated) germs to generate immunity against chicken cholera when challenged with newer, more virulent germs (Plotkin, 2005). In contrast to Jenner's smallpox vaccine, Pasteur used artificially generated milder, and therefore less pathogenic, germs to induce immunity, rather than simply use a milder variant of the disease as a prophylactic against its more virulent counterpart. Thus, whilst Jenner is credited with the concept of vaccination, Pasteur is more associated with the development of vaccines (Schwartz, 2001; Stern *et al.*, 2005). Indeed the term vaccine comes from the latin word for cow, *vacca*, and

was coined by Pasteur in homage to Jenner's work on cowpox (Hendriksen, 2008). Pasteur next extended his work to the development of an effective vaccine against anthrax; a disease caused by the bacterium Bacillus anthracis, a lethal disease which, at the time, was responsible for killing large numbers of sheep and even humans across Europe. He weakened the anthrax bacilli via an oxidising agent, potassium dichromate, and demonstrated the effectiveness of his vaccine in a famous, public experiment; where all the sheep inoculated with his vaccine survived following administration of anthrax bacteria. The non-vaccinated cohort of animals, of course, all died (Bazin, 2003; Lombard *et al.*, 2007; Schwartz, 2001). Pasteur's vaccines, containing weakened disease strains formulated in solutions suitable for injection, are regarded as the first examples of protein therapeutics generated *ex vivo (*Materi *et al., 2007)*. Pasteur also developed the first vaccine for the treatment of rabies; a virus which is ultimately fatal in humans. Even today, unless immediate post-exposure vaccination is given prior to the onset of symptoms, survival is minimal. Whilst Pasteur could not visibly detect the rabies virus, due its effects on the nervous system he and his colleagues were able to trace it to the brain and spinal cord. Pasteur successfully grew the virus in rabbits and obtained an attenuated form of the disease through desiccating infected animals' spinal cords. In actual fact, Pasteur had killed, rather than attenuated, the virus and his rabies vaccine was consequently the first example of what is now termed an inactivated vaccine (Schwartz, 2001). Using this vaccine, he found he could prevent rabies in his animal models. He was, of course, naturally hesitant about using the vaccine on humans; the risk being that if his vaccine still contained live virus it could potentially infect a patient with the fatal disease. The decision was taken out of his hands, however, when a young boy, nine year-old Joseph Meister, was brought to him after being bitten several times by a rabid dog. Knowing the boy was likely to die, Pasteur inoculated him a total of 13 times using various preparations of desiccated infected rabbit spinal cord, the last inoculation containing the most virulent sample. Joseph survived, his

bites healed and he did not contract rabies. This was a phenomenal development in the treatment of the previously incurable disease, and brought world-wide acclaim to the already famous Pasteur (Bazin, 2003; Lombard *et al.*, 2007; Schwartz, 2001).

1.2.4 Discovery of Proteins

In 1838, the concept of a protein was introduced through the work of the chemists Gerardus Johannes Mulder and Jons Jakob Berzelius, indeed Berzelius is credited with coining the term protein (Vickery, 1950). Their work elucidated that it was many different substances, or proteins, present in the blood and other biological fluids, which were responsible for the therapeutic effects observed in different experiments, such as those by Blundell, Jenner and Pasteur. With this discovery dawned the realisation that these proteins could potentially be harvested for use as therapeutics. However, the necessary tools to purify and formulate these proteins into usable drugs were not yet available. It would not be until the introduction of purified insulin, in 1922, that the true power of protein therapeutics, once purified, could begin to be realised (Materi *et al.*, 2007).

1.2.5 Diabetes and the Purification of Insulin

Diabetes mellitus is the umbrella term used to describe a collection of diseases resulting from either insufficient or complete lack of insulin production by the pancreas (type 1 diabetes mellitus), or the inability of cells to respond to insulin (type 2 diabetes mellitus) (Bastaki, 2005; Joshi *et al.*, 2010). Insulin is secreted in response to high blood glucose levels; resulting in the cellular absorption of glucose, which is subsequently stored as glycogen as part of the body's energy reserves (Taylor *et al.*, 1988). The resulting high blood glucose levels and lack of insulin in patients with diabetes can have severe and fatal consequences. Increased hunger, dehydration, urination, nausea, abdominal pain and vomiting are typical symptoms of diabetes (Koch, 1999; Newton *et al.*, 2004). Diabetic

ketoacidosis occurs when the body switches from using glycogen as an energy reserve and instead uses fatty acids (Taylor *et al.*, 1988). Ketone bodies are formed following liver conversion of fatty acids into glucose. This causes the kidneys to increase excretion of the ketone bodies and excess glucose, which cannot be removed from the blood due to the lack of insulin (Fleckman, 1993). Due to osmotic diuresis, the excess glucose excreted in the urine results in increased water and electrolyte loss; potentially leading to fatal dehydration (Inward *et al.*, 2002). Diabetic-ketoacidosis, as well as hyperglycaemia and dehydration, can result in the patient slipping into a diabetic coma, which, whilst reversible, was a veritable death sentence prior to the introduction of insulin (Materi *et al.*, 2007; Siperstein, 1992). Death from diabetes was typically a long-drawn out process characterised by the patient wasting away over time. Furthermore, the majority of deaths associated with diabetes were typically adolescents, who were often suffering from diabetes mellitus type 1, which used to be referred to as juvenile diabetes (diabetes resulting from the autoimmune destruction of the β islets of Langerhans cells of the pancreas, which produce insulin). Consequently, much interest, both medically and publically, was invested in research to treat this disease (Materi *et al.*, 2007). Prior to 1922, it was known that patients who had died from diabetes often had damaged pancreases. Furthermore, dogs which had had their pancreases removed developed diabetes-like symptoms (King *et al.*, 2003). In 1920, Dr. Frederick Banting had the notion that extracts from the pancreas could be used to treat diabetes, provided that the pancreas had first been degenerated to the extent that only the insulin-producing cells remained; otherwise, the digestive enzymes, also produced by the pancreas and used for the digestion of food, could potentially degrade and harm the pancreas extract – thereby limiting its therapeutic utility (Rosenfeld, 2002). With the aid of Professor John J. R. Macleod and Charles Best, Banting ligated the pancreatic ducts of dogs to induce pancreatic degeneration (Joshi *et al.*, 2007). Following degeneration, the pancreases were removed and the remaining β islets of

Langerhans cells used to generate an extract, which they termed isletin (Busnardo *et al.*, 1983). They injected the isletin into dogs, which had had their pancreases surgically removed and had consequently developed diabetes, and found they could temporarily control the disease (King *et al.*, 2003). After further research, and switching to bovine pancreases as the source of isletin extract, they had acquired sufficient amounts to keep several dogs alive, and had also enlisted the help of the biochemist James Collip, to aid with the purification of isletin, which they had now begun referring to as insulin – a term that had independently been suggested by European researchers over a decade ago (Joshi *et al.*, 2007). In 1922, their insulin extract was tested in Toronto on a 14 year-old boy named Leonard Thompson. Thompson was near death and despite initially suffering from an allergic reaction to the first dose, he recovered following administration of a further-purified second dose (Bliss, 1993a; Bliss, 1993b). Further testing in dying patients proved to be just as effective and provided hope that the killer disease would soon be treatable; a few months later the pharmaceutical company Eli Lilly and Company provided further technical assistance to the extent that large quantities of relatively pure insulin could be obtained, and was soon on sale (Feasby, 1958). The availability of insulin saved millions of lives and dramatically changed the life-expectancy of patients suffering from diabetes; literally enabling them to live ordinary lives. Insulin is consequently regarded as the first purified protein therapeutic, and set the precedent for all other protein therapeutics in the years to come (Materi *et al.*, 2007).

1.2.6 Limitations in the Manufacture and Efficacy of Therapeutic Proteins

The effects observed following the introduction of insulin were truly astounding. Similarly, vaccination was also a life-changer for countless people. Throughout the early 20th century further protein therapeutics, be they vaccines or otherwise, were developed and often proved to be as equally effective as their more illustrious predecessors;

particularly now these protein products were further purified in order to reduce the incidence of allergic reactions – typically observed following administration of earlier protein therapeutics. Purified vaccines for diseases such as German measles, polio, tuberculosis, typhus, yellow fever, mumps, chicken pox and influenza were all first developed in the 20th century. Despite a plethora of new and exciting protein-based therapies becoming available, they were still subject to hindrances that limited their effectiveness. Continuing with the example of insulin, there were several factors that limited its utility. Primarily, both the costs involved and the availability of bovine pancreases were detrimental factors in providing sufficient amounts of purified insulin to diabetics (Leader *et al.*, 2008). A further limiting factor was the high incidence of allergic reactions to insulin. Despite being purified, insulin was still being sourced from animal, rather than human, material and was, therefore, often recognised and subsequently targeted by the immune system (Schernthaner, 1993). Of course, all protein therapies derived from animal material will be inherently more immunogenic than those of human origin due to their recognition as non-self proteins (Schellekens, 2005). Other limitations, not limited to the production of insulin, include difficulties resulting from the sheer amount of animal material often required to obtain the desired protein in a pure form; it was often necessary to process tonnes of material to get the final product. These sorts of starting material to product ratios are untenable as well as being expensive (Materi *et al.*, 2007). It was clear that for therapeutic proteins to achieve complete viability as drugs new methods would have to be developed in order to obtain large amounts of the desired protein, preferably of human origin, and without requiring excess amounts of starting material.

1.2.7 Recombinant DNA Technology

The answer to generating large amounts of human proteins lay in the elucidation of the structure of DNA, by Watson and Crick in 1953, and the subsequent development of

recombinant DNA techniques, that enable bacteria to produce large amounts of human proteins (Chance *et al.*, 1993). Once the structure of DNA had been discovered, it was found that DNA was structurally identical between organisms. Recombinant DNA (rDNA) is DNA that has been formed from different sources and is possible due to this structural identity (Miller *et al.*, 1980). Again, insulin was the first protein to be artificially produced by rDNA technology (Pavlou *et al.*, 2004). In 1955, insulin became the first protein to have its sequence fully determined (Sanger, 1988). In 1973, Stanley Cohen and Herbert Boyer developed a technique using rDNA to insert genes into bacteria, with the bacteria subsequently producing the protein encoded by the foreign gene (Brown, 2005). In 1978, this technology was used to insert the human gene for insulin into *Escherichia coli* (*E. coli)* (Johnson, 1983). Plasmids, circular DNA found in bacteria that can replicate independently of chromosomal DNA, from *E. coli* were removed and used as cloning vectors. The plasmids were first cut open and a synthetic version of the human insulin gene (for the A and B chains of insulin) inserted. The plasmids were then closed and inserted back into the bacteria. Following bacterial division and replication, human insulin A and B chains were produced, which were then separated, purified and combined to form active insulin (Miller *et al.*, 1980; Pickup, 1986). Due to the structural identity between bacterial and human DNA, and despite being produced by *E. coli,* the insulin produced causes far less allergic reactions in comparison to animal-sourced insulin (Pickup, 1986). It is also absorbed quicker and acts faster than animal insulin (Heinemann *et al.*, 1993). Furthermore, producing recombinant insulin is less expensive and generates superior quantities in comparison to purifying insulin from animal pancreases, as well as being safer and better tolerated (Leader *et al.*, 2008; Pickup, 1986). In 1983, Eli Lilly marketed the first recombinant insulin product approved by the FDA, which they called humulin (Brown, 2005; Chance *et al.*, 1993; Johnson, 1983; Materi *et al.*, 2007; Pavlou *et al.*, 2004). Due to the aforementioned advantages of recombinant insulin over animal-sourced insulin, almost

all insulin available on the market today is human recombinant. Recombinant technology resulted in the ability to inexpensively manufacture large-scale amounts of purified therapeutic proteins, which have reduced immunogenicity in comparison to their animal derived counterparts (Leader *et al.*, 2008). Following the success with insulin, more and more human proteins were generated by recombinant technology for therapeutic use; examples include human growth hormone, factor VIII and erythropoietin (Pavlou *et al.*, 2004).

1.3 PEGYLATION

1.3.1 Improving Protein-based Therapies

Despite the century's worth of research devoted to developing and refining the large-scale manufacture of therapeutic proteins, and the overwhelming success of recombinant technology, they unfortunately still suffered from several disadvantages that are inherent to their protein nature, rather than limitations due to their origin or purification – problems which had of course dogged therapeutic proteins prior to the advent of recombinant technology. Therapeutic proteins, regardless of source, are rapidly degraded *in vivo* by circulating proteolytic enzymes and are also rapidly cleared by the renal system (Brown, 2005; Kang *et al.*, 2009). Consequently, therapeutic proteins require frequent, parenteral routes of administration, which in turn does not promote patient compliance, in order to maintain effective plasma concentrations of the drug (Duncan, 2003; Ryan *et al.*, 2008). Furthermore, as previously mentioned, most therapeutic proteins available at this time were sourced from animal material and consequently were often responsible for adverse immunological effects. Subsequently, protein modifications were required that could overcome these limitations, and thus the potential of proteins as drugs become fully realised. The first PEGylated proteins were synthesised in the 1970's and

formed the basis of what is now considered pioneering research by Drs. Frank F. Davis and Abraham Abuchowski. The synthesis of the first PEGylated proteins coincided with the expansion of the field of biotechnology, which was seeded in the aforementioned developments in recombinant DNA technology. It was after an extensive literature search by Davis that he realised that conjugating polymers to proteins may decrease their immunogenicity (Veronese *et al.*, 2009). His interest became focused on polyethylene glycol due to its improved properties, namely its non-immunogenicity, solubility in both aqueous and organic solvents, hydrophilicity, structural flexibility and non-toxicity, over other polymers, such as polyvinylalcohol and poly(vinylpyrrolidone) (Davis, 2002).

1.3.2 Early Research

In 1976, Davis and Abuchowski coupled mPEG, either 1,900 or 5,000 Da, to bovine serum albumin (BSA) and injected the conjugates either intramuscularly or intravenously to rabbits. They observed a loss of immunogenicity and extended circulating life in comparison to unmodified BSA (Abuchowski *et al.*, 1977b). In the same year, they conjugated the two mPEGs to bovine liver catalase and elicited similar results: enhanced circulatory half-life with maintained enzymatic activity and no immune response to the PEG-catalase, this time in a mouse model (Abuchowski *et al.*, 1977a). These key findings demonstrated the potential of PEGylation as a drug delivery system to improve the PK and immunological profiles of proteins.

1.3.3 The Chemistry of PEGylation

PEG is synthesised from anionic ring opening polymerisation of ethylene oxide, during which repeat units of ethylene glycol are formed and polymerised together to form PEG – the structures of which are presented in figure 1.1. This process begins via nucleophilic attack of the epoxide ring (Roberts *et al.*, 2002). PEG is synthesised when

hydroxide ions are used as the nucleophile, whereas monomethoxy PEG (mPEG) is synthesised when methoxide ions are used (figure 1.1) (Roberts *et al.*, 2002). The benefit of using mPEG is apparent in the next step in the synthesis of PEGylated proteins. PEG first needs to be activated through the addition of a functional group at one of the termini, in order to form a PEGylating agent suitable for protein coupling; mPEG has one terminal hydroxyl group available for functionalisation – the other hydroxyl group is capped with a methyl group, thus preventing the formation of cross-linked PEGylated proteins and improving homogeneity of the end product (Fee, 2007; Harris *et al.*, 2001; Kozlowski *et al.*, 2001). The functional group selected to activate the PEG should be based upon which groups are available on the target molecule to which the PEG will be coupled (Roberts *et al.*, 2002). Consequently, for proteins, reactive amino acids are targeted, such as lysine, serine and arginine, as well as the N-terminal amino acid group, of which lysine and the N-terminal amino acid group are the most common reactive groups used to activate PEG (Harris *et al.*, 2003; Harris *et al.*, 2001; Kozlowski *et al.*, 2001; Payne *et al.*, 2010).

1.3.3.1 First-generation PEG Chemistry

The first PEGylated proteins were synthesised from PEGs activated with a range of different functional groups, such as PEG *p*-nitrophenyl, PEG succinimidyl carbonate and PEG carbonylimidazole, to couple to either α or ε amino groups, predominantly on lysine (Kozlowski *et al.*, 2001; Roberts *et al.*, 2002). Low MW mPEGs were used to manufacture first-generation PEGylated proteins. However, functionalisation of mPEG often resulted in a heterogeneous mixture of activated mPEG with high levels of diol impurities (Roberts *et al.*, 2002). Together, these resulted in limitations such as cross-linked PEG proteins and unstable linkages. Furthermore, first-generation coupling techniques were restricted to low MW PEG since the diol content of PEG increases with MW, resulting in a higher prevalence

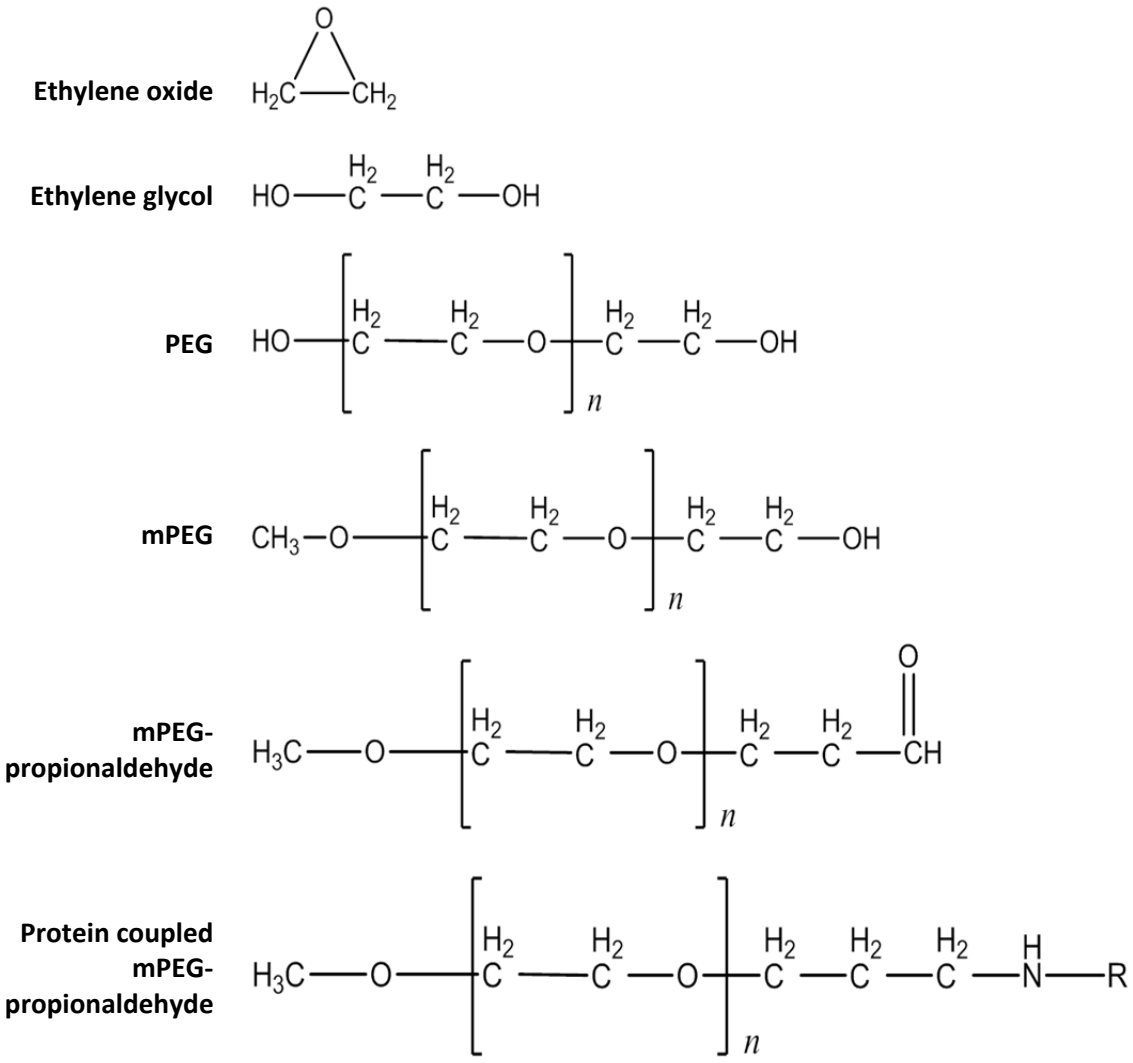

Figure 1.1: PEG structures

Structures of PEG ranging from its synthesis from ethylene oxide to protein coupled mPEG-propionaldehyde, a second-generation PEG chemistry.

of cross-linked PEG proteins when using high MW PEGs (Kozlowski *et al.*, 2001; Roberts *et al.*, 2002).A further downside of this is that it is actually higher MW PEGs, such as those above 20 kDa, which result in substantially improved PK profiles when conjugated to proteins (Yamaoka *et al.*, 1994).

1.3.3.2 Second-generation PEG Chemistry

Second-generation PEG chemistry was developed to overcome the limitations associated with first-generation PEG chemistry, and resulted in improved end-product homogeneity of PEGylated proteins due to reduced diol contamination and side reactions, as well as the ability to conjugate higher MW PEGs to proteins (Kozlowski *et al.*, 2001). One of the most widely used second-generation PEG chemistries is mPEG-propionaldehyde, which attaches to protein through amine conjugation – the structures of which are presented in figure 1.1, and is also the method by which PEGylated proteins have been synthesised in this thesis. Under acidic conditions, the aldehyde linker of mPEG-propionaldehyde is primarily selective for the N-terminal α-amine group due to its lower pK_a in comparison to other nucleophiles present on the protein (Roberts *et al.*, 2002). Conjugation using aldehydes results in the formation of a carbon-nitrogen double bond (also known as a Schiff base), which is subsequently reduced to form a stable amine linkage as shown in figure 1.1 (protein coupled mPEG-propionaldehyde) (Kozlowski *et al.*, 2001). This high selectivity results in much improved homogeneity of PEGylated proteins than those produced using first-generation PEG chemistry.

1.3.4 Consequences of PEGylation

1.3.4.1 Reduced Renal Clearance

PEG is a polymer consisting of repeating units of ethylene glycol, each of which can bind to approximately two water molecules; PEG chains are consequently highly hydrated and possess hydrodynamic radii that are between 5 – 10 fold greater than would be expected for a protein of similar MW; subsequently the effective size of PEG, in solution, is further enhanced (Gaberc-Porekar *et al.*, 2008; Gursahani *et al.*, 2009; Kozlowski *et al.*, 2001). The coupling of PEG to biologics increases the overall MW of the conjugate. This increase in size, further enhanced by the hydration of PEG, results in reduced glomerular

filtration of the conjugate and thus the therapeutic protein moiety is retained in the circulation, as part of a conjugate, for far longer than its unmodified form (Caliceti *et al.*, 2003). It is now firmly established experimentally that conjugation with PEG over 20 kDa in MW results in significantly reduced renal elimination of the attached protein moiety (Webster *et al.*, 2007; Yamaoka *et al.*, 1994).

1.3.4.2 Reduced Proteolytic Degradation

The coupling of PEG to the surface of proteins acts to sterically hinder the function of proteases and effectively masks the protein from enzymatic degradation (Fishburn, 2008). The flexibility of PEG chains, however, still allows receptor-drug interactions and thus a therapeutic response is still elicited despite the attachment of a large PEG moiety. In actual fact, due to the extended circulating half-lives of PEGylated proteins, resulting from reduced proteolytic degradation and reduced renal clearance, the *in vivo* efficacy of PEGylated proteins is typically much greater in comparison to the unmodified protein; since the protein is present for far longer in the circulation it has more opportunities to bind to its target, which is enough to overcome any inhibitions in receptor-drug binding due to the attached PEG moiety (Fishburn, 2008; Gaberc-Porekar *et al.*, 2008). The protective effect of PEG in this regard has been termed the shroud model, which postulates that PEG chains wrap themselves around the protein to secure an effective shield against proteolytic degradation (Pai *et al.*, 2011). However, for effective protection the shroud model depends on several factors: the size of the protein, the size of the PEG and the number of PEG chains coupled to the protein. Mono-PEGylated proteins, where the size of the PEG is comparable to the protein, are also reported to adopt a dumbbell configuration where the PEG exists as a random coil adjacent to the protein (Pai *et al.*, 2011). Whilst both models can be used to explain the protection imparted onto the coupled protein the dumbbell model may confer

a stronger, localised protection at the site of conjugation whereas the shroud model may confer overall protection to the entire molecule, albeit comparatively weaker.

1.3.4.3 Reduced Immunogenicity

The employment of proteins as drugs is further limited due to the high incidence of immune responses associated with their use. Although foreign proteins generally tend to be more immunogenic, neutralising antibodies have been generated against recombinant human protein therapies, which may result in reduced biologic activity and therefore compromise successful drug treatment. It is widely reported that the steric hindrance generated by coupling PEG to protein, which reduces the proteins degradation, is also accountable for the reduced immunogenicity observed with PEGylated proteins, in contrast to the original protein (Fishburn, 2008). In this case, the PEG shields epitopes on the protein from recognition by the immune system (Caliceti *et al.*, 2003). The immunogenicity of a protein may also be enhanced through aggregation. PEGylation has been demonstrated to prevent coupled proteins from aggregating together through shielding hydrophobic sites present on the protein (Veronese *et al.*, 2008). Whilst these two effects are likely explanations they do not encompass all possible mechanisms for reducing protein immunogenicity and, at present, comprehensive investigations into these pathways are lacking (Veronese *et al.*, 2009). It is this lack of data that forms the basis of Chapters 4, 5 and 6 and will be discussed in more detail in section 1.6.2

1.3.4.4 Improved Physicochemical Properties

Further benefits of PEG as the polymer of choice for pharmaceutical conjugation include its solubility in both organic solvents and water. The solubility of hydrophobic drugs is improved following conjugation with PEG and their aggregation in solution is reduced

also. PEG also imparts greater stability over temperature and pH ranges, and therefore helps extend the shelf life of drugs (Fishburn, 2008; Pasut *et al.*, 2012).

Polydispersity is another factor to be considered when conjugating polymers to proteins. Polydispersity, measured by the polydispersity index (PDI), describes the range of differing masses of individual polymers within a given sample. The low polydispersity of PEG, in comparison with other polymers, represents a further advantage, as this helps improve the homogeneity of PEGylated compounds formed during their synthesis; thus reproducible, inter-individual biologic effects are achieved (Pasut *et al.*, 2007). However, as yet, the only monodisperse PEGs available are below 1 kDa in MW, and thus would not be applicable for pharmaceutical conjugation as the low MW would not confer suitable protection (Veronese *et al.*, 2009).

1.3.5 Clinically Available PEGylated Pharmaceuticals

The first PEGylated drug acquired regulatory approval from the United States Food and Drug Administration (FDA) in 1990. Since then the field of PEGylation has expanded, particularly in terms of coupling techniques, and has established itself as the routinely applied stratagem to improve the efficacy, half-life and immunogenicity of biologics.

1.3.5.1 Pegademase

PEGylated adenosine deaminase (Pegademase/Adagen®) was the first PEGylated drug (Vellard, 2003). It was manufactured by Enzon, a company set up by Davis and Abuchowski. It was indicated for the treatment of adenosine deaminase deficiency type severe combined immunodeficiency (SCID), where the enzyme adenosine deaminase is lacking in individuals who have inherited two copies of the defective gene, located on chromosome 20 (Bax *et al.*, 2000; Engel *et al.*, 2007; Vellard, 2003). Adenosine deaminase is responsible for the breakdown of purines, which are constituents of DNA (Cristalli *et al.*,

2001). A lack of adenosine deaminase leads to a build up of deoxyadenosine triphosphate (dATP); a derivative of the purine base adenosine, which is used in DNA synthesis (Bax *et al.*, 2000). Accumulation of dATP results in the inhibition of the enzyme ribonucleotide reductase, which is responsible for the generation of deoxyribonucleotides – the single units of DNA (Booth *et al.*, 2009; Cohen *et al.*, 1978). This, in turn, inhibits DNA synthesis and subsequently cellular division (Bax *et al.*, 2000). This particularly affects T and B lymphocyte proliferation and subsequently compromises immune function, leading to SCID (Bax *et al.*, 2000; Cristalli *et al.*, 2001). Patients with SCID are highly vulnerable to infectious diseases, such as pneumonia and meningitis, due to their compromised immune systems, which can be fatal, particularly in young children (Alcais *et al.*, 2009; Booth *et al.*, 2009; Hirschhorn *et al.*, 1983). Treatment of SCID usually consists of bone-marrow transplantation in order for the donor stem cells to develop into lymphocytes in the patient, thus restoring the patient's immune system (Bax *et al.*, 2000). Pegademase is used for patients who are not suitable for, or who have failed, bone-marrow transplantation and is also recommended for infants and children. Pegademase is a form of enzyme replacement therapy and was actually the first successful application of such for an inherited disease (Cristalli *et al.*, 2001; Vellard, 2003). Pegademase metabolises dATP, thereby preventing the inhibition of ribonucleotide reductase, and consequently allows DNA synthesis/cellular division of T and B lymphocytes to proceed unimpeded; resulting in restoration of immune function (Burnham, 1994). Early attempts of enzyme replacement therapy were relatively unsuccessful for the treatment of adenosine deaminase deficiency type SCID. However, following PEGylation of adenosine deaminase results were much improved; effective levels of adenosine deaminase could be maintained, with the added bonus of reduced immunogenicity observed also (Booth *et al.*, 2009; Vellard, 2003). Since then, patients treated with pegademase develop much improved immune restoration and function.

1.3.5.2 Pegaspargase

In 1994, Enzon produced PEGylated L-asparaginase (Pegaspargase/Oncaspar®) for the treatment of acute lymphoblastic leukemia (ALL) (Dinndorf *et al.*, 2007). ALL results from the uncontrolled production of lymphoblasts (immature lymphocytes) from lymphoid stem cells in the bone marrow (Chessells, 2001; Masetti *et al.*, 2009). These immature cells (leukemic cells) crowd the bone marrow, preventing proper generation of both red and white blood cells, as well as not maturing into normal lymphocytes; resulting in the inability to properly fight infection, as well as problems deriving from insufficient red blood cell production, such as anemia (Chan, 2002). Asparagine is an amino acid involved in protein and DNA synthesis. However, it is not an essential amino acid as cells can synthesise their own asparagine via the enzyme asparagine synthetase, which generates asparagine from aspartate; another amino acid (Graham, 2003). Some leukemic cells, however, lack asparagine synthetase and are consquently incapable of synthesising their own asparagine (Graham, 2003; Narta *et al.*, 2007). These cancerous cells are conseqeuntly dependent on exogenous sources of asparagine for growth and development (Narta *et al.*, 2007). Antineoplastic therapy for ALL, therefore, focuses on depleting circulating asparagine through administration of L-asparaginase, an enzyme which converts asparaginase to aspartate and ammonia; thus limiting the supply of available asparaginase to leukemic cells (Graham, 2003; Masetti *et al.*, 2009). Patients receiving unmodified asparaginase often suffered from hypersensitivity reactions (Graham, 2003; Narta *et al.*, 2007). Frequent administration was also required due to the generation of neutralising antibodies, as well as proteolytic degradation of the drug in the circulation (Zeidan *et al.*, 2009). These limitations were overcome through PEGylation (Masetti *et al.*, 2009). Pegaspargase exhibits prolonged half-life in comparison to asparaginase alone, and also reduces the number of injections required to maintain effective drug levels (Zeidan *et al.*, 2009). Pegaspargase was

also associated with decreased immunogenicity and improved safety and tolerability in therapy-naive patients (Graham, 2003; Narta *et al.*, 2007).

1.3.5.3 Peginterferon α-2b

The third PEGylated drug to become clinically available was peginterferon α-2b (PegIntron®) approved in 2001, manufactured by Schering-Plough, for the treatment of chronic hepatitis C (Kang *et al.*, 2009). Hepatitis C is caused by the hepatitis C virus and primarily effects the liver (Alter, 2007). In general, the infection is asymptomatic, and symptoms are not usually observed until significant liver damage has already occurred (Hoofnagle *et al.*, 2006; Strader *et al.*, 2004). Symptoms include fatigue, flu-like symptoms, weight loss and gastrointestinal problems (Wooten, 2011). Chronic infection is likely as the virus persists in the liver. Patients who are untreated for chronic hepatitis C, or who have suffered from chronic hepatitis C for several years, often develop cirrhosis of the liver, which can result in liver failure (Hoofnagle *et al.*, 2006). Patients can also develop liver cancer, which can be fatal – as can liver failure also (Perz *et al.*, 2006). Hepatitis C is a global health problem and is usually transmitted through contact with infected blood, such as from blood transfusions, use of contaminated equipment and the sharing of contaminated needles (Aghemo *et al.*, 2010; Shepard *et al.*, 2005). It is estimated to have a global prevalence of 3% (Halfon *et al.*, 2010; Torresi *et al.*, 2011).

Interferons belong to a class of proteins known as cytokines and possess antiviral activity (Thompson *et al.*, 2011). Cytokines are signalling molecules secreted by cells of the immune system in order to regulate immunity and inflammation (Tamiya *et al.*, 2011). Inteferons are produced and released by cells when they become infected; thereby warning neighbouring cells to the viral infection and inducing changes in these cells geared toward fighting the virus (Aghemo *et al.*, 2010). Interferon α-2b binds to its receptors, interferon-α receptor 1 and 2, and initiates the JAK-STAT signalling pathway. Induction of

this pathway culminates in DNA transcription of interferon-α-inducible genes, some of which are involved in cell cycle control and the immune response; up-regulation of these proteins inhibits viral replication, suppresses the cell cycle, induces apoptosis, and thus help combat viral infection (Aghemo *et al.*, 2010; Chung *et al.*, 2008). Interferon α-2b also stimulates production of the T_h1 T-helper cell subset, which culminates in enhanced phagocytic activity of macrophages; stimulation of cytotoxic T-lymphocytes, which will destroy virus-infected cells; and the stimulation of B cells – leading to B cell proliferation and antibody production (Aghemo *et al.*, 2010; Chung *et al.*, 2008). Administration of interferon α-2b initially resulted in poor response rates due to its rapid elimination by the renal system, high absorption and tissue distribution; consequences of its low MW. These effects contributed to large variations in concentrations in between doses (Aghemo *et al.*, 2010). Consequently, at low concentrations effective viral suppression was not occurring, which led to poor response rates. Interferon α-2b was, therefore, a prime candidate for PEGylation and was PEGylated non-selectively with 12 kDa PEGs to produce peginterferon α-2b; a mixture of positional isomers (Bukowski *et al.*, 2002). Peginterferon α-2b exhibits improved bioavailability and half-life such that dosing could be reduced from 3 times a week, for native interferon α-2b, to just once a week for peginterferon α-2b , whilst still maintaining effective concentrations sufficient for suppression of viral replication. Peginterferon α-2b has since been used successfully to treat hepatitis C, and is administered in combination with ribavirin – a nucleoside inhibitor (Aghemo *et al.*, 2010).

1.3.5.4 Other Clinically Approved PEGylated Therapeutics

The success of these first PEGylated protein pharmaceuticals was critical in demonstrating that PEGylation could be used as a viable tool to improve the PK profiles of biologics. This was primarily due to the success of peginterferon α-2b, since treatment with pegademase and pegaspargase, whilst successful, was relatively limited in comparison;

indeed SCID, whilst a serious a disease, is fortunately rare. The success of peginterferon α-2b was further reinforced following the development of peginterferon α-2a (Pegasys®) in the same year, again for the treatment of hepatitis C. Peginterferon α-2a incorporates a 40 kDA branched PEG, as opposed to a 12 kDa PEG for peginterferon α-2b (Reddy *et al.*, 2002). The attachment of a larger PEG moiety resulted in peginterferon α-2a retaining only 7% of the native proteins antiviral activity (as opposed to 28% for peginterferon α-2b) but still resulted in increased efficacy in comparison to the native protein – due to the PEGylated versions much extended residence time (Bailon *et al.*, 2001). Peginterferon α-2a and peginterferon α-2b have since become blockbuster drugs, as have pegfilgastrim (Neulasta®) and mPEG-epoetin beta (Mircera®) for the treatments of chemotherapy-induced neutropenia and anemia, respectively (Jevsevar *et al.*, 2010). At the time of writing, there are currently 10 PEGylated pharmaceuticals clinically available, detailed in table 1. Peginesatide (Omontys®), developed by Affymax and Takeda, is not included; having since been recalled due to incidences of serious hypersensitivity reactions including fatal anaphylaxis (Fishbane *et al.*, 2013). Doxorubicin HCl liposome (Doxil®) is also not included as the therapeutic agent, doxorubicin, is itself not PEGylated; it is the liposome, used as the drug vehicle, that is (Gabizon *et al.*, 2003). Each PEGylated pharmaceutical in table 1 demonstrates improved efficacy combined with reduced dosing frequency, both of which provide improved pharmacological benefits and convenience to the patient when compared to their unmodified counterparts.

Table 1. Clinically available PEGylated Pharmaceuticals

Brand name/Generic name (Company)	Therapeutic agent	Indication	Year approved
Adagen® /Pegademase (Enzon)	Adenosine deaminase	SCID	1990
Oncaspar®/Pegaspargase (Enzon)	Asparaginase	ALL	1994
PegIntron®/Peginterferon α-2b (Schering-Plough)	Interferon α-2b	Hepatitis C	2001
Pegasys®/Peginterferon α-2a (Hoffman-La Roche)	Interferon α-2a	Hepatitis C	2001
Neulasta®/Pegfilgastrim (Amgen)	Granulocyte-colony stimulating factor	Neutropenia	2002
Somavert®/Pegvisomant (Pharmacia & Upjohn)	Growth Hormone Antagonist	Acromegaly	2003
Macugen®/Pegaptanib (OSI/Pfizer)	Anti-VEGF aptamer	Age-related Macular Degeneration	2004
Mircera®/PEG-epoetin beta	Erythropoietin	Anemia	2007
Cimzia®/Certolizumab pegol (UCB)	Anti-TNF Fab'	Crohn's Disease & Rheumatoid arthritis	2008
Krystexxa®/Pegloticase (Savient Pharmaceuticals)	Uricase	Chronic gout	2010

1.3.5.5 PEG Conjugates in Development

PEGylation has been suggested as a viable option for the passive delivery of anticancer drugs to tumours. Tumours, due to their enhanced angiogenesis, often have proportionately more vasculature than normal tissue and, furthermore, this vasculature is often highly permeable. Tumours often also have poorly developed lymphatic drainage. In combination, these two properties contribute toward what is termed the enhanced permeability and retention (EPR) effect (Duncan, 2006). Low MW anticancer drugs, which are conjugated to PEG, may therefore selectively accumulate in tumours due to the EPR effect, and the increase in MW as a consequence of PEGylation (Joralemon *et al.*, 2010). Currently, there are no low MW anticancer drugs that have been PEGylated clinically available, though there are several that have been evaluated in clinical trials. This is in part due to the low drug loading observed with PEGylated anticancer drugs, despite the EPR effect, as one PEG chain is usually coupled to a single drug molecule. Focus is currently on developing branched, multi-arm PEGs for conjugation with low MW anticancer drugs that

would provide a higher drug payload per PEG chain, and thus improve efficacy further. PEGylated anticancer drugs that have undergone clinical trials include PEG-paclitaxel, PEG-camptothecin, PEG-irinotecan and PEG-SN38, though this list is not exhaustive (Pasut *et al.*, 2009).

1.4 BIODISTRIBUTION OF MACROMOLECULES

Protein and non-protein molecules, such as PEG, differ from low MW compounds, such as most drugs, in several important respects in their disposition (Findlay *et al.*, 2000).

1.4.1 Proteins

As previously described, protein macromolecules must be administered parenterally to avoid enzymatic degradation by the digestive system (Mahmood *et al.*, 2005). Intravenous (IV) administration of macromolecules results in delivery directly into the systemic circulation. However, for other routes of administration, such as subcutaneous (SC), intramuscular (IM), or intraperitoneal (IP), the rate at which the macromolecule enters the systemic circulation depends on several factors, such as its MW, its physicochemical properties, and the rates of blood or lymph supply to the administration site (Takakura *et al.*, 1998). For example, for low MW macromolecules (1 kDa or less) entry into the systemic circulation will occur primarily through absorption into blood capillaries, whereas for higher MW macromolecules (20 kDa or larger) absorption will occur predominantly through the lymphatic system (Bocci, 1989; Mahmood *et al.*, 2005). Following entry into the systemic circulation, macromolecules are distributed intracellularly by extravasating from the microvasculature into the interstitial fluid and subsequently across cellular membranes into the cell (Michel, 1996). Macromolecules may extravasate through several different pathways, for example, directly through the endothelial cell of the capillary, or through inter-endothelial cell junctions (Takakura *et al.*,

1998). Again, properties of the molecule will affect its passage into the interstitial fluid. Furthermore, some may bind to plasma proteins, such as albumin, which can either inhibit or improve transport across membranes (Fasano *et al.*, 2005). Exchange from the vasculature into the cell is also affected by the permeability of the endothelium of the tissue through which exchange is occurring. For example, capillaries in the liver are composed of discontinuous endothelium, which allow facile transport into the interstitial fluid, whereas continuous endothelium makes up the majority of the microvasculature of the brain, resulting in a highly impermeable barrier which macromolecules cannot easily cross (Aird, 2007; Takakura *et al.*, 1998). Following passage into the interstitial fluid, intracellular distribution of a macromolecule is again governed by its physicochemical properties. For example, large MW macromolecules may only be internalised by endocytosis – in particular receptor-mediated endocytosis or pinocytosis – rather than diffusion across the membrane (Greish *et al.*, 2003). Internalisation via endocytosis almost inevitably leads to degradation by the lysosome, which will be discussed in more detail in section 1.6 (Bareford *et al.*, 2007). Macromolecules which bind to their target receptor on the surface of the cell are often subsequently internalised by receptor-mediated endocytosis, again culminating in lysosomal degradation (Krippendorff *et al.*, 2009). Macromolecules are also cleared through renal elimination. Again, this can be dependent on the MW of the molecule, as well as other factors, such as its overall charge. Low MW macromolecules are quickly eliminated as they can be easily filtered by the glomerulus, although if they are bound to albumin, for example, it can result in reduced glomerular filtration (Maeda *et al.*, 1992; Takakura *et al.*, 1994). As the MW of a macromolecule increases, however, its ability to pass through the glomerulus decreases (Hashida *et al.*, 1996). Following glomerular filtration, macromolecules may be degraded or excreted intact in the urine, though some may be reabsorbed (Mahmood *et al.*, 2005). Macromolecules may also be eliminated following receptor-mediated endocytosis and pinocytosis by

hepatocytes, where they will subsequently be degraded (Torchilin *et al.*, 2003). Some macromoledules may also be excreted in the bile following hepatic uptake (Mahmood *et al.*, 2007). Macromolecules may also be eliminated if neutralising antibodies are generated against them. In this case, antibody binding results in increased clearance of the macromolecule by the mononuclear phagocyte system (Jennings *et al.*, 2009).

1.4.2 PEG

Whereas the disposition of proteins is well understood, there are currently limited data available concerning the metabolism, excretion and disposition of PEG when coupled to protein in man (Webster *et al.*, 2007; Working, 1997). However, there are data available for free, unconjugated PEG.

1.4.2.1 Metabolism of PEG

The metabolism of PEG is MW-dependent, such that for PEGs of increasing MW metabolism becomes a less prevalent pathway of clearance. Metabolism is mediated by alcohol dehydrogenase, which oxidises alcohol groups to carboxylic acids (Herold *et al.*, 1989; Webster *et al.*, 2007; Webster *et al.*, 2009). These metabolites have been observed in burns patients who were treated with an antimicrobial cream containing three different MW PEGs; PEG 300, PEG 1000 and PEG 4000 Da. PEG was absorbed following topical application and entered the systemic circulation, resulting acute renal failure which ultimately proved fatal (Bruns *et al.*, 1982). This fatal syndrome, characterised by acidosis, has been replicated in rabbits and is similar to the toxicity observed following ingestion of ethylene glycol; a component of antifreeze and also the repeating unit of PEG (Herold *et al.*, 1982). Whilst ethylene glycol formation, in both humans and animals, has not been observed so far, oxalic acid, a major metabolite of ethylene glycol and mediator of toxicity, has been found and may be responsible for the renal toxicity that has been observed with

PEG (Webster *et al.*, 2009). Whilst PEG can be metabolised, the formation of toxic metabolites from PEG is unlikely given the high MW of the PEGs routinely used, and the relatively low amounts of PEG administered (Webster *et al.*, 2007). Indeed, the MW of PEGs typically conjugated to biologics is over 5 kDa (Molineux, 2003; Veronese *et al.*, 2005). Consequently, for PEGs routinely coupled to therapeutic agents clearance by metabolism would represent a very small fraction of the dose, and subsequently ought to limit potential toxicity associated with PEG metabolism; indeed, larger MW PEGs have been seen to be quite safe when administered orally (Working, 1997).

1.4.2.2 Disposition of PEG

Studies concerning the disposition of PEG have predominantly been generated following oral administration, consequently there is limited data regarding the disposition of PEG, either in a free form or protein-coupled, following parenteral administration (Working, 1997). The absorption of PEG following oral administration is MW-dependent, such that little PEG over 1 kDa is absorbed (Gursahani *et al.*, 2009; Webster *et al.*, 2007; Working, 1997). Absorption of PEG through the skin is also MW-dependent and is not thought to represent a viable route to the systemic circulation on undamaged skin (Tsai *et al.*, 2003). Though skin absorption can occur easily on damaged skin, as seen with burns victims, previously described (Herold *et al.*, 1989).

In animal disposition studies (rodent, dog and rabbit) in which PEG is administered intravenously, the majority of the dose of unconjugated PEG is found rapidly excreted in the urine and faeces (Carpenter *et al.*, 1971; Shaffer *et al.*, 1948; Shaffer *et al.*, 1950). In a disposition study in cats, PEG was also shown to be eliminated through biliary clearance, though this is a minor clearance pathway (Friman *et al.*, 1993; Webster *et al.*, 2007). Similar results have also been found in humans, with approximately 96% of a dose of 6 kDa PEG found excreted in the urine from 6 men (Shaffer *et al.*, 1947). However, it should be noted

that these studies largely utilise PEGs of a MW that would not commonly be coupled to biologics, i.e. from 400 Da to 6 kDa.

A study investigating the effect of PEG MW (6 – 190 kDa ^{125}I-labeled PEG) on tissue internalisation in mice, found that higher MW PEGs persisted in the circulation for longer, and were less likely to be excreted in urine. PEG was shown to accumulate in liver, skin, muscle and bone regardless of MW, but higher MW PEGs (above 50 kDa) were more readily internalised by macrophages and Kupffer cells (Yamaoka *et al.*, 1994).

Two studies have provided evidence for the vacuolation of renal tubular endothelial cells in rodents as a consequence of PEG, coupled to either tumour necrosis factor binding protein (TNF-bp) or haemoglobin, administration. In these studies the PEG-linked proteins were filtered by the glomerulus and reabsorbed, resulting in vacuolation of the endothelial cells. Often, vacuolation was reversible, but perhaps more surprisingly was that animals with distinct morphological abnormalities did not exhibit reduced renal function (Bendele *et al.*, 1998; Conover *et al.*, 1996). The PEG MWs used in these studies were between 5 and 50 kDa, and consequently would typically be used for biologic conjugation. It is, therefore, not inconceivable that vacuolation may occur in man, particularly in patients receiving chronic dosing of a PEGylated agent, though the evidence, and indeed the toxicological relevance, of this is currently unsubstantiated.

1.5 BIOANALYSIS OF MACROMOLECULES

1.5.1 Protein Analytical Limitations

In comparison to low MW drugs, the bioanalysis of proteins and other macromolecules is fraught with difficulties that can preclude reliable assessment – a requirement for accurately determining the PK parameters of the administered macromolecule. Immunoassays (western blotting, ELISA (enzyme-linked immunosorbent

assay) and liquid chromatography-tandem mass spectrometry (LC-MS/MS) are the predominantly applied techniques for the bioanalysis of therapeutically administered proteins in biological tissues and fluids. However, each method has limitations that prevent their use as a universal tool for the bioanalysis of proteins.

1.5.1.1 Immunoassay

Analysis of proteins by immunoassays is generated from reactions between an antibody and an antigen. These methods are often highly sensitive, rapid, cost-effective and require less sample volume than LC-MS/MS (Ewles *et al.*, 2011; Findlay *et al.*, 2000; Yang *et al.*, 2007). Furthermore, they are able to analyse large MW proteins that cannot be analysed by LC-MS/MS, since their mass-to-charge (*m/z*) ratios are above the range typical of the majority of spectrometers (Ewles *et al.*, 2011). Immunoassays also represent quick, facile techniques with high throughput (Campbell *et al.*, 2011; Wadhwa *et al.*, 2010). However, despite being a relatively quick technique, it can often take months to optimise and validate the assay due to the time required to generate the antibody to the protein of interest, which can often limit the utility of immunoassays in the early development of biologics (Ewles *et al.*, 2011; Findlay *et al.*, 2000; Yang *et al.*, 2007). Once the assay is validated, however, it can provide rapid analysis – providing that subsequent re-optimisation is not required, for example due to loss of biological activity of the antibody resulting from storage conditions, or re-optimisation due to variation between antibody lots (Findlay *et al.*, 2000). A further hindrance to the bioanalysis of proteins by immunoassay is their specificity. The analysis of proteins in biological matrices can be artificially altered due to the presence of the endogenous protein, thereby preventing accurate determination of PK parameters (Findlay *et al.*, 2000). Furthermore, abundant endogenous proteins, such as albumin, present in the sample can also complicate analysis, should the antibodies used in the assay be non-specific for the protein of interest (Ewles *et*

al., 2011). Analysis by immunoassay may also not be able to distinguish between the parent protein and reactive metabolites, should the metabolite differ structurally from the parent drug at positions other than the antibodies binding epitope(s) (Findlay *et al.*, 2000).

1.5.1.2 Liquid Chromatography-tandem Mass Spectrometry

LC-MS/MS can offer improved specificity and accuracy over immunoassays due to the samples being separated prior to detection by MS, which can resolve proteins/peptides from their structurally similar reactive metabolites, even if they have only minor modifications, which often cannot be achieved by immunoassay analysis (Ewles *et al.*, 2011). Method development for LC-MS/MS also does not require the generation of specialist reagents and consequently can be fully validated for use within days rather than months, as well as also offering the benefits of high throughput analysis (Ezan *et al.*, 2009). Analysis of proteins in biological samples by LC-MS/MS can be limited by the complexity of the sample, however. Whereas for immunoassays, a specific antibody may be found for the detection of the protein of interest in the sample, when analysed by LC-MS/MS all proteins from the sample will be analysed, which may reduce the sensitivity of the technique and can also make analysis challenging (Ewles *et al.*, 2011). Consequently, methods to clean up samples prior to LC-MS/MS analysis are often employed, such as protein precipitation (Campbell *et al.*, 2011). However, this process is non-selective, cannot remove all endogenous proteins in the sample, and can also result in analyte loss, either through direct precipitation of the protein of interest, or due to co-precipitation – where the analyte protein is co-precipitated out of solution when bound to an endogenous protein (Ezan *et al.*, 2009; Yang *et al.*, 2007). Whereas immunoassays are suitable for the analysis of large MW proteins, LC-MS/MS is suitable for the analysis of low MW proteins and peptides, such as below 5 kDa (Ewles *et al.*, 2011). For the analysis of larger proteins, they first need to be proteolytically digested via trypsin to produce surrogate peptides. It is these peptides

that are then subsequently analysed as representatives of the intact protein (Nowatzke *et al.*, 2011). However, this process has several limitations. For example, monitoring only one surrogate peptide can reduce the selectivity of the technique, since the chosen peptide may not fully represent the protein; for example if post-translational modifications to the protein have occurred at sites other than the surrogate peptide then this information will not be quantified (Campbell *et al.*, 2011; Ewles *et al.*, 2011). Furthermore, this requires further optimisation of the digestion and sample clean up steps for each peptide analyte, which may become time consuming if more than one surrogate peptide selected for analysis (Campbell *et al.*, 2011). Trypsin will also digest endogenous proteins present in the sample, which can further complicate analysis (Ewles *et al.*, 2011).

1.5.2 PEG Analytical Limitations

Methods that have been employed for the bioanalysis of PEG, and consequently PEGylated therapeutics, have been hindered by inherent difficulties relating to the PEG moiety. It is due to these issues that this thesis will present alternative methodologies suitable for the bioanalysis of PEGylated proteins.

1.5.2.1 Spectroscopy

Analytical difficulties for measuring PEG derive from PEG's transparency, its non-fluorescence and the absence of a UV chromophore contained within its structure (Webster *et al.*, 2009). Consequently, PEG is troublesome to detect using standard spectroscopy techniques.

1.5.5.2 Radiolabeling

Radiolabeling, the incorporation of a radioactive element, such as ^{3}H and ^{14}C, into a molecule, has proven to be a useful tool to monitor the metabolism and biological fate of

various compounds. However, the utility of radiolabeling is restricted by excess cost, and is therefore often confined to small scale studies in only a small percentage of laboratories. Furthermore, the data generated from radiolabeling PEGylated proteins may not provide sufficient detail and/or correctly represent the *in vivo* clinical situation due to the positioning of the radiolabel during the labelling process. If the radiolabel is applied to the protein then any degradation or metabolism of the conjugate, that may occur *in vivo,* will not provide information on the biological fate of the PEG moiety; just that concerning the protein. Secondly, positioning the radiolabel within the PEG may alter its structure and therefore may affect the pharmacokinetics of the conjugate. Furthermore, if the radiolabel is situated near the terminal hydroxyl groups of PEG this could affect the conjugation of PEG to proteins and/or the incorporation of the methyl cap on the remaining hydroxyl group; again, potentially altering the pharmacokinetics of the conjugate (Webster *et al.*, 2009).

1.5.2.3 Mass Spectrometry

Whilst the low polydispersity of PEG is beneficial in terms of conjugate homogeneity and reproducible therapy, it does represent a barrier when analysing PEG and PEGylated proteins by MS (Mero *et al.*, 2009). Due to their polydispersity they do not produce a single peak, but instead each different MW species of PEG, formed during ionisation, present in the sample is represented by a peak of their own. Each of these peaks in the spectrum is separated from adjacent peaks by a mass of ~44 Da – the MW of PEGs subunits. Analysing metabolic changes to the PEG and/or its metabolites is therefore a significant challenge. Moreover, PEGs of increasing MW are poorly ionised and thus, for larger PEGs, those that would be routinely conjugated to therapeutic proteins, the use of MS as an analytical tool may not be wholly appropriate (Mero *et al.*, 2009; Webster *et al.*, 2009).

1.6 PEG KNOWLEDGE LIMITATIONS

Despite the plethora of data validating the beneficial properties of PEGylation, and the success of existing PEGylated agents, there are several limitations still to be addressed regarding our fundamental understanding of PEGylated proteins. The body of work contained within this thesis is directed at resolving these issues.

1.6.1 Lack of Metabolism and Biodistribution Studies

As previously described in section 1.4.2., there is still a serious lack of data regarding the metabolism, disposition and biological fate of PEG when conjugated to proteins, which is in part due to the analytical limitations outlined in section 1.5.2., and consequently detailed knowledge of the effect of PEGylation on a proteins disposition is poorly understood. A knowledge gap therefore exists regarding the safety of PEGylated therapeutics, to which this thesis attempts to address.

1.6.2 Mechanisms of Reduced Immunogenicity

As previously mentioned, the reduced immunogenicity observed with PEGylated proteins is primarily attributed to the shielding effect of PEG. In this situation, PEG is believed to prevent the binding of antigenic epitopes on the biologic to B cell receptors, thus preventing their activation and consequently eliciting an immune response. However, the induction of immune-mediated responses involves various, intricately linked pathways to which the effect of PEGylation may involve some or all of the mechanisms involved. As yet, a complete explanation has not been fully elucidated (Veronese *et al.*, 2009). In terms of generating an immune response against a PEGylated biologic, there are several immunological processes involved; internalisation of the protein, processing of the protein into peptides, binding of the peptides to major histocompatability complex (MHC)

molecules to form complexes that are then presented on the surface of the cell, and finally, recognition by B and T lymphocytes.

1.6.2.1 MHC class II Pathway

The MHC class II pathway of antigen processing primarily utilises peptides that have been generated from lysosomes present in APC (Delamarre *et al.*, 2006). Typically, these peptides are generated from exogenous protein that have been internalised by the cell by endocytosis (Schroder *et al.*, 2010). Endocytosis is a compartmentalised process, which itself can be further subdivided into different categories, such as phagocytosis and macropinocytosis, but once internalised they follow a general endocytic pathway culminating in the lysosome (Pillay *et al.*, 2002). Material is initially internalised inside vesicles, which usually form when the plasma membrane invaginates extracellular material and pinches off to form a vesicle. These vesicles fuse with early endosomes, which then mature into late endosomes – characterised by a decrease in pH. Late endosomes then fuse with lysosomes, and any material, such as a biologic, present in the lumen of the late endosome will subsequently be present in the lysosome (Pillay *et al.*, 2002). The lysosome contains many different hydrolase enzymes, which include various protease enzymes to degrade internalised protein (Schroder *et al.*, 2010). These enzymes have an acidic optimum pH and consequently an acidic environment is maintained inside the lysosome through the action of proton pumps (Schroder *et al.*, 2010). The digestion of internalised protein via the various lysosomal proteases results in the formation of peptides, of which certain peptides will bind to MHC class II molecules. MHC class II molecules are synthesised in the endoplasmic reticulum and are transported to the lysosome with the peptide-binding groove of the molecule blocked by the invariant chain (Ii), a protein which prevents cellular peptides from binding to MHC class II molecules during translocation to the lysosome (Jensen, 2007). Inside the lysosome, the Ii is sequentially cleaved by cathepsin S (a

lysosomal cysteine protease) until only a section of the invariant chain, the class II-associated invariant chain peptide (CLIP), remains (Colbert *et al.*, 2009; Jensen, 2007; Watts, 2004). CLIP is subsequently removed from the MHC class II molecule, facilitated by the protein human leukocyte antigen-DM (HLA-DM), which causes dissociation of CLIP from the molecule – leaving it free for peptides present in the lumen of the lysosome to bind (Jensen, 2007; Watts, 2004). Once a peptide-MHC II complex has been formed it is transported to the cell surface, where the antigen (peptide) can be displayed for recognition by $CD4^+$ T cells, which express the specific T cell receptors (TCR) against the complex (Watts, 2004). Once this binding has occurred, co-stimulatory molecules present on the $CD4^+$ T cell and the complex interact, which results in a secondary signal that is necessary for activation of the naive $CD4^+$ T cell (however, this secondary/verification signal would not be required for activation of memory T cells) (Croft *et al.*, 1997; Linsley *et al.*, 1993). After these two signals have been established, the T cell proliferates through autocrine signalling, whereby it releases interleukin 2 (IL-2) which subsequently acts on the cell itself to activate its proliferation pathways (Jenkins *et al.*, 2001). After proliferation, the progenitor cells mature and differentiate into regulatory T cells, memory T cells and effector T cells (Kaech *et al.*, 2002; Seder *et al.*, 2003). Effector T cells secrete cytokines that can activate and stimulate other components of the immune system, such as macrophages, $CD8^+$ T cells and B cells (Jelley-Gibbs *et al.*, 2000; Jenkins *et al.*, 2001). The activation of antigen-specific B cells causes them to proliferate and increases their production of drug-specific neutralising antibodys, culminating in a long lasting antibody response that can inhibit or even preclude a biologic's effectiveness (Baker *et al.*, 2010; Chirino *et al.*, 2004). Furthermore, drug-specific activation of $CD8^+$ T cells can result in hypersensitivity reactions (Kalish *et al.*, 1999). These problems, with regards to PEGylated biologics, will be discussed in more detail in section 1.7.

1.6.2.2 MHC class I Pathway

In general, antigen processing through the MHC class I pathway was typically thought to be restricted to endogenous protein (Voeten *et al.*, 2001). Historically, this pathway was not thought to be involved in the presentation of peptides originating from extracellular protein. However, certain APCs, primarily DC, have the ability to cross-present antigen, whereby exogenous protein, which would typically be processed via the MHC class II pathway, can be processed via the MHC class I pathway and used to stimulate naive $CD8^+$ T cells (Amigorena *et al.*, 2010; Jensen, 2007). Cross-presentation usually occurs against proteins originating from tumours and viral infections, which do not easily infect APC and therefore would not usually be processed via the MHC I pathway by these cell types (Amigorena *et al.*, 2010). In this case, extracellular protein escapes the endocytic pathway into the cytosol, where they are degraded by the proteasome (Amigorena *et al.*, 2010; Jensen, 2007). Normally, the proteasome degrades damaged or unwanted endogenous proteins selected for degradation by ubiquitination – a post translational modification whereby ubiquitin chains are coupled to protein substrates; targeting them for degradation by the 26S proteasome (Glickman, 2000). The proteasome consists of a catalytic core particle (the 20S proteasome) – a barrel-like structure comprised of four heptameric rings, of which the two inner rings (composed of the β subunits (the two outer rings are composed of α subunits)) each possess three subunits with proteolytic ability – that is flanked either side by either one or two 19S regulatory caps, which are involved in directing ubiquitinated proteins into the catalytic 20S proteasome; together forming the 26S proteasome (Burlet-Schiltz *et al.*, 2005; Emmerich *et al.*, 2000; Glickman, 2000; Khan *et al.*, 2001; Niedermann *et al.*, 1999). Exogenous proteins that escape the endocytic pathway are degraded into peptides by the proteasome, which are then transported into the endoplasmic reticulum via the transporter associated with antigen processing (TAP) (Burlet-Schiltz *et al.*, 2005; Jensen, 2007; Niedermann *et al.*, 1996). Once inside the endoplasmic

reticulum peptides are loaded onto MHC class I molecules, which then translocate, through the Golgi apparatus, to the cell surface for display and recognition by $CD8^+$ T cells (Androlewicz, 2001; Burlet-Schiltz *et al.*, 2005). Again, activation of $CD8^+$ T cells requires two signals; the initial recognition of the peptide-MHC class I complex by the specific TCR on the $CD8^+$ T cell followed by interactions between co-stimulatory molecules (Curtsinger *et al.*, 2003; Pardigon *et al.*, 1998). Clonal expansion of the $CD8^+$ T cell then occurs, resulting in increased numbers of T cells capable of recognising the displayed antigen on other cells. Once recognised, these cells will be destroyed through the release of cytotoxins, such as perforin (Zhang *et al.*, 2010). MHC class I molecules are present in all nucleated cells, whilst proteasomes are also constitutively expressed, and so nearly all cell types can display peptides as a complex with MHC class I molecules (Jensen, 2007). However, during infection and stress, proinflammatory cytokines lead to the formation of what is termed the immunoproteasome – where the catalytic subunits of the 20S proteasome are substituted with inducible immunosubunits (Khan *et al.*, 2001). The immunoproteasome possesses enhanced ability to generate different peptide repertoires that can be loaded onto MHC class I molecules easier than if they were generated from the normal, constitutive proteasome (Androlewicz, 2001; Yewdell, 2005).

1.6.2.3 Potential effects of PEGylation

Hypothetically, PEGylation could inhibit or alter these two pathways at several different points (Veronese *et al.*, 2009). The attachment of PEG may inhibit or reduce internalisation of the protein into APCs and/or organs of the immune system, such as lymph nodes. PEG may confer protection against lysosomal and/or proteasomal degradation inside the APC, or alter the processing of the protein; thereby favouring non-immunogenic peptide production or a peptide repertoire containing fewer immunogenic peptides. PEG may also alter the distribution of the protein, as a conjugate, in cells or

tissues involved in immunogenicity. Echoing the lack of metabolism studies is the lack of investigation into these possible mechanisms of reduced immunogenicity. Whilst the mechanisms may differ between different PEGylated proteins, due to the size of the PEGs involved, linearity/branching of PEG and nature of the attached protein, and thus designing out adverse immunological effects may be a customised process for each conjugate; a complete understanding of how immunogenicity is reduced in the first place is paramount to ensuring successful PEGylated drug design in the future.

1.7 SAFETY AND EFFICACY ISSUES

The information outlined in section 1.5 clearly demonstrates a practical need to develop robust, analytical techniques to monitor the biological fate of both the PEG and protein components of PEGylated conjugates in order to inform drug safety science regarding their metabolism and disposition. Furthermore, addressing the gaps in our understanding regarding mechanisms of reduced immunogenicity may improve novel PEGylated drug design by further reducing the frequency of adverse drug reactions. Importantly, safety issues have arisen with PEGylated proteins in both human and animal models, which may be attributable to the currently poorly understood mechanics of PEGylated protein immunogenicity. Furthermore, neutralising antibodies have been reported against both the PEG and protein moieties of PEGylated proteins, resulting in reduced efficacy. These reports outline a functional need to address these issues.

1.7.1 Immunogenicity: PEG Moiety

Despite PEGylation being able to reduce the original immunogenicity of an attached protein this does not preclude the immune recognition of PEG itself, which, in some cases, is reported to result in hypersensitivity reactions. Neutralising anti-PEG antibodies, which may be pre-existing, may also act to increase the clearance of PEGylated

conjugates and therefore reduce their circulating half-life and attenuate effective treatment. This is termed accelerated blood clearance. Safety and efficacy issues resulting from antibody-mediated responses to the PEG moiety have been reported in both animal models and patients.

1.7.1.1 In Animal Models

Various PEGylated proteins have been used to demonstrate that PEGylation can prevent the binding of protein-specific antibodies. However, in these same studies a new immunogenicity was generated against PEG itself. Specific, anti-PEG antibodies have been recognised as far back as 1983 against proteins such as uricase, superoxide dismutase and ovalbumin; modified to various degrees with PEG (Richter *et al.*, 1983). In these studies, antibodies generated in animal models against the native protein were shown to be incapable of recognising the PEGylated version of the same protein. However, antibodies generated against a PEGylated protein were shown to be cross reactive with other PEGylated proteins; for example, antibodies generated against PEGylated uricase conjugates were shown to bind to PEGylated superoxide dismutase also, indicating the specificity of the antibodies for PEG (Tsuji *et al.*, 1985).

Numerous reports provide evidence for the accelerated blood clearance of a second dose of PEGylated liposomes in rodent models, as well as hypersensitivity reactions targeted against the PEG component of the liposome (Dams *et al.*, 2000; Ishida *et al.*, 2006a; Ishida *et al.*, 2005; Ishida *et al.*, 2006b; Ishida *et al.*, 2008a; Ishida *et al.*, 2008b; Ishida *et al.*, 2003; Laverman *et al.*, 2001; Wang *et al.*, 2007). Liposomes are vesicles composed of a lipid bilayer, which is used to encapsulate pharmaceuticals and consequently serves as a drug vehicle (Lian *et al.*, 2001). PEGylation is used to extend the circulating half-life of liposomes, and consequently the pharmaceutical agent contained therein, through sterically hindering interactions with plasma proteins and subsequent

uptake by the mononuclear phagocyte system (Immordino *et al.*, 2006). However, the safety and efficacy of PEGylated liposomes has been called in to question following issues occurring after repeat administrations. A single treatment regime of PEGylated liposomes induced acute hypersensitivity, which developed within minutes of re-administration in mice, and was characterised by lethargy, facial swelling and high mortality rates at higher doses (Judge *et al.*, 2006). Furthermore, accelerated blood clearance has been observed following repeat administration of PEGylated liposomes; resulting in reduced half-life and efficacy of the drug contained within the liposome (Ishida *et al.*, 2006a). It was shown that, following the first dose of PEGylated liposome, high amounts of anti-PEG IgM were secreted. The high amounts of anti-PEG IgM antibody were subsequently responsible for the clearance of the second dose of PEGylated liposomes (Wang *et al.*, 2007). The specificity of the antibodies to the PEG moiety was confirmed using ELISA; antibodies generated against a single injection of PEGylated liposomes were shown to be reactive against other PEGylated lipids but not native lipid; indicating the antibodies were targeted against the PEG moiety. It is not yet fully elucidated why anti-PEG IgM is secreted in response to PEGylated liposomes. However, further research has revealed that IgM may be secreted in a T lymphocyte-independent manner (Koide *et al.*, 2010). Furthermore, the binding of IgM to the second dose of PEGylated liposomes may also activate the complement system; resulting in increased clearance of the second dose by Kupffer cells and macrophages, which internalise complement-coated particles (Ishida *et al.*, 2006c).

1.7.1.2 In Humans

Interestingly, a recent study has shown that unconjugated PEG can activate the complement system in human sera within minutes; characterised by increases in the serum levels of products of complement activation, namely: C3d, Bb, C3a-desArg and SC5b-9 (Hamad *et al.*, 2008). Moreover, complement activation was observed using therapeutically

relevant PEG doses. The study utilised PEGs with MWs between 1,960 and 11,600 Da and found that higher MW PEGs were more effective complement activators. Consequently, it is feasible that clinically available PEGylated drugs may also cause complement activation, in line with this study, since some clinically available PEGylated drugs utilise PEGs above 11,600 Da, such as peginterferon α-2a (Pegasys), which is coupled to a 40 kDa PEG (Keating, 2009).

In 2007, a study detected anti-PEG antibodies in the sera of 12 out of 15 patients that were treated with pegaspargase (Armstrong *et al.*, 2007). The presence of anti-PEG was associated with rapid clearance of the drug, which may preclude effective drug therapy. Rapid clearance of pegaspargase is reported for up to a third of all patients receiving the drug for the treatment of ALL and thus the presence of anti-PEG may not be confined to a small subset of the population (Armstrong *et al.*, 2006). Hypersensitivity reactions are also known to occur with pegaspargase, over a range of doses, and can be either acute or delayed (Zeidan *et al.*, 2009). These can range from mild hypersensitivity reactions to anaphylaxis (Dinndorf *et al.*, 2007).

A recent study has shown that pre-existing anti-PEG may reside in up to 25% of the healthy population, and would thus corroborate the findings observed with pegaspargase clearance rates (Armstrong, 2009). This same study also purports that this represents an increase from a prevalence of 0.2% anti-PEG antibodies in the healthy population, originally reported in 1984 by Richter and Akerblom, to 25% in 2009 (Richter *et al.*, 1984). Other than differences in the sensitivity of the techniques employed between the two time points, passive hemagglutination in 1984 and flow cytometry in 2009, the only other explanation concluded by the authors is the increased exposure to PEG present in every day items over the subsequent years. Indeed, PEG and PEG-related compounds are extensively used in the cosmetics industry, as drug excipients and are found in such products as fertilisers, pesticides, toothpaste, food, drink, aerosols and shampoo (Armstrong, 2009; Fruijtier-

Polloth, 2005). If correct, pre-existing anti-PEG may constitute a significant obstacle to effective treatment with PEGylated agents in years to come.

Pegloticase (Krystexxa®), approved in 2010 for the treatment of treatment-failure gout, has been shown to be successful in reducing plasma uric acid levels, due to the action of the enzyme uricase, which metabolises uric acid (Reinders *et al.*, 2010; Sundy *et al.*, 2008). Antibodies to various PEGylated uricase conjugates have previously been generated in animal models (Tsuji *et al.*, 1985). Prior to pegloticase, earlier studies in humans during a Phase I study of PEG-uricase found specific anti-PEG antibodies present in 5 out of 13 patients, of which 3 of these 5 patients also exhibited injection-site reactions 8 to 9 days after injection (Ganson *et al.*, 2006). These 5 patients had much faster clearance of PEG-uricase in comparison to the remaining 8 patients, which was associated with the presence of IgG and IgM antibodies. During a 6 month, placebo-controlled clinical trial of pegloticase, 58% of patients did not respond to therapy and 26-31% of patients suffered from infusion reactions; again, these were associated with the generation of neutralising anti-pegloticase antibodies (Reinders *et al.*, 2010).

1.7.2 Immunogenicity: Protein Moiety

Antibodies specific to the protein, rather than the PEG, are also known to be associated with hypersensitivity reactions and accelerated blood clearance of PEGylated proteins; suggesting that immunogenicity is not completely abrogated following PEGylation and, furthermore, may not hold true for all PEGylated proteins and/or patients.

1.7.2.1 In Animal Models

A recent study in mice found that repeated injections of PEGylated recombinant human butylcholinesterase (PEG-rHu BChEs) resulted in circulating anti-rHu BChE antibodies and rapid clearance of the conjugate. BChE is used as prophylactic against

organophosphorous compounds, which are used as nerve agents, as it is an effective bioscavenger of such compounds. To maintain efficacy, multiple administrations are required to allow for therapeutic concentrations of the enzyme to remain in the circulation. Consequently, a PEGylated form of rHu BChE was synthesised to meet such requirements. A first injection of PEG-rHu BChE was shown to have an increased half-life in comparison to unmodified rHu BChE. However, following a second injection, the bioavailability was drastically reduced and the presence of neutralising antibodies was detected. These antibodies were shown to be specific for the enzyme, rather than the PEG. Thus, whilst PEGylation could extend the circulatory stability of rHu BChE it could not reduce its immunogenicity in mice; culminating in rapid clearance of the conjugate following multiple administrations (Chilukuri *et al.*, 2008).

1.7.2.2 In Humans

Treatment with interferon α can result in the generation of neutralising antibodies in patients (Lallemand *et al.*, 2010). Interferon α specific antibodies have also been detected in patients receiving treatment for hepatitis C with peginterferon α-2b or peginterferon α-2a, and has been associated with loss of antiviral activity; indeed, it is reported that up to 50 – 60% of patients do not respond to therapy or suffer relapse at the end of treatment, which may or may not be due to the presence of neutralising antibodies (Halfon *et al.*, 2010). One particular case study of a patient enrolled on a high-dose peginterferon α-2b course found virtually undetectable levels of circulating peginterferon α-2b, no virologic response to treatment, and the levels of interferon α specific antibodies increased after just one week of treatment (van der Eijk *et al.*, 2006). As yet there are very few large-scale, unbiased studies regarding the association of neutralising antibodies attenuating virologic reponse to peginterferon (α-2b or α-2a) therapy (Boo *et al.*, 2007; Halfon *et al.*, 2010; Sasayama *et al.*, 2010). Whilst the effect of neutralising antibodies on

abrogating antiviral activity cannot currently be discounted other factors, such as host genotype, are also reported to contribute toward the poor clinical outcome observed in non-responders (Halfon *et al.*, 2010).

1.7.3 Peginesatide (Omontys®)

Peginesatide is a PEGylated peptide mimetic erythropoiesis stimulating agent; possessing high affinity binding to the erythropoietin (EPO) receptor but is sequentially unrelated to EPO (Mikhail, 2012). It was approved in 2012 by the FDA for the treatment of anaemia in adult patients currently undergoing dialysis (Moran, 2012). In phase II and III clinical studies peginsatide was well tolerated (Valliant *et al.*, 2013). However, peginesatide was voluntarily recalled by Affymax and Takeda in 2013 due to hypersensitivity reactions occurring amongst patients (Eckardt, 2013). To date, it was reported that more than 25,000 patients had been administered peginesatide. Of these, 0.2% of patients suffered from hypersensitivity reactions of which a third of these cases were classified as serious in nature, and included 19 cases of anaphylaxis, of which 3 patients died (0.02% of patients) (Eckardt, 2013). Hypersensitivity was reported to occur within 30 minutes of administration, but there are no reports of hypersensitivity occurring following subsequent dosing (Eckardt, 2013; Locatelli *et al.*, 2013). As of yet, there is too little information available to establish whether the neutralising antibodies, observed in clinical trials, and the hypersensitivity reactions, observed post-marketing, were a consequence of antibodies to either the PEG or peptide moiety. Nevertheless, the case of peginesatide serves as a reminder that PEGylation is not a universal answer for the safe reduction of protein immunogenicity.

1.7.4 Summary

The information outlined in this section clearly reveals that, contrary to the widely-accepted dogma that PEG is non-immunogenic, anti-PEG antibodies can be generated in both animal models and humans, and are associated with hypersensitivity reactions and reduced drug efficacy. Injection of PEGylated proteins, such as ovalbumin and uricase, in animal studies has resulted in the generation of anti-PEG antibodies that were shown to be cross-reactive for PEG. In humans, anti-PEG antibodies are associated with reduced activity of clinically available PEGylated biologics, such as pegaspargase and pegloticase, and can also result in hypersensitivity reactions, which can be fatal, as was the case with peginesatide. Furthermore, the generation of anti-interferon α antibodies has been linked with reduced antiviral activity of both peginterferon α-2b and α-2a; indicating that PEGylation may not be universally able to reduce the immunogenicity of attached proteins, as previously thought. Alarmingly, anti-PEG antibodies have been detected in up to 25% of healthy blood donors, which may compromise the efficacy of existing and future PEGylated biologics. Whilst PEGylated biologics are, in general, widely tolerated, safe, and effective therapeutic agents, it is clear that pre-screening for anti-PEG antibodies prior to onset of therapy may become the norm for the continued safe and effective use of this class of pharmaceuticals.

1.8 THESIS AIMS

The primary aims of this thesis are method discovery and optimisation for the bioanalysis of PEGylated proteins, due to the analytical limitations that currently exist regarding the bioanalysis of both PEG and proteins. In order to comprehensively analyse the *in vivo* metabolism, disposition and biological fate of PEGylated proteins, suitable, quantitative analytical tools, that provide structural information concerning both the PEG and protein moieties as well as the overall molecular integrity of the conjugate, are required. Consequently, these will help inform drug safety science and simultaneously

improve our fundamental understanding of the field, which, as described earlier, is currently lacking. The effect of PEGylation on the immunogenicity of proteins is also poorly understood. Subsequently, the effect of PEGylation, in particular PEG MW, on PEG-protein cellular internalisation and antigen processing, processes which are involved in the immune response, was assessed. The following experimental aims were defined:

1) Develop an analytical platform capable of determining the *in vivo* kinetics, disposition and biological fate of a model PEGylated protein. This platform will: encompass both the PEG and protein moieties of the conjugate for analysis and quantification; be able to analyse a range of biological tissues and fluids; represent a facile, inexpensive, yet comprehensive, platform for the bioanalysis of PEGylated proteins.

2) Define the effect of PEGylation on the cellular internalisation of model PEGylated proteins and the potential consequences for immunogenicity. The effect of PEGylation, in particular PEG molecular weight, on uptake by dendritic cell, a model APC, will be assessed.

3) Define the effect of PEGylation on the *in vitro* processing of model PEGylated proteins and the potential consequences for immunogenicity. Human proteasome and lysosome fractions will be used to assess the effect of PEGylation, in particular PEG molecular weight, on both the MHC class I and II pathways of antigen processing, respectively; both in terms of overall protection against degradation, and on the peptide repertoires generated by the two pathways.

CHAPTER 2

Disposition of PEGylated Proteins: Gel-Based Analysis

CONTENTS

Disposition of PEGylated Proteins: Gel-Based Analysis

2.1 INTRODUCTION

The assessment of both the disposition and biological fate of PEGylated proteins has been hampered by limitations in the bioanalytical methods available to determine these properties, as described in the general introduction. Addressing this issue requires the discovery and development of novel platforms to allow the detection and quantification of PEGylated compounds in biological matrices. This chapter describes the development of gel-based assays to monitor the kinetics and biological fate of a model PEGylated protein – PEG-insulin – in a rodent model. Chapter 3 will describe the development of a ^{1}H NMR protocol to quantify the amount of PEG-insulin excreted in urine samples from the same rodent model. Combined, these two independent techniques provide an analytical platform to: 1) evaluate the structural integrity of PEGylated conjugates by monitoring both the PEG and protein components, and 2) determine the kinetics of the conjugate and its *in vivo* disposition in biological matrices.

Due to the very different physicochemical properties of the polyethylene glycol and polypeptide moieties of PEG-proteins, it is unlikely that a single bioanalytical assay will adequately detect the entire compound. Consequently, a multifaceted gel-based platform was required in order to report on the individual components of the conjugate. A sodium dodecyl sulphate-polyacrylamide gel electrophoresis (SDS-PAGE) method, incorporating a barium iodide stain to detect PEG, first described in 1992, was modified for the detection of PEG in biological tissues and fluids (Kurfurst, 1992). The use of western blotting, using both anti-PEG and anti-insulin antibodies, was employed to further assess the structural integrity, of both the PEG and protein components of the conjugate, as well as the disposition in tissues and fluids.

The disposition and biological fate of a model PEGylated protein, ^{40K}PEG-insulin (synthesised in-house), was assessed in a rodent model using the aforementioned methodology. Plasma, urine, liver and kidney samples were collected, and ^{40K}PEG-insulin

content and conjugate integrity determined in each sample over a period of 28 days, following a single dose of ^{40K}PEG-insulin.

2.2 METHODS AND MATERIALS

All reagents were purchased from Sigma-Aldrich Company Ltd (Dorset, UK), unless otherwise stated.

2.2.1 Synthesis and Purification of ^{40K}PEG-insulin

^{40K}PEG-insulin was synthesised using methodology adapted from (Dou *et al.*, 2007). Insulin (human recombinant from yeast), at 1 mg/mL, was dissolved in 0.02 M sodium acetate containing 0.20 M sodium chloride, pH 4.5. Activated 40 kDa branched polyethylene glycol (NOF Sunbright GL2-400AL3, NOF Corporation, Tokyo, Japan) was added at a 2:1 PEG:protein molar ratio to 50 mL insulin solution. Sodium cyanoborohydride, from a 1.0 M stock in ddH_2O, was added to the reaction mixture, to a final concentration of 3 mM, and the reaction left for 20-40 hours in the dark. The reaction mixture was then dialysed (Spectra, MWCO 5,000) against 20 mM sodium acetate, pH 4.0, and subsequently diluted 3-fold following buffer exchange. Cation exchange chromatography was used to purify the reaction mixture: ~ 1 mg ^{40K}PEG-insulin (3 mL of reaction mixture) was loaded on a 5 mL SP Hitrap HP column (GE Healthcare, Amersham), that had been equilibrated in 20 mM sodium acetate (pH 4.0), at a rate of 0.1 mL/min. The column was then washed with 3 column volumes of 20 mM sodium acetate at 1 mL/min. ^{40K}PEG-insulin was eluted using a 0.00 – 0.25 M sodium chloride linear gradient over 30 minutes, during which 1 mL fractions were collected. The bicinchoninic acid (BCA) assay (Fisher Scientific, Loughborough, UK) was used to determine the protein concentration of the purified ^{40K}PEG-insulin. Matrix assisted laser desorption ionisation time-of-flight mass spectrometry (MALDI-ToF-MS) was used to determine the MW of purified ^{40K}PEG-insulin.

^{40K}PEG-insulin was diluted in 0.1% trifluoroacetic acid (TFA) and mixed 1:8 v/v with sinapinic acid (LaserBio-Labs, Sophia-Antipolis, France), that had been dissolved in 50% acetonitrile/0.05% TFA (v/v), and then spotted onto the MALDI target plate. Molecular weight (MW) determination was performed using a Voyager DE Pro (Applied Biosystems, Foster City, CA)) in linear positive ion mode using bovine serum albumin (BSA) to calibrate.

2.2.2 28 Day Disposition Study

All experiments were performed in accordance with criteria outlined in a license granted under the Animals (Scientific Procedures) Act 1986. Male Wistar rats were intravenously administered ^{40K}PEG-insulin (4 mg/kg, dosing volume: 4 mL/kg) by continuous infusion over 15 minutes. Animals were maintained in metabolism cages for collection of urine and faeces and divided into two cohorts; the first cohort housed from days 0 – 14 and the second from days 14 – 28. Blood samples were taken by venopuncture of the tail vein on days 1, 3, 7 and 14 for the first cohort and on days 7, 14, 21 and 28 for the second. Liver and kidneys were harvested on days 14 and 28 and snap frozen in liquid nitrogen.

2.2.3 Dialysis of Urine Samples

Urine samples were dialysed (Spectra, MWCO 12-14,000), to remove salt content, against 0.1% NaCl for 2 hours at room temperature, 0.01% sodium chloride overnight at 4^{o}C, and then against ddH_2O for 2 hours at room temperature.

2.2.4 Deproteination of Plasma and Urine Samples

Acetone precipitation was used to remove protein content from plasma samples and from urine samples also; following their dialysis. Ice-cold acetone was added at a ratio of 4:1 (v/v) to 10 µL plasma samples and to 100 – 300 µL urine samples. Samples were kept

on ice for 10 minutes prior to centrifugation at 3,000 rpm for 10 minutes. Supernatants were removed and subsequently dried to complete dryness via vacuum centrifugation.

2.2.5 SDS-PAGE

Immediately before loading, dried samples were reconstituted in ddH_20 and Laemmli sample buffer (0.1 M tris-hydrochloride, 3.0% SDS, 15% glycerol, 0.2% bromophenol blue and 5% β-mercaptoethanol) and boiled for 10 minutes at 100^oC. Samples were allowed to cool and then separated by 12% SDS-PAGE using a Hoefer SE250 mini-gel system. Gels were run at 4^oC and a current of 40 mA/gel for 35 minutes. Following electrophoresis, gels were either transferred to nitrocellulose membrane or stained for PEG directly by the BaI_2 colorimetric stain.

2.2.6 BaI_2 Colorimetric Stain

Following electrophoresis, gels were rinsed in ddH_20 and then placed in 20 mL 5.0% glutaraldehyde solution for 30 minutes with gentle agitation, at room temperature. Glutaraldehyde solution was then replaced with 20 mL 0.1 M perchloric acid for a further 30 minutes. 5 mL 5.0% barium chloride solution was then added slowly, still with gentle agitation, and after ~2 minutes 2 mL 0.1 M iodine solution was added. After several minutes bands can be visualised and gels de-stained with ddH_2O prior to scanning (GS800 with Quantity One Software). Densitometry was performed using TotalLab 1-D Gel Analysis Software.

2.2.7 Western Blotting

Following electrophoresis, gels were transferred to nitrocellulose membrane at 300V and 250 mA for 1 hour at 4^oC. Blots were blocked in 5% non-fat milk (BioRad, Hertfordshire, UK) in TST (0.1% Tween, 20 mM tris-HCl, 150 mM NaCl, pH 8) with gentle

agitation at room temperature for up to 1 hour and then kept overnight at 4°C. Blots were returned to room temperature prior to incubation with primary antibodies for either PEG (rabbit anti-PEG IgG polyclonal serum antibody, 1:3000 dilution in 5% non-fat milk in TST, generated in-house (Pfizer, Sandwich, UK)) or insulin (guinea pig polyclonal IgG to insulin, 1:1000 dilution in 5% non-fat milk in TST (Abcam, ab7842)), both for 2 hours at room temperature with gentle agitation. After four 5 minute washes in TST, blots were incubated with corresponding secondary antibodies to PEG (goat anti-rabbit conjugated with horse radish peroxidise, 1:3000 dilution in 5% non-fat milk in TST (Dako, P0448, Cambridge, UK) or insulin (rabbit anti-guinea pig IgG conjugated with horse radish peroxidise, 1:3000 dilution in 5% non-fat milk in TST (Abcam, ab6771)), both for 1 hour at room temperature with gentle agitation. Blots were washed again (4 x 5 minute washes) and specific bands visualised by ECL detection (Perkin Elmer).

2.2.8 ^{40K}PEG-insulin Recovery Following Dialysis and Deproteination

A concentration range of ^{40K}PEG-insulin was spiked into ddH_20, control rat plasma or control rat urine. Urine and plasma samples were prepared for gel electrophoresis as described in sections 2.2.3 and 2.2.4. Samples in ddH_20 were untreated. All samples were separated by SDS-PAGE (2.2.5) and the resulting bands following BaI_2 colorimetric staining (2.2.6) were analysed by densitometry. The ratio of band volume between un-extracted (ddH_20 samples) and extracted (plasma and urine samples) ^{40K}PEG-insulin was used as a correction factor for pharmacokinetic (PK) analysis of urine and plasma obtained during the course of the 28 day disposition study.

2.2.9 ^{40K}PEG-insulin Integrity in Control Rat Plasma

A concentration range of ^{40K}PEG-insulin was spiked into control rat plasma and incubated at 37°C. Aliquots were taken at t = 0, 24, 48, 72 and 168 hours. Samples were

prepared for electrophoresis as described in section 2.2.4 and analysed by SDS-PAGE and western blot, sections 2.2.5 and 2.2.7 respectively.

2.3 RESULTS

An analytical platform capable of measuring all components of the PEGylated conjugate was successfully developed, as shown in figure 2.1. The methods utilised in this platform were developed, optimised and validated using spiked control biological samples. Once fully characterised, the disposition, structural integrity and biological fate of ^{40K}PEG-insulin in biological tissues and fluids, from a rodent disposition model, were determined.

2.3.1 ^{40K}PEG-insulin Recovery

Preliminary work analysing PEG-spiked rat plasma revealed it was necessary to first clean up samples due to the BaI_2 stain forming unwanted complexes with plasma proteins. Abundant plasma proteins such as albumin were particularly visible. Indeed, albumin, with a MW of approximately 66 kDa, resolves at a similar MW to ^{40K}PEG-insulin (due to PEG's steric hindrance/water association - resulting in a higher-than-anticipated MW when resolved on a gel), which potentially would have complicated analysis, particularly when using the BaI_2 stain as a semi-quantitative measure of PEG disposition. Rat urine contains albumin too: indeed, rodent urine is naturally abundant in proteins due to urine-spotting (when rats and mice spot urine to scent-mark their territory). To reduce unwanted protein backgrounds both plasma and urine samples were first deproteinated by acetone precipitation. Urine samples were also dialysed, against NaCl, prior to deproteination to further aid removal of proteins below the dialysis tubing molecular weight cut-off (MWCO), and also to reduce salt content; this aspect of dialysis is, however, perhaps more applicable to ^{1}H NMR analysis of urine samples where differences in the ionic strength between

samples can result in altered chemical shifts for the same compound, as described in more detail in Chapter 3.

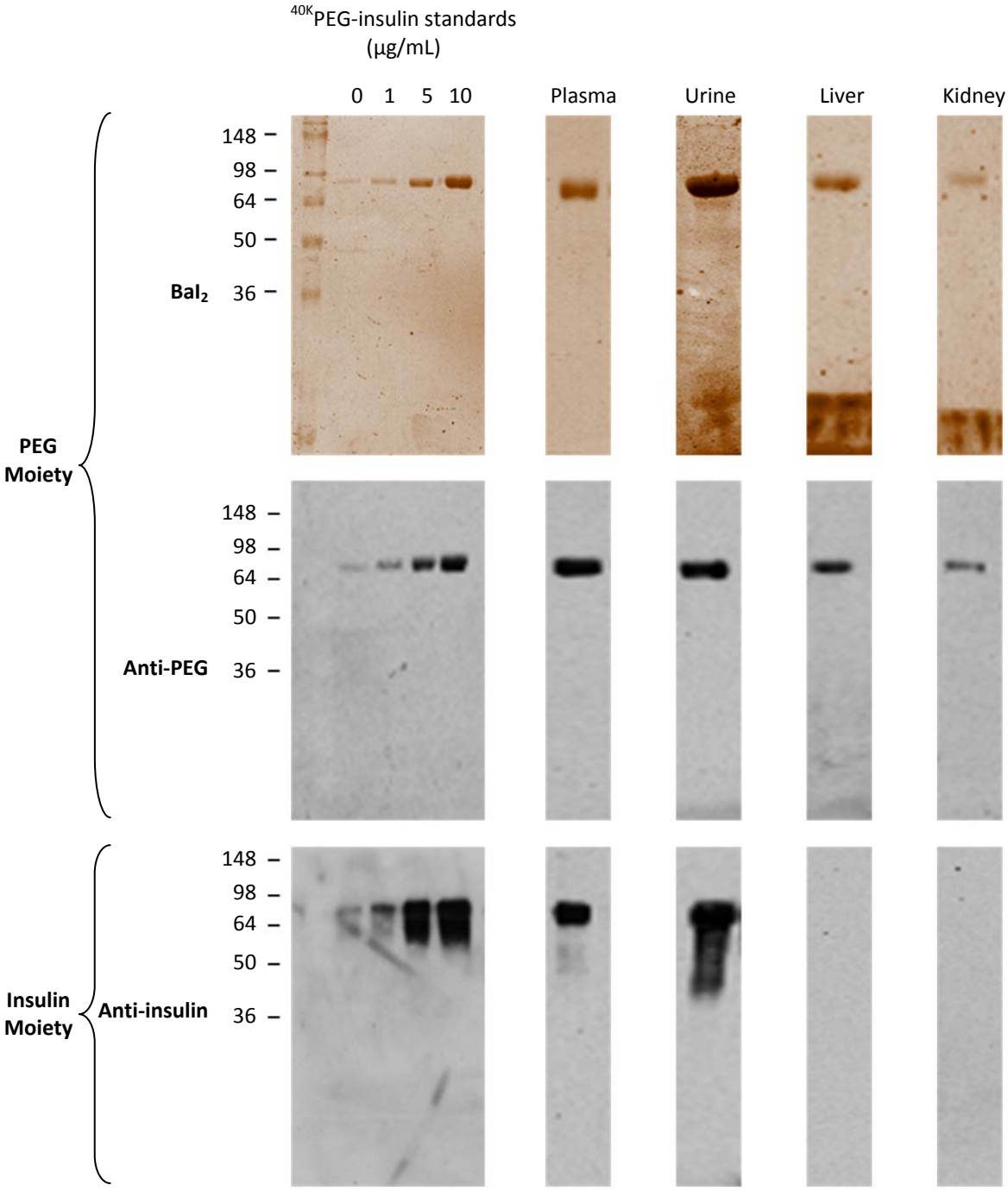

Figure 2.1: Gel-assay specificity for ^{40K}PEG-insulin

Both the PEG and protein moieties of PEGylated insulin could be simultaneously monitored by using all 3 assays, for both ^{40K}PEG-insulin standards and biological samples. Images are typical examples of each sample type and were taken from analyses of samples from the 28 day disposition study. No insulin bands were detected in the anti-insulin western blots of liver and kidney tissue in any sample on the days (14 and 28 post-dose) analysed, which is

likely due to complete metabolic cleavage of the conjugate and/or degradation of the insulin whilst still attached to PEG.

Both of these processes were shown to remove background protein content, selectively leaving only the PEG signal visible following BaI_2 staining (data not shown). However, following sample processing it was apparent that loss of ^{40K}PEG-insulin signal was occurring in processed samples in comparison to their equivalent unprocessed counterparts. Subsequently, control recovery experiments were performed to correct for loss of ^{40K}PEG-insulin signal following sample processing. In relation to unprocessed spiked samples, signal loss of ^{40K}PEG-insulin, in both processed urine and plasma samples, was shown to be highly consistent across a range of ^{40K}PEG-insulin concentrations; as seen in figures 2.2 (urine correction) and 2.3 (plasma correction). For urine samples, the average recovery was determined to be 45.6%, whilst for plasma samples the average recovery was 43.9%. Subsequently, all quantitative data generated from urine or plasma, either through the BaI_2 stain, western blot or ^{1}H NMR, were corrected accordingly to account for the signal loss that occurred during sample preparation.

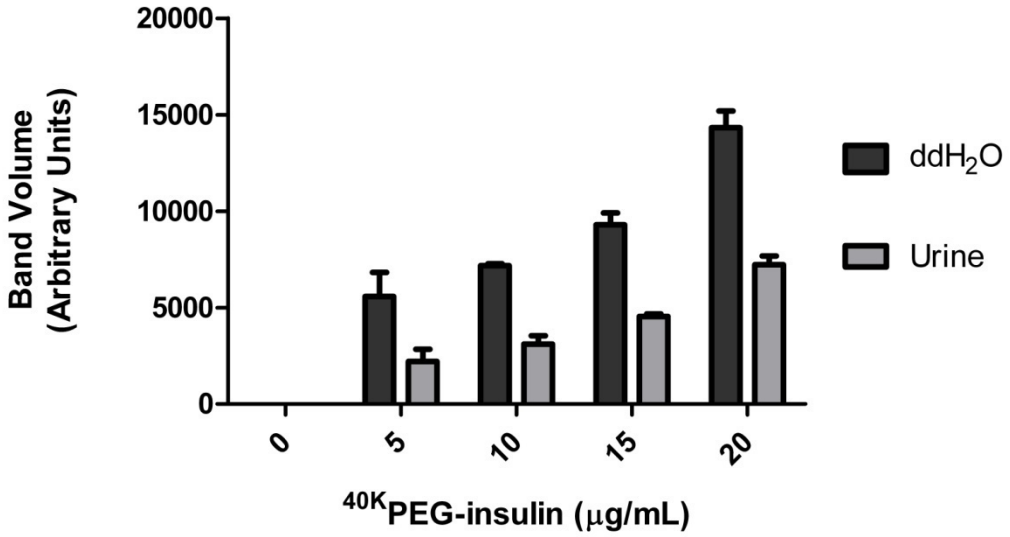

Figure 2.2: Signal loss of ^{40K}PEG-insulin in control urine following sample processing

^{40K}PEG-insulin was spiked into ddH_2O and control rat urine. Urine samples were processed as described and analysed by the BaI_2 stain followed by densitometry. Data are presented as n=4 ± SEM.

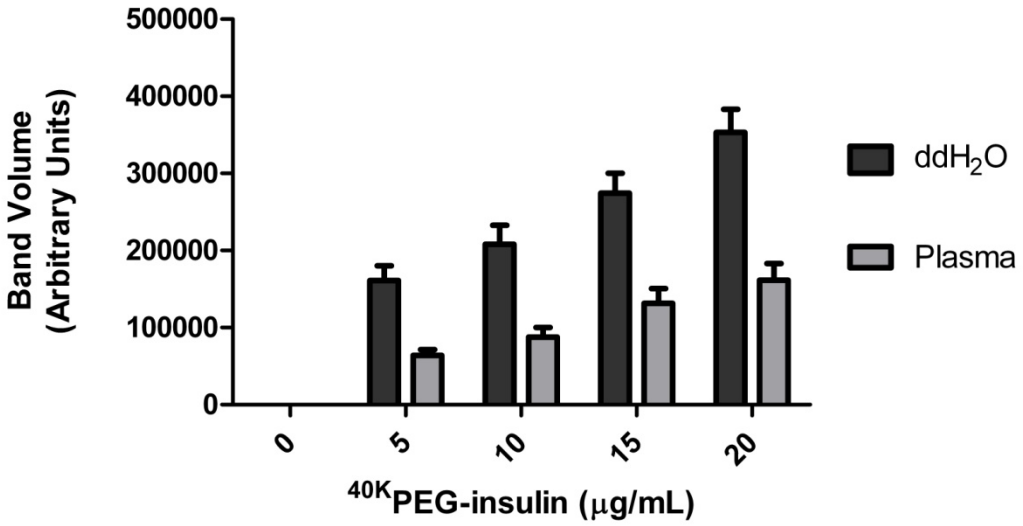

Figure 2.3: Signal loss of ^{40K}PEG-insulin in control rat plasma following sample processing

^{40K}PEG-insulin was spiked into ddH_2O and control rat plasma. Plasma samples were processed as described and analysed by the BaI_2 stain followed by densitometry. Data are presented as n=4 ± SEM.

2.3.2 28 Day Disposition Study

2.3.2.1 Plasma Concentration of ^{40K}PEG-insulin

Analysis of plasma samples across the 28 day study by the BaI_2 stain and western blot, for both PEG and insulin, initially revealed that ^{40K}PEG-insulin was present intact in the plasma for all 7 animals until approximately day 7; specific PEG and insulin bands, resolving at the corresponding MW of ^{40K}PEG-insulin, were detected by all three assays (figure 2.4). After day 7, however, insulin was only detected on day 14 for one animal (rat 7) and not at all on days 21 and 28 for any animal. Whereas PEG was detected by both the BaI_2 stain and anti-PEG western blot in all time-points analysed, up to and including day 28, and in all animals. Taken together, these data indicate that the insulin moiety of the conjugate is

either metabolically cleaved or progressively degraded to the extent that after days 7 – 14 only a PEG moiety remains in the circulation, which is no longer recognised as intact ^{40K}PEG-insulin. The highest plasma concentration of ^{40K}PEG-insulin appeared to be on day 1, with

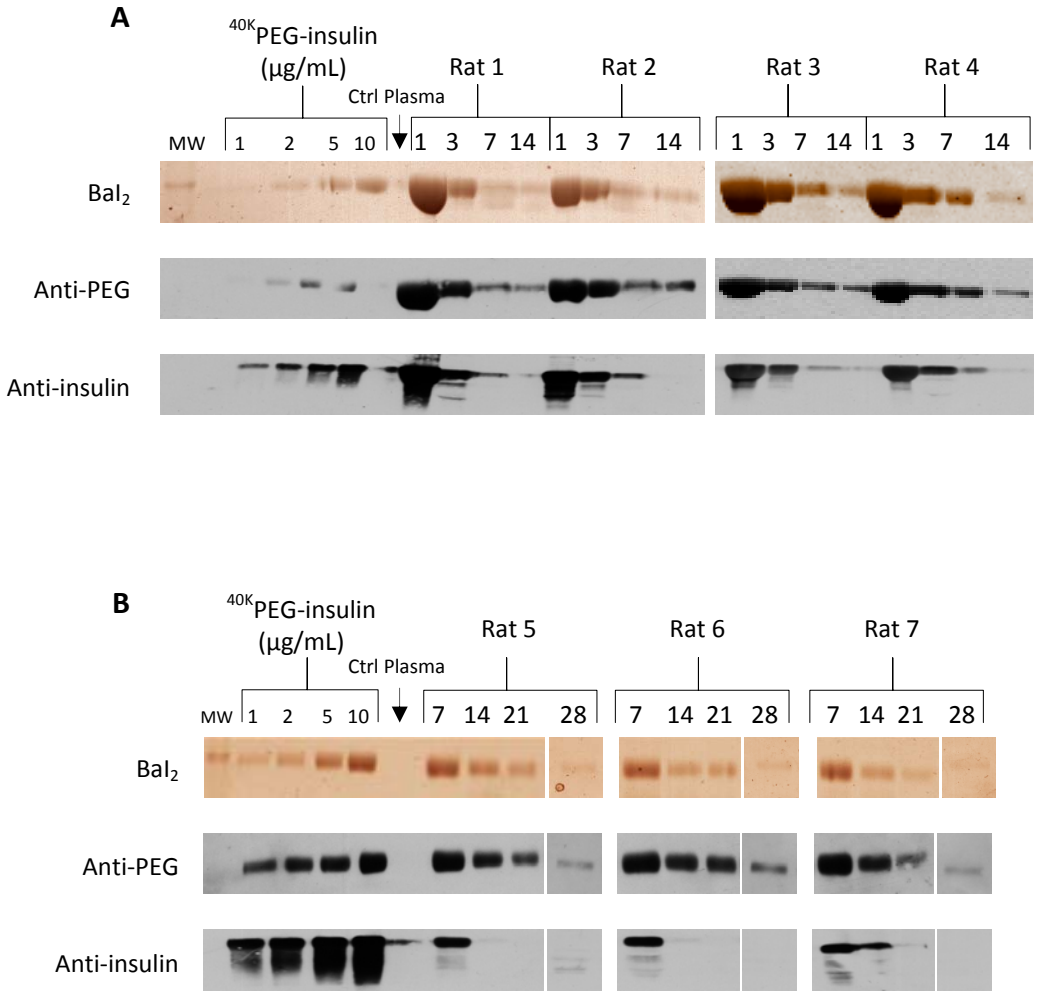

Figure 2.4: Analysis of plasma samples from the 28 day disposition study

Plasma samples from the 28 day disposition study were processed as described and analysed by the Bal_2 stain and western blots probed for both PEG and insulin. A) Days 1 – 14 for rats 1 – 4. B) Days 7 – 28 for rats 5 – 7.

the signal intensity for both PEG and insulin bands decreasing over the 28 days; albeit the insulin signal disappears entirely whilst PEG persists throughout the time-course. This is reflected in the mean plasma concentrations, derived from densitometry performed on the

anti-PEG western blots, presented in table 2.1; with the highest concentration of ^{40K}PEG-insulin found to be 131.3 µg/mL on day 1, which decreases to 2.7 µg/mL by day 28, although this concentration is likely to be reflective of just a PEG moiety, no longer

Day	Rat 1	Rat 2	Rat 3	Rat 4	Rat 5	Rat 6	Rat 7	Mean Plasma Concentration (µg/mL)
1	125.1	139.4	112.3	148.4				131.3 ± 15.9
3	25.1	36.3	37.4	47.0				36.4 ± 9.0
7	11.5	17.8	20.6	29.9	16.8	18.4	20.0	19.2 ± 5.6
14	4.3	5.9	17.2	12.3	5.6	7.3	8.6	8.8 ± 4.5
21					1.9	4.7	1.5	2.7 ± 1.8
28					1.8	4.2	2.1	2.7 ± 1.3

Table 2.1: Plasma concentration of ^{40K}PEG-insulin (µg/mL)

Densitometry of the anti-PEG western blots was performed on the plasma samples from the 28 day disposition study. Data are presented as n=3 ± SD.

conjugated to insulin, remaining in the circulation; based on the evidence provided by the anti-insulin western blots. The mean concentration after infusion at t = 0 was determined to be 228.8 µg/mL. The $t_{½}$ of ^{40K}PEG-insulin was calculated to be 131 hours.

2.3.2.2 Excretion of ^{40K}PEG-insulin in Urine

Urine samples analysed by the BaI_2 stain and anti-PEG western blot revealed that PEG was continually excreted in urine over the 28 day period by all 7 rats (figures 2.5 and 2.6, BaI_2 and anti-PEG data). However, in combination with analysis by anti-insulin western blot, it was found that after approximately day 7 ^{40K}PEG-insulin was no longer excreted as an intact conjugate, as was also observed in the analysis of the plasma samples. The insulin signal can be seen to continually reduce over the first 7 days in urine from rats 1, 2, 3 and 4 (figure 2.5, anti-insulin data), but by days 13 and 14 insulin could no longer be detected in the urine from these rats at all, as observed in figure 2.6 A (anti-insulin data). Accordingly,

no insulin signal in the urine collected on days 17, 21, 24 and 28 was detected at all for the second cohort of rats, rats 5, 6 and 7, (figure 2.6 B, anti-insulin data). Taken together, these data again indicate that the insulin moiety is either metabolically cleaved from PEG entirely

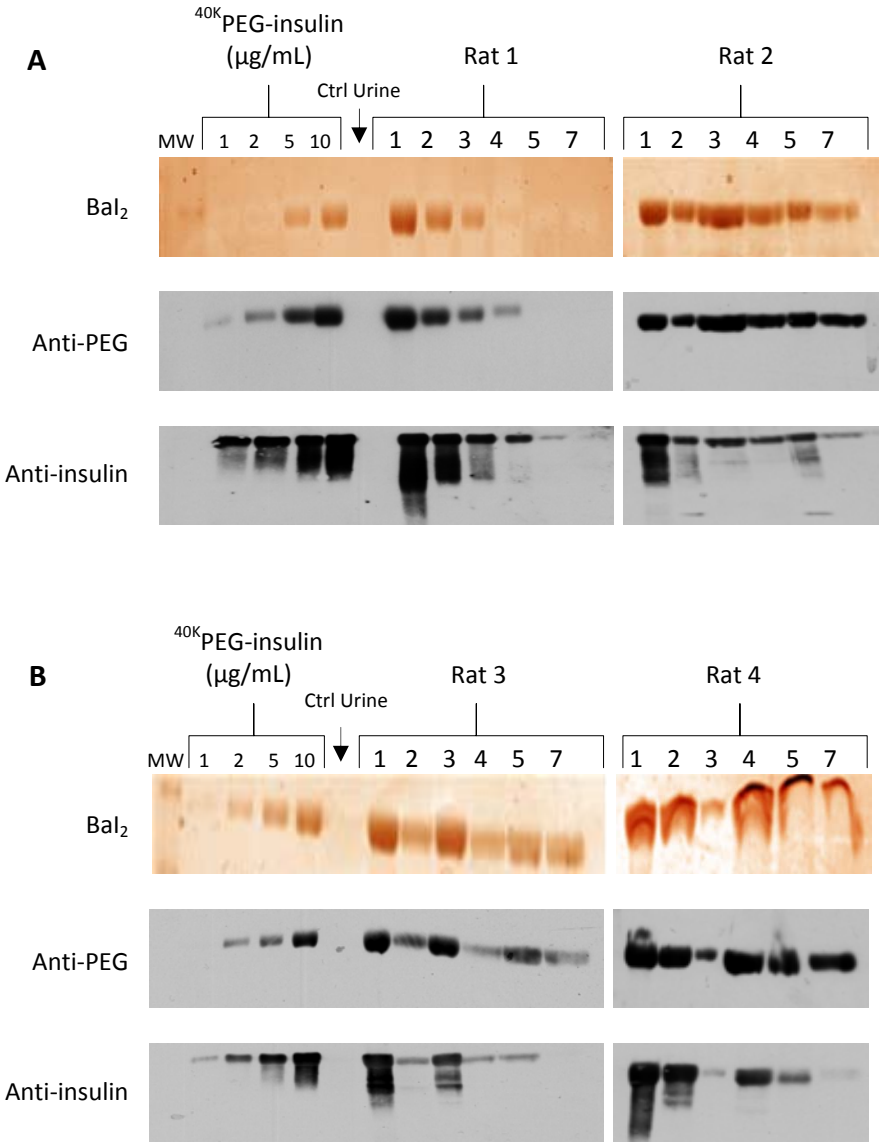

Figure 2.5: Analysis of urine samples from the 28 day disposition study (Days 1 – 7)

Urine samples from the 28 day disposition study were processed as described and analysed by the BaI_2 stain and western blots probed for both PEG and insulin. A) Days 1 – 7 for rats 1 and 2. B) Days 1 – 7 for rats 3 and 4.

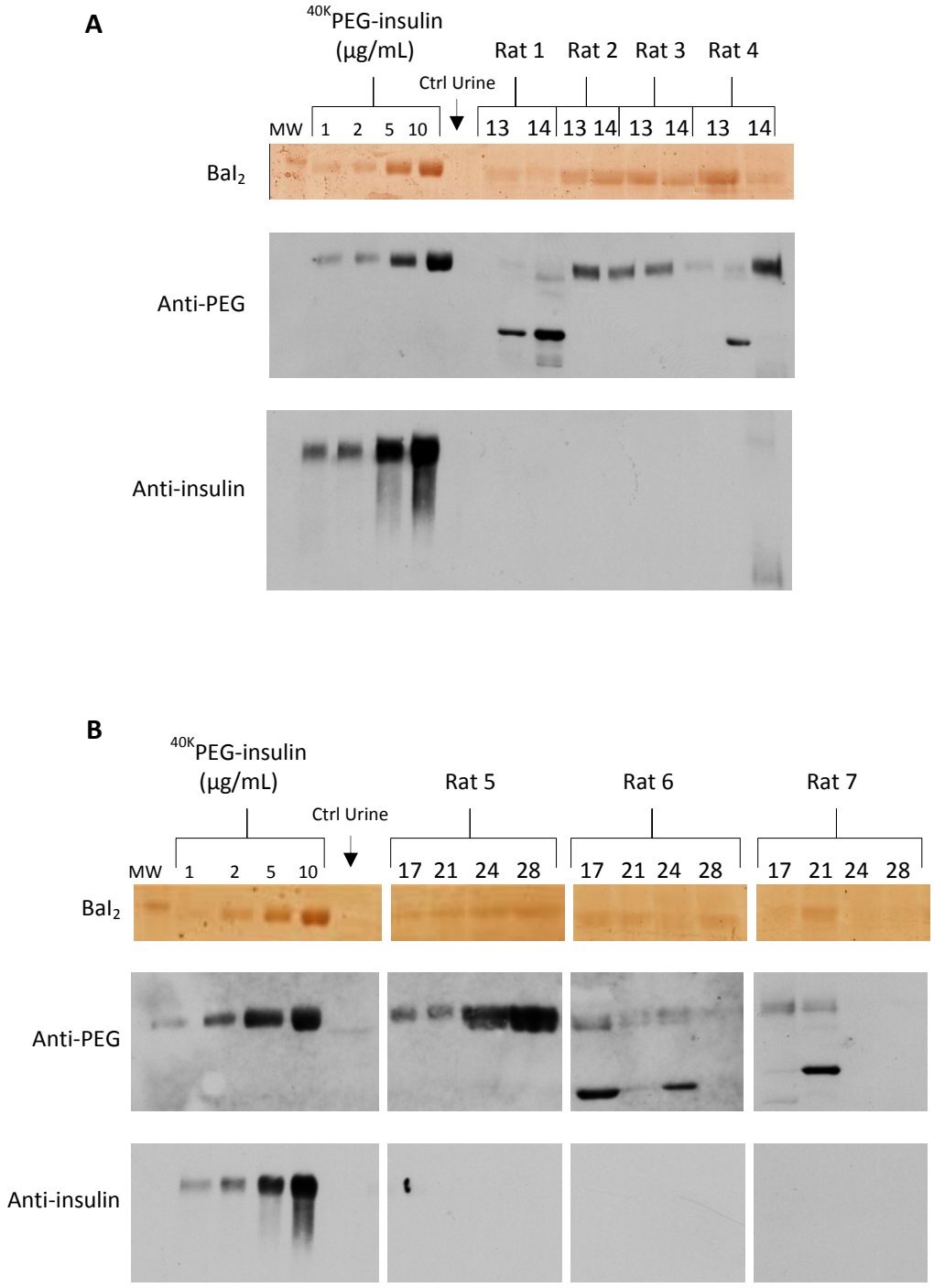

Figure 2.6: Analysis of urine samples from the 28 day disposition study (Days 17 – 28)

Urine samples from the 28 day disposition study were processed as described and analysed by the BaI_2 stain and western blots probed for both PEG and insulin. A) Days 13 and 14 for rats 1 – 4. B) Days 17 – 28 for rats 5 – 7.

or is incrementally degraded; to the extent that after day 7 only the remaining PEG moiety is excreted in the urine. Interestingly, in figure 2.6 A and B (anti-PEG data) on days 13 and 14 for rat 1, day 13 for rat 4, days 17 and 24 for rat 6 and day 21 for rat 7, a second PEG moiety, of lower MW, was observed. It was determined from the MW markers that the difference in MW between the two PEG moieties was 20 kDa; the lower MW moiety may, therefore, be due to loss of one of the 20 kDa PEG chains *in vivo*, as the activated PEG used to synthesise ^{40K}PEG-insulin was branched; consisting of two 20 kDa PEG chains.

The total amount of PEG excreted in the urine for each time-point analysed was determined from densitometry of the anti-PEG western blots, and is presented in table 2.2. In general, the total amount of PEG excreted reduced over time, although there were minimal increases on days 17 and 28 (mean PEG excreted). The cumulative total amount of PEG excreted for each rat, and the corresponding percentage of the dose this value represented, were determined; since urine could not be collected daily over the entire 28 day study, it is not possible to determine the absolute total amount of PEG excreted in the urine. However, it is clear that the majority of the dose is excreted in the first two weeks. Indeed, of the days analysed in the first two weeks (from rats 1 – 4) the mean total amount of PEG excreted was 608.4 µg, which represents 44.9% of the dose; whereas in the days analysed in the last two weeks (from rats 5 – 7) the average total amount of PEG excreted was only 11.8 µg, which represents just 0.9% of the dose.

Day	Rat 1 (µg)	Rat 2 (µg)	Rat 3 (µg)	Rat 4 (µg)	Rat 5 (µg)	Rat 6 (µg)	Rat 7 (µg)	Mean PEG excreted (µg)
1	453.8	323.1	202.5	316.7				324.01 ± 102.8
2	165.8	163.6	105.3	196.3				157.8 ± 38.0
3	50.2	36.0	89.1	41.7				54.2 ± 23.9
4	21.9	29.6	9.0	52.4				28.2 ± 18.2
5	n.d.	27.6	21.9	19.5				23.0 ± 4.2
7	n.d.	30.3	7.0	27.9				21.7 ± 12.8
13	9.0	12.3	3.5	3.3				7.0 ± 4.4
14	9.7	1.3	0.2	2.9				3.5 ± 4.2
17					5.9	3.3	5.0	4.8 ± 1.3
21					3.3	n.d.	3.1	3.2 ± 0.2
24					3.5	0.2	2.2	2.0 ± 1.7
28					7.9	0.9	n.d.	4.4 ± 5.0
Total excreted	710.4	623.8	438.5	660.7	20.6	4.4	10.3	
% of dose	52.4	46.0	32.3	48.7	1.5	0.3	0.8	

Table 2.2: Total amount of PEG (µg) excreted in the urine

Densitometry of the anti-PEG western blots was performed on the urine samples from the 28 day disposition study. Data are presented as n=3 ± SD; n.d. = not determined.

2.3.2.3 Accumulation of ^{40K}PEG in Liver

To assess the amount of ^{40K}PEG-insulin, if any, remaining in the livers of each rat, homogenates were generated from livers collected on either day 14 (rats 1 – 4) or day 28 (rats 5 – 7), prepared for gel electrophoresis and analysed by the BaI_2 stain and western blot; using both anti-PEG and anti-insulin antibodies. As was found in plasma and urine samples, a PEG moiety was detected on days 14 and 28 by both the BaI_2 stain and anti-PEG

western blot. However, bands on the anti-insulin western blot were not detected; indicating that a PEG moiety, that was no longer intact ^{40K}PEG-insulin, was accumulating in the liver tissue of each rat; as observed in figure 2.7. The percentage of the dose remaining in the liver was variable between animals, but in general on day 28 proportionately more PEG material had accumulated in

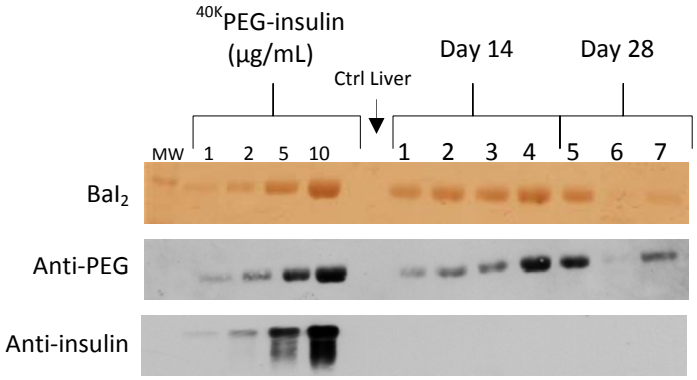

Figure 2.7: Accumulation of ^{40K}PEG in the liver

Liver tissue samples from days 14 (rats 1 – 4) and 28 (rats 5 – 7) were prepared for gel electrophoresis and analysed by the BaI_2 stain and western blots probed for both PEG and insulin.

the liver; approximately 30.78% of the dose was found to remain in the livers on day 28 compared to only 25.25% of the dose remaining on day 14 (table 2.3).

2.3.2.4 Accumulation of ^{40K}PEG in Kidney

The amount of ^{40K}PEG-insulin residing in the kidneys of the animals was also assessed in the same manner as the liver samples; kidney tissue was homogenised, prepared for gel electrophoresis and analysed by the BaI_2 stain and western blotting. Again, in kidneys harvested both on days 14 and 28 a PEG moiety was detected by both the BaI_2 stain and anti-PEG western blot. However, bands were not detected on the anti-insulin western blot; indicating that the PEG moiety accumulating in the kidneys of each rat is no longer intact ^{40K}PEG-insulin, as shown in figure 2.8. Again, more PEG material had

accumulated by day 28 in comparison to day 14, with 33.23% of the dose persisting in the kidneys on day 28 compared to 26.95% on day 14, as was also observed with the liver samples (table 2.3).

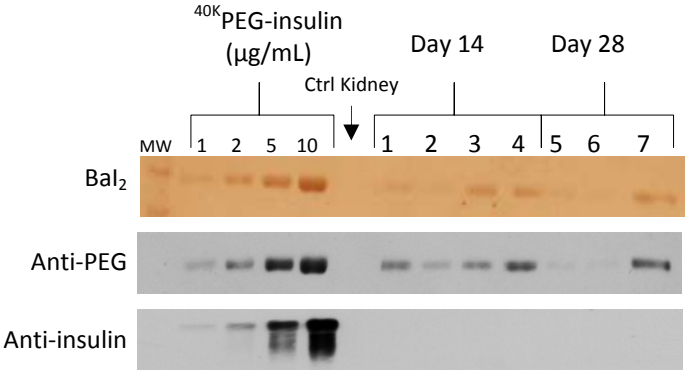

Figure 2.8: Accumulation of ^{40K}PEG in the kidneys

Kidney tissue samples from days 14 (rats 1 – 4) and 28 (rats 5 – 7) were prepared for gel electrophoresis and analysed by the BaI_2 stain and western blots probed for both PEG and insulin.

Rat	Day	Amount of PEG in whole Liver (µg)	% Dose Remaining in whole Liver	Amount of PEG in both Kidneys (µg)	% Dose Remaining in both Kidneys	Total amount of PEG in both Organs (µg)	% Dose Remaining in both Organs
1	14	129.47	9.35	35.94	2.60	165.41	11.95
2	14	231.30	17.58	1.59	0.12	232.89	17.70
3	14	276.67	21.15	12.10	0.93	288.77	22.08
4	14	696.31	52.91	41.64	3.16	737.95	56.07
	Mean	**333.44**	**25.25**	**22.82**	**1.70**	**356.26**	**26.95**
	SD	**249.62**	**19.09**	**19.08**	**1.42**	**259.41**	**19.85**
5	28	725.16	53.48	n.d.	n.d.	725.16	53.48

6	28	11.95	0.88	100.22	7.35	112.17	8.23
7	28	515.12	37.99	n.d.	n.d.	515.12	37.99
	Mean	**417.41**	**30.78**	**100.22**	**7.35**	**450.82**	**33.23**
	SD	**366.51**	**27.03**	**n.d.**	**n.d.**	**311.51**	**23.00**

Table 2.3: Total PEG content (µg) accumulating in liver and kidney tissue

Densitometry of the anti-PEG western blots was performed on liver and kidney samples from both days 14 and 28 for all 7 rats. Data are presented as n=3; n.d. = not determined.

2.3.3 ^{40K}PEG-insulin Integrity in Control Rat Plasma

The loss of insulin signal relatively early in urine and plasma samples, whilst the PEG moiety persisted for the full 28 days, combined with the fact no insulin signal was observed at all on days 14 and 28 in liver and kidney tissue raised the question of exactly where the proteolytic degradation of the insulin moiety was occurring. One possibility is that it occurs in the circulation, through the action of plasma proteases, or following cellular internalisation, potentially through the lysosomal and proteasomal pathways of protein processing. If degradation occurs intracellularly, it is possible that the liberated protein may be processed into peptides suitable for MHC binding and subsequent T cell recognition. Furthermore, cleavage of the therapeutic protein moiety from PEG may alter the intracellular disposition of the protein – potentially reducing its efficacy; a result which could be further exacerbated by the loss of protection imparted by PEG. To begin resolving this question the *in vitro* stability of ^{40K}PEG-insulin, spiked into control rat plasma, was assessed over a period of 7 days: 7 days being the time post-dose at which the majority of insulin signal had been lost *in vivo.* Furthermore, a concentration range of 3, 10 and 30 µg/mL ^{40K}PEG-insulin was used as these closely represented the *in vivo* levels observed in the animal samples after day 1. The stability of insulin and overall conjugate integrity was tracked using western blot for both PEG and insulin, as observed in figure 2.9 (30 µg/mL ^{40K}PEG-insulin data only). From figure 2.9 the densitometry reveals there is no significant

change in either the level of PEG or insulin over 7 days; indicating that the *in vivo* insulin signal loss observed is likely to be a consequence of ^{40K}PEG-insulin cellular internalisation and subsequent degradation, rather than degradation in the circulation.

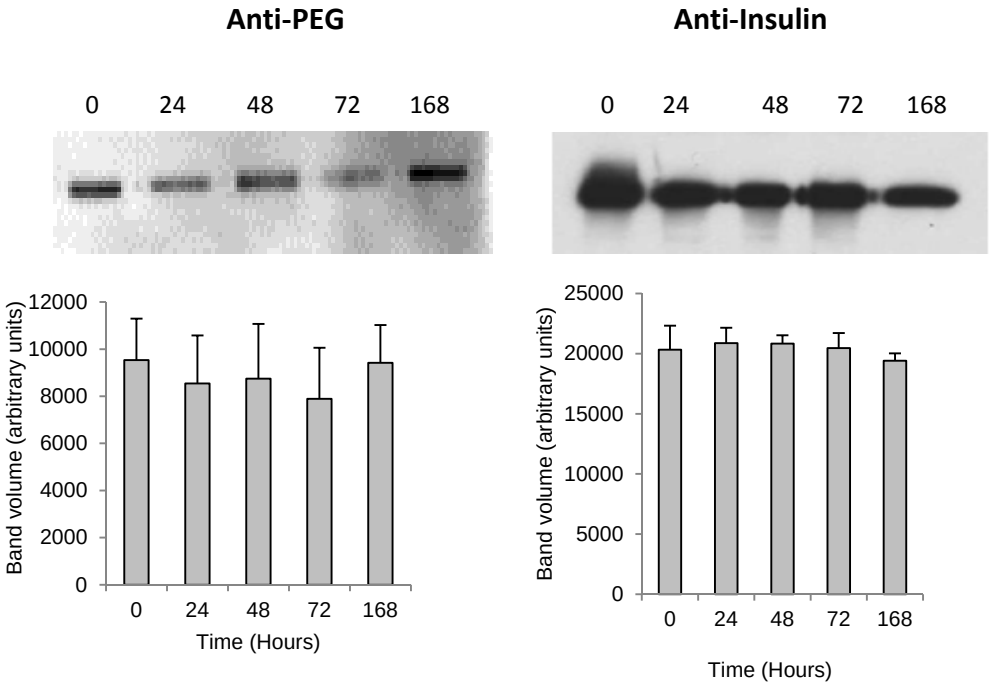

Figure 2.9: Stability of ^{40K}PEG-insulin in control rat plasma *in vitro*

^{40K}PEG-insulin (30 µg/mL) was spiked into control rat plasma and incubated for up to 168 hours at 37^{o}C. Aliquots were taken at the stated times, prepared for gel electrophoresis and analysed by either anti-PEG or anti-insulin western blotting. Data are presented as n=4 ± SEM (anti-PEG densitometry) and n=5 ± SEM (anti-insulin densitometry), with a representative western blot above each graph.

2.4 DISCUSSION

A gel-based analytical platform was developed to assess both the PEG and protein moieties of ^{40K}PEG-insulin *in vivo;* enabling the disposition, biological fate and pharmacokinetics of the conjugate to be determined in a rodent model. In combination, the use of three different assays allowed the structural integrity of the conjugate to be assessed over the 28 day study, as each assay is specific for different components of the conjugate. The BaI_2 stain and anti-PEG assays monitor PEG, whilst the anti-insulin assay is selective for insulin, together providing comprehensive, independent analysis of each moiety. Furthermore, the anti-PEG antibodies were shown to be much more sensitive for PEGylated protein, rather than PEG alone, indicating that the antibodies must also recognise the linker used to couple PEG to insulin. Consequently, using all three assays, it was possible to ascertain when 1) insulin had been metabolically cleaved entirely from PEG, or sequentially degraded to the extent the antibodies were no longer capable of recognising it as intact insulin (anti-insulin assay), 2) a PEG moiety still containing the linker was present in the samples (anti-PEG assay/BaI_2 stain), and 3) PEG, in any form, was still present in the samples (BaI_2 stain). The specificity of each assay is represented graphically in figure 2.10.

Sample clean up via deproteination and dialysis of control urine and plasma samples was necessary to produce gels suitable for densitometric analysis. Both of these

sample preparation methods were shown to be highly reproducible in removing abundant plasma and urinary proteins, and resulted in the formation of bands containing PEG or PEG-insulin only, following staining. PEG-insulin signal loss was also shown to be highly reproducible following sample preparation: results from a signal loss study, incorporating a range of different ^{40K}PEG-insulin concentrations, allowed the average recovery following preparation to be determined, thus providing a reliable measure to correct for signal loss in *in vivo* biological samples. Initially, these optimised methods were used to detect ^{40K}PEG-

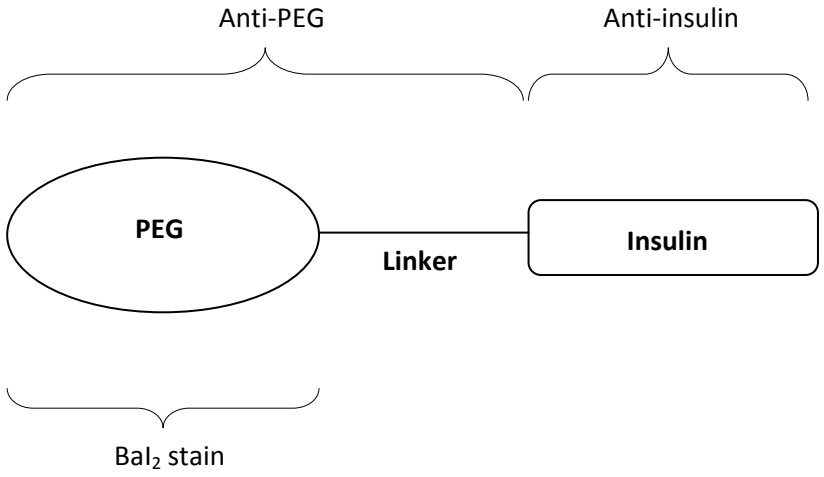

Figure 2.10: Specificity of gel-based assays

insulin in a 48 hour pilot study in rodents. However, it was found that ^{40K}PEG-insulin was cleared extremely slowly from the plasma (data not shown), and so the study was extended to 28 days. Male Wistar rats were intravenously administered a single dose of ^{40K}PEG-insulin and maintained for 28 days, during which plasma, urine, liver and kidney samples were collected. In plasma, both the BaI_2 stain and anti-PEG assay detected the PEG moiety over 28 days. However, the anti-insulin assay was only able to detect the insulin moiety until day 14. Taken together, these data indicate that cleavage of the conjugate, or sequential degradation of the insulin moiety, results in a PEG moiety circulating in the plasma after day 14, which is no longer recognised as intact ^{40K}PEG-insulin. This result was

also found when analysing the urine samples, however, the anti-insulin assay was no longer able to detect the insulin moiety after day 7. When analysing liver and kidney tissue harvested on days 14 and 28, the anti-insulin assay was unable to detect insulin in samples from any rat on either day. In contrast, both the BaI_2 stain and anti-PEG assay were able to detect the PEG moiety on both days in every sample. Taken together, these data indicate that a PEG moiety, which is no longer intact ^{40K}PEG-insulin, accumulates in liver and kidney tissue following a single dose of ^{40K}PEG-insulin. Despite the loss of insulin signal found in all samples, the coupling of PEG did have a profound effect in extending the retention time of insulin, which usually has a half-life of ~ several minutes in the circulation. Indeed, in this study, insulin was detected, as part of a conjugate, up to 14 days post-dose in the plasma. However, this should not detract from the fact that this study is the first to demonstrate that PEGylated proteins may be metabolically cleaved *in vivo.* This is in clear contrast to the well-documented rationale behind PEGylation, whereby PEG is usually coupled permanently to a protein. The loss of insulin observed in this study could be explained by dissociation of the conjugate, resulting in rapid elimination of insulin whilst the PEG moiety, in some form, persists in both biological fluids and tissues. However, the progressive degradation of insulin, whist still coupled to the PEG, is also a possibility, which cannot be discounted. Given that the conditions used for the anti-PEG assay in this study were not sensitive enough for the assay to detect native PEG alone (data not shown), but the assay was still able to detect PEG far longer after the anti-insulin assay could no longer detect the insulin moiety, it is possible that progressive proteolytic degradation may be a more likely mechanism of insulin loss than complete conjugate cleavage; since the PEG antibodies appear to predominantly recognise the linker between PEG and protein, which is presumably still linking the PEG to insulin, albeit the insulin may be being progressively degraded over time – eventually culminating in complete signal loss once all insulin epitopes have been degraded. However, the complete metabolic cleavage of PEG-insulin

cannot be discounted either, as this explanation does not preclude the possibility that complete cleavage of the conjugate results in the linker remaining intact, resulting in the PEG antibodies still being able to detect the PEG moiety, with the insulin then being rapidly eliminated or degraded. Further studies are required to elucidate the exact mechanism by which insulin signal is lost.

The site of conjugate cleavage or degradation was not apparent during analysis of samples from the 28 day disposition study. These processes could occur in the circulation, through the action of circulating protease enzymes, or following cellular internalisation of the conjugate. To address this issue, the *in vitro* stability of ^{40K}PEG-insulin in control rat plasma was assessed over a period of 7 days; 7 days being a time at which significant insulin signal had been lost *in vivo.* It was found that the insulin moiety was stable over 7 days, with no loss of insulin signal occurring. Thus, it appears that PEGylation does protect coupled proteins from degradation in the circulation, but following cellular internalisation this protective effect is either lost or diminished to the extent that the attached protein is completely cleaved or degraded, leaving only a PEG moiety.

In conclusion, the three gel-based assays were developed into an analytical platform that could be used to independently monitor both the PEG and protein components of a PEGylated protein *in vivo;* providing a measure of the structural integrity of the conjugate. The assays revealed that PEGylated proteins can be cleaved or degraded following cellular internalisation, resulting in the protective effect of PEG being lost, and the accumulation of a PEG moiety in biological tissues. Cleavage of the conjugate may also alter the intracellular disposition of the protein moiety, which may have implications for the efficacy of the therapeutic agent. These methods were used to quantify ^{40K}PEG-insulin present in the plasma and excreted in the urine, and thus were able to generate PK data; consequently, these methods could be easily translated to clinical studies were the PK profiling of a PEGylated protein in the blood and urine of patients is required.

CHAPTER 3

Disposition of PEGylated Proteins: ^{1}H NMR Analysis

CONTENTS

Disposition of PEGylated Proteins: ^{1}H NMR Analysis

3.1 INTRODUCTION

This chapter describes the development and optimisation of a ^{1}H NMR method for the detection and quantification of ^{40K}PEG-insulin in urine samples from the 28 day disposition study, as described in chapter 2. The gel-based analytical platform provides only a semi-quantitative measure of ^{40K}PEG-insulin quantification. However, for ^{1}H NMR analysis, the use of an internal standard, which can be used throughout all analyses, can provide absolute quantification of the PEG moiety. Furthermore, since the comprehensive bioanalysis of PEGylated macromolecules has previously been relatively limited, ^{1}H NMR was used to validate the data obtained using gel-based methods developed in chapter 2. ^{1}H NMR analyses the hydrogen atoms present within compounds. The repeating unit of PEG contains four hydrogen atoms and has a MW of 44 Da, therefore, for 40 kDa PEG, there are approximately 909 repeating units together containing approximately 3636 hydrogen atoms; per single 40 kDa PEG chain. As each of the hydrogen atoms present in the repeating unit of PEG are in the same chemical environment, they will, therefore, all resonate at the same chemical shift. This results in a single, strong resonance signal that is easily identifiable in a ^{1}H NMR spectrum. The use of ^{1}H NMR is consequently ideally suited to the detection and quantification of PEG. In this chapter, a method, encompassing sample preparation through to ^{1}H NMR analysis, has been optimised for the quantification of ^{40K}PEG-insulin excreted in the urine of animals from the 28 day disposition study: thus providing complementary information in combination with the gel-based analytical platform with regards to the detection and quantification of PEGylated proteins in biological fluids.

3.2 METHODS AND MATERIALS

All reagents were purchased from Sigma-Aldrich Company Ltd (Dorset, UK), unless otherwise stated.

3.2.1 Urine Samples

Urine samples were obtained during the course of the 28 day disposition study, as described in section 2.2.2.

3.2.2 Dialysis of Urine Samples

Urine samples were dialysed (Spectra, MWCO 12-14,000) against 0.1% sodium chloride for 2 hours at room temperature, 0.01% NaCl overnight at 4^{o}C and then against ddH_2O for 2 hours at room temperature.

3.2.3 Deproteination of Urine Samples

For ^{1}H NMR analysis, 1 mL of dialysed urine was deproteinated by addition of ice-cold acetone (VWR International, Leicestershire, UK) at a 1:1 (v/v) ratio. Samples were kept on ice for 10 minutes and then centrifuged for a further 10 minutes at 3,000 rpm. Supernatants were removed and depleted of H_2O by vacuum centrifugation until complete dryness. Samples prepared in ddH_2O were only depleted of H_2O by vacuum centrifugation (i.e. were not dialysed and/or deproteinated).

3.2.4 Sample Preparation

Following H_2O depletion, samples were reconstituted in 600 µL methanol-d_4 and centrifuged for 8 minutes at 13,300 rpm. Supernatants were then removed and transferred into 535-PP NMR tubes.

3.2.5 ^{1}H NMR Analysis

All ^{1}H NMR data were acquired at 300 Kelvin on a Bruker 600 MHz Avance 3, with CryoProbe, and analysed using TopSpin 2.1 software.

3.2.6 ^{1}H NMR Optimisation

For accurate and sensitive quantification of ^{40K}PEG-insulin, optimisation of the various parameters involved in producing ^{1}H NMR data is required. Once optimal conditions were defined they were used throughout for subsequent quantification of ^{40K}PEG-insulin excreted in urine across the 28 day study. The following parameters were optimised using ^{40K}PEG-insulin spiked into control rat urine and/or ddH_2O, and validated using urine samples from the 28 day disposition study.

Temperature

All samples, from either the 28 day disposition study or those used during parameter optimisation, were analysed at 300 Kelvin. All samples were allowed an equilibration period within the probe, prior to analysis, to ensure all analyses occurred at a constant temperature.

Shimming Procedure

To achieve homogeneity of the magnetic field the Z shims were first auto calibrated using the Topshim function in the TopSpin 2.1 software whilst the sample was spinning at 20 Hz. Once calibrated, spinning stopped and the X and Y shims were then manually adjusted using the interactive parameter adjustment display (GS) in combination with the Lock Display.

Receiver Gain

The receiver gain (RG) was ascertained using the *rga* command in the TopSpin 2.1 software, which automatically determines the optimum RG for a given sample.

Number of Scans

The optimal number of scans (NS) was determined using control urine samples spiked with ^{40K}PEG-insulin. It was defined as the NS after which an increased NS did not improve resolution of the PEG signal.

Relaxation Delay

The relaxation delay (D1) was determined following an inversion recovery experiment set up with variable delay times from 0.1 – 10 seconds over 12 increments.

Offset Frequency

The offset frequency was adjusted for each sample using *GS*.

90^o Pulse

The 90^o pulse length was determined for each sample using *GS*

EFP Window Function

Following acquisition, the free induction decay (FID) was processed using the *efp* command in the TopSpin 2.1 software, which combines commands for em (applies an exponential window function), ft (Fourier transforms the spectrum) and phase, which sets the phase correction.

3.2.7 Internal Standard

Nicotinamide was selected as the internal standard (IS) from which ^{40K}PEG-insulin excreted in the urine across the 28 day disposition study would be quantified.

3.2.7.1 Preparation

Nicotinamide (12.5 mM) was prepared in ddH_2O before being freeze-dried and reconstituted in D_2O (99.0%). The IS was then transferred into a stem coaxial insert.

3.2.7.2 Proton Signal Selection

A concentration range of ^{40K}PEG was analysed with the IS in triplicate. The resonance signal of PEG at ~3.65 ppm was integrated manually with all 4 proton signals from nicotinamide to generate 4 standard curves. The proton signal which resulted in the highest coefficient of determination (R^2) out of the 4 standard curves was selected as the signal used to quantify PEG content in the 28 day urine samples.

3.2.8 ^{40K}PEG-insulin Quantification in Urine Samples

All 28 day urine samples were analysed with the nicotinamide IS, coaxially inserted within the NMR tube, and ^{1}H NMR spectra were acquired with: a constant receiver gain of 32, 32 scans and a relaxation delay of 3.0 seconds. The 90^o pulse was calibrated for each individual sample and varied between 8.57 – 9.77 µs. To suppress the residual solvent peak (CD_3OH) at 4.87 ppm, from methanol-d_4, the 1H offset frequency was also individually calibrated and varied between 2919 – 2924 Hz. Following data acquisition and Fourier Transform all spectra were processed using an exponential window function (EFP)

3.2.9 Limit of Detection Determination

The limit of detection (LOD) was determined from a concentration range of ^{40K}PEG spiked into control urine, in triplicate. Relative integration was used to compare the PEG signal, for each concentration, with 3 artefact signals that were within ± 0.5 ppm of the PEG signal, and the average taken. It was defined as the point at which the area under the PEG signal became 3:1 greater than the observed artefacts. This stringent method was also

applied to the 28 day disposition study to ascertain at which timepoints the amount of ^{40K}PEG-insulin excreted in the urine could no longer be accurately detected.

3.3 RESULTS

3.3.1 ^{1}H NMR Optimisation

The signal-to-noise ratio (S/N) was used to optimise several of the parameters outlined in section 3.2.6, since this ratio is indicative of the intensity of the PEG signal in comparison to noise intensity (i.e. background). A higher S/N produces less noise interference and clearer resolution of the PEG signal – a prerequisite for accurate ^{40K}PEG-insulin quantification.

Receiver Gain and EFP Window Function

The RG and use of the EFP window function were the first parameters optimised. The *rga* command in the TopSpin 2.1 software routinely indicated a RG of 32 in both ddH_2O and control rat urine samples spiked with a concentration range of ^{40K}PEG-insulin. A RG of 32 was also routinely indicated when analysing urine samples from the 28 day disposition study. Following acquisition the ^{1}H NMR spectra obtained from ^{40K}PEG-insulin standards were processed using the EFP window function in the TopSpin 2.1 software. The *efp* function combines three commands, the *em* (which applies an exponential multiplication to the data, which improves S/N), *ft* (which Fourier transforms the data) and phase (which corrects for errors due to Fourier transform). The S/N was used to monitor the effect of increasing the RG and using EFP on the resolution of the PEG signal at each concentration of ^{40K}PEG-insulin analysed (Figure 3.1). Figure 3.1 shows the different S/N observed between the same samples analysed with a RG of either 1 or 32 and with or without processing by EFP. From figure 3.1 it can be clearly seen that the effect of EFP processing

acts to more than double the S/N for each concentration analysed, at both a RG of 1 and 32, compared to the same samples analysed without EFP. This indicates the EFP window function improves the resolution of the PEG signal and therefore should aid in accurate ^{40K}PEG-insulin quantification. The effect of increasing RG can also be observed in figure 3.1; a RG of 32 results in approximately a 10-fold increase in S/N for each concentration, in both samples processed with EFP and samples without processing, compared to the same samples analysed with a RG of 1.

The effect of EFP processing is apparent in figure 3.2, were the improved resolution of the PEG signal (1 µg/mL ^{40K}PEG-insulin in ddH_2O) following EFP processing is shown along with the same sample analysed without processing. Background interference is clearly reduced in the EFP processed data and the base of the PEG signal can be clearly defined.

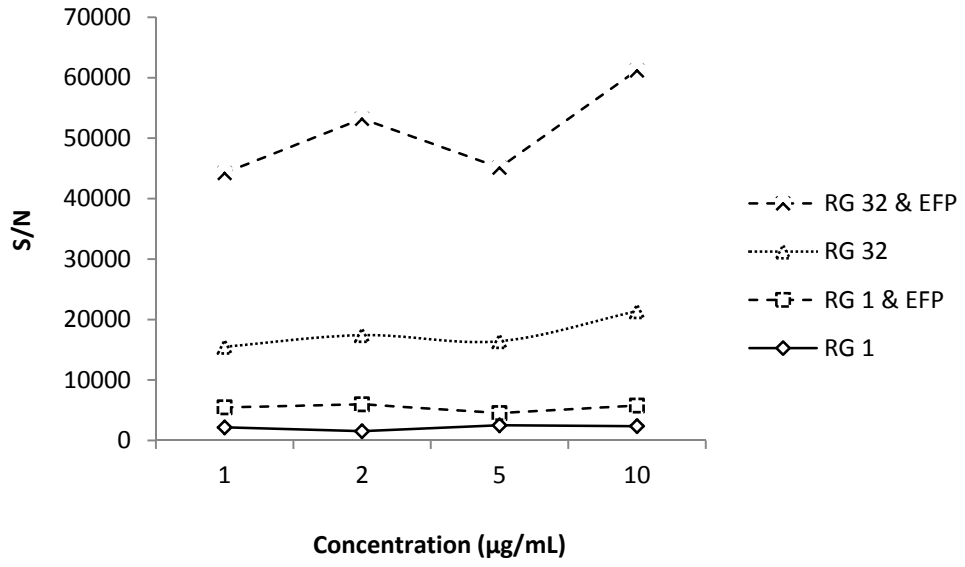

Figure 3.1: Effect of RG and EFP processing on the S/N of ^{40K}PEG-insulin standards

^{40K}PEG-insulin was spiked into control rat urine and prepared for ^{1}H NMR analysis as described. Samples were analysed with a RG of 1 and repeated with a RG of 32, S/N was calculated for both sets of data both with and without EFP processing.

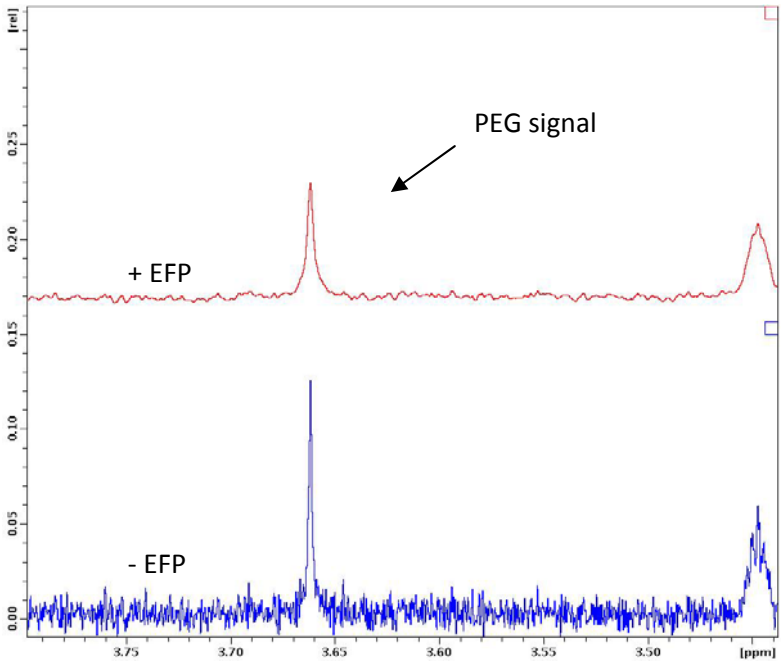

Figure 3.2: Effect of EFP processing on ^{1}H NMR spectra

^{40K}PEG-insulin (1 µg/mL) was spiked into ddH_2O and prepared for ^{1}H NMR analysis as described. The sample was analysed with (red trace) and without (blue trace) EFP processing.

This is extremely important in ensuring that quantification of the PEG signal is not artificially increased due to the presence of excess background noise and, even more crucially, from potentially un-removed urinary protein signals, which resonate in the same area of the spectrum as PEG but are hidden by excess background.

The effect of EFP processing and data acquisition with a RG of 32 was validated in urine samples from the 28 day disposition study (figure 3.3). In figure 3.3, days 1 – 7 urine samples, from rat 1, were analysed with a RG of 1 and days 13 – 24 urine samples, from rat 5, were analysed with a RG of 32, both with and without EFP processing, and the S/N for all 4 conditions determined. Again, figure 3.3 shows that the effect of EFP processing acts to approximately double the S/N for each time point analysed, at both a RG of 1 and 32. From day 13 onwards the effect of increasing RG from 1 to 32 again acts to improve the S/N approximately 10-fold for all time points with and without EFP processing. The improved S/N observed with a RG of 32 and EFP processing was particularly crucial since PEG signals

at the later time points were not detectable with a RG of 1 and without EFP processing. This result was also observed with lower concentrations of ^{40K}PEG-insulin standards analysed in control urine (data not shown). The results in figure 3.1 and 3.2 clearly highlight the requirement for optimisation to improve resolution of the PEG signal, particularly at low concentrations of PEG, which was subsequently validated in urine samples from the 28 day disposition study.

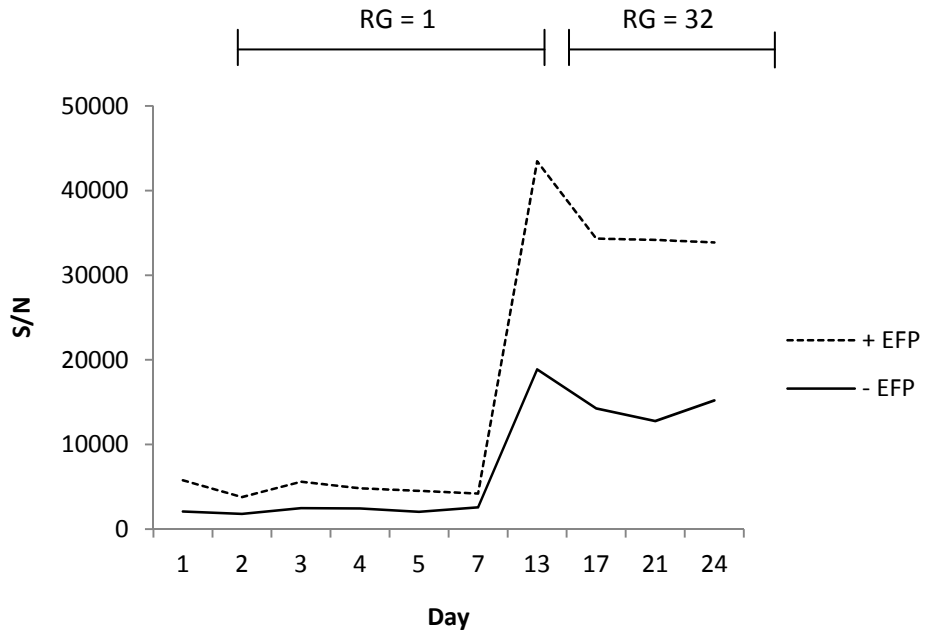

Figure 3.3: Effect of RG and EFP processing on the S/N of urine samples from the 28 day disposition study

Urine samples from rat 1 (days 1 – 7) and rat 5 (days 13 – 24) were prepared for ^{1}H NMR analysis as described. Days 1 – 7 samples were analysed with a RG of 1 and days 13 – 24 analysed with a RG of 32. All samples were analysed with and without EFP processing and the S/N calculated.

Shimming Procedure

Shimming is the process of adjusting the magnetic field within the spectrometer to attain homogeneity. The quality and resolution of spectra is dependent on field homogeneity and it is therefore vitally important to ensure the magnetic field is homogenous relative to the sample. Differences in field homogeneity may arise between samples due to concentration changes, different sample positions and the presence and

movement of un-dissolved particles. To counteract this, samples were spun in the spectrometer at 20 Hz to provide movement to the particles within the sample. Spinning helps reduce the inhomogeneity along the X and Y axes but not the Z axis, the axis about which the sample is spun. During spinning, the *Topshim* function was used to auto calibrate the shim magnets along the Z axis. Once calibrated, the sample was stopped from spinning and the X and Y shims were then manually adjusted. The *Lock Display* was used to measure improvements in shimming. The *Lock Display* shows the intensity of the lock signal resulting from the solvent peak, in this case the signal from methanol-d_4. Improved field homogeneity results in an increase in the intensity of the lock signal, which is observed in the *Lock Display*. The shimming end point occurs when the intensity of the lock signal can no longer be increased through adjustments made to the shim magnets. Poor shimming results in asymmetry and broad peak shoulders of signals in the spectrum. The *GS* was used to monitor the effects of shimming in real-time, as the *GS* allows visualisation of the spectra that would be acquired using the settings currently in place. In practice, the *GS* window display focussed on the residual solvent peak at 3.31 ppm as this peak is a pentet and thus provided a reliable visual aid, in combination with the Lock Display, of when magnetic field homogeneity had been attained.

The shimming procedure outlined above was determined in ^{40K}PEG-insulin standards, spiked intro control rat urine, and was subsequently applied to all urine samples from the 28 day disposition study. However, since analysis occurred over many days the spectrometer was often calibrated for other users' samples. Thus it was necessary each time the spectrometer was used to calibrate all the shim magnets (X, Y and Z) of the spectrometer prior to analysis of actual samples. This allowed the magnets of the spectrometer to be at the same starting position each time it was used for analysis of ^{40K}PEG-insulin standards and/or 28 day urine samples; thus allowing reproducibility in shimming procedure between analyses on different days. The shim magnets of the

spectrometer were first calibrated with 2 mM sucrose in 90% H_2O/10% D_2O (Bruker) on each day the spectrometer was used and the calibration saved as a shim file. The shim file was loaded, prior to implementing the shimming procedure outlined above, for each individual sample analysed on that particular day.

The effect of good shimming and a homogenous magnetic field can be observed in figure 3.4 (rat 2, day 4 urine sample). Figure 3.4 focuses on the PEG signal acquired without optimised shimming (blue trace) and with optimised shimming (red trace) from the same urine sample. The PEG signal in the blue trace is much broader and asymmetrical in comparison to the PEG signal in the red trace. Figure 3.4 clearly shows the benefit and utility of optimising the shimming conditions for each sample; allowing accurate and reproducible quantification of ^{40K}PEG-insulin excreted in the urine across the 28 day disposition study.

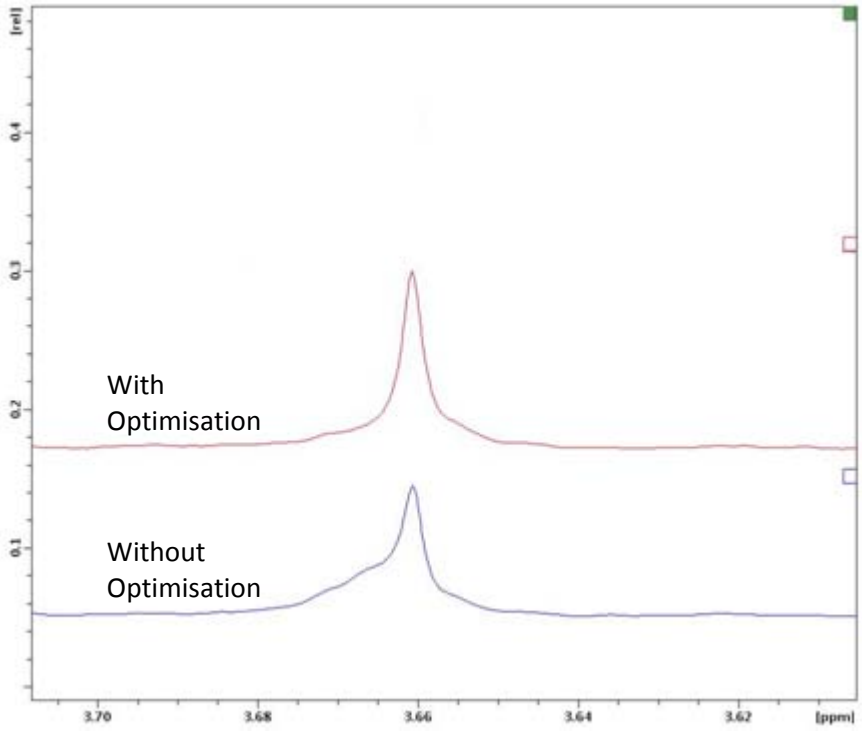

Figure 3.4: Effect of optimised shimming on PEG signal resolution

Urine from rat 2 (day 4) was prepared for ^{1}H NMR analysis as described. The sample was analysed both with the optimised shimming procedure (red trace) and without (blue trace).

Number of Scans (NS)

The NS is the number of times data acquisition for a single experiment occurs. The signals detected during each acquisition are added together (signal averaging) and contribute toward the final spectrum. An increased NS increases the magnitude of the NMR signal and improves S/N. The optimum NS was defined as the NS after which increasing the NS did not increase PEG signal resolution, i.e. the intensity of the PEG signal was not increased relative to the baseline – even if S/N was improved. The optimum NS was calculated from ^{40K}PEG-insulin standards in control rat urine and determined to be 32 scans. In figure 3.5, the spectra obtained from the same sample of ^{40K}PEG-insulin (10 µg/mL) analysed with 32 (blue trace), 128 (red trace) and 256 scans (green trace) are overlaid. Increasing the NS past 32 did improve the S/N, with ratios of 463.49, 907.15 and 1141.80 for 32, 128 and 256 scans, respectively. However, this did not relate to improved resolution and detection of the PEG signal: whilst the intensity of the PEG signal generated from 128 and 256 scans appears much greater to the signal generated from 32 scans, in relation to the overall spectrum the PEG signal was not actually enhanced at higher NS, i.e. sensitivity was not enhanced, and consequently no significant benefit would be obtained using a higher NS. Furthermore, this would have unnecessarily prolonged the overall analysis time.

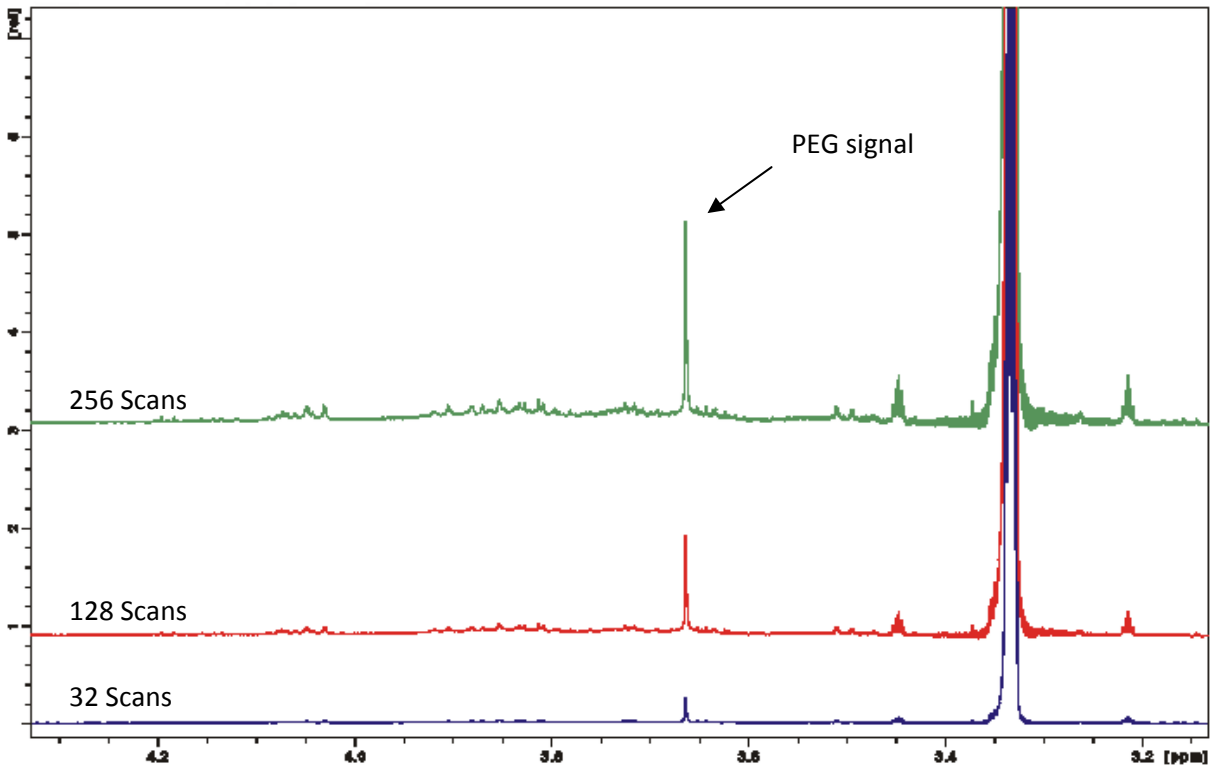

Figure 3.5: Effect of NS on PEG signal resolution

^{40K}PEG-insulin (10 µg/mL) was spiked into control rat urine and prepared for ^{1}H NMR analysis as described. The sample was analysed with 32 (blue trace), 128 (red trace) and 256 scans (green trace).

Relaxation Delay (D1)

The D1 is the time between each scan (acquisition) during the course of the experiment. The D1 is required to allow the nuclei of interest to fully relax before being pulsed with radiofrequency in the following scan. Without sufficient D1 the nuclei become saturated and this reduces the intensity of the signal during each scan. Following radiofrequency pulsing the net magnetisation of the sample returns to equilibrium along the Z axis, the axis along which the nuclei are oriented within the magnetic field. This is termed spin-lattice relaxation (T_1) and it occurs through interactions between the nuclei and their surroundings, or lattice. The D1 length should be sufficient to allow T_1 to occur and should typically be between 1 – 5 times the length of T_1. T_1 is calculated from an

inversion recovery experiment – an experiment set up to determine at what time point the nuclei of interest are relaxed. An overview of the inversion recovery experiment is given in figure 3.6. Briefly, the nuclei are aligned in the direction of the applied magnetic field (B_0), which is along the Z axis. A 180^o pulse flips the nuclei into the –Z plane after which T_1 begins and the nuclei start to relax. After a variable delay a 90^o pulse flips the net magnetisation into the XY plane – the plane in which NMR signals are detected. With a variable delay of T=0 the nuclei are not given sufficient time to relax and so the 90^o pulse tips the net magnetisation into the –X plane resulting in negative signals. With a variable delay of T<T1 approximately half are relaxed resulting in no observable signal. With a variable delay of T≥T1 net magnetisation has returned to equilibrium and thus the 90^o pulse tips the nuclei into the X plane and a positive signal is observed. The variable delay at which no signal is observed is termed t_{null} and T_1 is calculated from t_{null} using the equation $T_1 = t_{null}/\ln(2)$ (De Graaf, 2008).

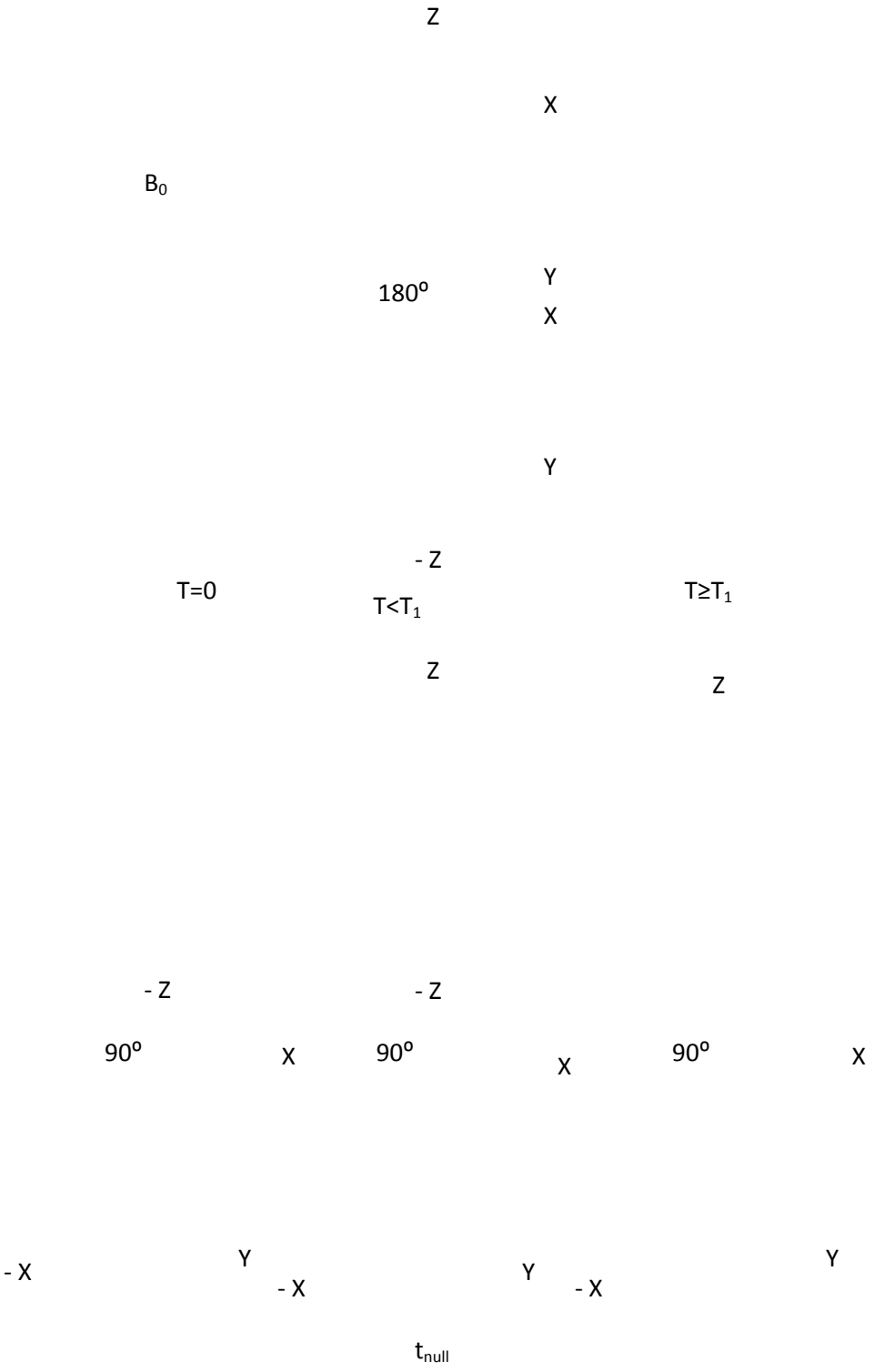

Figure 3.6: Inversion recovery overview

Schematic of the inversion recovery experiment; an initial pulse flips the nuclei 180° into the –Z plane. T_1 begins and after a variable delay a 90° pulse flips the nuclei into the XY plane. In this plane signals are detected and t_{null} can be ascertained – as the variable delay at which no signal is detected.

In figure 3.7, the spectra acquired with a range of variable delays from 0.1 to 10 seconds are overlaid. Figure 3.7 focuses on the PEG signal at 3.65 ppm and clearly indicates a t_{null} time of 1.0 second. Thus the T_1 of PEG is 1.44 seconds (1.0/ln(2)) (to two decimal places). The optimised D1 time therefore lies between 1.44 – 7.20 seconds, since D1 = (1 x 5)T_1.

To confirm PEG relaxation, the same ^{40K}PEG-insulin sample, spiked into control rat urine, was analysed with a D1 of 2.0 seconds and then with a D1 of 7.20 seconds, figure 3.8. Relative integration was used to determine if the area under the PEG signal (i.e. the intensity of the signal) significantly altered between the two D1 times. The PEG signal was integrated with a peak which had a t_{null} time of 0.1 seconds (data not shown) and was therefore guaranteed to be fully relaxed, at either 2.0 or 7.20 seconds, and could therefore be used as a reliable reference signal in both datasets. In figure 3.8 the intensity of the PEG signal essentially remains unchanged between the two D1 times; with a value of 17.4223 for a D1 of 2.0 seconds (panel A) and 17.4407 for a D1 of 7.20 seconds (panel B). Thus, with a D1 of 2.0 seconds the PEG signal was shown to be relaxed. However, a D1 of 3.0 seconds was used to analyse urine samples from the 28 day disposition study to ensure complete relaxation between data acquisitions.

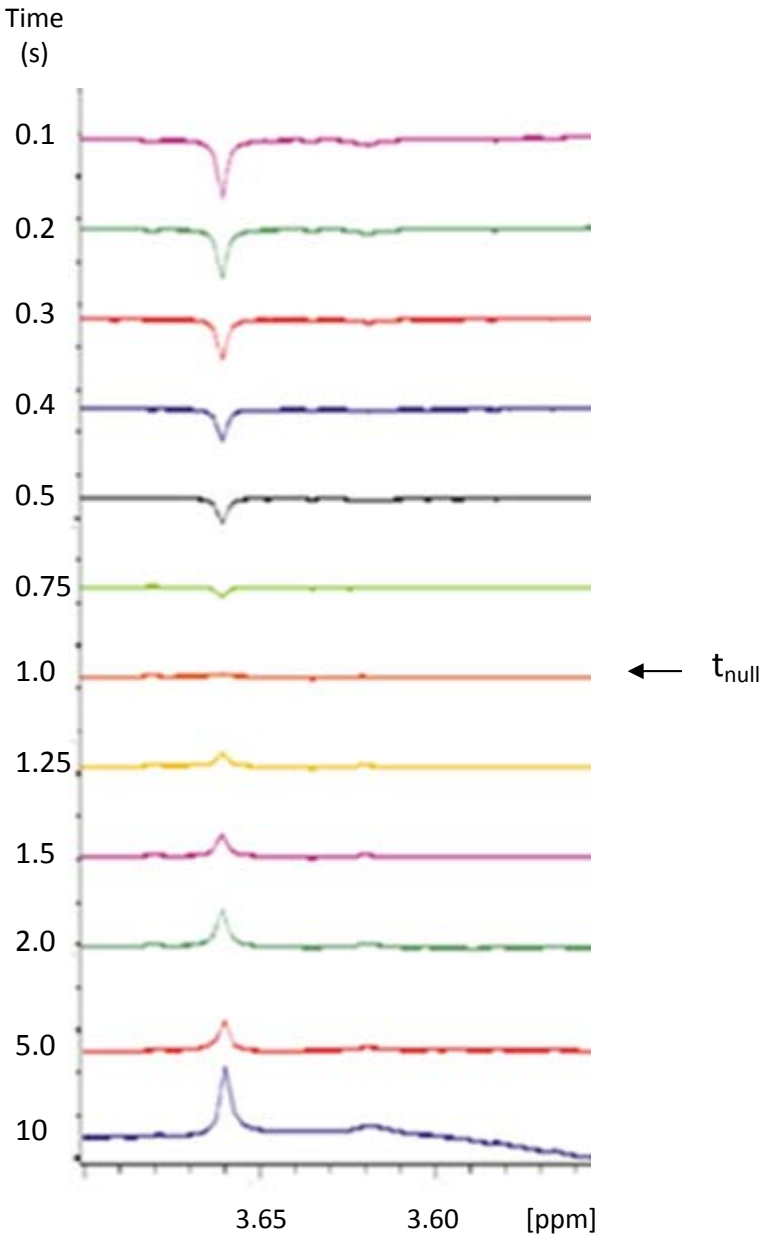

Figure 3.7: Inversion recovery of ^{40K}PEG-insulin

^{40K}PEG-insulin (10 µg/mL) was spiked into control rat urine and prepared for ^{1}H NMR analysis as described. The inversion recovery experiment was set up with variable delay times from 0.1 – 10 seconds and the spectra generated overlaid. T_{null} is the variable delay at which no signal can be observed and was found to be at 1.0 second.

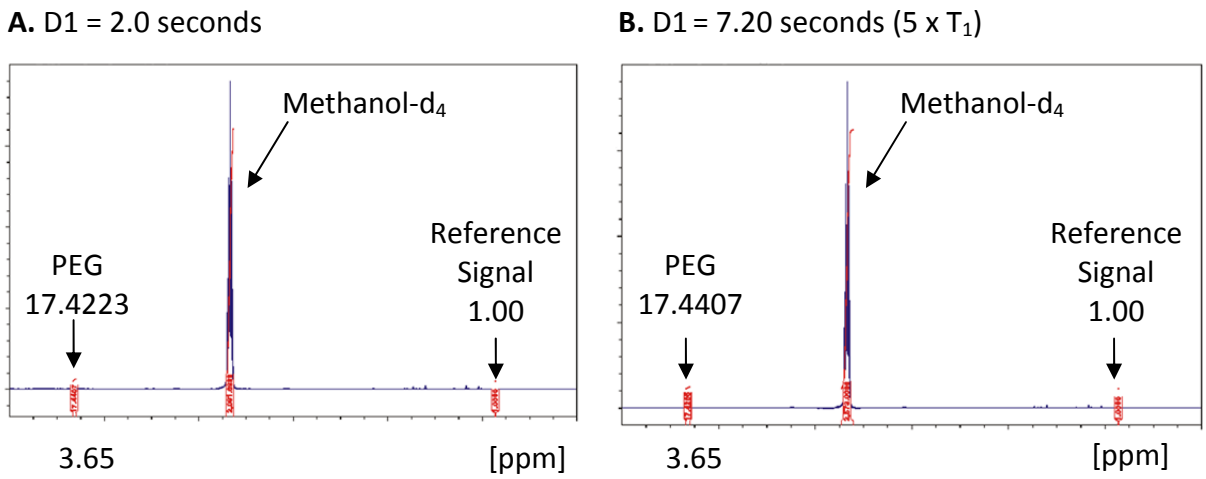

Figure 3.8: Comparison of PEG signal intensity analysed with different D1 times

^{40K}PEG-insulin (10 µg/mL) was spiked into control rat urine and prepared for ^{1}H NMR analysis as described. The sample was analysed with a D1 of 2.0 seconds (**A**) and again with a D1 of 7.20 seconds (**B**). The area under each PEG signal between the two datasets was compared relative to the area under a reference signal (automatically given the value of 1.00) that had previously been shown to be fully relaxed at both D1 times. Relative to the reference signal, the area under the PEG signal did not significantly alter between the two data sets; 17.4223 for D1 = 2.0 seconds and 117.4407 for D1 = 7.20 seconds.

Offset Frequency

The deuterated solvent methanol-d4 has residual signals which resonate at 3.31 and 4.87 ppm, figure 3.9 A. PEG resonates at 3.65 ppm and thus the residual signal at 3.31 ppm is too close to the PEG signal to be suppressed from the spectrum by a pulse. However, the residual signal at 4.87 can be removed by optimising the spectrometer frequency offset to suppress this residual resonance. The frequency offset is the centre of the spectral window, which for all ^{1}H NMR analyses for PEG was 5.0 ppm. Using the *GS*, the residual resonance at 4.87 ppm can be suppressed by manually adjusting the frequency offset (O1) for each individual sample, the effect of which can be seen in figure 3.9B.

A. Rat 2 (day 1) urine sample without O1 optimisation

B. Blank control urine with O1 optimisation

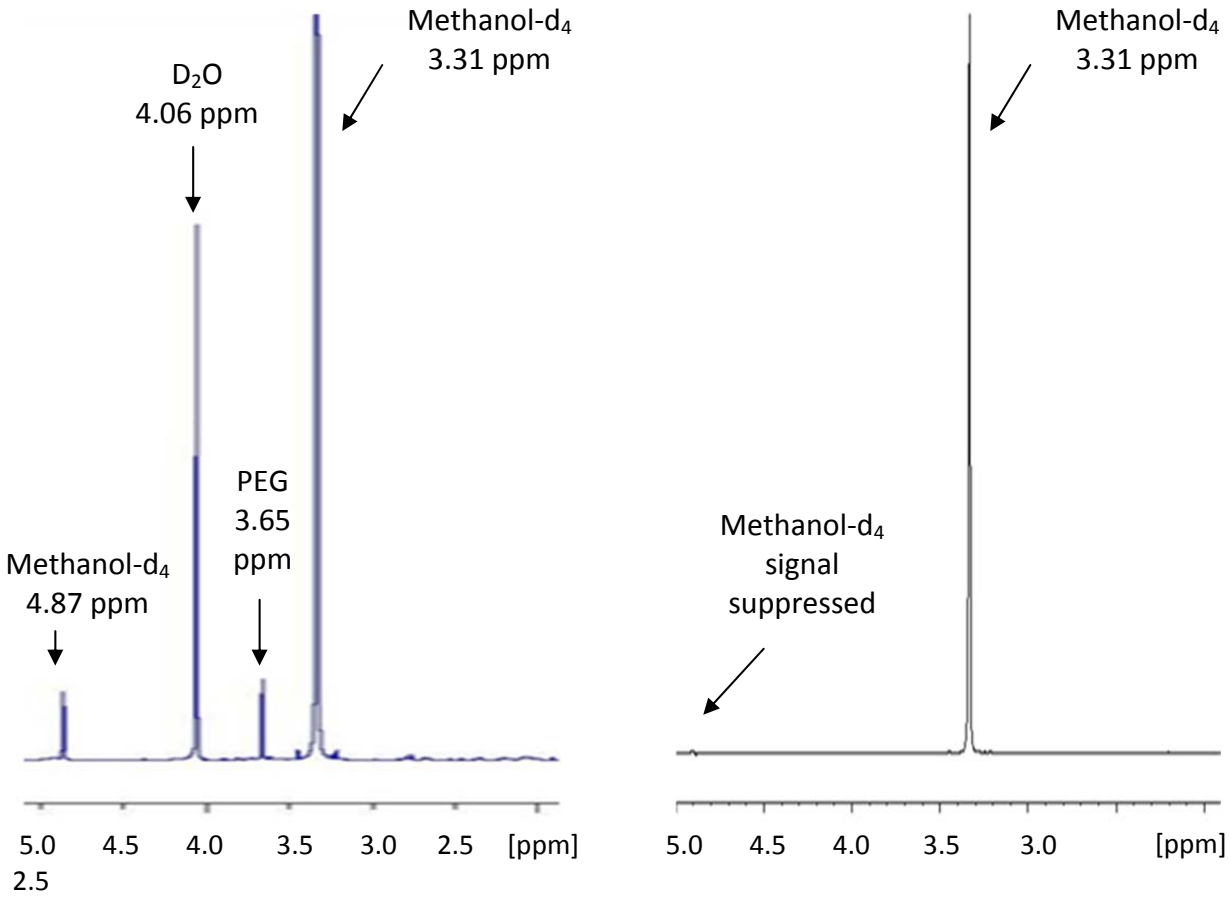

Figure 3.9: Suppression of residual methanol-d_4 resonance at 4.87 ppm

Rat 2 (day 1) urine sample (**A**) acquired without O1 optimisation compared with control blank urine (**B**) acquired with O1 optimisation. **A** shows the two residual methanol-d_4 resonances at 3.31 and 4.87 ppm, with the PEG signal at 3.65 ppm and D_2O (Nicotinamide IS solvent) residual resonance at 4.06 ppm. **B** shows the effect of optimising the O1 with respect to suppressing the residual methanol-d_4 signal at 4.87 ppm.

3.3.2 Internal Standard

Nicotinamide has 4 proton signals that resonate downfield from PEG and methanol-d_4, which therefore make it an ideal IS as it does not interfere with signals of interest, i.e. PEG, as seen in figure 3.10. Furthermore, it is non-volatile and its protons are non-labile. In theory, each of the 4 proton resonances could be utilised as the reference peak from which ^{40K}PEG-insulin excreted in urine could be quantified, these are labelled A – D in figure 3.10. To establish which signal to use a concentration range of ^{40K}PEG was analysed with nicotinamide (prepared as described in section 3.2.7.1) and 4 standard curves generated from relative integration of the PEG signal, in each concentration, with all 4 signals of nicotinamide individually, as seen in figure 3.11. The signal labelled A gave the highest coefficient of determination (R^2) (0.9927) and was consequently selected as the reference signal to quantify ^{40K}PEG-insulin content excreted in the urine across the 28 day disposition study. A standard curve generated from the average relative integration ratio of PEG against all 4 proton resonances of nicotinamide combined was also produced and elicited an R^2 of 0.9899 (data not shown).

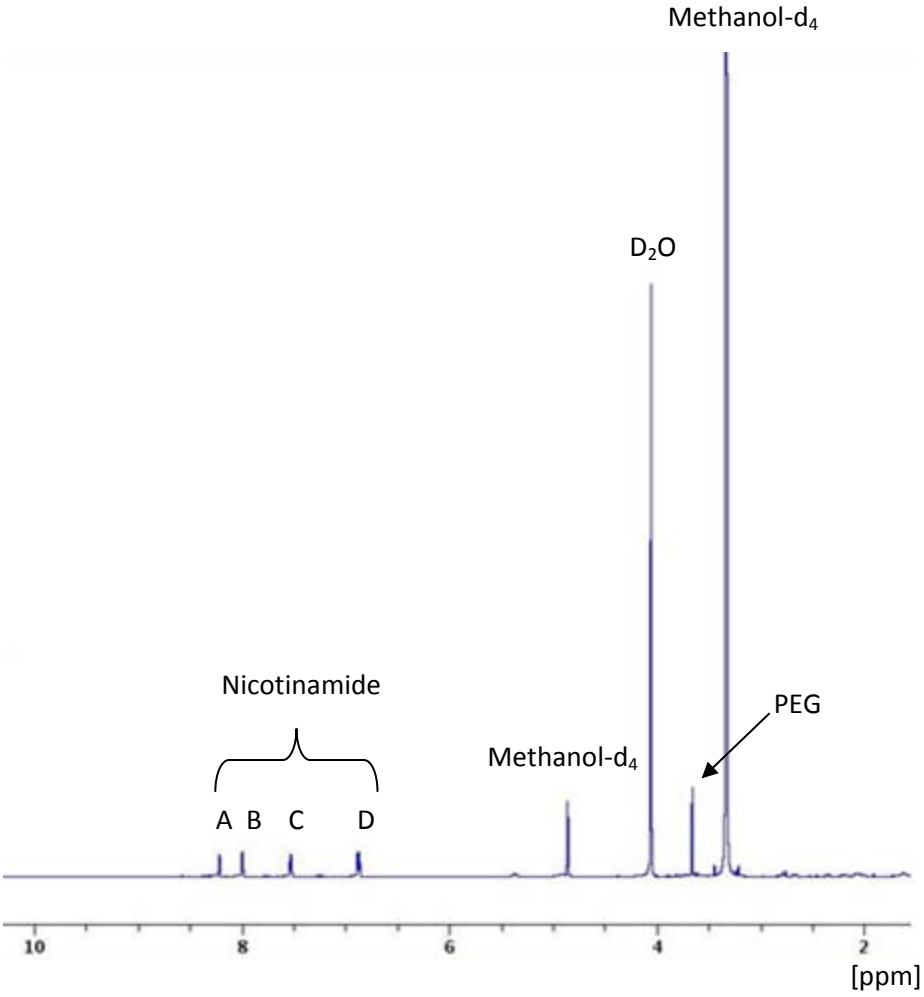

Figure 3.10: Proton resonances of nicotinamide

Rat 2 (day 1) urine sample analysed with nicotinamide IS. The 4 proton resonances of nicotinamide are labelled A – D and resonate downfield from PEG and the residual solvent resonances.

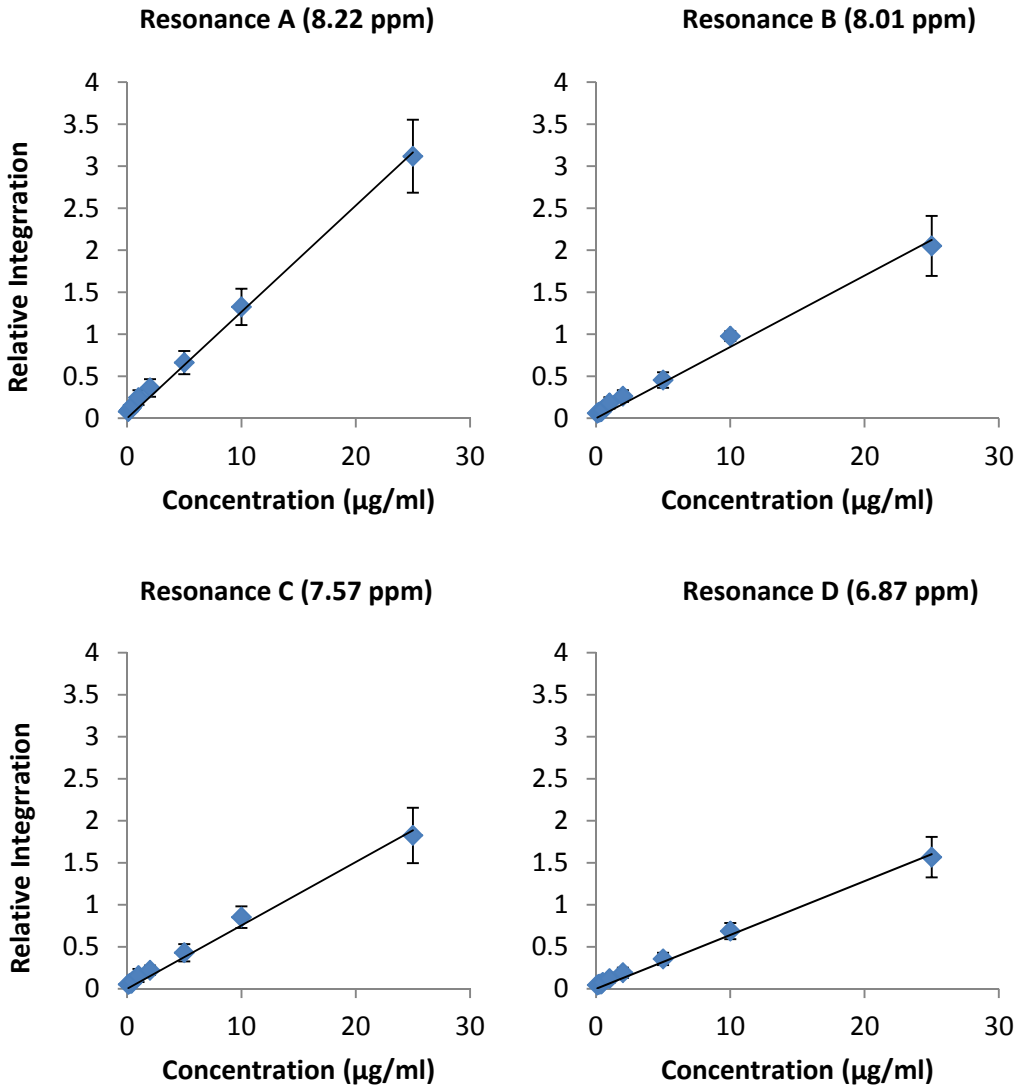

Resonance	Equation	R^2
A	y = 0.1266x	0.9927
B	y = 0.0849x	0.9853
C	y = 0.0755x	0.9868
D	y = 0.0641x	0.9907

Figure 3.11: ^{40K}PEG standard curves generated against each proton resonance of nicotinamide

A concentration range of ^{40K}PEG, in triplicate, was spiked into control rat urine and prepared for ^{1}H NMR analysis as described. The PEG signal was integrated manually with each proton signal from nicotinamide (labelled A – D: corresponding to figure 3.10) and standard curves generated. Data are presented as the mean ± SD, n=3. The equation of the straight line (with an intercept at 0, 0) is given in the table with the accompanying R^2 value for each nicotinamide resonance. The nicotinamide signal labelled A produced the standard curve with the highest R^2 (0.9927) and was thus used as the reference signal to quantify ^{40K}PEG-insulin excretion in the 28 day disposition study

3.3.3 ^{40K}PEG-insulin Quantification in Urine Samples

Once the ^{1}H NMR data acquisition parameters had been optimised as described in section 3.2.6, and validated from selected urine samples from the 28 day disposition study, all subsequent urine sample analyses utilised the optimised parameters as detailed in section 3.2.8. Using the nicotinamide IS the concentration of ^{40K}PEG-insulin excreted in each urine sample was calculated. From the known total volume of urine collected each day the total amount of PEG excreted daily in the urine could be calculated for each individual rat. These data are given in table 3.1, along with the average total amount of PEG excreted daily for all animals combined; which is presented graphically in figure 3.12. The data in figure 3.12 and table 3.1 has been corrected for loss of ^{40K}PEG-insulin during processing as outlined in section 2. From table 3.1 and figure 3.12 it is clear that ^{40K}PEG-insulin is excreted rapidly from day 1 onward until days 3/4, after which the amount excreted levels off, apart from a slight increase between days 13 and 17. Of the 10 time points analysed across the 28 day study the amount of ^{40K}PEG-insulin excreted in the urine equated to approximately 34.9% of the dose.

Day	Rat 1	Rat 2	Rat 3	Rat 4	Rat 5	Rat 6	Rat 7	Total PEG excreted (mean ± SD)
1	330.3	265.8	52.4	175.7				206.1 ± 120.5
2	102.4	92.8	33.3	63.6				73.0 ± 31.2
3	48.5	39.0	11.2	24.6				30.8 ± 16.4
4	40.6	34.9	18.0	28.3				30.4 ± 9.7
5	35.8	21.1	13.8	10.7				20.3 ± 11.1
7	23.7	17.5	6.6	9.4				14.3 ± 7.8
13	29.0	18.2	24.3	12.3				20.9 ± 7.3
17					52.6	15.4	32.9	33.6 ± 18.7
21					22.2	9.2	31.6	21.0 ± 11.2
24					22.8	9.7	24.3	22.6 ± 12.2
Total	610.2	489.3	159.7	324.6	108.6	34.2	88.8	473.0
% of Dose	45.0	36.1	11.8	23.9	8.0	2.5	6.6	34.9

Table 3.1: Total amount of PEG (µg) excreted daily into urine

Urine samples from the 28 day disposition study were prepared for ^{1}H NMR analysis as described. Each time point was analysed in triplicate to determine the average concentration of PEG present in the urine using the nicotinamide IS. The total PEG excreted (µg/day) was then determined. Data is presented as the total amount of PEG excreted daily in the urine for each animal, from which the average amount of PEG excreted daily between all animals was subsequently determined (far right column. The data was corrected for signal loss as outlined in section 2.

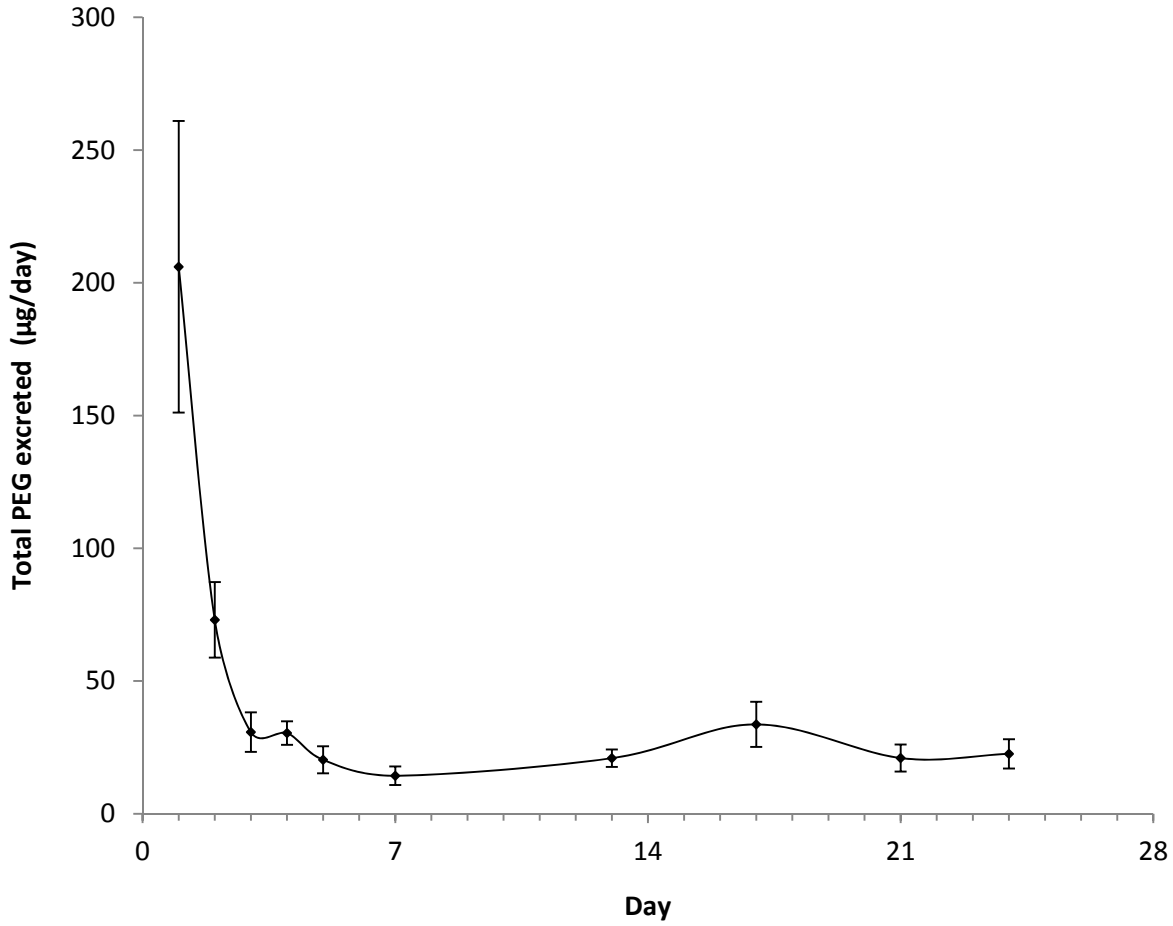

Figure 3.12: Total PEG excreted daily into urine for all rats combined

The total amount of PEG excreted daily for all animals combined (data from table 3.1) is presented ± SEM.

3.3.4 Limit of Detection Determination

The LOD was determined by comparing the intensity of the PEG signal against 3 artefact signals, within ± 0.5 ppm of the PEG signal, by relative integration and averaging the ratio. The rationale for using this method to determine the LOD is highlighted in figure 3.13. Figure 3.13 shows the spectra acquired from a day 24 urine sample (rat 6), a time which contained the lowest amounts of PEG. At these later timepoints artefact signals, possibly from un-removed urinary proteins, are of similar intensity to the PEG signal and in some cases appeared to overlap with the PEG signal. Similar artefact signals were observed

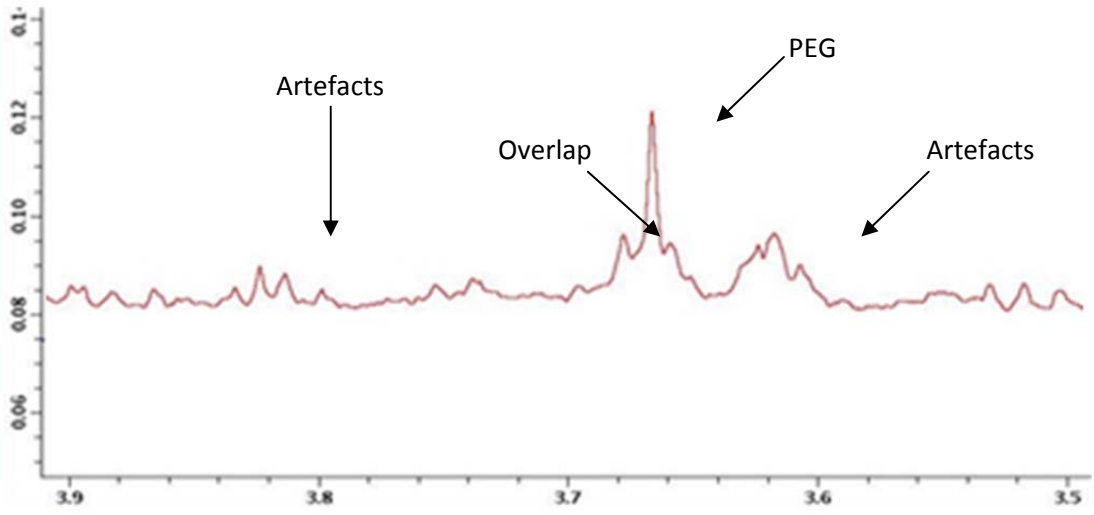

Figure 3.13: Day 24 urine sample from rat 6

Rat 6 day 24 urine sample prepared for ^{1}H NMR analysis as described and acquired with optimised parameters as outlined in section 3.2.8. Highlighted are the PEG signal and artefact signals also present in the sample. Also highlighted is potential overlap of the PEG signal by these artefact signals.

in low concentration ^{40K}PEG standards (data not shown). For accurate detection this represented a significant barrier and thus a stringent method to determine the LOD was required. To this end, a concentration range of ^{40K}PEG, in triplicate, was spiked into control rat urine and prepared for ^{1}H NMR analysis as described. The ratios obtained of PEG signal intensity relative to 3 artefact signals was averaged for each concentration of ^{40K}PEG and the LOD defined as the concentration at which PEG signal intensity became 3:1 greater than the average intensity of the artefact resonances. The LOD was determined to be 0.5 µg/mL as shown in figure 3.14. When this method for determining the LOD was applied to urine samples from the 28 day disposition study it was found that all PEG signals in the time-points analysed were indeed 3 times greater than artefact signals present in the sample, as shown in figure 3.15.

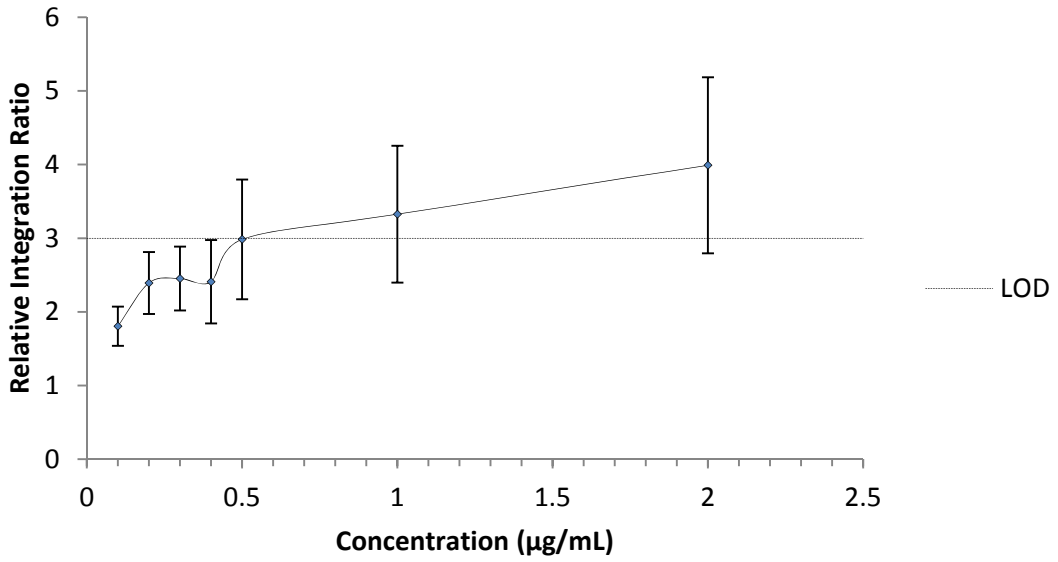

Figure 3.14: Limit of detection determination in ^{40K}PEG standards

A concentration range of ^{40K}PEG, in triplicate, was spiked into control urine and prepared for ^{1}H NMR analysis as described and acquired with optimised parameters as outlined in section 3.2.8. The intensity of the PEG signal was integrated manually with 3 artefact signals resonanting ± 0.5 ppm of the PEG signal and the average taken. Data are presented as the mean relative integration ratio ± SD, n=3. The LOD was determined to be 0.5 µg/mL: the concentration at which PEG signal intensity became 3 times greater than potentially overlapping artefact signals.

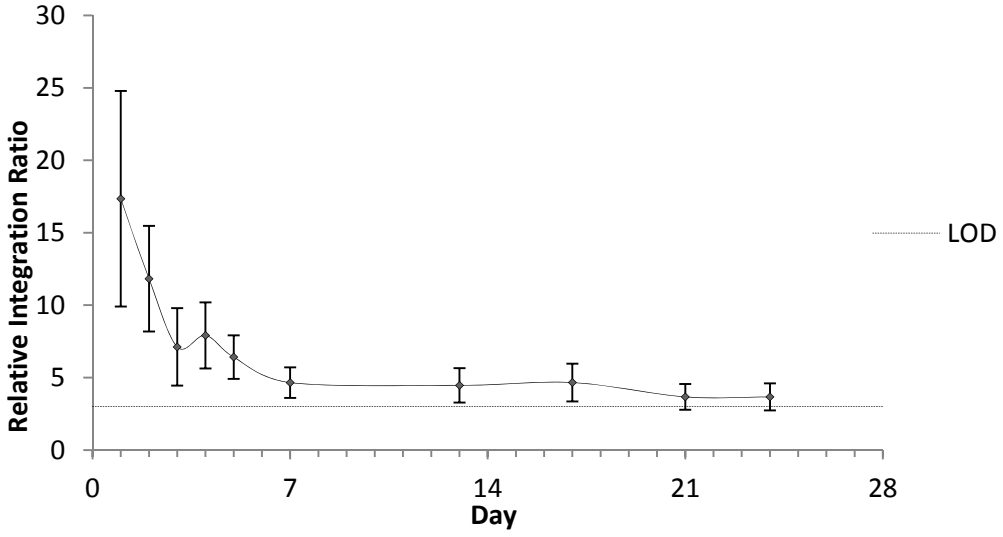

Figure 3.15: Limit of detection method applied to 28 day urine samples

Urine samples from the 28 day disposition study were prepared for ^{1}H NMR analysis as described. The LOD method as described in section 3.3.4 was applied to each time-point for each rat (n=3) and the results averaged. Data are presented as the mean relative integration ratio for all animals combined ± SD

3.4 DISCUSSION

Chapter 2 described the development of a gel-based analytical platform to independently monitor both the PEG and protein components of a PEGylated protein; thereby providing a measure of the disposition, pharmacokinetics and structural integrity of the conjugate in a rodent model, and could potentially be translated to the analysis of samples generated from clinical studies. Here, a ^{1}H NMR method was developed and optimised for the detection and quantification of PEGylated proteins, and was used to quantify the amount of ^{40K}PEG-insulin excreted in urine from rodents from the 28 day disposition study; thus adding an extra facet to the gel-based platform described in chapter 2 in terms of absolute quantification, since the gel-based methods provide only semi-quantitative information. PEG contains many hydrogen atoms each in the same chemical environment, which all contribute toward a single resonance peak that can be easily identified. The straight-forward identification of PEG by ^{1}H NMR potentially represents a facile, uncomplicated tool to monitor the PEG moiety of PEGylated proteins. However, since the area under the curve of each resonance signal is directly proportional to the number of protons which produce the signal, this reduces the ability of ^{1}H NMR to simultaneously monitor the insulin component of the conjugate, as, in comparison to PEG, the numbers of hydrogen atoms present in insulin are significantly lower. However, this does not preclude the use of ^{1}H NMR as an effective tool to quantify PEG excreted in urine. Indeed, with ^{1}H NMR a sealed IS could be used to produce a fully quantitative assay, allowing for robust analysis between samples. In this study, nicotinamide was selected as the IS, as it is non-labile, non-volatile, and resonates downfield from the PEG resonance. Urine samples from the 28 day disposition study were prepared for ^{1}H NMR analysis as they were for gel-based analysis, by dialysis and deproteination, which was shown to reproducibly remove abundant urinary proteins in gel-based analyses. The presence of urinary proteins could potentially complicate ^{1}H NMR analysis and consequently both

dialysis and deproteination were again used to clean up urine samples prior to analysis. This kept sample preparation identical between both gel-based and ^{1}H NMR platforms, ensuring reliable comparisons could be made between the data generated by each assay. Prior to analysing urine samples from the 28 day disposition study, the various spectrometer parameters involved in producing ^{1}H NMR spectra were optimised. This was crucial to ensure accurate and reliable quantification of PEG could be maintained during analysis of each sample. Once these parameters were defined, they were used throughout for all subsequent analyses of urine samples collected during the 28 day disposition study. ^{1}H NMR analysis confirmed that ^{40K}PEG-insulin was excreted rapidly in the urine from day 1 to day 3, after which the amount excreted remained relatively stable throughout the remaining time points, with slight increases in PEG excreted on days 4 and 17. The sensitivity of ^{1}H NMR, under the conditions used in this study, was sufficient to detect PEG in all urine samples analysed, with the LOD and LOQ defined as 0.5 μg/mL and 10 μg/mL, respectively, but could not provide full quantification after day 3, when the amounts of PEG excreted fell below the LOQ. Despite this, quantification of PEG by ^{1}H NMR was commensurate with the values obtained using gel-based methods. Using a Bruker 600 MHz spectrometer, ^{1}H NMR was not sensitive enough to monitor the protein moiety of the conjugate. Future advancements in NMR technology, coupled with the use of more powerful spectrometers, such as a Bruker 800 MHz or Bruker 1 GHz spectrometer, may result in the capability to simultaneously monitor each component of a PEGylated protein using ^{1}H NMR. Increased sensitivity may also allow the detection and quantification of PEG in other biological fluids and tissues: urine was selected for initial ^{1}H NMR analysis due to the relative ease in concentrating urine samples; future increases in sensitivity may therefore preclude the necessity of sample concentration and allow for detection of PEG in other samples, such as plasma. Furthermore, when translated to clinical studies, deproteination may not be required to improve abundant urinary proteins since human

urine typically has a much lower protein content; hence, there may be much less analyte loss during sample preparation and consequently this may improve the sensitivity of the assay. Thus, the conclusion from this study was that ^{1}H NMR can be used as a tool to measure the urinary excretion of PEG, with benefits such as high specificity, since PEG produces a single resonance peak, and absolute quantification, using an internal standard. Coupled with the gel-based analytical platform, ^{1}H NMR provides complementary information with regards to assessing the pharmacokinetics, disposition and biological fate of PEGylated proteins; with similar analysis parameters to the gel-based assays, such as identical LOD, sample preparation and run-time, as well as offering the benefit of absolute quantification of the PEG moiety – as detailed in table 3.2.

	Gel-Based Platform	**^{1}H NMR**
LOD	0.5 µg/mL	0.5 µg/mL
Structural Analysis	PEG, Linker, Protein	PEG
Sample Volume	100 – 300 µL	1 mL
Sample Preparation	Dialysis and deproteination	Dialysis and deproteination
Overall Time	2 days	2 days
Analysis Requirements	Routine laboratory equipment	Specialist equipment
Quantification	Semi	Absolute

Table 3.2 Comparison of the gel-based analytical platform and ^{1}H NMR

CHAPTER 4

Cellular Internalisation of PEG

CONTENTS

Cellular Internalisation of PEG

4.1 INTRODUCTION

The evidence acquired in chapter 2 indicate that ^{40K}PEG-insulin undergoes cellular internalisation, after which either full metabolic dissociation of the conjugate or progressive proteolytic degradation of the insulin moiety occurs, both of which culminate in tissue retention of PEG. This raises several interesting possibilities: 1) dissociation of PEGylated proteins may result in the protective shielding effect of PEG being lost, presumably resulting in increased degradation of the therapeutic agent and consequently reducing its efficacy; 2) dissociation may subsequently alter the intracellular disposition of the liberated protein moiety, again potentially affecting the efficacy of the biologic; and 3) dissociation of the conjugate may result in the liberated protein moiety becoming available for immunological processing. As described in the general introduction, there is little data concerning the disposition and metabolism of a PEGylated protein in man. Consequently, the effect of PEGylation on the internalisation and cellular disposition of a coupled protein is poorly understood. Therapeutically, a range of different PEG MWs and linkers are conjugated to proteins for the purposes of improving their PK properties. In this chapter, the effect of PEG MW on the cellular internalisation of PEG was assessed. The body of work in this chapter is the first of three chapters devoted to developing methodology to assess the effect of PEGylation on the internalisation and intracellular processing of proteins, in order to 1) assess the poorly understood effect of PEGylation on cellular internalisation; 2) begin addressing the poorly understood mechanics of how PEGylation reduces the immunogenicity of proteins; and 3) continue the investigations described in chapters 2 and 3 to determine if intracellular processing pathways are capable of degrading/cleaving PEGylated proteins . The data described in chapter 2 clearly showed PEG accumulation in both liver and kidney tissue. In this chapter, the gel-based assays and ^{1}H NMR, described in chapters 2 and 3, respectively, were initially tested as tools to assess the cellular internalisation of ^{40K}PEG-insulin in HepG2 cells(a human liver cell line), in order to replicate

in vitro what had been observed *in vivo*. Next, the internalisation of different MW PEGs by bone-marrow derived dendritic cell (DC) – a model APC – was assessed by flow cytometry and fluorescence microscopy, as well as insulin – continuing the use of insulin as a model protein.

4.2 METHODS AND MATERIALS

All reagents were purchased from Sigma-Aldrich Company Ltd (Dorset, UK), unless otherwise stated.

4.2.1 Cell Culture

4.2.1.1 HepG2 Cell

HepG2 (Health Protection Agency) cell line was cultured in Dulbecco's Modified Eagle Medium (DMEM), supplemented with 10% Foetal Calf Serum (FCS) and 2 mM penicillin-streptomycin, and maintained in a humidified atmosphere (5% CO_2) at 37^{o}C.

4.2.1.2 Dendritic Cell Generation

Immature Dendritic Cell

Bone marrow-derived immature dendritic cells (iDC) were generated from C57BL/6 mice. *Femora* and *tibiae* were removed and both ends cut. Bone marrow was flushed from each bone in Hanks Balanced Salt Solution (HBSS). Cells were washed in HBSS and seeded at 3 x 10^6 cells/dish in 100 mm microbiological petri dishes. Culture medium was RPMI-1640 medium supplemented with: 10% FCS, 50 µM 2-mercaptoethanol, 2 mM HEPES, 1 mM sodium pyruvate, 2 mM L-glutamine, 100 IU/mL streptomycin, 100 µg/mL penicillin

and 10 ng/mL GM-CSF. Cells were maintained in a humidified atmosphere (5% CO_2) at 37°C. Culture medium was refreshed on day 3 and iDC used experimentally on day 7.

Mature Dendritic Cell

Mature dendritic cells (mDC) were generated from iDC via overnight incubation with lipopolysaccharide (1 µg/mL) on day 6. Differentiation was assessed by light microscopy and mDC were used experimentally on day 7.

4.2.2 Cell Dosing and Lysate Preparation

4.2.2.1 HepG2 Cell

Cells were seeded in 24-well plates (3 x 10^5 cells/well) in 1 mL culture media and allowed to adhere overnight. Culture media was replaced with conditioned media (culture media containing ^{40K}PEG-insulin or ddH_2O as vehicle control) and cells incubated for the stated times. Conditioned media was then removed and cells washed with phosphate-buffered saline (PBS) (2 x 100 µL). Cell lysates were collected in 100 µL TEAB buffer (0.5 M tetraethylammonium borohydride, 0.1% sodium dodecyl sulphate). Conditioned media and lysates were stored at -20°C prior to gel electrophoresis.

4.2.2.2 Dendritic Cell

iDC were seeded in 24-well plates (5 x 10^5 cells/well) in 1 mL culture media and allowed to adhere for a minimum of 2 hours. Culture media was replaced with conditioned media and cells incubated for the stated times. Plates were then centrifuged at 900 RCF for 5 minutes at 4°C and conditioned media removed. Cells were washed in 1 mL RPMI-1640 medium and re-centrifuged. Cell lysates were collected in 100 µL TEAB buffer. Conditioned media and lysates were stored at -20°C prior to gel electrophoresis.

4.2.3 SDS-PAGE

Cell lysates (10 µL) were deproteinated (1:1 v/v) and prepared for analysis by gel electrophoresis as described in sections 2.2.4 and 2.2.5, respectively

4.2.4 BaI_2 Colorimetric Stain and Western Blot

Gels were stained with the BaI_2 stain or transferred to nitrocellulose membrane and probed for either PEG or insulin as described in sections 2.2.6 and 2.2.7, respectively.

4.2.5 ^{1}H NMR

100 µL samples were deproteinated (1:1 v/v) and prepared for ^{1}H NMR analysis as described in sections 3.2.3 and 3.2.4, respectively. Data was acquired at 300 Kelvin using a Bruker 800 MHz Avance III with CryoProbe and analysed using TopSpin 2.1 software. Parameter optimisation was essentially as described in section 3.2.8 for ^{40K}PEG-insulin quantification in urine samples using a Bruker 600 MHz spectrometer.

4.2.6 Flow Cytometry

iDC and mDC were generated as described and 5 x 10^5 cells were used per condition. DCs were incubated at 37^{o}C in a humidified atmosphere with either 5 kDa PEG-FITC or 40 kDa PEG-FITC (1 mg/mL) in a 100 µL total volume of RPMI-1640 medium, for the indicated times. Baseline controls were kept at 4^{o}C. Cells were washed twice with stain buffer (2% FBS, 1 mM EDTA in sheath fluid) and then incubated with Cd11c$^{PE\text{-}Cy5.5}$ antibody (Invitrogen) at 4^{o}C for 30 minutes in the dark. CD11c is an abundant transmembrane integrin protein used as a marker for DC. Cells were then washed twice more with stain buffer and reconstituted in 800 µl sheath fluid (for immediate analysis) or fixed in 800 µl 1% PFA (for future analysis). The degree of PEG-FITC cellular internalisation was assessed using a BD FACS Canto II Flow Cytometer (BD Biosciences, UK) and analysed with Cyflogic^{TM}

software, CyFlo Ltd, Finland. Gates were defined as shown in figure 4.7, which restrict analysis to internalisation of PEG-FITC by the DC population only. Internalisation of $Dextran^{FITC}$ (40 kDa, Invitrogen) was used as positive control for DC endocytic ability by incubating DCs with $Dextran^{FITC}$ (0.5 μg/mL) and analysed as above.

4.2.7 Fluorescence Microscopy

iDC and mDC were generated as described. Cells were seeded in 12-well plates (5 x 10^5 cells/well) in 1 mL culture media and allowed to adhere for a minimum of 2 hours. Culture media was replaced with conditioned media containing either 5 kDa PEG-FITC (100 μg/mL or 1 mg/mL), 40 kDa PEG-FITC (100 μg/mL or 1 mg/mL) or RMPI-1640 medium (vehicle control), and incubated at either 37°C or 4°C for the indicated times. Cells were incubated in reverse chronological order such that each time-point ended at the same time. Conditioned media was replaced with culture media containing Hoechst stain (Invitrogen, Paisley, UK), which stains DNA, at 2 μg/mL and left for 20 minutes at room temperature. Hoechst stain was removed and cells washed with PBS (3 x 1 mL) and then fixed in 1 mL paraformaldehyde (PFA) (4% in PBS) at room temperature for 10 minutes. PFA was removed and cells washed twice (2 x 1 mL) and stored in PBS at 4°C in the dark. Images were acquired using a Zeiss Axio Observer with a 20x objective, with identical exposure times for each channel (Blue channel (Hoechst): 20 ms; Green channel (FITC) 162 ms). Post-acquisition image processing (background subtraction) was performed using AxioVision 4.8 software.

4.2.7.1 Insulin-rhodamine

Insulin was labelled with rhodamine (a fluorophore) using a commercially available kit (Lightning-Link®, Innova Biosciences, Cambridge, UK) as per the manufacturer's instructions. Insulin-rhodamine was incubated with DC (200 μg/mL) to assess their ability to

internalise fluorescently-labelled insulin, as well as fluorescently-labelled PEG, and was analysed by fluorescence microscopy as described, exposure time for Red channel (Rhodamine): 85 ms.

4.3 RESULTS

4.3.1 BaI_2/Western Blot Analysis

The BaI_2 colorimetric stain and western blot analyses were initially used to detect endocytosis of PEG and ^{40K}PEG-insulin *in vitro.* ^{40K}PEG-insulin was incubated with both HepG2 and iDC for the indicated times and both conditioned media and cell lysates prepared for SDS-PAGE as described. At 1, 2 and 4 hours post-dose no detectable levels of ^{40K}PEG-insulin were found in cell lysates at either 10, 25 or 50 µg/mL ^{40K}PEG-insulin, by either the BaI_2 stain or western blotting, or in any cell type (not shown). ^{40K}PEG-insulin, at each concentration, was detected, however, in the conditioned media. No detectable levels of ^{40K}PEG-insulin were found in the cell lysates at 6 hours post-dose also, in either HepG2 (Figure 4.1) or iDC (Figure 4.2). Again, ^{40K}PEG-insulin was detected in the conditioned media. A lower MW PEG, 20 kDa PEG, was incubated with HepG2 at 50 µg/mL but could not be detected by the BaI_2 colorimetric stain at 1, 2 or 4 hours post-dose (not shown) or at 6 hours post-dose (Figure 4.3). The incubation times were then extended to 24 hours and the resulting HepG2 cell lysates analysed for ^{40K}PEG-insulin content. At 24 hours post-dose, ^{40K}PEG-insulin could be detected weakly by all three assays; however the BaI_2 stain could only detect PEG at 100 µg/mL ^{40K}PEG-insulin (Figure 4.4). Therefore, more sensitive and specific techniques were required, since a non-specific band was also detected in the control lysate sample.

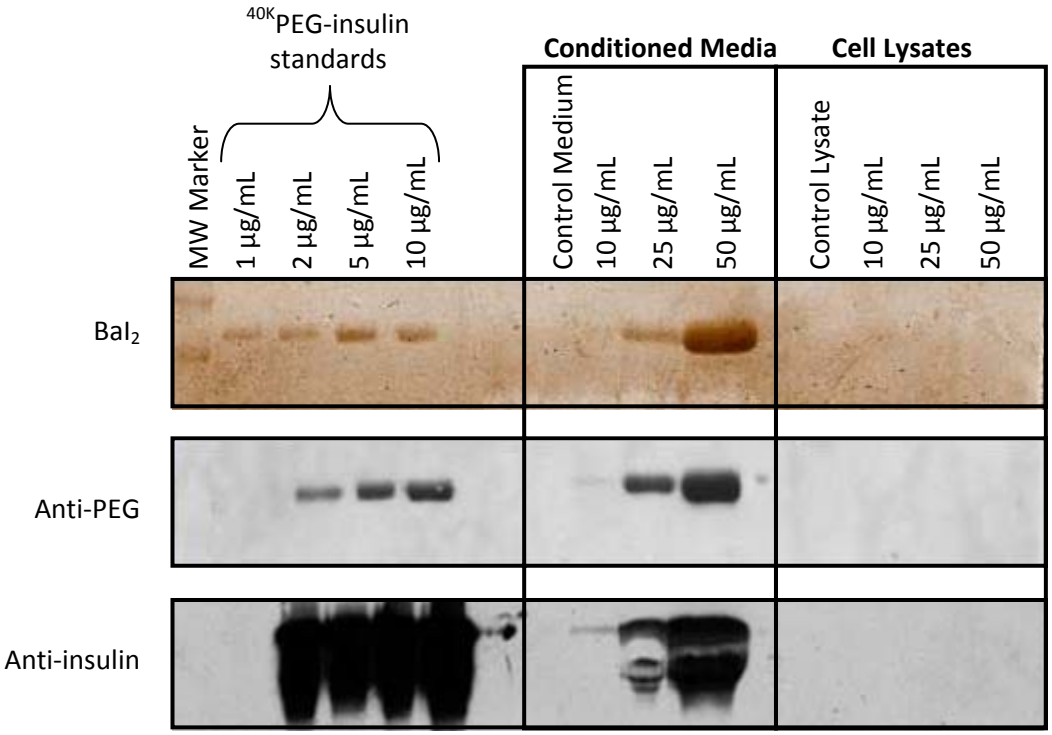

Figure 4.1: ^{40K}PEG-insulin internalisation by HepG2 is not detectable 6 hours post-dose

A concentration range of ^{40K}PEG-insulin was incubated with HepG2 cells for 6 hours and both the conditioned media and cell lysates analysed for ^{40K}PEG-insulin content using the BaI_2 stain and Western blot.

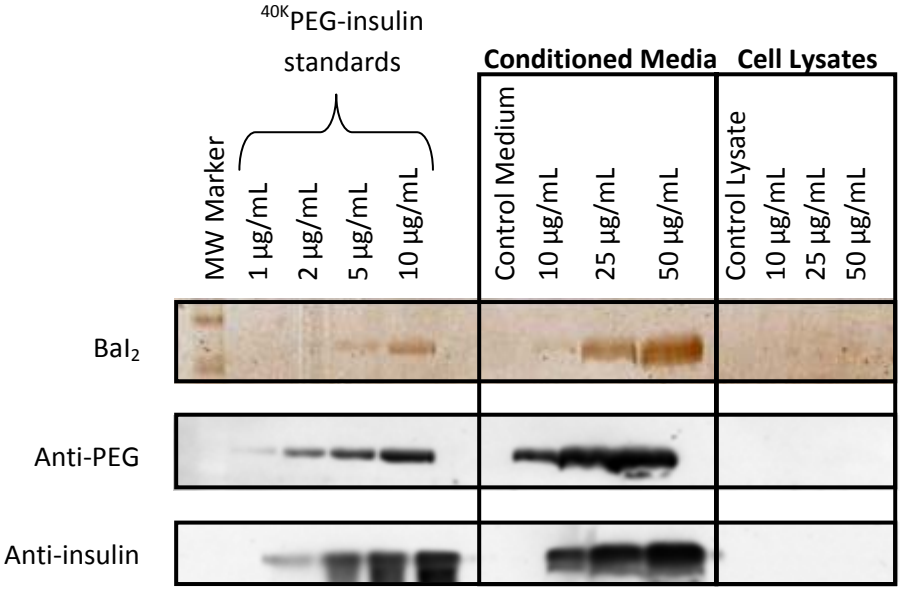

Figure 4.2: ^{40K}PEG-insulin internalisation by iDC is not detectable 6 hours post-dose

A concentration range of ^{40K}PEG-insulin was incubated with iDCs for 6 hours and both the conditioned media and cell lysates analysed for ^{40K}PEG-insulin content using the BaI_2 stain and Western blot.

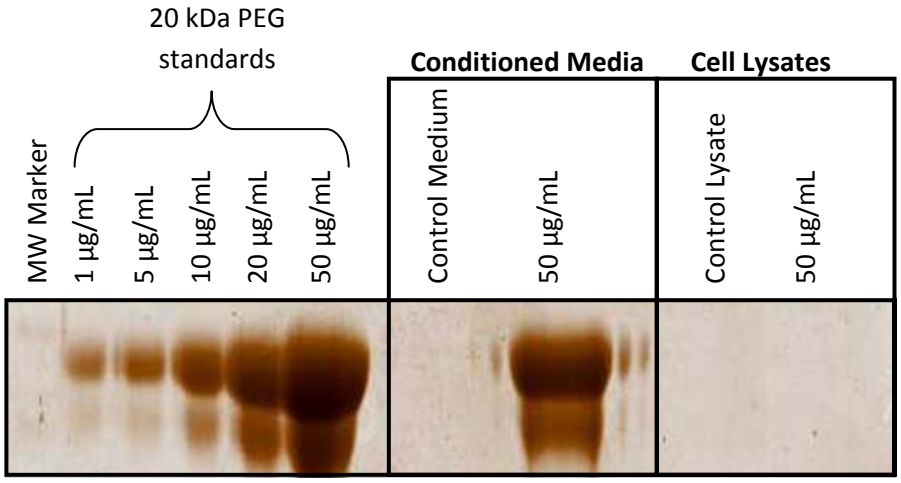

Figure 4.3: Internalisation of 20 kDa PEG by HepG2 cells is not detectable 6 hours post-dose

20 kDa PEG was incubated with HepG2 cells for 6 hours and both the conditioned media and cell lysates analysed for 20 kDa PEG content using the BaI_2 stain.

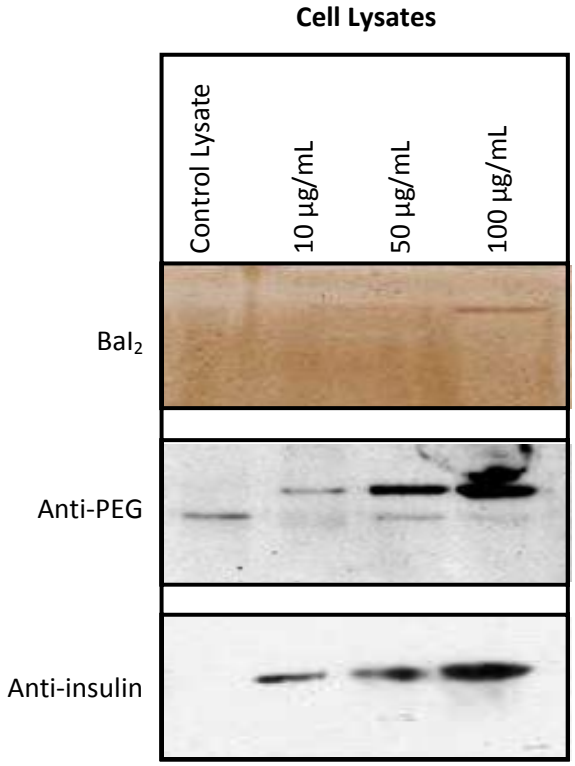

Figure 4.4: ^{40K}PEG-insulin internalisation by HepG2 cells is detectable 24 hours post-dose

^{40K}PEG-insulin was incubated with HepG2 cells for 24 hours and both the conditioned media and cell lysates analysed for ^{40K}PEG-insulin content using the BaI_2 stain and Western blot.

4.3.2 ^{1}H NMR Analysis

The utility of ^{1}H NMR as a tool for monitoring PEG and PEGylated protein endocytosis was assessed. HepG2 were dosed with ^{40K}PEG-insulin for 24 hours and conditioned media and lysates collected and prepared for ^{1}H NMR analysis as described; ddH_2O was used as vehicle control. The PEG signal in the conditioned medium sample could be clearly detected (Figure 4.5, blue trace) despite the fact that it overlapped with residual signals resonating between 3.65 – 3.73 ppm, which were also observed in the control media sample (Figure 4.5, red trace). A weak signal, resonating at the chemical shift of PEG, was found in the conditioned lysate sample (Figure 4.6, blue trace). However, in the control lysate sample (Figure 4.6, red trace) a residual signal was observed that resonated at the same chemical shift of PEG and was of comparable intensity to the signal observed in the

conditioned lysate. It is therefore unlikely that any reliable, quantitative assessments of ^{40K}PEG-insulin internalisation by HepG2 could be acquired using ^{1}H NMR. Given the presence of interfering resonances and the fact that the PEG signal in the conditioned lysate was barely visible, if it was indeed PEG, the utility of ^{1}H NMR as a tool to measure cellular internalisation was not investigated further; even with lysates generated from iDC, which actively internalise antigen from their environment.

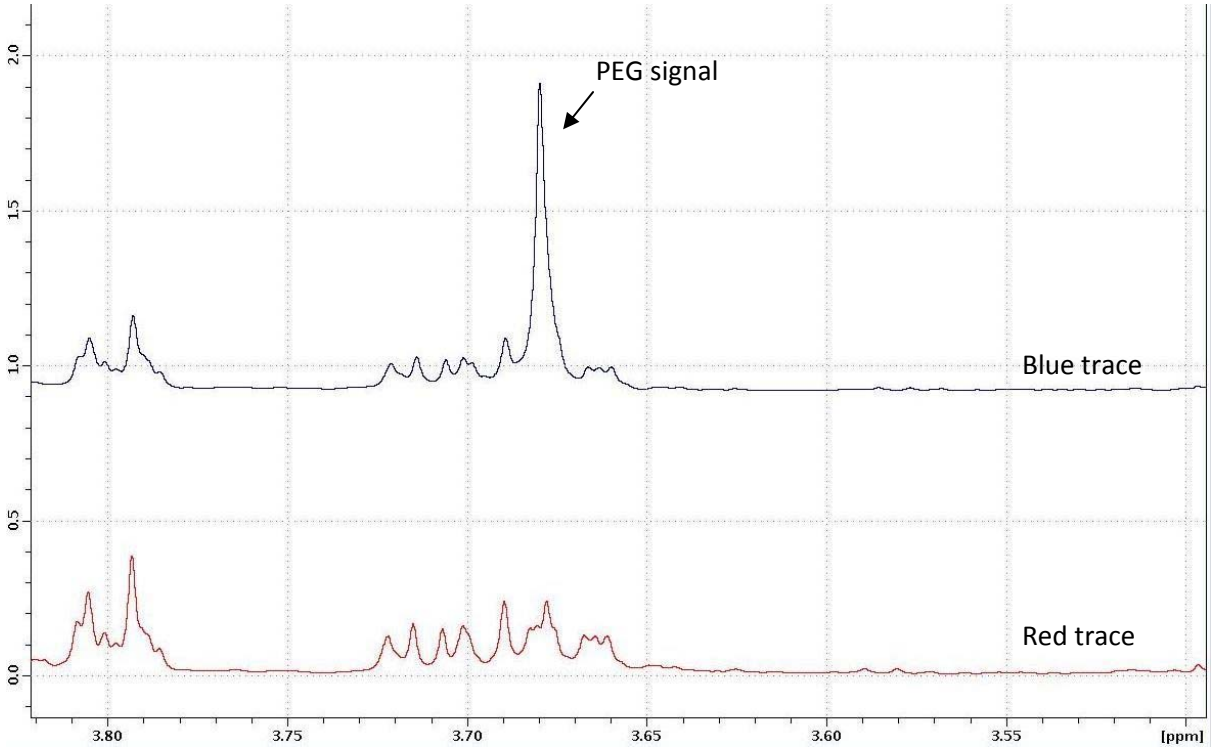

Figure 4.5: ^{40K}PEG-insulin is detectable in conditioned medium by ^{1}H NMR

^{40K}PEG-insulin was incubated with HepG2 cells for 24 hours after which the conditioned medium (blue) was removed and prepared for ^{1}H NMR analysis as described. ddH_2O was used as vehicle control (red).

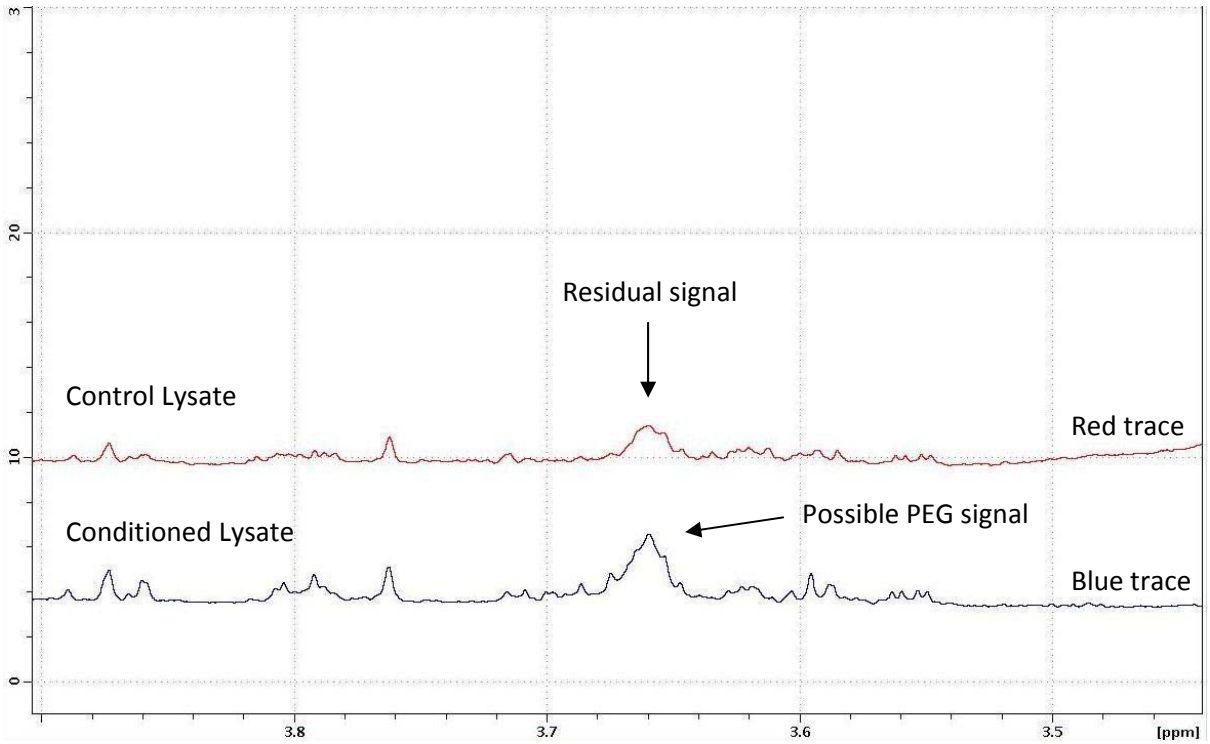

Figure 4.6: Possible PEG signal in conditioned lysate analysed by ^{1}H NMR

^{40K}PEG-insulin was incubated with HepG2 cells for 24 hours, after which conditioned lysate (blue) was prepared for ^{1}H NMR analysis as described. ddH_2O was used as vehicle control (red).

4.3.3 Flow Cytometry Analysis

Internalisation of PEG and PEGylated proteins was next assessed using flow cytometry, which requires the use of fluorescently labelled probes. Both iDC and mDC were incubated with two different MW PEG probes: 5 kDa and 40 kDa PEG-FITC. In comparison to iDC, mDC have a reduced endocytic phenotype and consequently the number of visible cells acquiring fluorescence was predicted to be less. Therefore, mDC were used to determine if endocytosis was the process by which PEG was being internalised, rather than simple diffusion, since the number of visible mDC that acquire fluorescence should be lower in comparison to iDC. The DC population was selected via gating, in which cells were selected for analysis based on the characteristic size and granularity of DC, as well as

selecting cells for analysis that only express high levels of the DC marker CD11c, as described in figure 4.7. Consequently, analysis was restricted to the DC population.

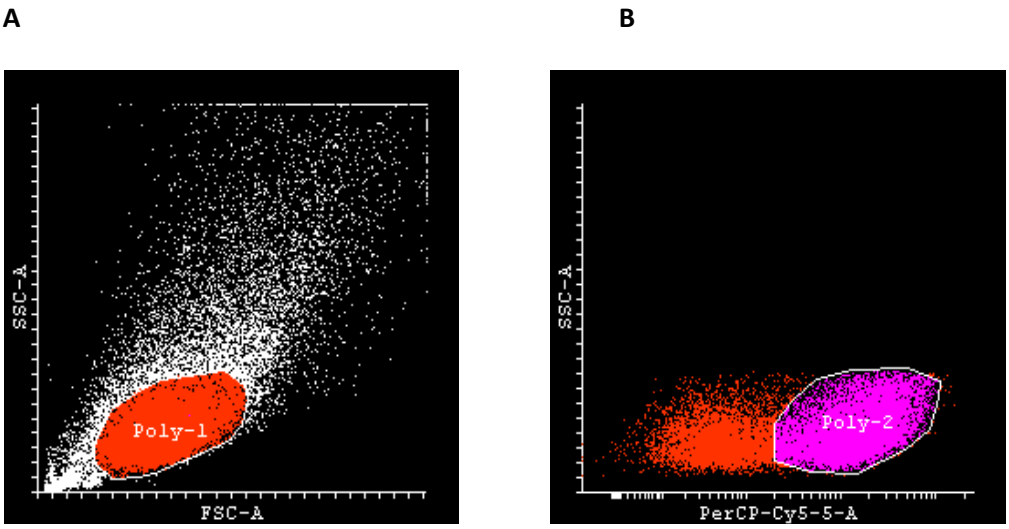

Figure 4.7: Gating

Analysis was restricted to the DC population only through the use of gating. A) Selection of DC population by size and granularity (cellular internal complexity). Forward-Scattered/Side-Scattered (FSC/SSC, respectively) plot represents cellular distribution by size (FSC) and granularity (SSC), enabling selection of the DC population, defined by the region Poly-1, based on characteristic DC size and granularity. Poly-1 was generated from unlabelled DC. B) Selection of DC population by expression of the DC marker CD11c. A DC population, Poly-2, was selected based on high expression of CD11c. Poly-2 was generated from DCs incubated with $Cd11c^{PE\text{-}Cy5.5}$ antibody only. Thus, in combination, these two gates, defined by the regions Poly-1 and Poly-2, restrict analysis to the DC population only, and were applied to all subsequent analyses.

Both iDC and mDC were incubated with 5 kDa PEG-FITC over 90 minutes and internalisation assessed by flow cytometry. In comparison with iDC, mDC internalised 5 kDa PEG-FITC at a lower rate, as shown in figure 4.8 C, as predicted. This indicated that uptake of 5 kDa PEG-FITC by iDC was most likely occurring through endocytosis and was not simply a result of the probe adhering to the cells over time, as, if this was the case, the percentage of visible cells acquiring fluorescence is likely to have been similar for both cell types. Next, both 5 kDa PEG-FITC and 40 kDa PEG-FITC were incubated with iDC over 2 hours. Perhaps surprisingly, both probes appeared to be internalised by iDC at almost identical rates (figure 4.9 C). The majority of uptake appeared to occur in the first 20 minutes, with approximately 50% of cells acquiring fluorescence when incubated with either probe. These data indicated that iDC can internalise PEG, and presumably PEGylated proteins, regardless of PEG MW. However, in these experiments it was possible that signal saturation had occurred since the percentage of visible cells acquiring fluorescence in all experiments quickly reached a plateau. This is most likely because of the relatively high concentrations of PEG-FITC incubated with the DC in these experiments, which was a direct consequence of the inability to detect cellular internalisation by either the gel-based assays or ^{1}H NMR in previous experiments. Therefore, since the aim of these experiments was to determine whether PEG MW can alter the cellular internalisation of a protein, higher concentrations of PEG-FITC were used with flow cytometry analysis, in comparison to earlier experiments, to enhance the detection of internalised PEG-FITC; rather than keeping the concentrations of the PEG probes in line with the *in vivo* plasma concentrations of ^{40K}PEG-insulin observed in the disposition study in chapter 2, concentrations which were used in earlier internalisation experiments. Consequently, to validate the results found using flow cytometry, fluorescence microscopy was subsequently used to assess the internalisation of PEG-FITC.

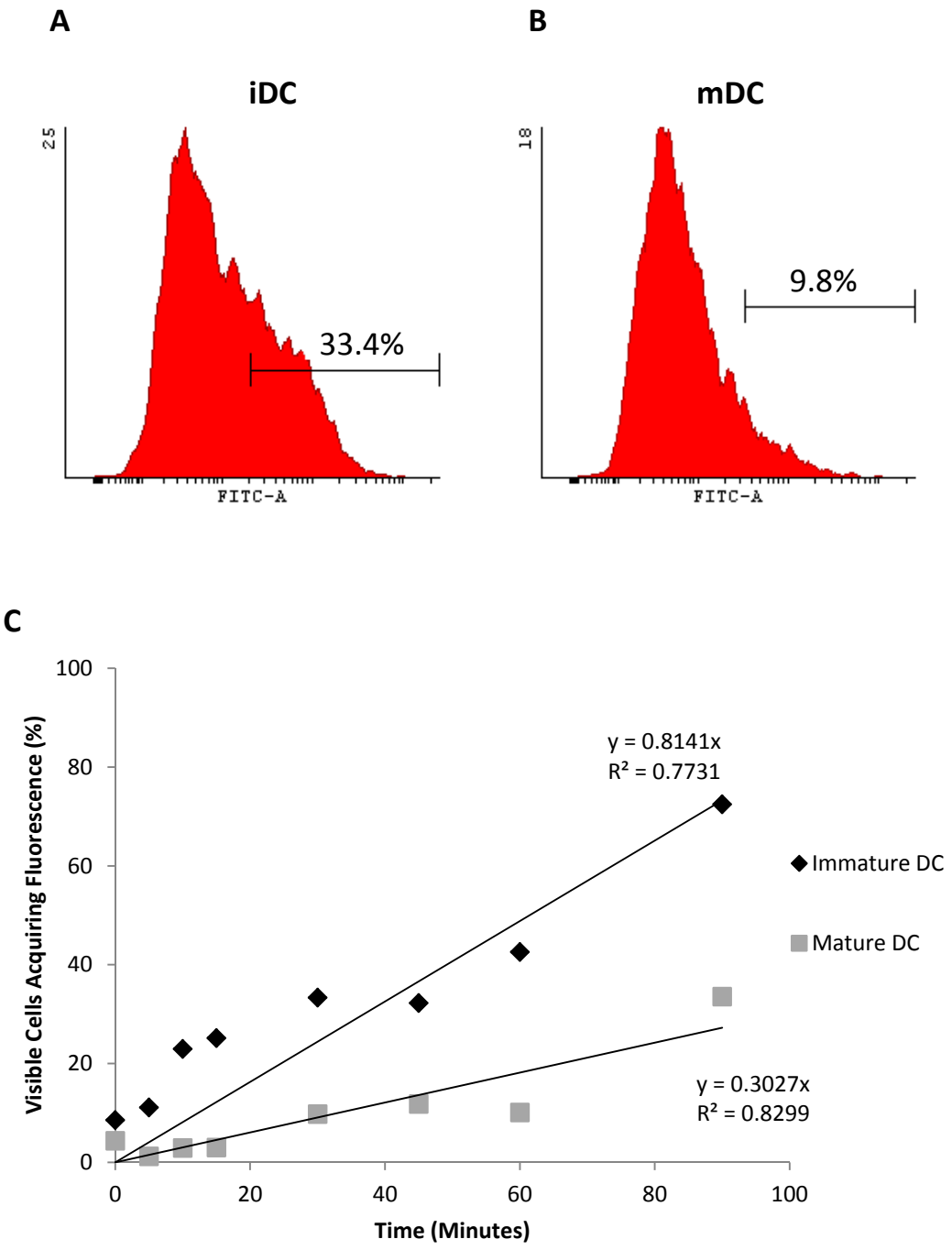

Figure 4.8: Differential internalisation of 5 kDa PEG-FITC by iDC and mDC

5 kDa PEG-FITC was incubated with either iDC or mDC for the stated times and internalisation determined by flow cytometry. A) Histogram plot of iDC incubated with 5 kDa PEG-FITC for 30 minutes, the percentage of visible iDC that have acquired fluorescence is indicated above the marker. B) Histogram plot of mDC incubated with 5 kDa PEG-FITC for 30 minutes, the percentage of visible mDC that have acquired fluorescence is indicated above the marker. C) Differential internalisation of 5 kDa PEG-FITC by iDC and mDC presented graphically as the percentage of visible cells acquiring fluorescence, with linear trend lines for each data set (intercept at (0, 0)).

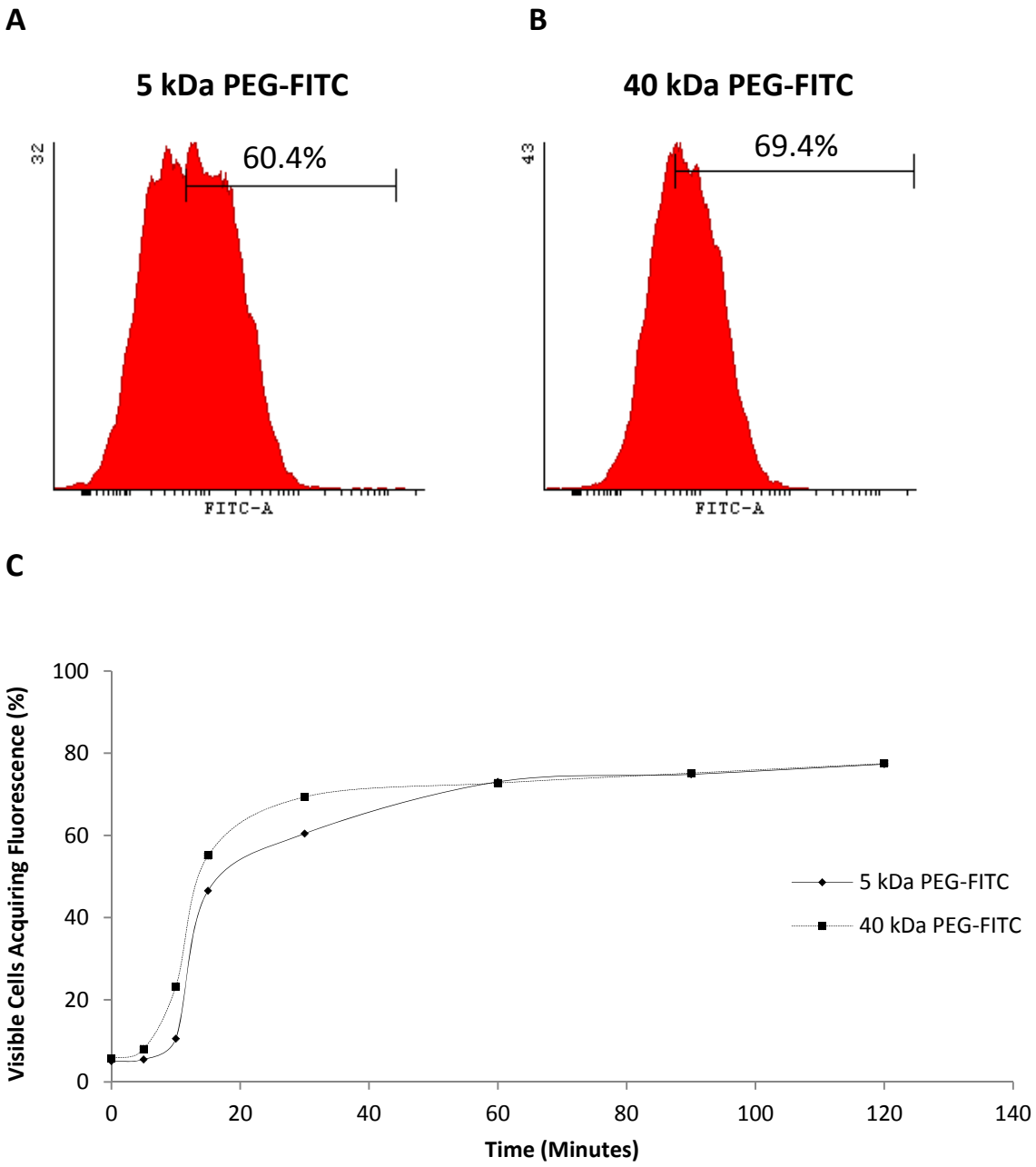

Figure 4.9: Similar internalisation of 5 kDa PEG-FITC and 40 kDa PEG-FITC by iDC

5 kDa PEG-FITC and 40 kDa PEG-FITC were incubated with iDC for the stated times and internalisation determined by flow cytometry. A) Histogram plot of iDC incubated with 5 kDa PEG-FITC for 30 minutes, the percentage of visible iDC that have acquired fluorescence is indicated above the marker B) Histogram plot of iDC incubated with 40 kDa PEG-FITC for 30 minutes, the percentage of visible iDC that have acquired fluorescence is indicated above the marker . C) Similar internalisation of 5 kDa PEG-FITC and 40 kDa PEG-FITC by iDC, presented graphically as the percentage of visible cells acquiring fluorescence.

4.3.4 Fluorescence Microscopy Analysis

Fluorescence microscopy offers the benefit of visually being able to ascertain the degree of endocytosis by iDC. In these experiments, the use of low temperature (4^{o}C) was used as a control for endocytosis, as well as the use of mDC, since endocytosis is an energy-dependent process; requiring heat in order to enable internalisation. Both 5 kDa and 40 kDa PEG-FITC were again used as probes for PEG internalisation by iDC. Two doses of PEG-FITC were used, 100 μg/mL and 1 mg/mL, and both were detected using fluorescence microscopy; however, the data presented in this chapter is generated from the 1 mg/mL concentrations only. Furthermore, a fluorescently-labelled insulin probe (insulin-rhodamine) was synthesised using a labelling kit purchased from Innova, in order to assess the internalisation of insulin alone by iDC.

The internalisation of 40 kDa PEG-FITC by iDC was first assessed using fluorescence microscopy over 24 hours. Hoechst staining was used to stain DNA, producing a bright, blue-fluorescence. Subsequently the nuclei of Hoechst-stained cells were easily visible as blue discs. FITC, a derivative of fluorescein, is a synthetic fluorophore which emits green fluorescence. Thus, the cellular internalisation of PEG-FITC can be easily ascertained using a combination of fluorescence microscopy and Hoechst staining. As observed in figure 4.10, 40 kDa PEG-FITC was internalised by iDC in a time-dependent manner over 24 hours; indicated by increased accumulation of green fluorescence in comparison to earlier time-points. No green fluorescence was observed in any of the corresponding vehicle control samples. Next, insulin-rhodamine was incubated with iDC over 24 hours. Rhodamine emits red fluorescence and therefore internalisation of insulin-rhodamine is indicated by increased accumulation of red fluorescence over time; which was exactly what was observed when the samples were analysed, as shown in figure 4.11. Again, no fluorescence was observed in any of the corresponding vehicle control samples.

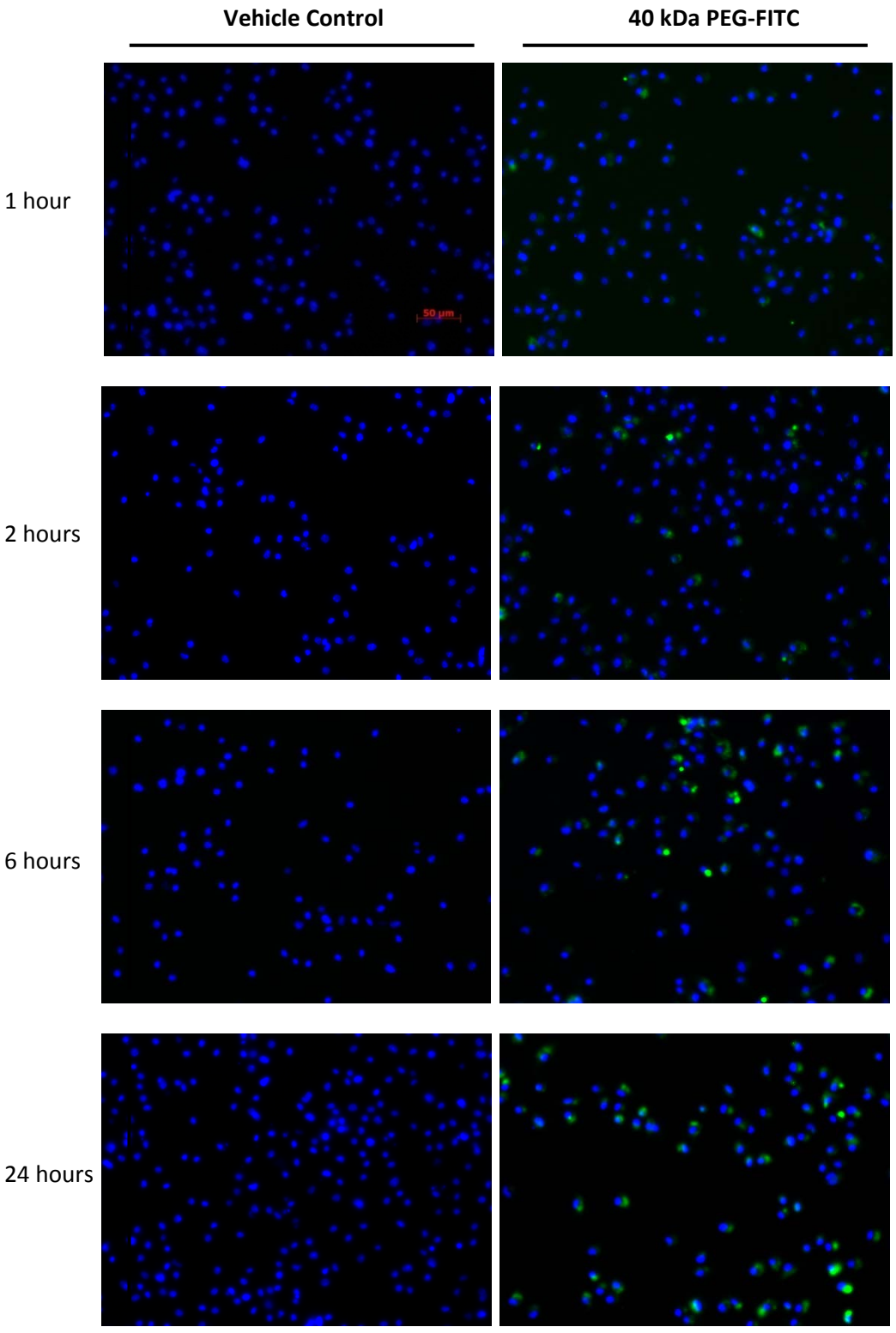

Figure 4.10: iDC internalise 40 kDa PEG-FITC

40 kDa PEG-FITC (1 mg/mL) was incubated with iDC at 37^{o}C over 24 hours and internalisation was assessed by fluorescence microscopy, as described.

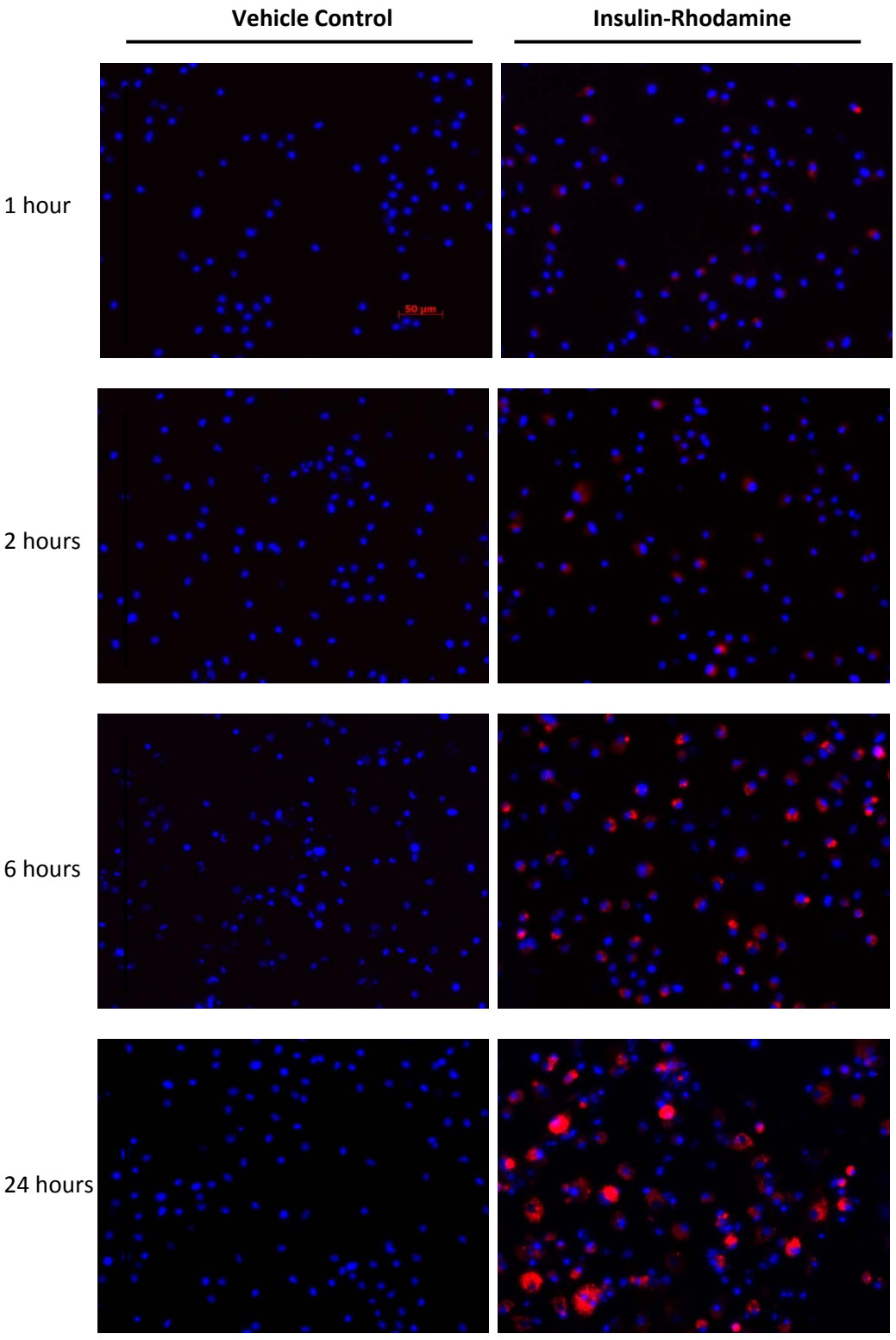

Figure 4.11: iDC internalise insulin-rhodamine

Insulin-rhodamine (200 µg/mL) was incubated with iDC at 37^{o}C over 24 hours and internalisation was assessed by fluorescence microscopy, as described.

5 kDa PEG-FITC was then incubated with iDC over 24 hours. Internalisation was again shown to be time-dependent and no fluorescence was observed in the vehicle control samples (data not shown). In comparison with 40 kDa PEG-FITC at 24 hours, the internalisation of both PEG-FITC probes was shown to be equivalent; as seen in figure 4.12. The number of visible cells which have acquired fluorescence when incubated with either 5 kDa or 40 kDa PEG-FITC (figure 4.12 B), as well as the signal intensity, presented as the mean corrected pixel intensity of internalised fluorescence (figure 4.12 C), are comparable between the two probes, indicating that PEGs of a MW between 5 and 40 kDa appear to be internalised by iDC to a similar degree.

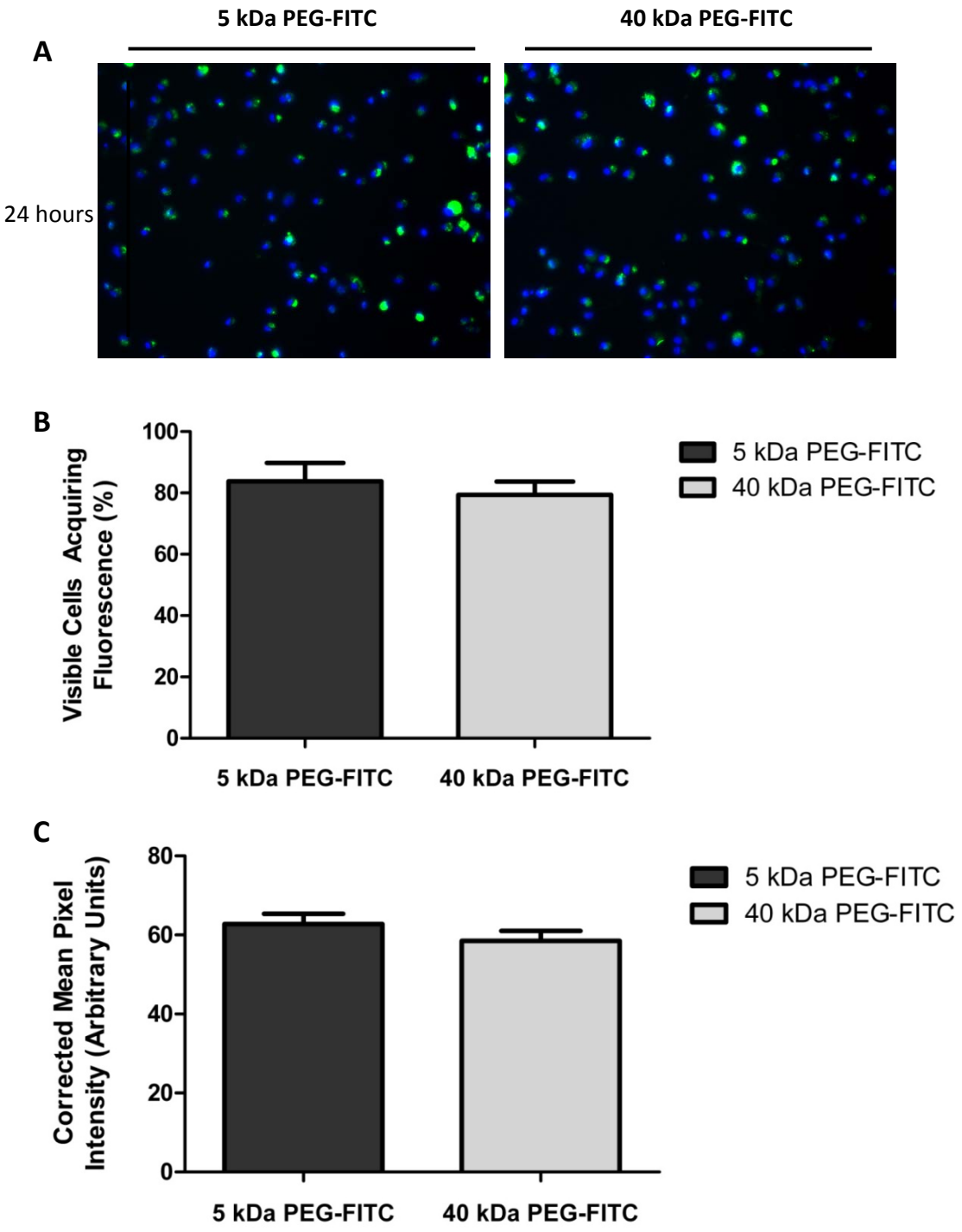

Figure 4.12: iDC internalise 5 kDa and 40 kDa PEG-FITC to a similar degree

5 kDa and 40 kDa PEG-FITC (1 mg/mL) were incubated with iDC at 37^{o}C over 24 hours and internalisation was assessed by fluorescence microscopy, as described. A) Representative images. B) The percentage of visible cells acquiring fluorescence. Data are presented as n=3 + SEM. C) Mean pixel intensity of acquired PEG-FITC fluorescence by each iDC present in all images (n=3) corrected for background intensity, + SEM. Images were analysed using ImageJ software.

To confirm these data and ensure that internalisation by endocytosis was indeed responsible for the apparent increases in fluorescence observed, the internalisation for both 5 kDa and 40 kDa PEG-FITC was compared between iDC and mDC, and also iDC incubated at 4^{o}C. As seen in figure 4.13, mDC exhibit a much reduced capacity to internalise 5 kDa PEG-FITC over the same time period in comparison to iDC; with both the number of cells acquiring fluorescence and the intensity of fluorescence signal highly diminished.

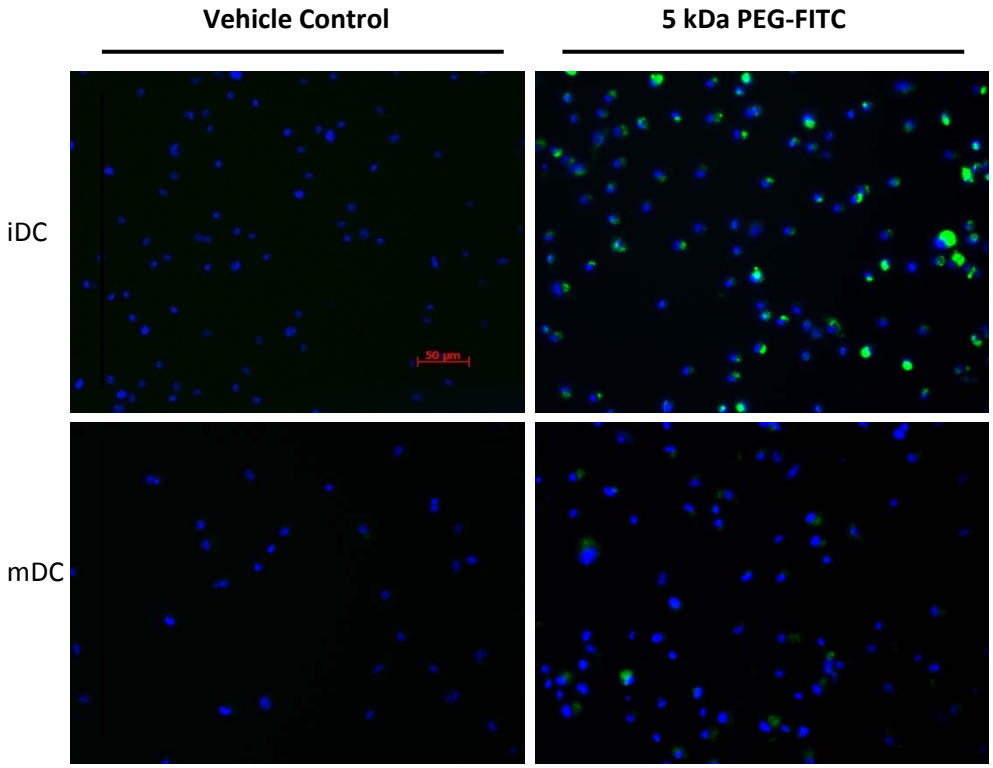

Figure 4.13: mDC exhibit reduced endocytic capacity for 5 kDa PEG-FITC

5 kDa PEG-FITC (1 mg/mL) was incubated with both mDC and iDC at 37^{o}C over 24 hours and internalisation was assessed by fluorescence microscopy, as described.

This result was also found when 40 kDa PEG-FITC was incubated with both mDC and iDC (figure 4.14).

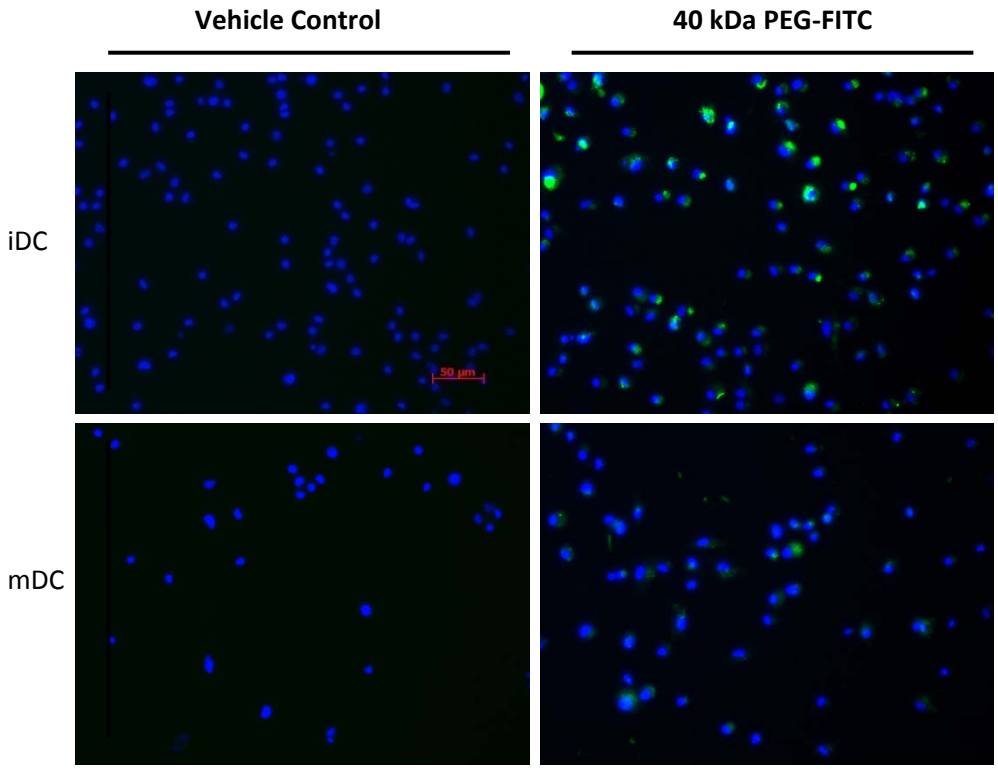

Figure 4.14: mDC exhibit reduced endocytic capacity for 40 kDa PEG-FITC

40 kDa PEG-FITC (1 mg/mL) was incubated with both mDC and iDC at 37^{o}C over 24 hours and internalisation was assessed by fluorescence microscopy, as described.

Next, the internalisation of both probes by iDC was assessed when cells were incubated at 4^{o}C. For both 5 kDa and 40 kDa PEG-FITC absolutely no internalisation was detected at all at 4^{o}C, figures 4.15 and 4.16, respectively. Taken together, these data indicate that iDC are indeed capable of internalising PEG, over a range of MWs concordant with the sizes of PEG currently used therapeutically, and that endocytosis, as expected, is the process by which internalisation occurs.

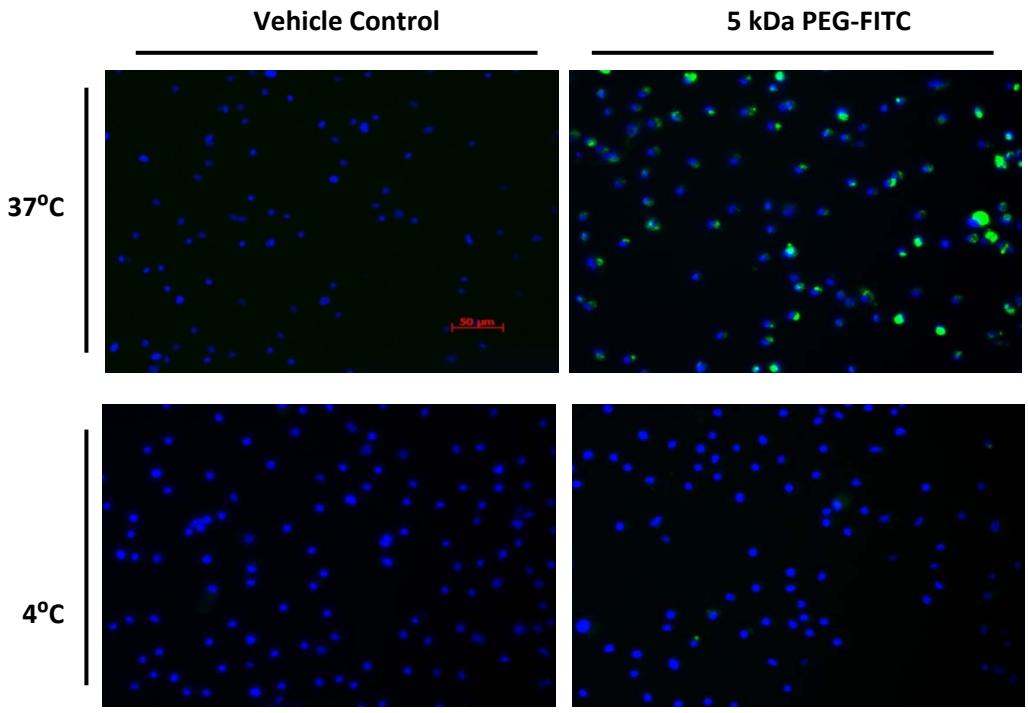

Figure 4.15: Endocytosis of 5 kDa PEG-FITC by iDC is inhibited at 4°C

5 kDa PEG-FITC (1 mg/mL) was incubated with iDC at both 4°C and 37°C over 24 hours and internalisation was assessed by fluorescence microscopy, as described.

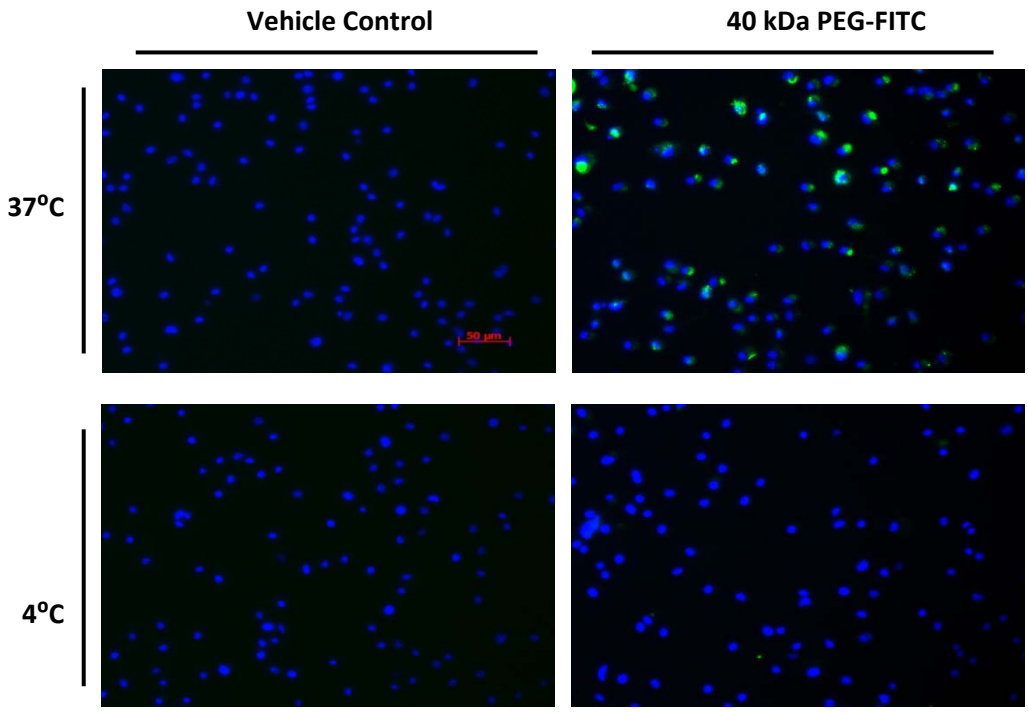

Figure 4.16: Endocytosis of 40 kDa PEG-FITC by iDC is inhibited at 4°C

40 kDa PEG-FITC (1 mg/mL) was incubated with iDC at both 4°C and 37°C over 24 hours and internalisation was assessed by fluorescence microscopy, as described.

4.4 DISCUSSION

Cellular internalisation followed by intracellular degradation/dissociation of ^{40K}PEG-insulin was shown to be the likely mechanism for the loss of insulin signal observed in chapter 2. It is also a requirement for immunological processing, of which various immune-mediated adverse drug reactions have been reported for a variety of PEGylated biologics, both in clinical trials and for those already marketed for therapeutic use. Furthermore, the precise effects that PEGylation may have on the immune response to proteins are currently poorly understood, as described in more detail in the general introduction. Potentially, PEGylation, in particular PEG MW, may have an effect on the cellular internalisation and disposition of a protein, which may have further repercussions in the generation of immune responses against the coupled protein. In this chapter, several different methodologies were assessed as tools to monitor the effect of PEGylation on the internalisation of proteins, in order to address the current limitations in our knowledge.

Initially, the multi-analytical platform described in chapters 2 and 3 was used to monitor the cellular internalisation of ^{40K}PEG-insulin. In chapter 2, a PEG moiety was shown to accumulate in the liver tissue of animals dosed with ^{40K}PEG-insulin. Consequently, these early studies focused on HepG2 cells (a human liver cell line) for early testing of cellular internalisation, as well as iDC generated from mice; thereby, attempting to replicate what had previously been observed *in vivo* in a suitable *in vitro* model, whilst also beginning to assess the internalisation of PEGylated proteins by APC. The gel-based assays, described in chapter 2, were first used to detect a range of ^{40K}PEG-insulin concentrations, incubated with both HepG2 and iDC, over a period of 6 hours. No ^{40K}PEG-insulin was detected in the cell lysates by any of the three assays, in either of the cell types, or at any timepoint. Furthermore, even when dosed with a lower MW PEG, 20 kDa PEG, no PEG was detected in the cell lysates. It was only when extending the incubation period to 24 hours that the internalisation of ^{40K}PEG-insulin could be detected by the gel-based assays. However, due

to the small size of the bands and inability to detect internalisation prior to 24 hours, techniques with enhanced sensitivity were required in order to provide improved monitoring of PEG and PEGylated protein internalisation. Furthermore, the anti-PEG assay also produced non-specific bands, which may have limited analysis. Subsequently, the utility of ^{1}H NMR was assessed, as described in chapter 3. Despite proving to be a useful tool for the detection and quantification of ^{40K}PEG-insulin in urine it was not amenable to the detection of internalised ^{40K}PEG-insulin, even at 24 hours post-dose and using a more powerful Bruker 800 MHz spectrometer, compared to the Bruker 600 MHz used in chapter 3. The spectrometer was capable of detecting PEG in conditioned media; however, the resonance signal was clearly overlapping with other resonances that had not been removed by deproteination of the sample. These overlapping signals were also observed in control media. When cell lysates were analysed 24 hours post-dose, again, a residual resonance at the same chemical shift as PEG was visible in the control cell lysate. Whilst a signal at PEG's chemical shift was detected in the corresponding conditioned cell lysate it was roughly equivalent to the signal observed in the control cell lysate. Indeed, it is likely that this residual resonance was contributing the majority of the signal observed for the apparent PEG signal in the conditioned cell lysate. Thus, under these conditions, ^{1}H NMR, whilst sensitive, was shown to be inadequately specific for the detection of internalised PEG, and alternative methods were sought. The methods selected were flow cytometry and fluorescence microscopy, which can be used to detect fluorescently labelled compounds. Two different fluorescently labelled PEGs, 5 kDa and 40 kDa PEG-FITC, were used to assess if PEG MW can affect internalisation by iDC. Ideally, sophisticated dual-labelled PEGylated proteins, with different fluorophores attached separately to the PEG and protein moieties of the conjugate, would provide the best analytical substrate for these methods. Since these were not available, the internalisation of different MW PEG-FITC species was compared with that of insulin labelled with rhodamine, using a commercially available kit.

In these experiments, the use of mDC was used as a negative control for internalisation by endocytosis. Endocytosis is the process by which iDC internalise foreign antigen. When iDC internalise antigen they are stimulated to become mDC, which typically have a much reduced endocytic capacity, but enhanced ability to process and present antigen. Therefore, the internalisation of PEG-FITC by mDC should be reduced in comparison with iDC. Using flow cytometry initially, the internalisation of 5 kDa PEG-FITC by mDC was shown to be reduced in comparison to iDC, as expected. Interestingly, the internalisation of both 5 kDa and 40 kDa PEG-FITC by iDC was shown to be remarkably similar, despite the 35 kDa difference in MW. However, under the initial conditions used for these flow cytometry experiments signal saturation was potentially causing the number of cells acquiring fluorescence to plateau rapidly, and so the focus then became on assessing the utility of fluorescence microscopy to further validate this finding. Again, in these experiments the use of mDC as a negative control for endocytosis was incorporated. Additionally, incubations at 4^{o}C were also used as a negative control for endocytosis, since low temperatures inhibit the energy-dependent process. Using fluorescence microscopy, 5 kDa PEG-FITC, 40 kDa PEG-FITC and insulin-rhodamine were all internalised in a time-dependent manner over 24 hours. No fluorescence was detected in the vehicle controls or in conditions incubated at 4^{o}C, and internalisation by mDC was consistently lower in comparison. Taken together, these data indicate that iDC are internalising all three probes by endocytosis. Interestingly, when comparing the number of cells acquiring fluorescence at 24 hours post-dose between iDC incubated with 5 kDa and 40 kDa PEG-FITC, the numbers were again remarkably similar; with 83.8% ± 6.0 of iDC internalising 5 kDa PEG-FITC compared to 79.4% ± 4.4 of iDC internalising 40 kDa PEG-FITC. These data are approximately equivalent to the data obtained using flow cytometry, despite the onset of saturation. Furthermore, when comparing the mean pixel intensity of internalised fluorescence between the two probes at 24 hours dose, the numbers are again remarkably

similar, with a mean pixel intensity of 62.8 ± 2.6 (arbitrary units) for 5 kDa PEG-FITC, compared to 58.5 ± 2.5 for 40 kDa PEG-FITC. Whilst these data can not quantify the actual amounts of each probe internalised, the signal intensity of internalised PEG-FITC does provide a semi-quantitative indicator of overall differences in the internalisation of each probe, of which there was shown to be minimal difference at 24 hours. Taken together, these data support the finding that iDC internalise PEGs between 5 and 40 kDa to a similar degree in terms of the overall number of PEG-FITC molecules internalised, since each PEG is coupled to one FITC molecule.

In conclusion, whilst the multi-analytical platform, described in chapters 2 and 3, is capable of measuring the *in vivo* disposition and biological fate of PEGylated proteins over 28 days, it was not amenable for the *in vitro* monitoring of the effect of PEGylation on cellular internalisation over 24 hours. Whilst the gel-based assays could detect internalisation at 24 hours, the sensitivity of the assays would have hindered analysis, particularly as longer timepoints would have been required to adequately investigate the effect of PEGylation on cellular internalisation, which, when analysed *in vitro*, would have represented a difficult scenario too different to the *in vivo* environment. Consequently, alternative techniques were assessed. Fluorescence microscopy was shown to be a sensitive technique for the detection of fluorescently labelled PEG and insulin internalisation, which was confirmed to occur by endocytosis through the use of appropriate negative controls – rather than simply adhering to the surface of the cells. Again, the internalisation of two different MW PEGs was shown to be incredibly similar. Insulin-rhodamine was also internalised by iDC. Ideally, a dual-labelled probe would have provided complementary information on both the PEG and protein moieties, in a similar vein to the gel-based assays as described in chapter 2. However, such analytes were not readily available. Whilst in theory it was possible to also fluorescently label ^{40K}PEG-insulin, since, according to the manufacturer's instructions the rhodamine is covalently linked to

free amine groups, of which insulin has up to four, the PEG moiety is covalently linked to the N-terminal α-amino group and may also protect the remaining amine groups from conjugation. Thus, in all likelihood a heterogeneous mixture of rhodamine labelled ^{40K}PEG-insulin would have been formed, which potentially would have limited conclusions drawn from comparisons between internalisation of the two probes. Furthermore, given that iDC appear to have no difficulty in internalising either 5 kDa or 40 kDa PEG-FITC, it is unlikely that the addition of insulin (MW ~ 5.8 kDa) to either PEG MW would have significantly altered its internalisation by endocytosis by iDC. The two different PEGs used in this study are of MWs routinely attached to therapeutic proteins to improve their pharmacokinetics. These data indicate that PEG MW is unlikely to alter the internalisation of proteins by iDC over the clinically relevant PEG MW range used in this study; since both probes, in terms of the number of PEG molecules, were internalised to a similar degree.

CHAPTER 5

Intracellular Disposition of PEGylated Proteins: Lysosomal Degradation

CONTENTS

Intracellular Disposition of PEGylated Proteins: Lysosomal Degradation

5.1 INTRODUCTION

Lysosomal degradation is the major route for exogenous protein degradation in the cell. The internalisation of exogenous protein, such as a PEGylated protein, by endocytosis culminates in its degradation inside lysosomes; the end-point of the endocytic pathway. As described in the general introduction, the lysosome is a vesicle containing many different hydrolase enzymes, which, together, are capable of digesting the majority of macromolecules that enter the organelle. Furthermore, lysosomal hydrolase enzymes are also involved in processing internalised proteins into peptides for display to the immune system, the next step *en route* to producing an immune response. Certain peptides will be bound by MHC class II molecules present in the lysosome, forming peptide-MHC II complexes that subsequently translocate to the plasma membrane for display and recognition by $CD4^+$ T cells – stimulation of which initiates a cascade of events; involving proliferation and differentiation of the stimulated $CD4^+$ T cell, and eventually culminating in the generation of neutralising antibodies (nAb) against the original antigen or protein, which can compromise efficacy and precludes effective drug therapy – forcing clinicians to adopt alternative drug regimens, as described in the general introduction. As mentioned in previous chapters, how PEGylation may alter the intracellular disposition, or reduce the immunogenicity, of a coupled protein is poorly understood. PEGylation is not a universal tool to ameliorate the immunogenicity of a given protein, and, furthermore, PEGylation can also result in a new immunogenicity targeted against PEG itself. This chapter aims to address these issues and continues the body of work described in earlier chapters by focussing on the effect of PEG MW on intracellular degradation of a model protein (insulin), mediated by the lysosome, which has potential implications for the immune processing of a PEGylated protein. This chapter consequently describes the enrichment of a lysosome fraction derived from human liver.

5.2 METHODS AND MATERIALS

All reagents were purchased from Sigma-Aldrich Company Ltd (Dorset, UK), unless otherwise stated.

5.2.1 Lysosome Enrichment from Human Liver

An enriched lysosome fraction (L^+) from human liver was obtained, characterised and used to degrade insulin and a series of PEGylated insulins through adapting existing methods as well as protocols from lysosome isolation kits (Sigma-Aldrich: catalogue number LYSISO1, Pierce: catalogue number 89839) (Egger *et al.*, 2011; Wozniak *et al.*, 2008).

5.2.1.1 Liver Homogenisation and Centrifugation

Human liver (8.8 g starting material) was minced and placed in 4 volumes of 250 mM sucrose containing 10 mM tris-acetate, pH 7.0. Liver pieces were homogenised using an Oscillating Mill MM 400 at $30s^{-1}$ for 3 minutes. The homogenate was centrifuged at 1,000 *g* for 10 minutes at 4^oC. The post nuclear supernatant (PSN) was removed and the resulting pellet washed in 5 mL sucrose buffer, re-centrifuged and the resulting supernatant added to the original PSN. The PSN was then centrifuged at 20,000 *g* for 20 minutes at 4^oC. The supernatant was discarded and the pellet obtained suspended in 5 mL sucrose buffer. This fraction was termed the crude lysosomal fraction (CLF).

5.2.1.2 Calcium Chloride Precipitation

The CLF was adjusted to 8 mM calcium chloride ($CaCl_2$) (from a 250 mM stock solution) and placed on ice for 10 minutes, after which the CLF was centrifuged at 5,000 *g*

for 10 minutes at 4°C. The resulting supernatant was removed and divided into working aliquots and stored at -80°C to release lysosomal content. This was termed the L^+ fraction.

5.2.2 Synthesis of ^{20K}PEG-insulin and ^{30K}PEG-insulin

PEGylated insulin was synthesised as described in section 2.2.1. Both conjugates were synthesised using PEG reagents kindly donated by Dr. Reddy's.

5.2.3 Lysosomal Degradation of Insulin and PEGylated Insulin *in vitro*

Insulin and PEGylated insulin were incubated at 37 °C ± the L^+ fraction, at the stated amounts, in a 60 µL final volume of 100 mM citrate buffer containing 2 mM dithiothreitol (DTT), pH 4.5.

5.2.3.1 Western Blot Analysis

At the stated times, 10 µL aliquots were taken, diluted 1:2 with ddH_2O and stored at -80°C prior to analysis via western blot, as previously described in section 2.2.7. For detection of LAMP1 by western blot, the protocol was as described in section 2.2.7, but blots were blocked in 5% BSA and incubated at 4°C overnight in primary antibody (1:500 dilution) (Abcam, ab24170), secondary antibody (1:3000 dilution) was incubated for 1 hour at room temperature (Dako, P0448).

5.2.3.2 LC-ESI-MS/MS Analysis

Mass spectrometry (MS) was used to assess the effect of PEGylation on the peptide repertoires generated following lysosomal degradation. After 30 minute incubations, samples were passed through a 0.5 mL 3 kDa MWCO centrifugal filter (Amicon), according to manufacturers instructions, and stored at -80°C prior to delivery into a Triple TOF 5600 mass spectrometer (AB Sciex) by automated in-line reversed phase liquid chromatography

using an Eksigent NanoUltra cHiPLC System mounted with a microfluidic trap and an analytical column (15 cm x 75 µm) packed with ChromXP C_{18}–CL 3 µm, a NanoSpray III source was fitted with a 10 µm inner diameter PicoTip emitter (New Objective). Samples were loaded onto the trap in 0.1% formic acid, which was then washed for 10 minutes (2 µL/min) with 2% ACN/0.1% FA before switching in-line with the analytical column. A gradient of 2 – 50% (v/v) ACN/0.1% (v/v) FA was applied to the column over 75 minutes at a flow rate of 300 nL/min. Spectra were acquired automatically in positive ion mode using information-dependent acquisition powered by Analyst TF 1.5.1. software; using mass ranges of 400 – 1600 atomic mass units (amu) in MS and 100 – 1400 amu in MS/MS. Up to 25 MS/MS spectra were acquired per cycle (~ 10 Hz) using a threshold of 100 counts/second, with dynamic exclusion for 12 seconds and rolling collision energy. The instrument was automatically calibrated after every fifth sample using a β-galactosidase digest. Peptide sequences were identified with ProteinPilot software (v4.0) using the Paragon algorithm and the most recent version of the SwissProt database (Shilov *et al.*, 2007). No digestion enzyme was selected as the target specificities of the multiple lysosomal enzymes were unknown. Biological modifications were allowed. The differential detection of insulin peptides was confirmed via visual inspection of MS and MS/MS spectra.

5.3 RESULTS

An enriched lysosome fraction (L^+ fraction) was generated from human liver. The L^+ fraction was shown to contain functional lysosomes capable of degrading protein substrates.

5.3.1 Enrichment and Characterisation of the L^+ Fraction

Prior to enriching lysosomes from human liver, the methodology employed to do so was optimised using a variety of different starting materials. Lysosome fractions were

initially prepared from HepG2 cells, which were shown to contain functional lysosomes. A functional lysosome fraction was also obtained from mouse liver (data not shown), using identical methodology to that used for human liver tissue. An attempt was also made to acquire lysosomes from Epstein-Barr virus transformed human B cells (data not shown); however, this did not yield a functional fraction using our general methodology. Thus, the majority of method development occurred using HepG2 lysosome fractions, which was then applied to the generation of lysosomes from mouse liver, and finally translated to the enrichment of an L^+ fraction from human liver. From HepG2, a crude lysosomal fraction (CLF) was generated. By using western blot, the HepG2 CLF was shown to contain LAMP1 (lysosomal-associated membrane protein 1): an abundant lysosomal transmembrane protein that was used as a marker for lysosomes, as shown in figure 5.1 A. Next, the proteolytic capacity of the CLF was assessed using BSA as a model substrate, as shown in figure 5.1 B. BSA was incubated ± HepG2 CLF at a 1:1.6 (w/w) protein ratio of BSA to CLF over a period of 7 days. Degradation was assessed by SDS-PAGE and Coomassie stain. As shown in figure 5.1 B, BSA is stable over 7 days (though there is a slight loss in protein on day 7, which may be attributable to BSA auto-degradation), however, in the presence of HepG2 CLF BSA was degraded to the extent that the band was barely visible on day 7. To determine whether this loss of signal was lysosomal-mediated, repeat incubations were set up; either using CLF that had been boiled (to denature the lysosomal enzymes), or in the presence of leupeptin – a lysosomal protease inhibitor. In both these conditions, the degradation of BSA was inhibited to the extent that no loss of BSA signal was apparent when compared with the corresponding timepoints incubated without CLF, as also shown in figure 5.1 B. Thus, an enriched lysosome fraction was obtained from HepG2 cells and was shown to be proteolytically capable. Furthermore, aliquots of the HepG2 CLF were shown to be equally capable of degrading BSA after extended periods stored frozen at -80^{o}C (data not shown).

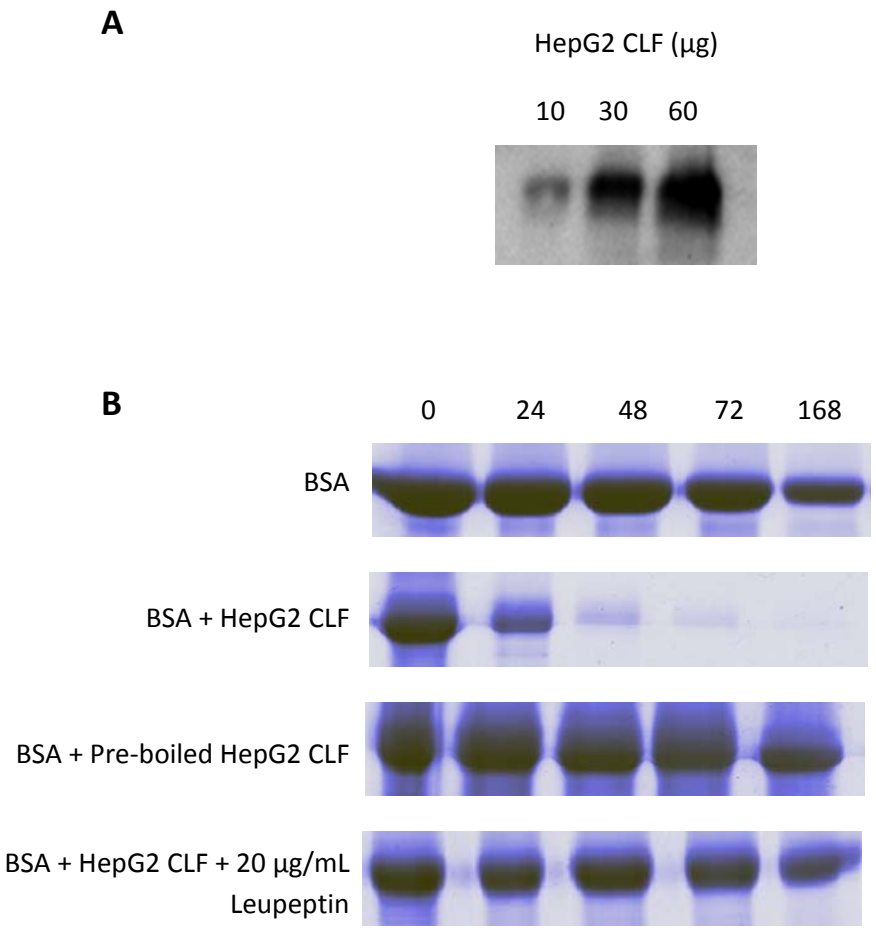

Figure 5.1: Characterisation and optimisation of lysosome fractions

A) Anti-LAMP1 western blot of 10, 30 and 60 µg CLF protein, originating from HepG2. B) Proteolytic capacity of lysosome fractions originating from HepG2. BSA (1 mg/mL) was incubated with HepG2 CLF (1.6 mg/mL) either alone, boiled (10 minutes at 100^{o}C) or in the presence of 20 µg/mL leupeptin (lysosomal protease inhibitor) over 7 days. Degradation was assessed by SDS-PAGE and coomassie stain. All data are representative examples taken from various experiments.

These methods were then applied to the generation of lysosome fractions from mouse liver and, eventually, human liver. The initial homogenisation step used to generate HepG2 CLF was mild sonication, however, for liver tissue, an oscillating mill was used since this was shown, under the conditions used in this study, to satisfactorily homogenise the tissue so that only ~75% of cells are disrupted, as determined by trypan blue exclusion; any

higher incurs the risk of also disrupting lysosome integrity. Furthermore, for generating lysosome fractions from liver tissues, an extra purification step, $CaCl_2$ precipitation, was incorporated. This step helps to remove residual endoplasmic reticulum and mitochondria, although it may also result in partial loss of lysosome yield. This step was shown to be successful in producing functional enriched L^+ fractions from liver tissues with much less residual protein content, as determined by comparing coomassie stains and the rates of BSA degradation between the CLF and L^+ fractions (data not shown). However, it was not as effective when used to further purify HepG2 CLF (data not shown), though this may be due to the much larger starting amounts of material available when preparing lysosomes from liver tissue in comparison from HepG2 cells. Thus, an enriched L^+ fraction was obtained from human liver that was shown to contain functional lysosomes.

5.3.2 Stability of PEG to lysosomal degradation

Initial degradation studies using lysosome fractions derived from HepG2 cells focused on the stability of the PEG component to lysosomal degradation. In these studies, it was shown that 40 kDa PEG, either alone (figure 5.2 A) or when coupled to insulin (figure 5.2 B), was stable over a period of 7 days when incubated with CLF, with no visible loss of signal observed when analysed by either the BaI_2 stain, for PEG alone (5.2 A), or the anti-PEG western blot, for PEG conjugated to insulin (5.2 B). Next, the stability of insulin alone and the insulin moiety of ^{40K}PEG-insulin were assessed over 7 days by either Coomassie stain or anti-insulin western blot. No insulin could be detected by either assay past day 0, indicating that shorter time courses were required to monitor the lysosomal degradation of insulin (data not shown). In these subsequent studies with shorter time course the L^+ fraction, from human liver, was used as the source of lysosomal proteases, and the effect of PEG MW on the lysosomal degradation of insulin was assessed.

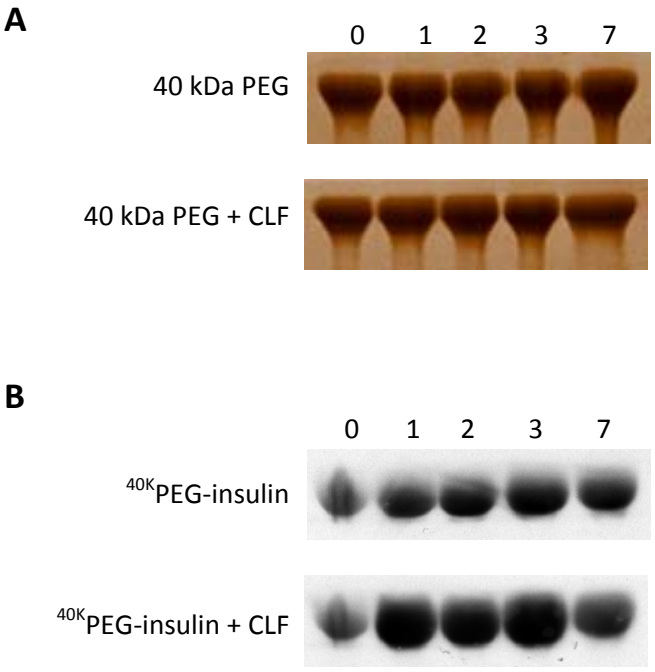

Figure 5.2: Stability of PEG to lysosomal degradation

40 kDa PEG (A) or ^{40K}PEG-insulin (B) was incubated ± HepG2-derived CLF, at a ratio of 1:1.6 mg/mL (PEG to CLF), over a period of 7 days. Stability was assessed by the BaI_2 stain (A) or anti-PEG western blot (B).

5.3.3 Lysosomal Degradation of Insulin and PEGylated Insulin

The effect of PEGylation on the lysosomal degradation of insulin was assessed using the enriched L^+ fraction, obtained from human liver, and the range of PEGylated insulins synthesised as described. Insulin and the three PEGylated insulins were incubated at 37°C ± L^+, at a ratio of 1:1.6 insulin to L^+ (w/w). The increase in MW between 20 kDa, 30 kDa and 40 kDa PEGylated insulin was taken into account such that incubations contained equivalent amounts of insulin to the non-PEGylated insulin incubation, as well as identical ratios of substrate to L^+. Degradation was assessed by SDS-PAGE and anti-insulin western blot. Over a 6 hour period, in the presence of L^+, insulin was completely degraded within 2 hours, with no insulin bands visible from this timepoint onwards, as shown in figure 5.3.

When insulin was PEGylated with either 20 kDa, 30 kDa or 40 kDa PEG, the insulin moiety was again degraded to completion within 2 hours regardless of the PEG MW attached, as shown in figures 5.4, 5.5 and 5.6, respectively. These data are summarised in figure 5.7, which shows the lysosomal degradation of insulin and all three PEGylated insulins overlaid. From figure 5.7, it is clear that PEG, between 20 and 40 kDa, has no protective effect against *in vitro* lysosomal degradation when conjugated to insulin.

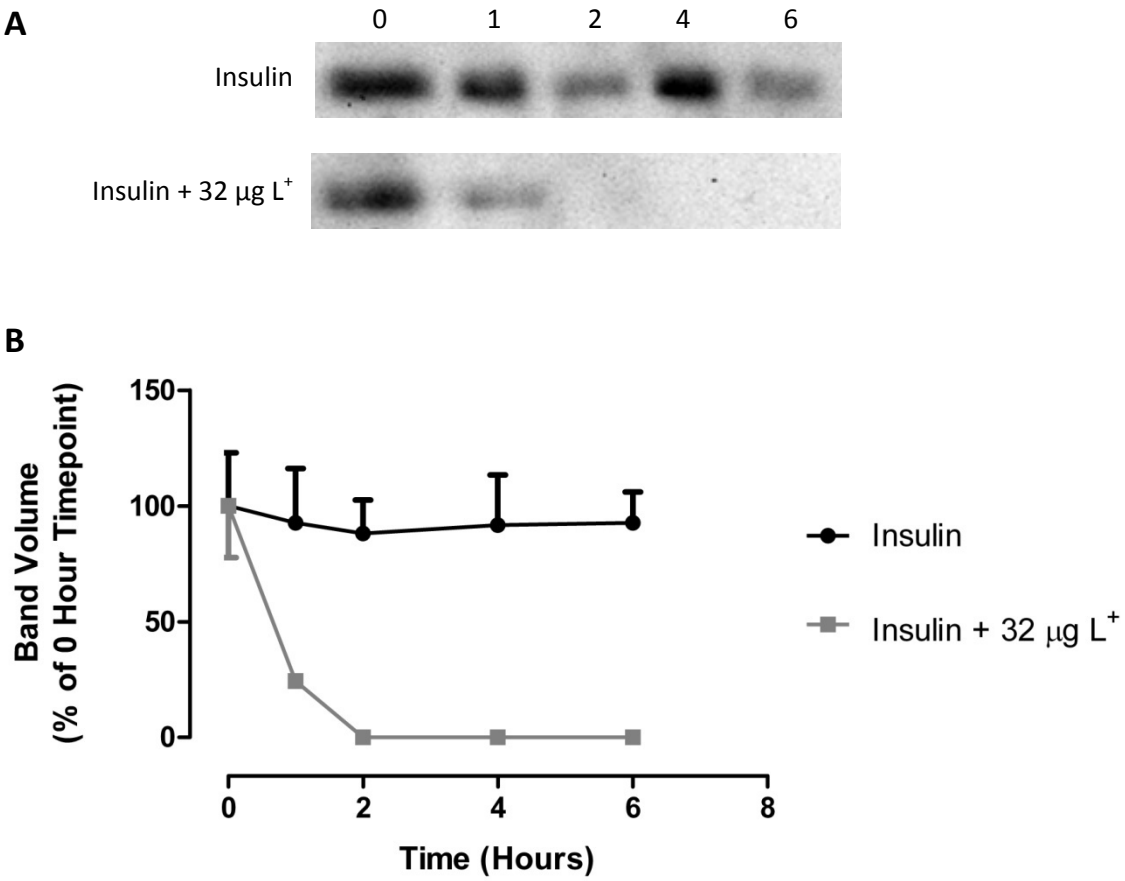

Figure 5.3: Lysosomal degradation of insulin

Insulin (20 μg) was incubated ± 32 μg L^+ fraction (human liver) over 6 hours. Degradation was assessed by SDS-PAGE and anti-insulin western blot. A) Representative blots; B) Densitometric analysis. Data are presented as the mean band volumes as a percentage of the 0 hour timepoint ± SEM. N=3.

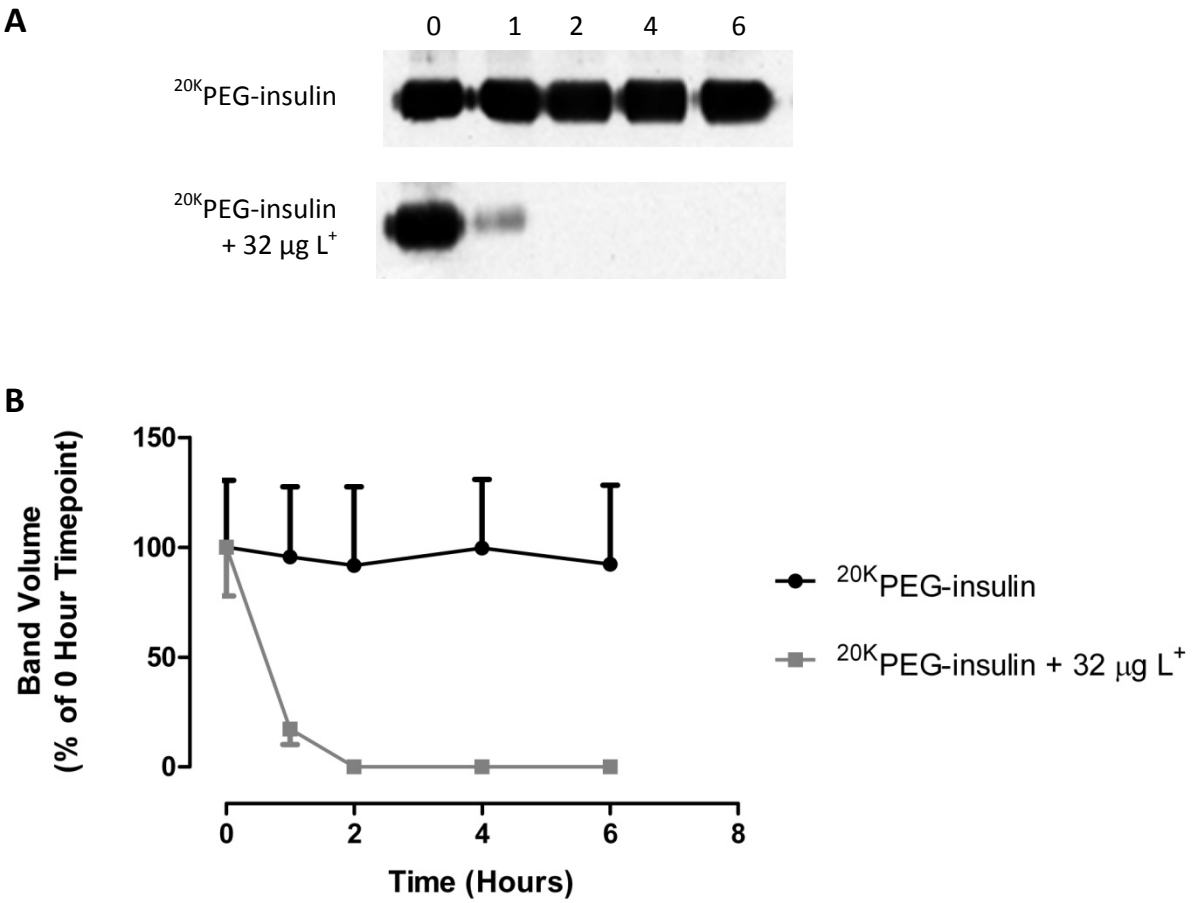

Figure 5.4: Lysosomal degradation of ^{20K}PEG-insulin

^{20K}PEG-insulin (88.8 µg, of which ~20 µg is insulin) was incubated ± 32 µg L^+ fraction (human liver) over 6 hours. Degradation was assessed by SDS-PAGE and anti-insulin western blot. A) Representative blots; B) Densitometric analysis. Data are presented as the mean band volumes as a percentage of the 0 hour timepoint ± SEM. N=3.

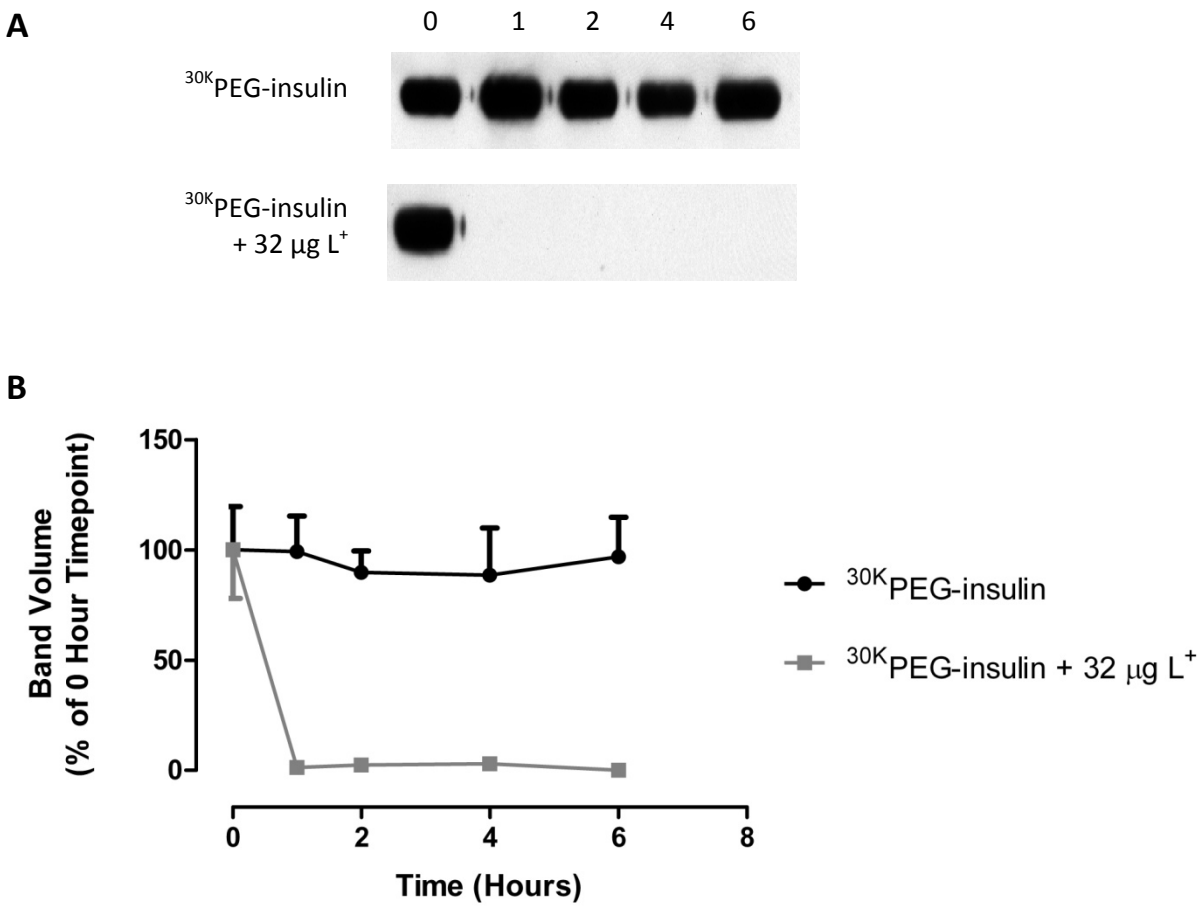

Figure 5.5: Lysosomal degradation of ^{30K}PEG-insulin

^{30K}PEG-insulin (123.4 µg, of which ~20 µg is insulin) was incubated ± 32 µg L^+ fraction (human liver) over 6 hours. Degradation was assessed by SDS-PAGE and anti-insulin western blot. A) Representative blots; B) Densitometric analysis. Data are presented as the mean band volumes as a percentage of the 0 hour timepoint ± SEM. N=3.

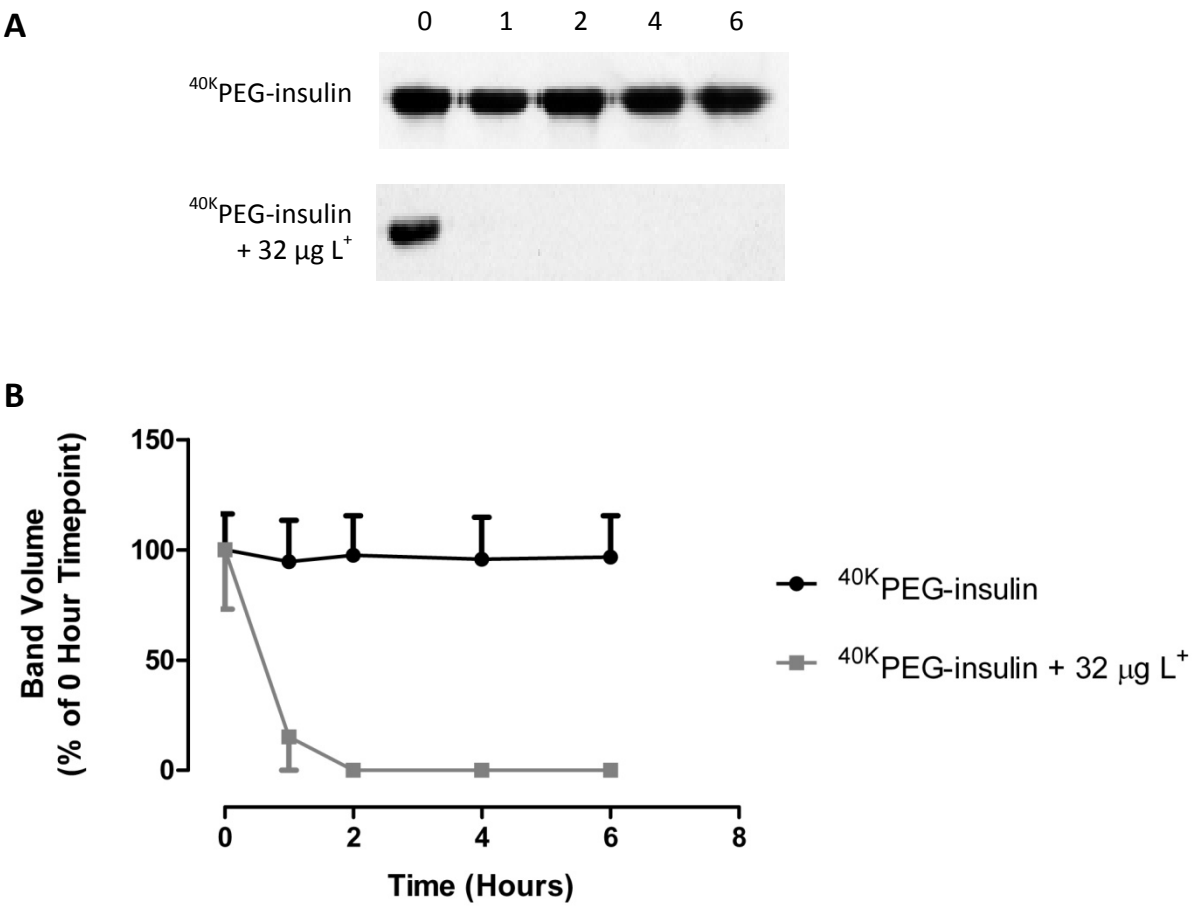

Figure 5.6: Lysosomal degradation of ^{40K}PEG-insulin

^{40K}PEG-insulin (157.7 µg, of which ~20 µg is insulin) was incubated ± 32 µg L^+ fraction (human liver) over 6 hours. Degradation was assessed by SDS-PAGE and anti-insulin western blot. A) Representative blots; B) Densitometric analysis. Data are presented as the mean band volumes as a percentage of the 0 hour timepoint ± SEM. N=3.

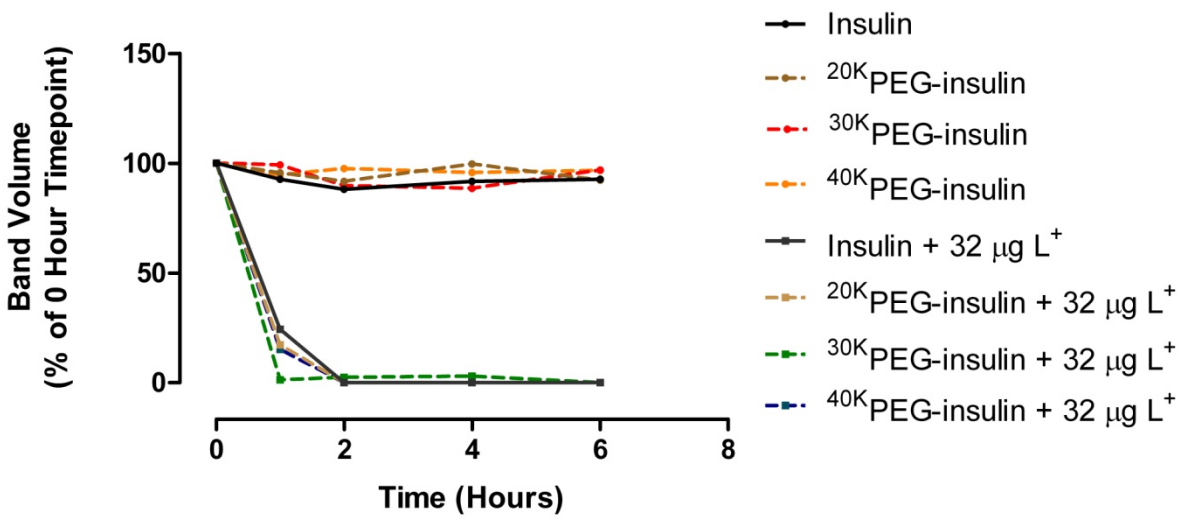

Figure 5.7: Lysosomal degradation comparison

Comparison of the lysosomal degradation of insulin with each PEGylated insulin. Data are presented as the mean band volumes as a percentage of the 0 hour timepoint. N=3.

To further confirm this, the study was repeated twice using reduced amounts of L^+ (4 and 16 μg). Degradation should proceed slower at lower concentrations of L^+, thus allowing a more detailed time course to be defined for the loss of insulin and potentially providing an opportunity to better ascertain if PEGylation does have a MW-dependent protective effect against lysosomal degradation. Slower insulin degradation with reduced amounts of L^+ was found for each PEGylated insulin, as shown in figures 5.8, 5.9 and 5.10, for ^{20K}PEG-insulin, ^{30K}PEG-insulin and ^{40K}PEG-insulin, respectively. In these figures, for all three conjugates, the slowest degradation of the insulin moiety was observed with 4 μg L^+, as expected, with the degradation of the insulin moiety in the presence of 16 μg L^+ similar to that observed with 32 μg L^+. In the presence of 4 μg L^+, there did appear to be a slight protective effect that was PEG MW-dependent, as shown in figure 5.11. When conjugated to either 20 kDa or 30 kDa PEG, the insulin moiety was degraded such that no insulin could be detected at either 4 or 6 hours. However, when conjugated to 40 kDa PEG, the insulin moiety could still be detected by anti-insulin western blot at both 4 and 6 hours post-incubation, albeit degradation had very nearly reached completion at these times. In the presence of 16 μg L^+, however, no MW-dependent protective effect of PEG was observed, as shown in figure 5.12. Here, insulin had been essentially degraded to completion by 2 hours, regardless of PEG MW attached. Taken together, these data indicate that PEG, between 20 and 40 kDa, does not impart protection against lysosomal degradation when conjugated to insulin under optimal conditions for lysosomal degradation. When using reduced amounts of L^+, where the enzyme concentrations may be rate-limiting, there did appear to be a slight PEG MW-dependent protective effect when insulin was conjugated to 40 kDa PEG. However, given that this protection with 40 kDa PEG offers only approximately 2 hours more time prior to complete degradation of the insulin moiety, the *in vivo* therapeutic implication of this finding may be insubstantial.

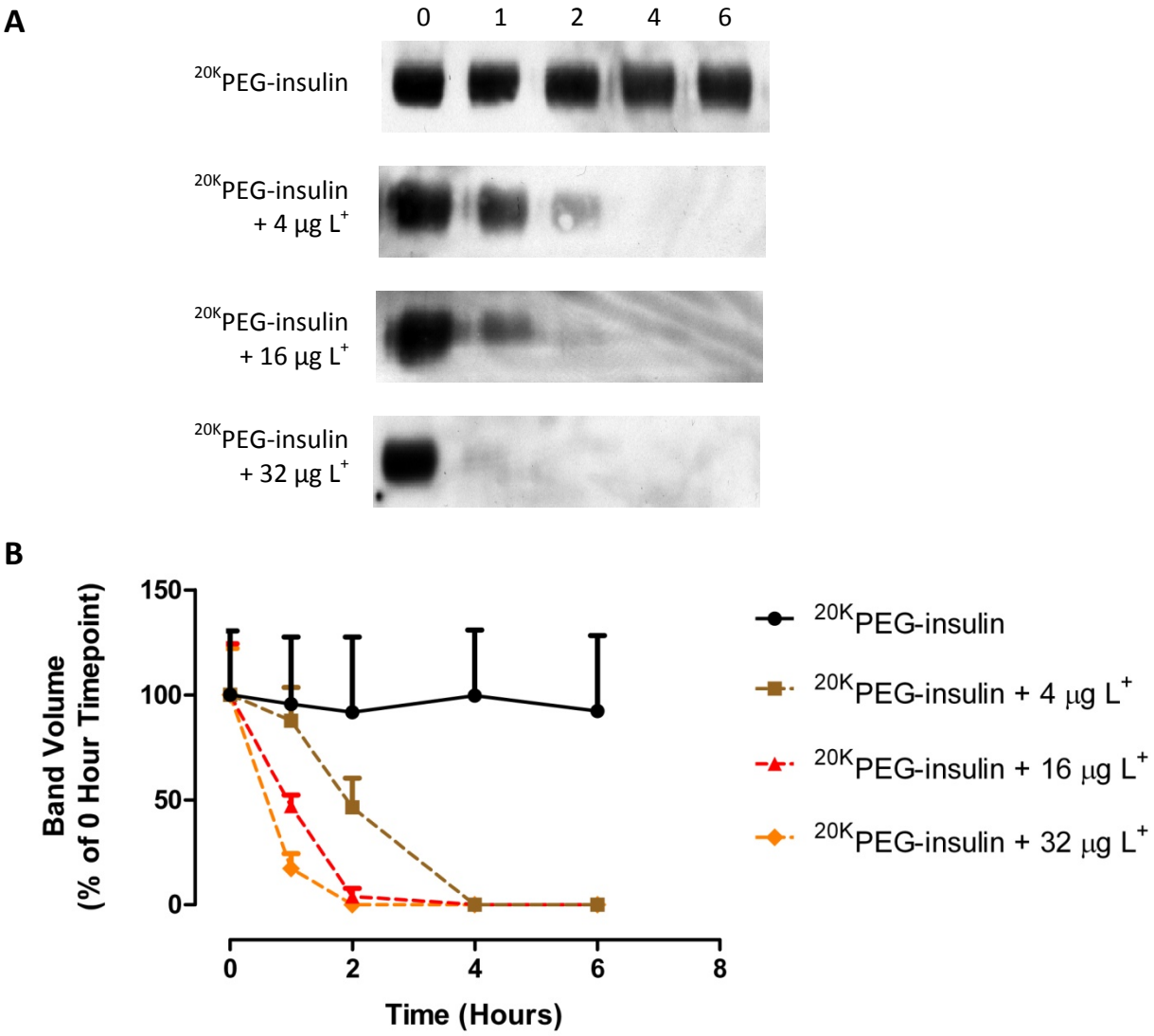

Figure 5.8: Lysosomal degradation of ^{20K}PEG-insulin with varying L^+

^{20K}PEG-insulin (88.8 µg) was incubated with either 4 µg or 16 µg L^+ fraction (human liver) over 6 hours and compared with the data acquired when incubated with 32 µg L^+ fraction. Degradation was assessed by SDS-PAGE and anti-insulin western blot. A) Representative blots; B) Densitometric analysis. Data are presented as the mean band volumes as a percentage of the 0 hour timepoint + SEM. N=3.

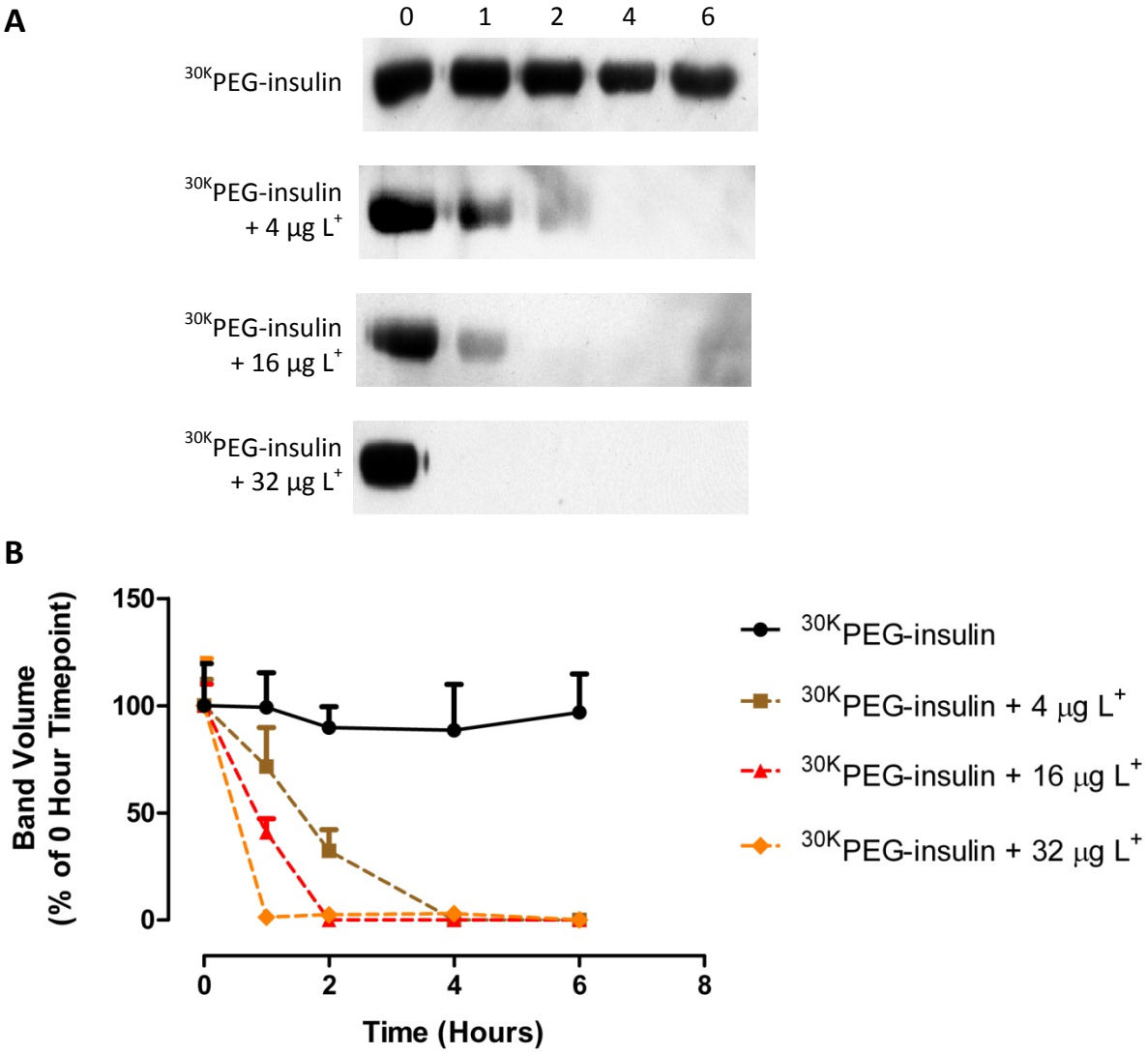

Figure 5.9: Lysosomal degradation of ^{30K}PEG-insulin with varying L^{+}

^{30K}PEG-insulin (123.4 µg) was incubated with either 4 µg or 16 µg L^{+} fraction (human liver) over 6 hours and compared with the data acquired when incubated with 32 µg L^{+} fraction. Degradation was assessed by SDS-PAGE and anti-insulin western blot. A) Representative blots; B) Densitometric analysis. Data are presented as the mean band volumes as a percentage of the 0 hour timepoint + SEM. N=3.

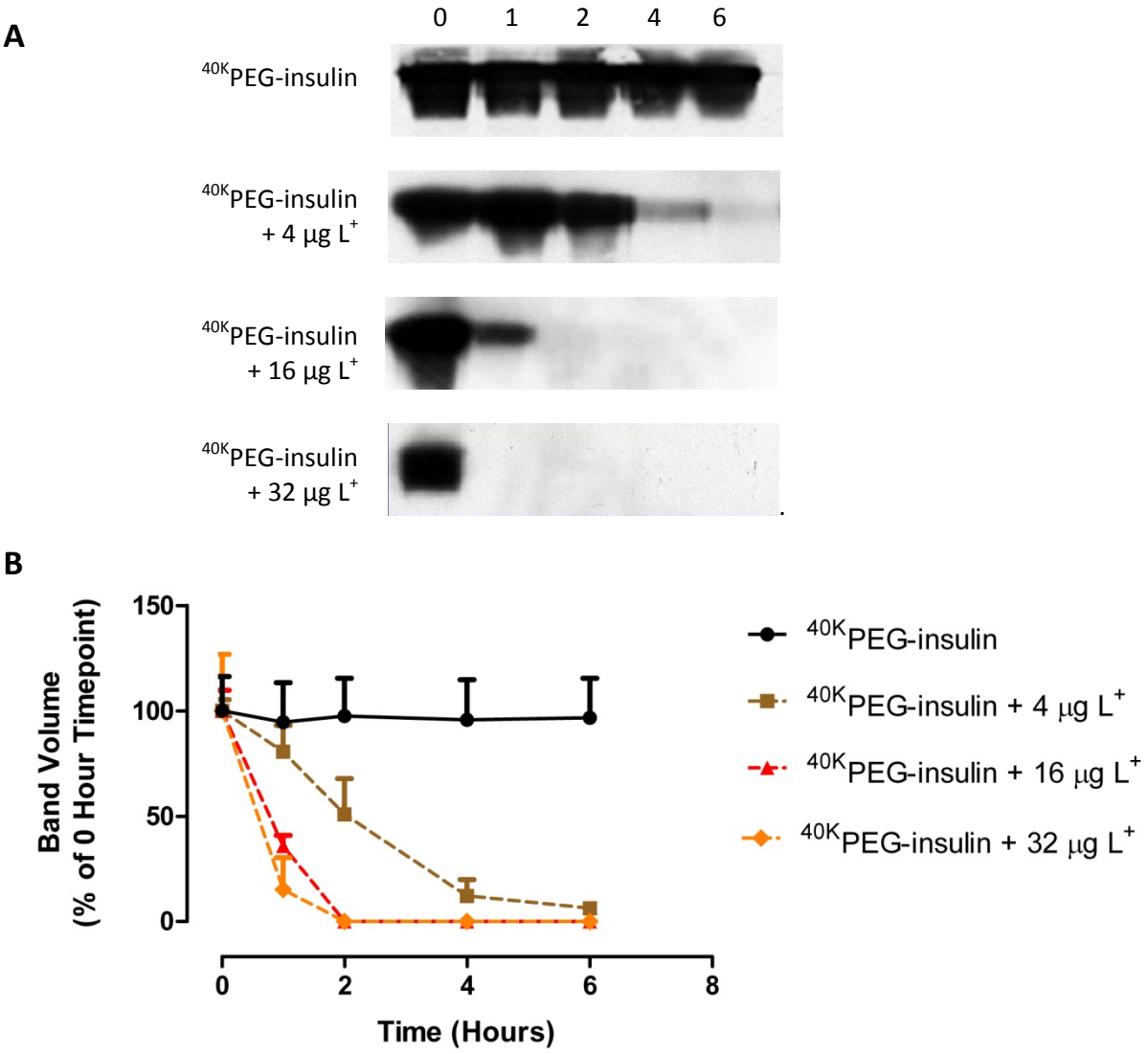

Figure 5.10: Lysosomal degradation of ^{40K}PEG-insulin with varying L^+

^{40K}PEG-insulin (157.7 µg) was incubated with either 4 µg or 16 µg L^+ fraction (human liver) over 6 hours and compared with the data acquired when incubated with 32 µg L^+ fraction. Degradation was assessed by SDS-PAGE and anti-insulin western blot. A) Representative blots; B) Densitometric analysis. Data are presented as the mean band volumes as a percentage of the 0 hour timepoint + SEM. N=3.

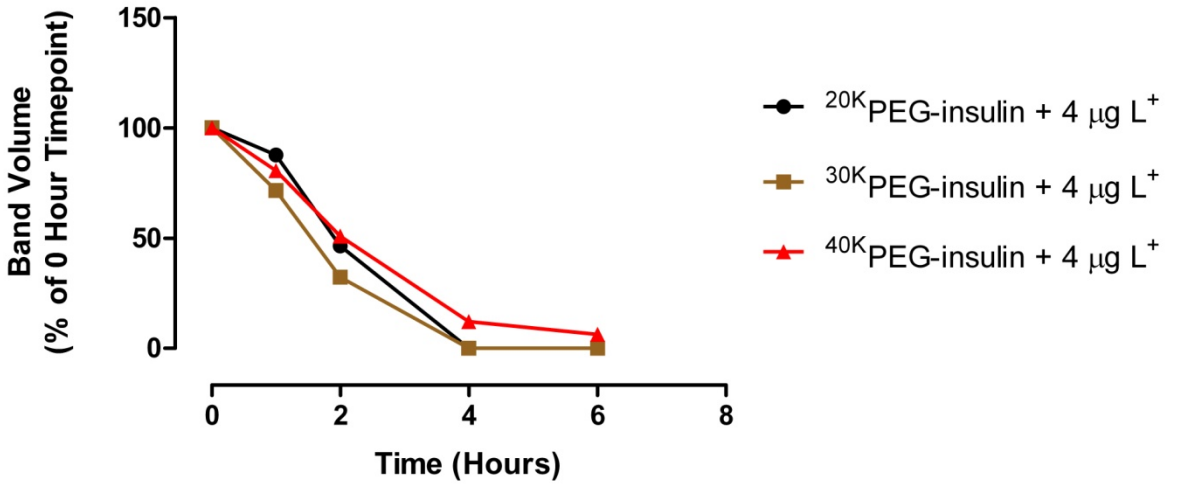

Figure 5.11: Comparison of lysosomal degradation of PEGylated insulin with 4 µg L^+

Comparison of the degradation of each PEGylated insulin in the presence of 4 µg L^+ fraction. Data are presented as the mean band volumes as a percentage of the 0 hour timepoint. N=3.

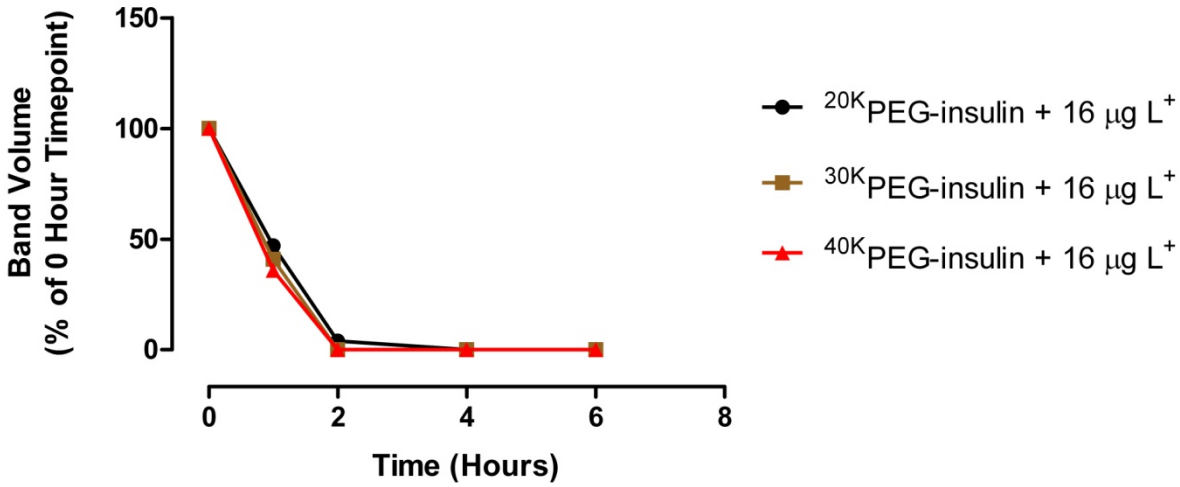

Figure 5.12: Comparison of lysosomal degradation of PEGylated insulin with 16 µg L^+

Comparison of the degradation of each PEGylated insulin in the presence of 16 µg L^+ fraction. Data are presented as the mean band volumes as a percentage of the 0 hour timepoint. N=3.

5.3.4 Effect of PEGylation on the Peptide Repertoire

Next, the effect of PEGylation on the peptide repertoire generated following lysosomal degradation was assessed using MS. The length of the incubation period used to generate samples for analyses was selected based on the time required for ~50% of the insulin moiety to be degraded, which, according to figure 5.7, was approximately 30 minutes for insulin alone, and for all three PEGylated conjugates (Tenzer *et al.*, 2005). Following 30 minute incubations the samples were passed through centrifugal filters, with a MWCO of 3 kDa, and the filtrates collected for analysis. These filters prevent intact insulin and PEGylated insulin from passing into the filtrate and consequently analysis was restricted to peptides generated following lysosomal degradation. Comparison of the peptides detected between each of the three PEGylated insulins following lysosomal degradation showed there was little difference in the peptides observed, such that almost identical peptide repertoires were generated between each PEGylated insulin, as shown in table 5.1. A total of 12 peptides were detected in the combined repertoires of PEGylated insulin, of which 9 (75%) were detected from all three conjugates, with only 3 (25%) peptides detected solely from one conjugate only; FFYTPKT, detected from ^{20K}PEG-insulin, and GIVEQCCT and VCGERGF, both detected from ^{40K}PEG-insulin. Interestingly, the peptide VCGERGF was the only peptide detected in any of the three PEGylated conjugate's repertoires that was not also detected in the peptide repertoire from non-PEGylated insulin. These data indicate that PEG MW, over a range of 20 – 40 kDa, has little effect on the peptides generated following lysosomal degradation, though some small differences were observed.

	Peptides Observed			
Chain	**Insulin**	**^{20K}PEG-insulin**	**^{30K}PEG-insulin**	**^{40K}PEG-insulin**
A	GIVEQCC	GIVEQCC	GIVEQCC	GIVEQCC
A	GIVEQCCT	-	-	GIVEQCCT
A	GIVEQCCTS	GIVEQCCTS	GIVEQCCTS	GIVEQCCTS
A	GIVEQCCTSIC	-	-	-
A	YQLENYCN	-	-	-
A	QLENYCN	QLENYCN	QLENYCN	QLENYCN
B	FVNQHLCG	-	-	-
B	FVNQHLCGSH	-	-	-
B	FVNQHLCGSHL	-	-	-
B	VNQHLCG	-	-	-
B	VNQHLCGSHL	-	-	-
B	VNQHLCGSHLVE	-	-	-
B	YLVCGER	YLVCGER	YLVCGER	YLVCGER
B	YLVCGERG	YLVCGERG	YLVCGERG	YLVCGERG
B	YLVCGERGF	-	-	-
B	LVCGERG	LVCGERG	LVCGERG	LVCGERG
B	LVCGERGF	LVCGERGF	LVCGERGF	LVCGERGF
B	-	-	-	VCGERGF
B	ERGFFYTPKT	-	-	-
B	FFYTPKT	FFYTPKT	-	-
B	FYTPKT	FYTPKT	FYTPKT	FYTPKT
B	YTPKT	YTPKT	YTPKT	YTPKT

Table 5.1: Peptides observed following lysosomal degradation

Sequences of the peptides observed following the lysosomal degradation of insulin, ^{20K}PEG-insulin, ^{30K}PEG-insulin and ^{40K}PEG-insulin. Highlighted in green are sequences detected in each repertoire. N=2.

However, when comparing the peptides generated from non-PEGylated insulin with each PEGylated insulin, there were ten unique peptides that were solely detected following the degradation of non-PEGylated insulin, which were predominantly from the N-terminus of the B chain, as presented graphically in figure 5.13A and B – where the peptides detected by MS from insulin alone (A) and PEGylated insulin (B) are highlighted within the amino acid structure of insulin. Insulin consists of two peptide chains (A and B chains) linked by two disulphide bridges (the A chain also has an internal disulphide bond)

(Blundell *et al.*, 1972). Six of the ten unique peptides detected following the lysosomal degradation of non-PEGylated insulin form the N-terminus of the B chain. The PEGylation chemistry used in this study to couple PEG to insulin is selective for the N-terminal α-amine due to its lower pK_a, as described in the general introduction. The N-termini of insulin consist of the amino acids glycine and phenylalanine for the A and B chains, respectively. The pK_a of the α-amine of phenylalanine is lower than that of glycine and consequently PEG, under the conditions used in this study, selectively couples to the B chain, as reflected in the MS data; where peptides forming part of the N-terminus of the A chain were detected following lysosomal degradation of each PEGylated insulin (and insulin alone), but not the B chain, as shown in figure 5.13B (Campbell *et al.*, 2010). These peptides are presumably still attached to PEG and consequently did not pass through the filter.

Taken together, these data indicate that altering PEG MW, over a range of 20 – 40 kDa, does not result in differential lysosomal degradation of the insulin moiety in terms of the peptide repertoires generated between each conjugate, despite the differences in the MW of the PEG attached. However, when compared to the peptide repertoire generated following degradation of non-PEGylated insulin, PEG, regardless of MW, can alter the distribution of the peptides that are formed; predominantly at the site of attachment – suggesting that PEG may confer stronger local protection as opposed to overall protection against lysosomal degradation; at least in terms of the peptides formed following lysosomal processing.

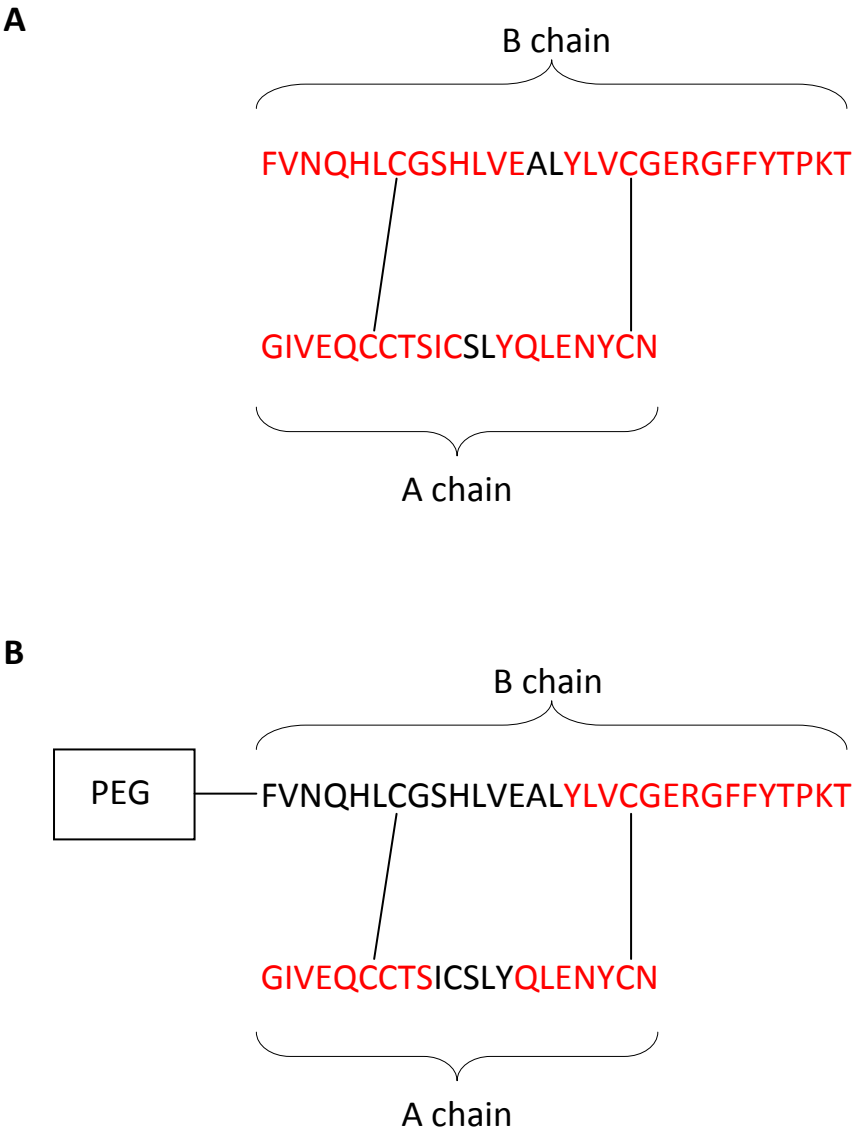

Figure 5.13: Differential peptide repertoires generated between insulin and PEGylated insulin

The amino acid structures of insulin (A) and PEGylated insulin (B), displaying the A and B chains linked by two disulphide bridges. Highlighted in red are the amino acids present in the unique peptides that were detected following the lysosomal degradation of non-PEGylated insulin (A) and all three PEGylated insulin conjugates combined (B).

5.4 DISCUSSION

An enriched lysosomal fraction (L^+) was obtained from human liver that was shown to possess specific lysosomal protease activity. Initially, existing methodology was adapted to enrich lysosome fractions from HepG2 cells and mouse liver. These fractions were shown to contain the specific lysosomal protein LAMP1, and proteolytic degradation in the presence of these fractions was inhibited in the presence of leupeptin – a lysosomal protease inhibitor – indicating that the degradation observed was indeed lysosomal-mediated. These methods were then applied to the enrichment of lysosomes from human liver, whilst also incorporating a further purification step – $CaCl_2$ precipitation. This extra step was shown to increase the purity of enriched lysosomes whilst still maintaining specific lysosomal activity. Thus, an L^+ fraction was obtained from human liver, which was used to assess the effect of PEGylation, in particular the effect of PEG MW, on the lysosomal degradation of a model protein, insulin. Prior to studying the fate of attached protein, the stability of the PEG moiety when incubated with lysosomal fractions was assessed. Using HepG2-derived CLF, over a period of 7 days no degradation was observed when CLF was incubated with either 40 kDa PEG alone or when 40 kDa PEG was conjugated to insulin; indicating the stability of PEG to lysosomal degradation. This result was not unexpected, given that, as discussed in the general introduction, metabolism of PEG represents a very minor clearance route particularly for PEG of the MW used in this study. Furthermore, metabolism of PEG is mediated by alcohol dehydrogenase, which is not a lysosomal hydrolase (Schroder *et al.*, 2010). The stability of the insulin moiety of ^{40K}PEG-insulin was also assessed over 7 days during this study, and could only be detected on day 0. Consequently, shorter time courses were employed to assess the lysosomal degradation of insulin and the effect of PEGylation on this process. In these studies, the L^+ fraction obtained from human liver was used. In the presence of L^+, insulin was degraded to completion within 2 hours, such that no insulin was detected by anti-insulin western blot.

When analysing the lysosomal degradation of ^{20K}PEG-insulin, ^{30K}PEG-insulin and ^{40K}PEG-insulin, such that the overall amount of insulin as part of the different sized conjugates was equivalent, it was found that the insulin moiety was still completely degraded within 2 hours, regardless of the MW of PEG attached; indicating that PEG, over the MW range used in this study, does not confer protection against lysosomal degradation. When considering the events that occur *in vivo* during lysosomal degradation and processing of internalised protein, it is perhaps not too surprising that PEGylation does not appear to confer protection against degradation; given that protein which enters the lysosome will be in an environment designed to efficiently degrade and process protein – an environment containing many different protease enzymes resulting in enzyme-to-substrate ratios heavily favoured toward enzymatic degradation. Thus, under the conditions used in this study, designed to closely replicate the *in vivo* situation, it was not unexpected that PEG was unable to protect against lysosomal degradation. Consequently, to further confirm this finding, the study was repeated using reduced amounts of L^+. Under these conditions, degradation of the insulin moiety ought to be slower and thus differential rates of lysosomal degradation occurring due to PEG MW-differences in PEGylation may be easier to track. Subsequently, repeat incubations of the three PEGylated insulins ± either 4 or 16 µg L^+ were analysed, over the same time course, by anti-insulin western blot. As expected, in the presence of 4 µg L^+ the insulin moiety, for all three conjugates, was degraded to completion the slowest. Whereas, in the presence of 16 µg L^+, degradation was similar to that when the insulin moiety was degraded by 32 µg L^+; with complete degradation again occurring within approximately 2 hours for all three conjugates, but with more insulin detected at 1 hour in comparison to the corresponding timepoint + 32 µg L^+. When comparing the degradation between the three conjugates, no MW-dependent protective effect of PEGylation was observed at all in the presence of 16 µg L^+, with essentially identical insulin degradation at each time point for all three conjugates. In the presence of

4 µg L^+, when coupled to either 20 kDa or 30 kDa PEG, the insulin moiety was degraded to completion within 4 hours. However, when coupled to 40 kDa PEG the insulin moiety could still be detected by western blot at both 4 and 6 hours, albeit degradation had essentially neared completion at 6 hours. Taken together, these data indicate only a slight PEG MW-dependent effect is observed when proteins are coupled to higher MW PEG when degraded in the presence of lower amounts of L^+.

Next, MS analysis was used to determine if PEGylation can alter the peptide repertoires generated following the lysosomal degradation of insulin and PEGylated insulin. Differences in the peptide repertoires between either ^{20K}PEG-insulin, ^{30K}PEG-insulin or ^{40K}PEG-insulin were minimal, such that only 3 peptides were not detected in all three repertoires, out of a total of 12 peptides detected in the combined repertoires from all three conjugates. In contrast, there was a distinct difference in the peptide repertoire generated from insulin alone in comparison to those generated from the three PEGylated insulins. In this study, PEG is coupled to insulin at the N-terminal of the B chain. Peptides originating from this terminal could not be detected in any of the repertoires generated from each of the three PEGylated insulins. However, B chain N-terminal peptides could be detected following the lysosomal degradation of non-PEGylated insulin, indicating that PEG confers selective protection from degradation at the site of attachment. Taken together, these data further support the finding that PEGylation, in terms of altering PEG MW, has little effect on the lysosomal degradation of insulin; be it in terms of overall protection against degradation or in the peptide repertoires generated – though PEG, regardless of MW, can provide local protection to the protein at the site of attachment.

The L^+ fraction described in this chapter obtained from human liver provides further evidence that the protein moiety of PEGylated proteins is degraded or metabolically cleaved following cellular internalisation, as suggested by the *in vivo* studies in chapter 2. *In vivo,* the cleavage of ^{40K}PEG-insulin could be clearly observed over time,

whilst ^{40K}PEG-insulin was shown to be stable *in vitro* in plasma, indicating that the cleavage of the conjugate did not occur in the circulation, but was a consequence of uptake into tissue compartments. Indeed, accumulation of PEG was demonstrated in liver and kidney several days post-dosing. *In vitro* cellular uptake of the intact conjugate was described in chapter 4. In this chapter, the effect of PEG MW on the lysosomal degradation of insulin was assessed and was shown to have no protective effect, regardless of PEG MW, under the conditions used in this study. With respect to potential immunological consequences, the next process by which PEGylation may have an effect is on the peptide repertoires generated following lysosomal proteolysis; potentially resulting in a repertoire containing fewer immunogenic peptides in comparison to the repertoire generated following proteolysis of the native protein. In this study it was shown that PEGylation has little effect with regards to the peptide repertoires generated between the three different PEGylated insulins, though some minor differences were observed, but can result in differences in the peptides generated when comparing PEGylated and non-PEGylated insulin; particularly at the site of attachment. However, to further support this view in a strictly immunological setting, it perhaps would be more appropriate to use lysosome fractions obtained from APC, such as DC and macrophages, which are intimately involved in the processing and presentation of antigen. However, for the purposes of assessing the effect of PEGylation on lysosomal degradation of the protein as a whole, rather than assessing the effect of PEGylation on the peptides generated, the use of liver derived lysosomes is appropriate. Furthermore, this proof-of-principle study clearly demonstrates the utility of using enriched lysosome fractions to assess the effect of PEGylation on the peptides generated following lysosomal degradation. Whilst the immunogenicity of insulin is no longer an important safety question *per se*, differences in the peptides generated between PEGylated and non-PEGylated insulin were observed. Differences such as these may become important when investigating the safety of future PEGylated agents. Indeed, this study may provide the

necessary tools to improve the safety of future PEGylated agents by tailoring the PEGylation process to prevent the generation of immunogenic peptides, particularly as PEG appears to offer local protection at the site of attachment. However, it should be borne in mind that only a single, relatively short, incubation time was explored in this study. Nevertheless, theoretically these data could mean that site-specific PEGylation may be used to selectively protect known immunogenic sequences present in the protein from forming in the lysosome, thereby preventing their binding to MHC class II molecules and subsequent recognition by the immune system.

In conclusion, an enriched L^+ fraction was generated from human liver and used to assess the effect of PEGylation on the lysosomal degradation of a model protein. PEG itself was stable to lysosomal degradation but could not confer protection against lysosomal degradation to PEG-coupled insulin. Furthermore, no PEG MW-dependent protective effect was observed under degradation conditions based on enzyme-to-substrate ratios typical of the *in vivo* situation. Only under conditions of low protease concentrations could a very slight PEG MW-dependent effect be observed with the highest MW PEG used in this study, 40 kDa PEG. Thus, under normal *in vivo* conditions, PEGylation, over a therapeutically relevant PEG MW range, appears to have no protective effect against lysosomal degradation in comparison to the degradation of the native protein, in this case insulin. Furthermore, the effect of PEG MW on the peptide repertoires generated also appeared to be minimal, with only minor differences observed in the repertoires generated between the three PEGylated insulins; further supporting the finding that PEGylation has little effect against lysosomal degradation. Indeed, PEG only confers local protection against lysosomal degradation at the site of attachment.

CHAPTER 6

Intracellular Disposition of PEGylated Proteins: Proteasomal Degradation

CONTENTS

Intracellular Disposition of PEGylated Proteins: Proteasomal Degradation

6.1 INTRODUCTION

Degradation by the proteasome is the major route of non-lysosomal protein degradation in the cell. This route was predominantly thought to be exclusive for endogenous protein degradation; however, as described in the general introduction, exogenous protein can also be degraded via the proteasome through cross-presentation. Cross-presentation primarily occurs in APC, such as DC, and refers to their ability to internalise, process and present exogenous protein through the MHC class I pathway, as opposed to the MHC class II pathway following lysosomal degradation. Proteins degraded and processed by the proteasome will form complexes with MHC class I molecules, which are then displayed on the surface of the cell for recognition by $CD8^+$ T cells. Once a complex has been recognised, and provided that sufficient co-stimulatory signals have occurred also, the $CD8^+$ T cell is activated and initiates the release of cytotoxins, such as perforin, which leads to the death of the cell displaying the peptide. Whilst the sources of protein for cross-presentation are generally from bacteria, tumours or virus-infected cells, it is possible that other exogenous proteins, such as those originating from a therapeutic protein or PEGylated protein, may also escape lysosomal degradation and subsequently be cross-presented following internalisation by APC. Given the fundamental lack of understanding concerning the mechanisms of how PEGylation affects protein intracellular disposition and reduces immunogenicity, as described in the general introduction, the potential role of PEGylation on protein degradation by the proteasome was investigated concurrently with the effect of PEGylation on lysosomal degradation. This chapter describes the purification of 20S proteasome from human liver, which was subsequently used to study the effect of PEGylation, using a range of different MW PEGs, on the proteasomal degradation of insulin.

6.2 METHODS AND MATERIALS

All reagents were purchased from Sigma-Aldrich Company Ltd (Dorset, UK), unless otherwise stated.

6.2.1 Purification of 20S Proteasome from Human Liver

20S proteasome from human liver was purified, characterised, and used to degrade insulin and a series of PEGylated insulins, from adapting previously described methodology to purify 20S proteasome from animal liver (Bardag-Gorce *et al.*, 2004; Beyette *et al.*, 2001; Conconi *et al.*, 1998; Conconi *et al.*, 1996; Di Noto *et al.*, 2005; Farout *et al.*, 2006; Friguet *et al.*, 2002; Rivett *et al.*, 1994).

6.2.1.1 Liver Homogenisation and Centrifugation

Human liver (10 g starting material) was minced in 100 mL 50 mM tris-HCl, containing 250 mM sucrose and 150 mM NaCl, pH 7.5. Liver pieces were homogenised using a TissueRuptor (Qiagen). The resulting homogenate was centrifuged at 10,000 *g* for 20 minutes at 4^{o}C. The homogenate supernatant was removed and further centrifuged at 100,000 *g* for 1 hour at 4^{o}C. The 100,000 *g* supernatant was removed and further centrifuged at 100,000 g for 5 hours at 4^{o}C. The resulting 100,000 *g*/5 hour pellet was resuspended in 5 mL 20 mM triethanolamine buffer, containing 150 mM NaCl and 15% (v/v) glycerol, pH 7.7.

6.2.1.2 Ammonium Sulphate Precipitation and Dialysis

Solid ammonium sulphate was added slowly to the 100,000 *g*/5 hour fraction to give a 35% saturated solution, at 4^{o}C, and left stirring for 1 hour, followed by a 15 minute centrifugation at 10,000 *g* (4^{o}C). The resulting supernatant was removed and further solid ammonium sulphate added to give a 60% saturated solution at 4^{o}C. The solution was

stirred for 1 hour, re-centrifuged and the resulting pellet resuspended in 2 mL 20 mM triethanolamine buffer. The sample was then dialysed against 1 L triethanolamine buffer (MWCO 12 – 14,000) overnight at 4^{o}C, with one buffer change.

6.2.1.3 Anion Exchange Chromatography

The ammonium sulphate dialysed fraction was loaded onto a DEAE 5PW anion exchange column (Waters) equilibrated in 10 mM tris-HCl, pH 7.2, and proteasomes eluted using a linear gradient of NaCl from 0.1 – 0.5 M over 30 minutes, during which fractions (1 mL) were collected. Active fractions containing specific proteasomal activity were pooled, concentrated and loaded onto a Mono Q HR 5/5 column (GE Amersham) equilibrated in 10 mM Tris-HCl, pH 7.2, and proteasomes again eluted using the same, linear NaCl gradient. Active fractions were pooled and concentrated and protein content determined by the Bradford assay.

6.2.2 Proteasomal Activity Assay

To a 96-well plate, 50 µL of each anion exchange fraction was added to 50 mM Hepes containing 50 µM boc-LSTR-AMC (prepared from a 10 mM stock in DMSO) in a 200 µL final volume, pH 7.8. Plates were incubated for 1 hour at 37^{o}C, after which the released fluorescence from each fraction was determined with Ex/Em wavelengths of 360 and 460 nm, respectively.

6.2.3 Proteasomal Degradation of Insulin and PEGylated Insulin *in vitro*

Insulin and PEGylated insulin were incubated ± 20S proteasome, at the stated amounts, at 37^{o}C in 50 mM Hepes containing 5 mM DTT, 100 mM NaCl, 1 mM $MgCl_2$, pH 7.8, in a 60 µL final volume.

6.2.3.1 Western Blot Analysis

Aliquots (10 µL) were removed at the stated times, diluted with ddH_2O and stored at -80^oC prior to SDS-PAGE/western blot analysis to assess degradation, as described in section 2.2.7.

6.2.3.2 LC-ESI-MS/MS Analysis

The peptide repertoires generated following proteasomal degradation were analysed by MS as described in section 5.2.3.2.; incubations were for 12 hours, however.

6.3 RESULTS

A 20S proteasome fraction was obtained from human liver using adapted methodology. This fraction was shown to be highly purified and capable of degrading protein. These proteasomes were subsequently used to assess the effect of PEGylation on the proteasomal degradation of insulin, a model protein.

6.3.1 Purification and Characterisation of Human Liver 20S Proteasome

Following homogenisation and differential centrifugation of human liver, the pellet was further purified using ammonium sulphate precipitation and dialysis. After dialysis, the resulting fraction was further purified using two ion exchange columns. Fractions were assessed for specific proteasomal activity using two fluorogenic probes, boc-LSTR-AMC and suc-LLVY-AMC, which assess the chymotrypsin-like and trypsin-like activity of the proteasomes, respectively. In their native state, the fluorophore AMC is quenched due to the attachment of the bulky blocking groups; succinyl (suc) and N-t-butyloxycarbonyl (boc). Cleavage of the peptide, linking AMC to the quenching group, by the proteasome results in the release of the fluorescent AMC, which can be measured fluorometrically. Thus, the presence of fluorescence in a fraction, over baseline values, indicates active proteasome

content. Following the second ion exchange step, active fractions were pooled, concentrated, and the protein content determined by the Bradford assay. To assess the purity of the final 20S proteasome fraction, 5 µg of protein from the fraction was resolved on an SDS-PAGE gel, alongside 5 µg of protein taken from earlier fractions, and stained with coomassie, as shown in figure 6.1. In figure 6.1, the final 20S fraction was resolved in lane G. In this lane the only protein bands visible are between ~22 and 35 kDa, which are the

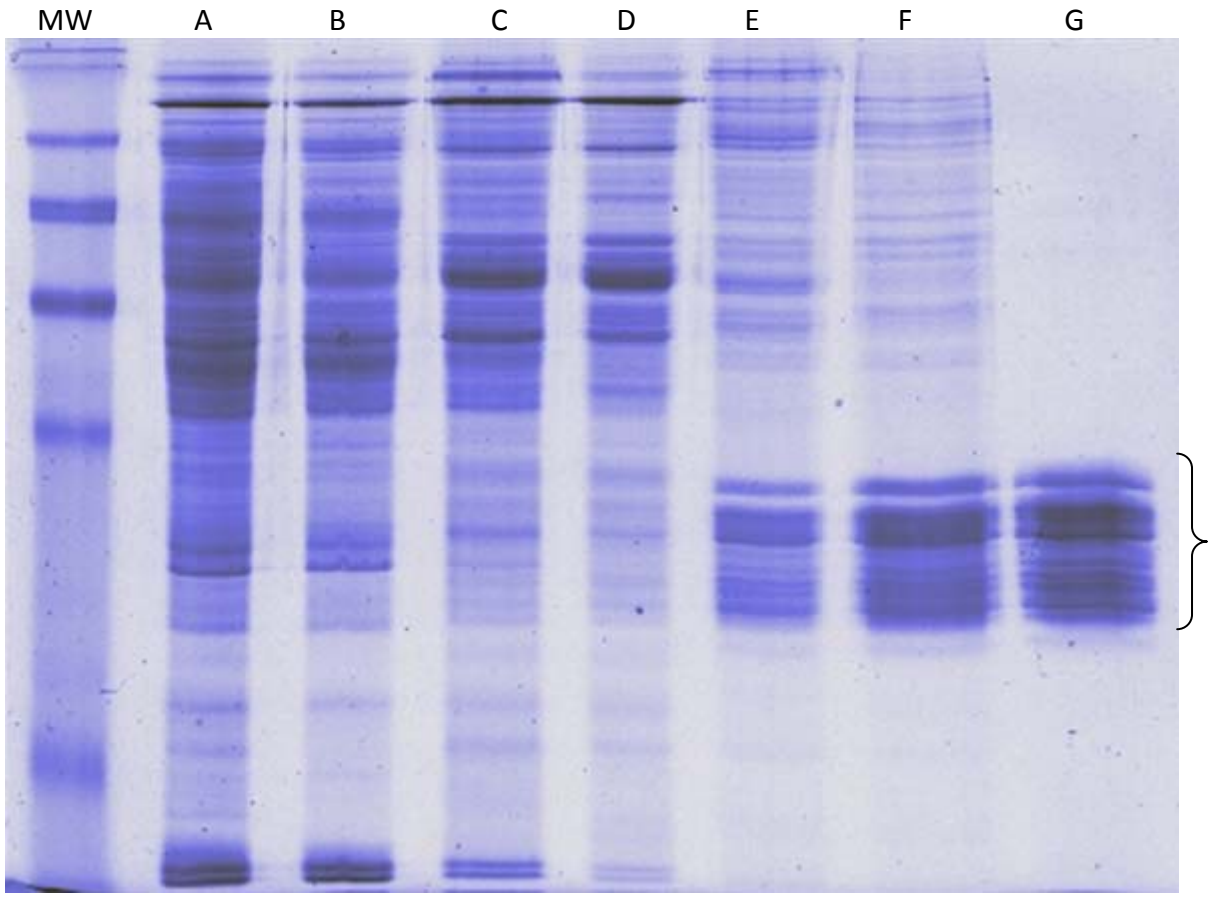

Figure 6.1: Purification of 20S proteasome from human liver

Protein (5 µg) from each fraction was loaded onto a 12% SDS-PAGE gel and stained with coomassie following electrophoresis. Lanes – A: Homogenate supernatant, B: 100,000 g/1 hour supernatant, C: 100,000 g/5 hour pellet, D: Ammonium sulphate dialysed fraction, E: DEAE (100,000 g/5 hour pellet) active fractions, F: DEAE (Ammonium sulphate dialysed fraction) active fractions, G: Mono Q (DEAE combined) active fractions. Bands highlighted in Lane G are the characteristic proteasomal subunits.

MWs of the individual proteasomal subunits, under reducing conditions. In fact, these characteristic bands appear visible as far back in the purification process as the final centrifugation step prior to ammonium sulphate precipitation (Lane C). The bands in lane G were excised from the gel, tryptically digested and analysed via reverse-phase HPLC. All 14 subunits which constitute the 20S proteasome were identified (data not shown) as well as 3 immunoproteasome subunits and proteasome activator complex subunits 1 and 2, all of which were identified with high sequence coverage, and represented 25% of the total number of proteins identified in the bands (19 out of 76). Once purified, the 20S proteasomes were assessed for activity using both fluorogenic probes in combination with MG132, a proteasome inhibitor, as shown in figure 6.2.

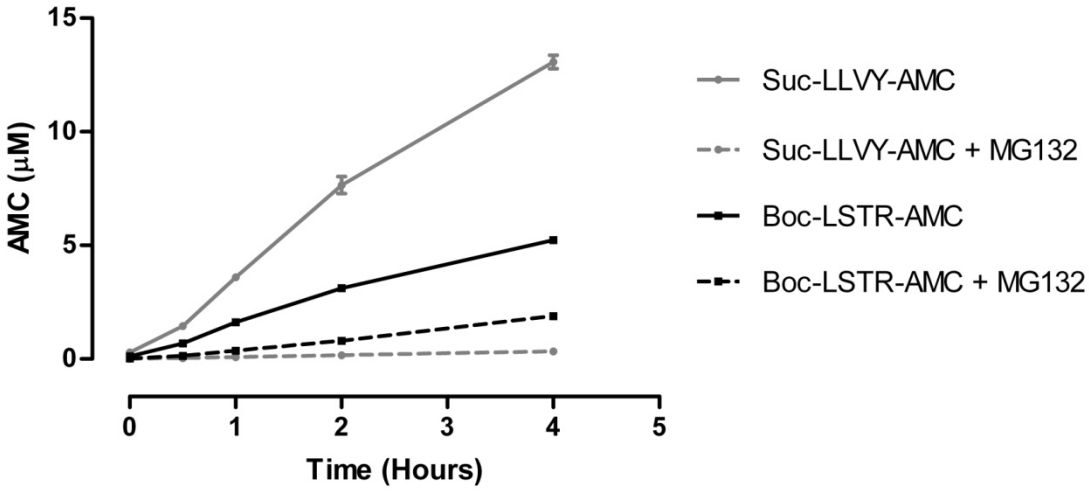

Figure 6.2: Inhibition of proteasomal activities

20S proteasome (1.0 µg/well) was incubated with either 50 µM suc-LLVY-AMC (trypsin-like activity) or 50 µM boc-LSTR-AMC (chymotrypsin-like activity), either alone or in the presence of 20 µM MG132 (proteasome inhibitor). Data are presented as the mean concentration of AMC (µM) ± SEM. N=3.

In figure 6.2, in the presence of MG132 both the trypsin-like and chymotrypsin-like proteasomal activities were inhibited, as indicated by the reduced concentration of AMC in

each well compared with the corresponding timepoints incubated without MG132. Indeed, trypsin-like activity (suc-LLVY-AMC data) was essentially completely inhibited over 4 hours. Next, the proteolytic capacity of the purified 20S proteasomes was assessed using insulin as a model substrate. Insulin was incubated ± 20S proteasome over 24 hours and degradation was assessed by SDS-PAGE and coomassie stain, as shown in figure 6.3.

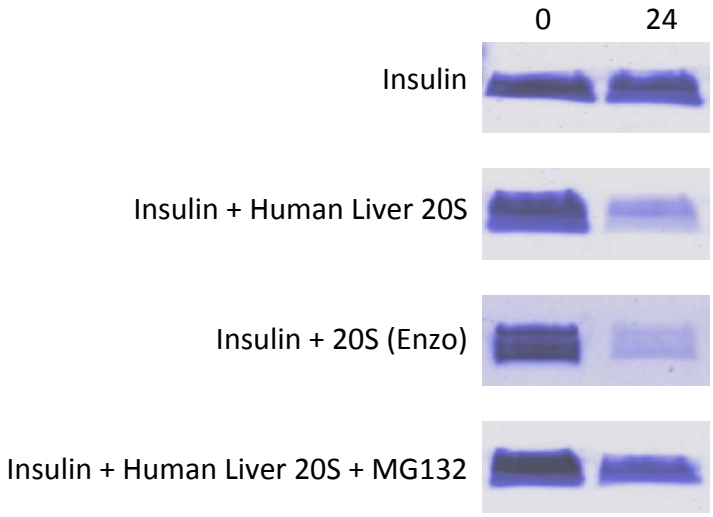

Figure 6.3: Proteolytic capacity of purified human liver 20S proteasome

Insulin (30 µg) was incubated either alone or in the presence of 2.5 µg 20S proteasome, purified from either human liver (± 20 µM MG132) or purchased from Enzo Life Sciences, over 24 hours. Degradation was assessed by SDS-PAGE and coomassie stain.

In figure 6.3, insulin was degraded to a large extent in the presence of 20S proteasome, but remained intact when incubated alone. Degradation by in-house purified 20S proteasome was compared with that of 20S proteasome purchased from Enzo Life Sciences (purified from human erythrocytes) under identical conditions. Both in-house purified 20S and commercial 20S proteasomes degraded insulin over 24 hours to a very

similar degree (figure 6.3). Furthermore, in the presence of MG132, degradation of insulin by human liver 20S proteasome was almost completely inhibited, as also shown in figure 6.3. Thus, a 20S proteasome fraction was obtained from human liver that was shown to be highly purified and capable of degrading protein.

6.3.2 Proteasomal Degradation of Insulin and PEGylated Insulin

The effect of PEGylation on the proteasomal degradation of insulin was assessed using purified human liver 20S proteasome and a range of PEGylated insulins, synthesised as described in chapter 5. Insulin and the three PEGylated insulins were incubated at 37^{o}C ± 20S proteasome at a ratio of 5:1 insulin to 20S (w/w). The increase in MW between 20 kDa, 30 kDa and 40 kDa PEGylated insulin was taken into account such that incubations contained equivalent amounts of insulin, as well as identical ratios of substrate to 20S. Degradation was assessed by SDS-PAGE and anti-insulin western blot. In the presence of 20S proteasome, insulin was degraded almost to completeness over 48 hours as shown in figure 6.4. When conjugated to 20 kDa PEG, the insulin moiety was also degraded almost to completeness over 48 hours, as shown in figure 6.5, indicating that 20 kDa PEG appears to confer no protection against proteasomal degradation. However, when conjugated to either 30 kDa or 40 kDa PEG, the insulin moieties were only degraded to approximately 50% at 48 hours, figures 6.6 and 6.7, respectively; indicating that at higher MWs PEG is able to confer partial protection against proteasomal degradation of insulin. This MW effect of PEG is best presented in figure 6.8, which contains the proteasomal degradation of insulin and all three PEGylated insulins overlaid. In figure 6.8, the proteasomal degradation of insulin and ^{20K}PEG-insulin is shown to be largely equivalent, whilst the partial protective effect of 30 kDa and 40 kDa PEG is clearly shown. The stability of insulin and the three PEGylated insulins without 20S proteasome was also shown to be stable over 48 hours (figures 6.4 – 6.8). Thus, the conclusion from this study was that PEGylation may only offer

insulin partial protection against proteasomal degradation when utilising PEGs above 20 kDa.

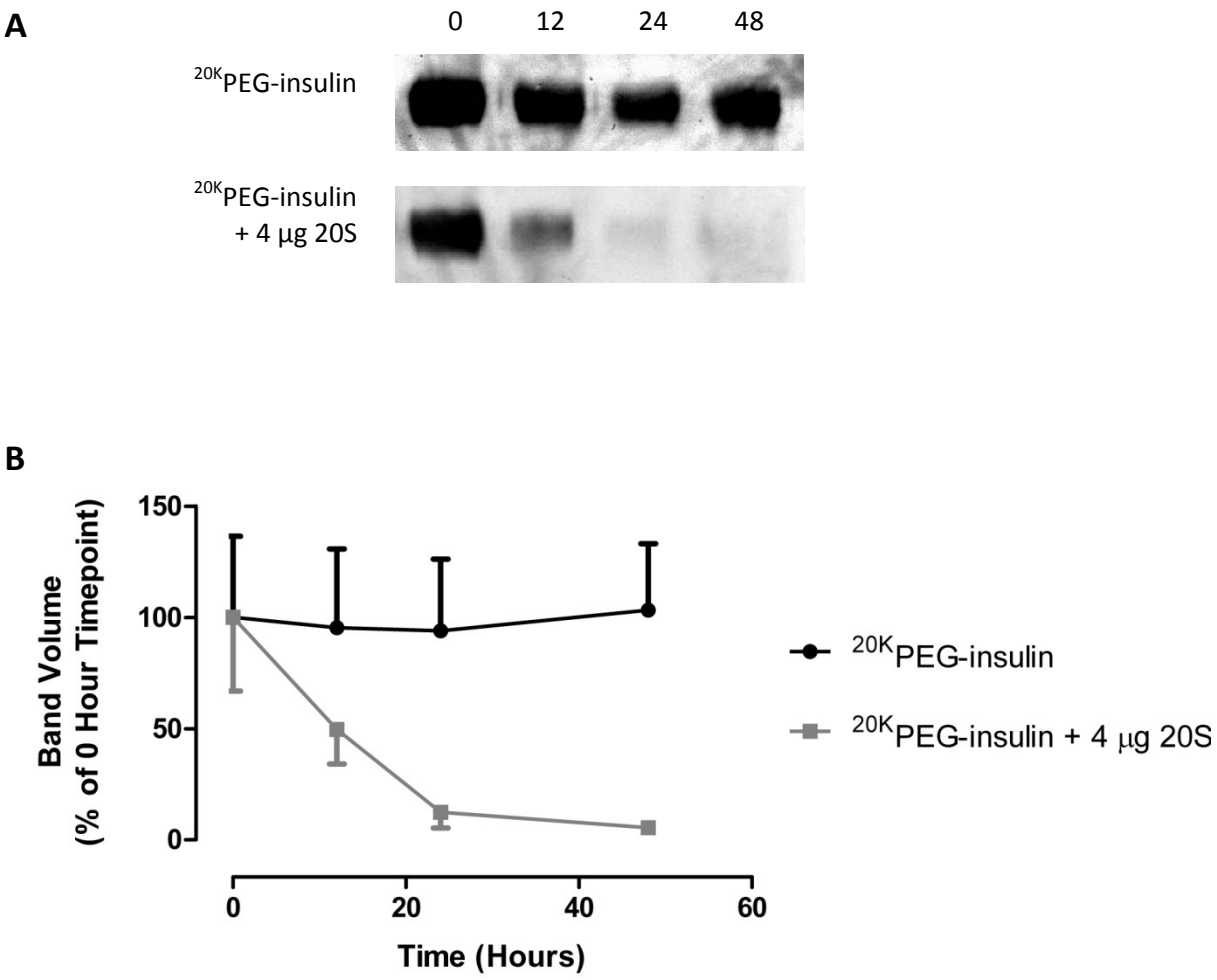

Figure 6.5: Proteasomal degradation of ^{20K}PEG-insulin

^{20K}PEG-insulin (88.8 μg, of which ~20 μg is insulin) was incubated ± 4 μg human liver 20S proteasome over 48 hours. Degradation was assessed by SDS-PAGE and anti-insulin western blot. A) Representative blots; B) Densitometric analysis. Data are presented as the mean band volumes as a percentage of the 0 hour timepoint ± SEM. N=3.

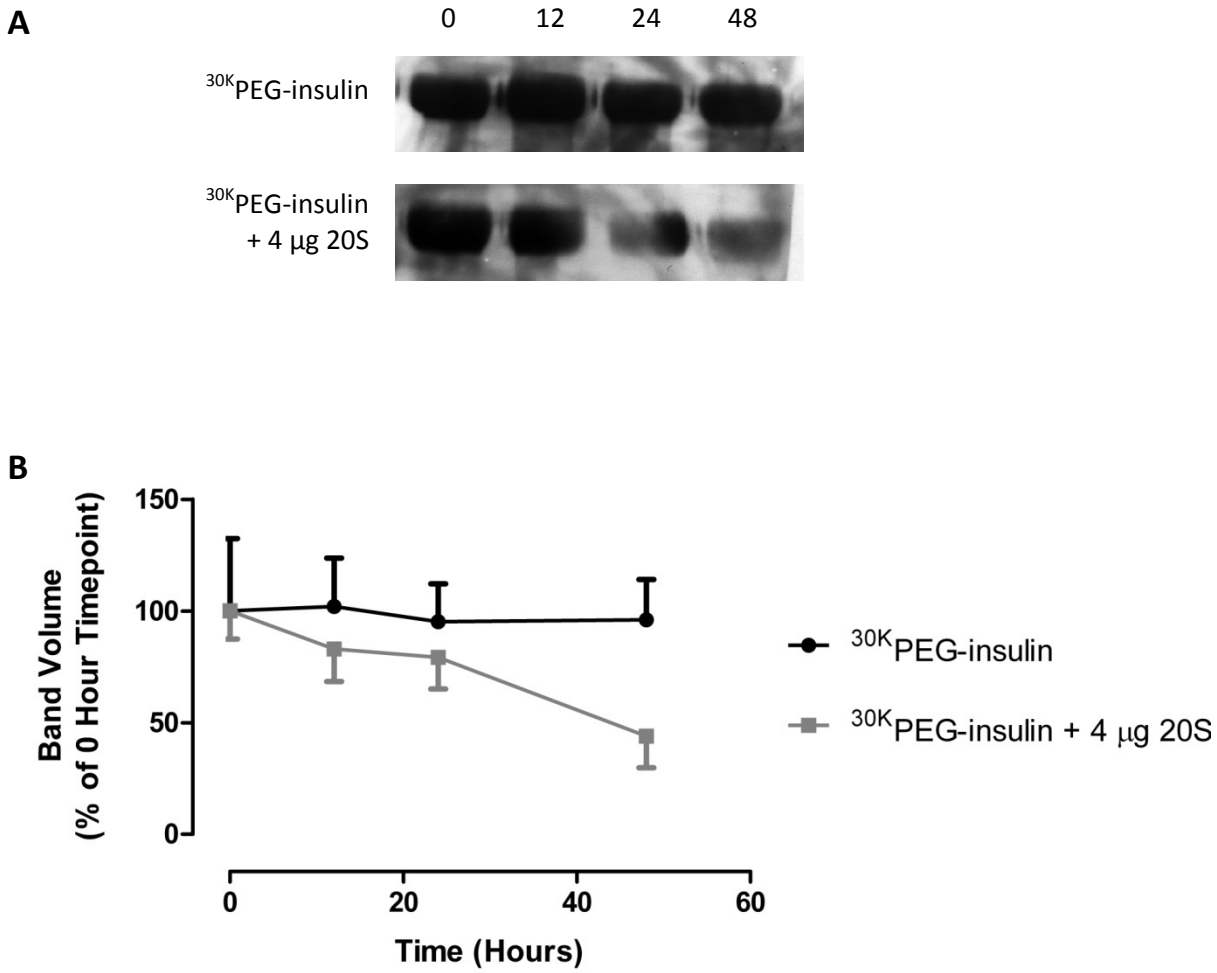

Figure 6.6: Proteasomal degradation of ^{30K}PEG-insulin

^{30K}PEG-insulin (123.4 µg, of which ~20 µg is insulin) was incubated ± 4 µg human liver 20S proteasome over 48 hours. Degradation was assessed by SDS-PAGE and anti-insulin western blot. A) Representative blots; B) Densitometric analysis. Data are presented as the mean band volumes as a percentage of the 0 hour timepoint ± SEM. N=3.

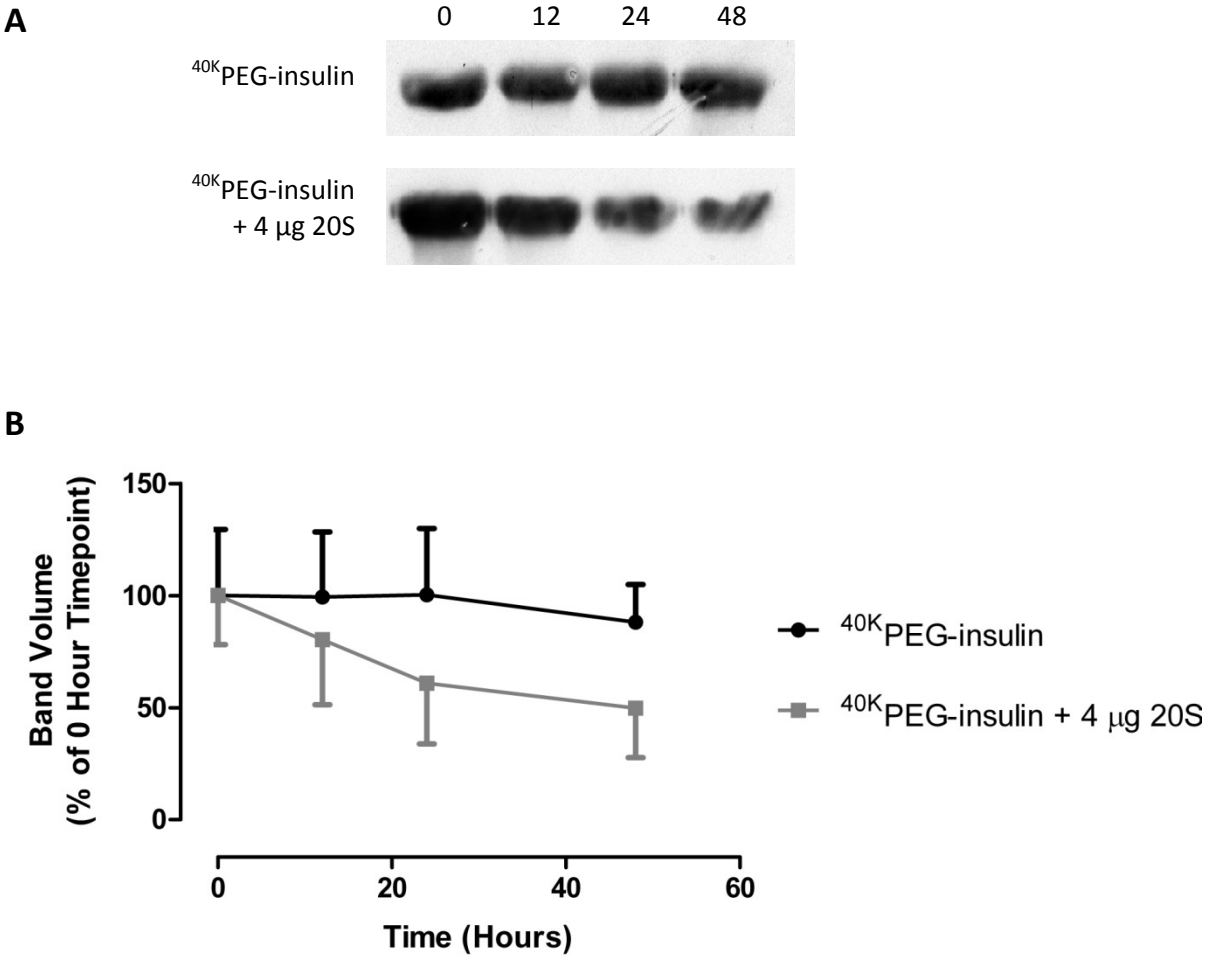

Figure 6.7: Proteasomal degradation of ^{40K}PEG-insulin

^{40K}PEG-insulin (157.7 µg, of which ~20 µg is insulin) was incubated ± 4 µg human liver 20S proteasome over 48 hours. Degradation was assessed by SDS-PAGE and anti-insulin western blot. A) Representative blots; B) Densitometric analysis. Data are presented as the mean band volumes as a percentage of the 0 hour timepoint ± SEM. N=3.

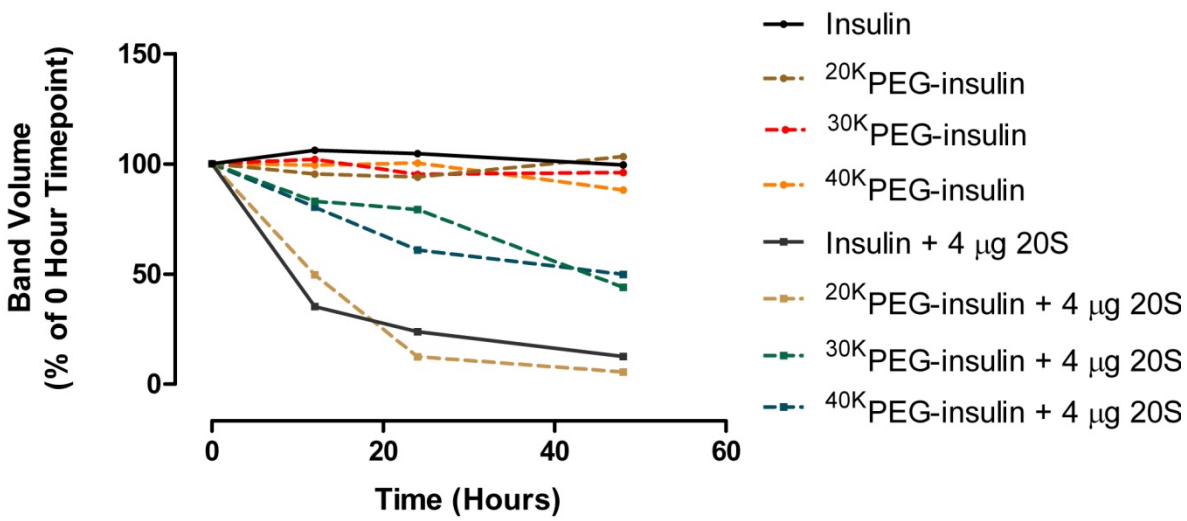

Figure 6.8: Proteasomal degradation comparison

Comparison of the proteasomal degradation of insulin with each PEGylated insulin. Data are presented as the mean band volumes as a percentage of the 0 hour timepoint. N=3.

6.3.3 Effect of PEGylation on the Peptide Repertoire

The effect of PEGylation on the peptide repertoires generated following proteasomal degradation was next assessed using MS. As for MS analysis of the lysosomal generated peptide repertoires, the incubation time selected was based on the time required for 50% of the insulin moiety to be degraded. However, since a PEG MW-dependent protective effect was observed following incubation with 20S proteasome, as shown in figure 6.8, the time selected was based on the degradation of insulin and ^{20K}PEG-insulin, which exhibited similar degradation; consequently 12 hours was chosen as the incubation time as this was approximately the time required for 50% of the insulin signal to be lost in both these samples.

A total of 73 different peptides were detected in the repertoires for both insulin and PEGylated insulin combined, of which 52 of these peptides (71.2%) were found in the repertoire from non-PEGylated insulin, as shown in table 6.1. Furthermore, the entire sequence of insulin was covered in these peptides, as seen in figure 6.9 A.

	Peptides Observed			
Chain	Insulin	^{20K}PEG-insulin	^{30K}PEG-insulin	^{40K}PEG-insulin
A	-	GIVEQ	-	-
A	-	GIVEQC	GIVEQC	GIVEQC
A	GIVEQCC	GIVEQCC	GIVEQCC	GIVEQCC
A	GIVEQCCT	GIVEQCCT	GIVEQCCT	GIVEQCCT
A	GIVEQCCTS	GIVEQCCTS	GIVEQCCTS	GIVEQCCTS
A	GIVEQCCTSI	GIVEQCCTSI	GIVEQCCTSI	-
A	GIVEQCCTSIC	-	-	-
A	GIVEQCCTSICS	-	-	-
A	-	-	IVEQCCT	-
A	-	-	CCTSICSL	-
A	TSICSLYQLE	-	-	-
A	TSICSLYQLENY	-	-	-
A	SICSLYQLE	-	-	-
A	SICSLYQLENY	-	-	-
A	-	-	ICSLYQLE	-
A	ICSLYQLENY	-	-	-
A	CSLYQLENY	-	CSLYQLENY	-
A	CSLYQLENYCN	-	-	-
A	-	SLYQLE	-	-
A	-	SLYQLEN	SLYQLEN	-
A	SLYQLENY	SLYQLENY	SLYQLENY	-
A	SLYQLENYCN	-	SLYQLENYCN	-
A	-	-	LYQLENY	-
A	-	-	LYQLENYCN	-
A	-	-	YQLENYC	-
A	-	YQLENYCN	YQLENYCN	-
A	-	QLENYCN	QLENYCN	-
B	FVNQHLCG	-	-	-
B	FVNQHLCGS	-	-	-
B	FVNQHLCGSH	-	-	-
B	FVNQHLCGSHL	-	-	-
B	FVNQHLCGSHLVE	-	-	-
B	FVNQHLCGSHLVEA	-	-	-
B	VNQHLCGSHLVE	-	-	-
B	NQHLCGSHLVE	-	-	-
B	QHLCGSHL	-	-	-
B	QHLCGSHLVE	-	-	-
B	HLCGSHL	HLCGSHL	HLCGSHL	-
B	HLCGSHLV	-	HLCGSHLV	-
B	HLCGSHLVE	HLCGSHLVE	HLCGSHLVE	HLCGSHLVE
B	HLCGSHLVEA	-	HLCGSHLVEA	-
B	HLCGSHLVEALYLVCGERGFFYTPKT	-	-	-
B	-	-	LCGSHLV	-
B	LCGSHLVE	LCGSHLVE	LCGSHLVE	LCGSHLVE
B	LCGSHLVEA	LCGSHLVEA	LCGSHLVEA	LCGSHLVEA
B	LCGSHLVEAL	-	-	-

B	-	-	CGSHLVE	CGSHLVE
B	GSHLVEALYL	GSHLVEALYL	-	-
B	-	-	SHLVEALY	-
B	SHLVEALYL	SHLVEALYL	-	-
B	VEALYLVCGE	-	VEALYLVCGE	-
B	EALYLVCGE	-	EALYLVCGE	-
B	EALYLVCGER	-	-	-
B	-	ALYLV	ALYLV	-
B	-	ALYLVC	-	-
B	ALYLVCGE	ALYLVCGE	ALYLVCGE	-
B	ALYLVCGER	-	ALYLVCGER	-
B	-	-	LYLVCGE	-
B	LYLVCGER	-	-	-
B	-	-	YLVCGER	YLVCGER
B	VCGERGF	-	-	-
B	VCGERGFFY	VCGERGFFY	-	-
B	VCGERGFFYT	VCGERGFFYT	VCGERGFFYT	-
B	VCGERGFFYTPKT	VCGERGFFYTPKT	VCGERGFFYTPKT	-
B	CGERGFFYTPKT	-	CGERGFFYTPKT	-
B	-	-	GERGFF	-
B	GERGFFYT	GERGFFYT	-	-
B	GERGFFYTPKT	GERGFFYTPKT	GERGFFYTPKT	GERGFFYTPKT
B	ERGFFYTPKT	ERGFFYTPKT	ERGFFYTPKT	ERGFFYTPKT
B	RGFFYTPKT	-	-	-
B	GFFYTPKT	GFFYTPKT	GFFYTPKT	-
B	FFYTPKT	-	FFYTPKT	-
B	-	FYTPKT	-	-

Table 6.1: Peptides observed following proteasomal degradation

Sequences of the peptides observed following the proteasomal degradation of insulin, ^{20K}PEG-insulin, ^{30K}PEG-insulin and ^{40K}PEG-insulin. Highlighted in green are sequences detected in each repertoire. N=2.

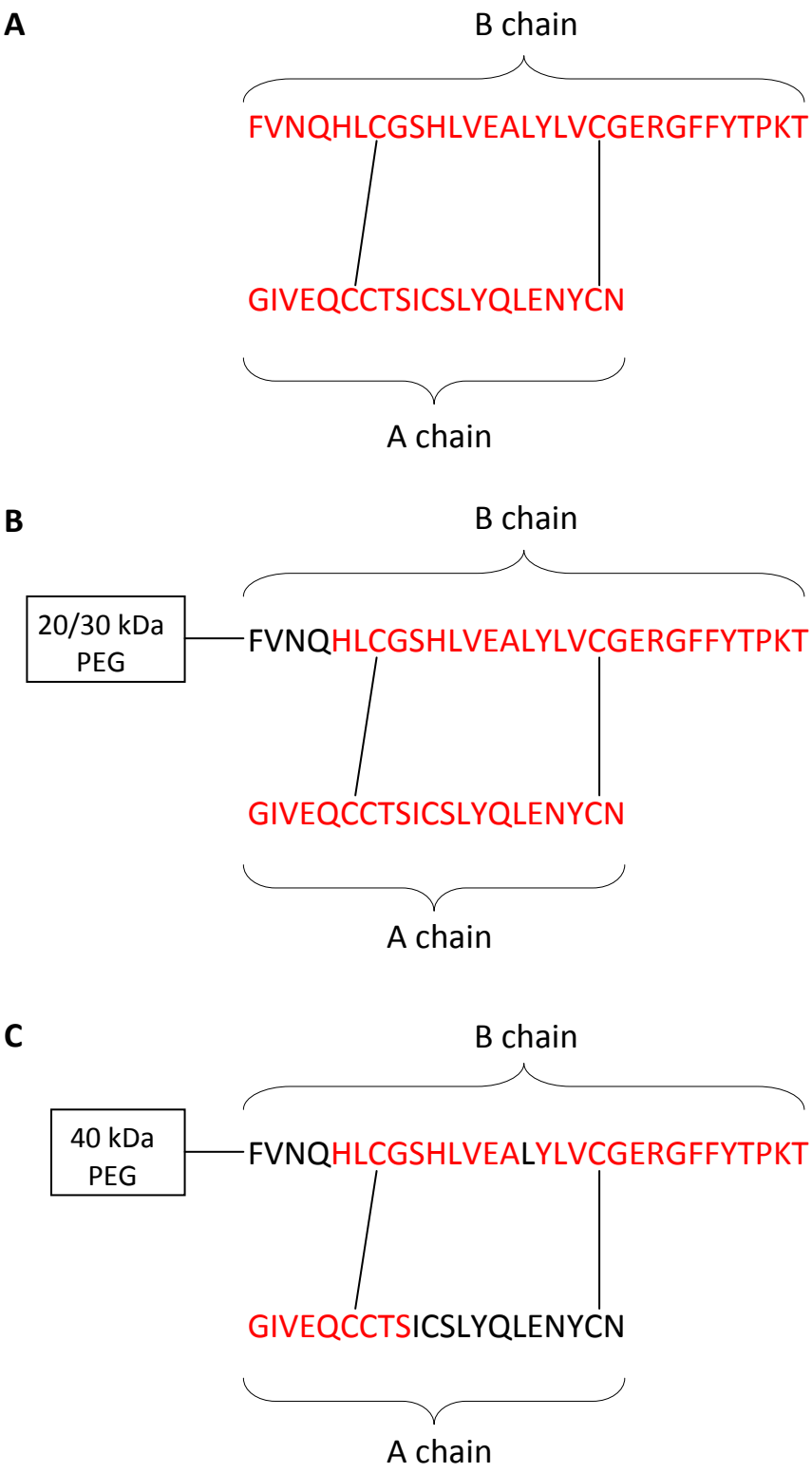

Figure 6.9: Differential peptide repertoires generated between insulin and PEGylated insulin

The amino acid structures of insulin (A) and PEGylated insulin (B and C), displaying the A and B chains linked by two disulphide bridges. Highlighted in red are the amino acids present in the unique peptides that were detected following the proteasomal degradation of non-PEGylated insulin (A), ^{20K}PEG-insulin and ^{30K}PEG-insulin combined (B), and ^{40K}PEG-insulin (C).

A total of 24 peptides (32.9%) were unique to the non-PEGylated insulin repertoire, of which 10 of these peptides (41.7%) form the N-terminus of the B chain, which is the site of PEG attachment. Again, as was observed in the lysosomal generated peptide repertoires, PEG, regardless of MW, confers local protection at this site, as shown in figure 6.9 B and C. Whereas there was little difference in the lysosomal generated repertoires between insulin and each PEGylated insulin, other than at the site of attachment, following proteasomal degradation there were only 8 peptides (11.0%) that were detected in the repertoires of both non-PEGylated insulin and all three PEGylated insulin conjugates. A total of 49 peptides were detected from the repertoires of each PEGylated insulin combined, 21 (42.9%) of which were not detected in the non-PEGylated insulin repertoire. Of these 49 peptides, 27 (55.1%) were unique to one conjugate, 13 (26.5%) were detected in two repertoires, and 9 (18.4%) were detected in the repertoires of all three conjugates; indicating there is much greater variation in the peptides formed following proteasomal processing in comparison to lysosomal processing. The largest difference, however, is in the number of peptides detected for each conjugate. For ^{20K}PEG-insulin, a total of 28 peptides were found, whilst for ^{30K}PEG-insulin a total of 41 peptides were detected. However, for ^{40K}PEG-insulin, only 11 peptides comprised the entire repertoire. As shown in figure 6.9 C, the majority of these "missing" peptides are from the C-terminus of the A chain, indicating that 40 kDa PEG can confer protection against proteasomal processing at both the N-terminus of the B chain and the C-terminus of the A chain, presumably through sterically hindering entry of these parts of the protein into the three catalytic active sites of the proteasome.

6.4 DISCUSSION

A 20S proteasome fraction was obtained from human liver that was shown to be highly purified and contain functional proteasome. By using SDS-PAGE followed by Coomassie stain, the purity of the 20S proteasome in the final fraction of the purification protocol was shown to be high; the only bands visible were in between the known MW range (~22 – 35 kDa) of the 20S proteasomal subunits (Beyette *et al.*, 2001). When these bands were excised and analysed by reversed-phase HPLC each proteasomal subunit was detected. Specific proteasomal activity, chymotrypsin-like and trypsin-like, by the purified 20S proteasome was identified through the use of fluorogenic probes. Furthermore, in the presence of MG132, a specific proteasome inhibitor, these activities were inhibited. Initial degradation studies of insulin, analysed by SDS-PAGE and Coomassie stain, indicated that insulin was degraded in the presence of purified 20S proteasome. The extent of degradation was comparable to that when commercial 20S proteasome, used as a positive control, was used to degrade insulin under the same conditions. In the presence of MG132, degradation of insulin by purified 20S proteasome was inhibited; providing further evidence that degradation was proteasome-mediated. Consequently, this fraction was used to assess the effect of PEGylation, in particular the effect of altering PEG MW, on the proteasomal degradation of insulin – a model protein. In the presence of 20S proteasome, insulin was degraded almost to completion over 48 hours. When analysing the proteasomal degradation of ^{20K}PEG-insulin, ^{30K}PEG-insulin and ^{40K}PEG-insulin, such that the overall amount of insulin as part of the different sized conjugates was equivalent to that of the non-PEGylated insulin incubation, a MW-dependent protective effect was identified. The degradation of the insulin moiety when conjugated to 20 kDa was found to be similar to the degradation of non-PEGylated insulin over 48 hours; indicating the lower MW PEG does not confer protection against proteasomal degradation when conjugated to insulin. However, when coupled to either 30 kDa or 40 kDa PEG, the insulin moiety was only

degraded to approximately 50% for both conjugates over 48 hours; indicating that PEG of a MW above 20 kDa can partially protect insulin from proteasomal degradation.

Next, the peptide repertoires generated from non-PEGylated insulin and PEGylated insulin following proteasomal degradation were assessed using MS. A total of 52 peptides were detected in the repertoire generated from non-PEGylated insulin, which together covered the entire sequence of insulin. When comparing the peptides from PEGylated insulin, there was a marked difference between the overall sequence coverage from the peptides generated between ^{20K}PEG-insulin and ^{30K}PEG-insulin, with that of ^{40K}PEG-insulin. Peptides from the N-terminus of the B chain could not be detected in the repertoires from all three conjugates. The N-terminus of the B chain is the site of PEG attachment; consequently, it appears that PEG can again confer local protection against proteasomal degradation at the site of attachment, as was also found following lysosomal degradation. For ^{20K}PEG-insulin and ^{30K}PEG-insulin, the entire remaining sequence of insulin was detected in their corresponding peptide repertoires. However, for ^{40K}PEG-insulin, peptides from the C-terminus of the A chain could not be detected. One explanation for this could be that 40 kDa PEG is sterically hindering the formation of these peptides. In terms of the overall degradation of the insulin moiety of PEGylated insulin, a PEG MW-dependent effect was observed, such that conjugation with either 30 kDa or 40 kDa PEG appeared to provide similar overall protection against degradation over 48 hours. At the peptide level, however, this similarity appears to end, with the 10 kDa increase in MW seemingly providing greater protection to C-terminal peptides. Despite the overall sequence coverage from the peptides detected between ^{20K}PEG-insulin and ^{30K}PEG-insulin being similar overall, there was still much variation in terms of the numbers of peptides which constitute each repertoire; with a total of 28 peptides detected in the repertoire of ^{20K}PEG-insulin and 41 peptides detected from ^{30K}PEG-insulin, with only 11 detected from ^{40K}PEG-insulin. Furthermore, there was also variation in the number of detected peptides common to each

conjugate, with 55.1% of the detected peptides unique to the repertoire of one conjugate only, and only 18.4% of detected peptides common to the repertoires of all three conjugates. In comparison to the repertoires generated following lysosomal degradation, 75% of the PEGylated insulin peptides detected were common to all three conjugates. Surprisingly, however, these figures both originate from the same total number of peptides common to PEGylated insulin, which was 9 between both pathways, as shown in table 6.2.

	Lysosomal Peptides				Proteasomal Peptides			
	Insulin	^{20K}PEG-insulin	^{30K}PEG-insulin	^{40K}PEG-insulin	Insulin	^{20K}PEG-insulin	^{30K}PEG-insulin	^{40K}PEG-insulin
No. of Peptides	21	10	9	11	52	28	41	11
A Chain Peptides	6	3	3	4	15	11	17	4
B Chain Peptides	15	7	6	7	37	17	24	7
Insulin Coverage (%)	92.2%	60.8%	60.8%	60.8%	100%	90.0%	92.2%	68.6%
A Chain Coverage (%)	93.3%	76.2%	76.2%	76.2%	100%	95.2%	100%	42.9%
B Chain Coverage (%)	90.5%	50%	50%	50%	100%	86.7%	86.7%	83.3%
Shared Insulin Peptides	-	10	9	10	-	19	23	8
Shared A Chain Peptides	-	3	3	4	-	5	7	3
Shared B Chain Peptides	-	7	6	6	-	14	16	5
No. of Peptides common to PEG-insulin	-		9		-		9	

Table 6.2: Differences in the peptide repertoires generated between lysosomal and proteasomal processing

There was also much more variation in the combined PEGylated insulin repertoires compared to non-PEGylated insulin in the proteasomal repertoires than in those generated following lysosomal processing. A total of 24 peptides were unique to non-PEGylated insulin following proteasomal degradation, compared to only 10 following lysosomal degradation. There were also more peptides detected overall following proteasomal degradation (73 peptides) compared to lysosomal degradation (22 peptides). Under the conditions used in these studies this is perhaps not surprising given that the substrate-to-enzyme ratio used in the lysosomal incubations was 1:1.6 (w/w), compared to 5:1 (w/w) for the proteasomal incubations. Furthermore, the L^+ fraction is comprised of many different

hydrolase enzymes with different specificities and capacities for proteolytic degradation, compared to only three proteolytic activities of the proteasome. Presumably, the difference in the overall number of detected peptides between the two pathways can be explained by these differences, since it is likely that once peptides are formed following lysosomal degradation they can be quickly hydrolysed down to their constitutive amino acids, or peptides too small for MS detection, due to the excess enzyme-to-substrate ratio. This explanation may also account for the much larger variation observed in the PEGylated insulin repertoires between the two pathways, but does not seemingly account for why 40 kDa PEG confers extra protection for C-terminal peptides when it appeared to confer similar overall protection as 30 kDa PEG.

Taken together, these data indicate that altering the MW of PEG can result in differential rates of proteasomal degradation of the attached protein and altered peptide repertoires, which has implications for both the overall disposition of PEGylated proteins and, potentially, for their immunogenicity. In order to assess this latter effect it would be important to characterise degradation by immunoproteasomes, in addition to the constitutive proteasome, as was the case here. Immunoproteasomes are the predominant form in APC, which contain immunoproteasomes under inflammatory conditions in response to pathogens. Whilst both the constitutive proteasome and the immunoproteasome produce peptides presented by MHC class I molecules to $CD8^+$ T cells, the immunoproteasome is reported to generate an altered peptide repertoire to that of the constitutive proteasome, a repertoire that is thought to contain more peptides with increased affinity for MHC class I molecules. Continuation of this project should, therefore, include the isolation of APC 20S proteasome to further support a role for PEGylation in immune processing.

In conclusion, 20S proteasome was purified from human liver and was used to assess the effect of PEGylation on the proteasomal degradation of a model protein. A MW-

dependent protective effect of PEG was found, such that increasing PEG MW provides enhanced protection against proteasomal degradation of the coupled protein. Whilst there was much variation in the peptide repertoires formed between the conjugates, this protection was focused at the site of PEG attachment regardless of PEG MW; as was also found in the peptide repertoires generated following lysosomal degradation. However, the addition of 40 kDa PEG to insulin did confer protection at the C-terminal of the A chain. Perhaps surprisingly, this was not observed following conjugation with 30 kDa PEG, despite the two appearing to confer equal overall protection when analysed using western blotting. Taken together, these data indicate that PEGylation with higher MW PEGs can prolong the stability of the coupled protein to proteasomal degradation, and can selectively protect peptides from degradation at the site of attachment. However, since exogenous protein degradation primarily occurs via lysosomal degradation, the clinical impact of site-specific PEGylation on proteasomal degradation may be relatively small. Furthermore, future studies focused on assessing the differences between the peptide repertoires generated following proteasomal degradation of protein and the corresponding PEGylated protein should include the immunoproteasome, which prevail under inflammatory conditions in the response to pathogens, rather than constitutive proteasome.

CHAPTER 7

Final Discussion

CONTENTS

7.1 PROTEIN PEGYLATION

Today, biologics represent an exciting and diverse class of pharmaceuticals. The last ten years has seen an increase in the number of biologics either approved for medical use, or entering clinical trials. The advantages of biologics over typical small molecule drugs are numerous. However, the disadvantages they possess, such as instability, rapid renal elimination, vulnerability to proteolytic degradation and immunogenicity, limit their utility. To counteract these limitations, biologics have been modified with various reagents, of which PEG has become the most common modification. PEG acts as a protective shield, inhibiting proteolytic degradation and immune recognition, whilst simultaneously reducing renal elimination due to increasing the overall MW. These benefits have been well validated, yet there is still relatively little known about the metabolism and disposition of PEGylated proteins. Whilst the disposition and metabolism of unconjugated PEG is well understood, though this data has predominantly been generated utilising PEGs with MWs that are not usually applied for pharmaceutical conjugation, the metabolism and disposition of PEGylated proteins is not. This, in part, is caused by difficulties in the bioanalysis of PEGylated macromolecules using routine analytical methods, such as MS and immunoassays. There have also been reports of neutralising antibodies and immune-mediated ADRs against the PEG moiety of PEGylated therapeutics, in both patients and animal studies, suggesting that PEGylation may not be a universally safe method for ameliorating the limitations associated with biologics.

In the studies described in this thesis, several methodologies were developed, optimised and assessed for their utility with regards to the bioanalysis of PEGylated proteins. These methods were developed in order to 1) determine the disposition and biological fate of PEGylated proteins, and 2) assess the effect of PEGylation on internalisation and intracellular degradation. To assess the disposition and biological fate of

PEGylated proteins, a multi-analytical platform, comprising three gel-based assays and ^{1}H NMR, was first established that was capable of tracking the *in vivo* disposition of a model PEGylated protein in biological matrices. This platform was applied to samples generated from a 28 day disposition study in rodents, whilst simultaneously providing information concerning the individual fate of both the PEG and protein moieties of the conjugate, as well as its overall structural integrity. To determine the internalisation and intracellular degradation of PEGylated proteins, by both the lysosomal and proteasomal pathways of protein degradation (processes which are also intimately involved in the immune response), flow cytometry, fluorescence microscopy, and enriched lysosome/purified proteasome fractions were utilised. The overall research programme and key data are presented graphically in figure 7.1.

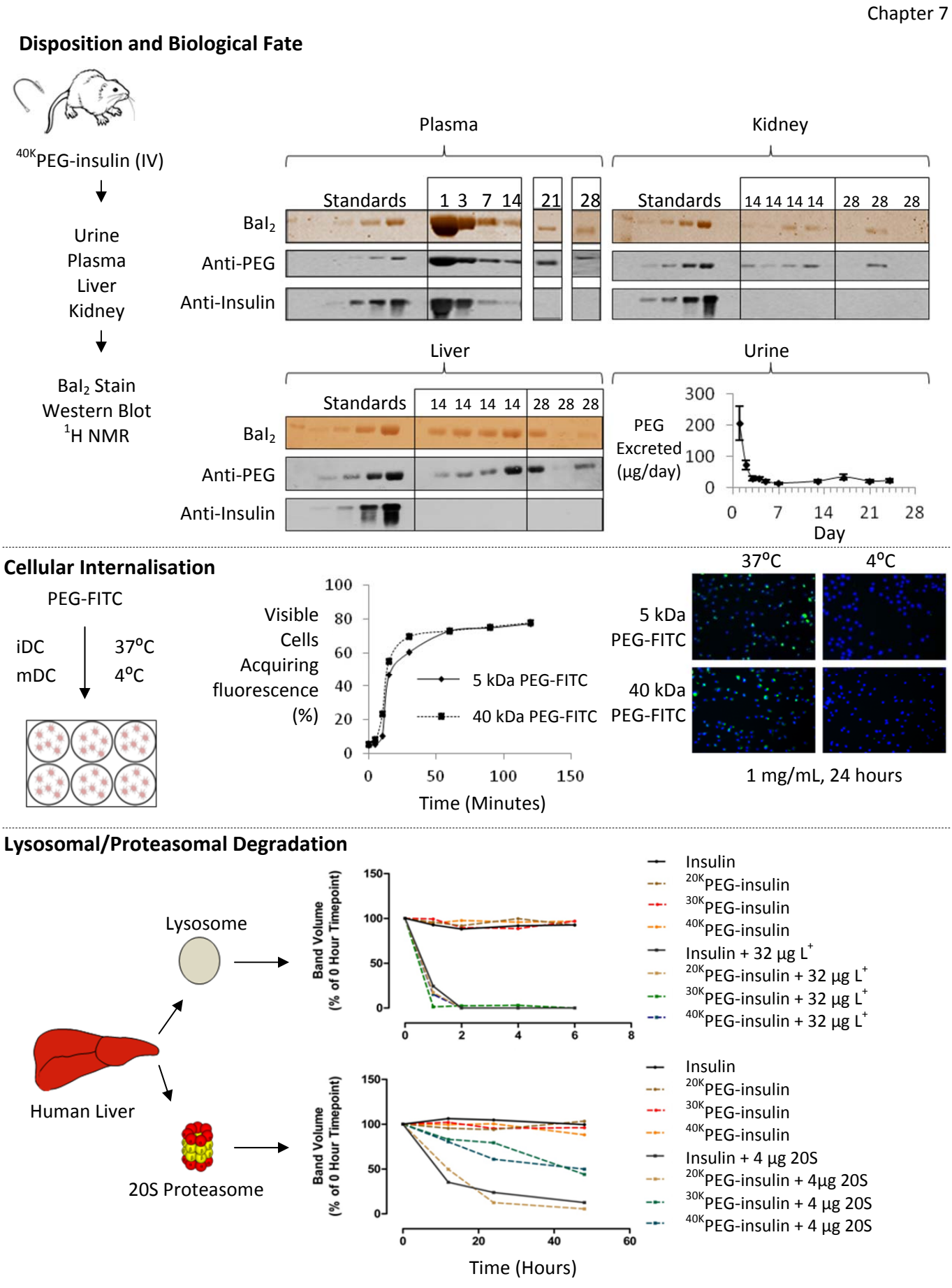

Figure 7.1: Schematic illustrating the conceptual basis of the studies and exemplar data from the individual facets of the research programme

7.2 DISPOSITION AND METABOLIC FATE OF PEGYLATED PROTEINS

As described in detail in the general introduction, there are inherent difficulties regarding the bioanalysis of PEG, and consequently PEGylated therapeutics. These difficulties have necessitated the development of alternative analytical approaches suitable for measuring the pharmacokinetics, disposition and biological fate of PEGylated proteins. In this project, a combination of three gel-based assays, which independently monitor both the PEG and protein moieties, and ^{1}H NMR, which monitors PEG, were developed, optimised and shown to be capable of measuring ^{40K}PEG-insulin circulating in plasma and excreted in urine, whilst also providing a measure of tissue retention in liver and kidney; thus allowing the disposition and PK parameters of the conjugate to be determined. Following a single dose of ^{40K}PEG-insulin both the anti-PEG western blot and ^{1}H NMR were able to detect the PEG moiety of the conjugate throughout the 28 day disposition study in urine, whilst the anti-PEG western was also capable of monitoring PEG in plasma (figures 2.4 – 2.6 and 3.12). Furthermore, anti-PEG western blotting could also detect PEG on days 14 and 28 in liver and kidney tissue (figures 2.7 – 2.8). The addition of PEG was shown to substantially prolong the half-life of the coupled insulin, from ~5 minutes, for unmodified insulin, to 131 hours for ^{40K}PEG-insulin. However, the use of anti-insulin western blotting revealed that the conjugate did not remain intact throughout the 28 day period, despite the PEGylation chemistry used in this study to couple 40 kDa PEG to insulin being second-generation, and therefore designed to provide a stable linkage between PEG and protein. In urine and plasma samples, the insulin moiety depleted over time until it was degraded completely by approximately days 7 and 14, respectively; leaving only PEG, in some form, circulating in plasma and excreted in urine (figures 2.4 – 2.6). Accordingly, in both liver and kidney tissue the insulin moiety could not be detected on either day 14 or 28, indicating that a PEG moiety, that was no longer intact PEG-insulin, was accumulating in these tissues (figures 2.7 – 2.8). The loss of insulin signal can be explained by either 1) sequential

degradation of the insulin moiety whilst still coupled to PEG, or 2) complete metabolic cleavage of the conjugate, after which insulin is rapidly excreted/degraded. The first explanation is in direct contrast with the rationale for PEGylating proteins, whereby the PEG moiety is used to protect the attached protein from proteolytic degradation. The second explanation again has repercussions regarding protection of the protein, as well as potentially altering its intracellular disposition following cleavage, but also opens up the interesting possibility that cleavage may result in the subsequently un-protected protein becoming available for immunological processing. Again, this would be contrary to the reasoning behind PEGylation – in order to reduce the immunogenicity of proteins. As described in the general introduction, it is reported that PEGylation reduces the immunogenicity of proteins through protecting antigenic epitopes on the protein's surface from recognition by the immune system. However, this does not preclude other, potential effects PEGylation may have on other processes involved in producing an immune response against a PEGylated protein, such as cellular uptake and subsequent degradation through the lysosomal and proteasomal pathways of protein degradation. Subsequently, the site of degradation becomes an important factor, since cellular uptake followed by conjugate cleavage would allow lysosomal and proteasomal processing and presentation to the immune system to occur. The site of degradation could not be determined *in vivo* from the 28 day disposition samples. However, the structural integrity of ^{40K}PEG-insulin was assessed *in vitro* in control rat plasma. Over a period of 7 days, a period in which major loss of insulin signal *in vivo* was observed*,* the insulin moiety of ^{40K}PEG-insulin was shown to be stable – with no loss of insulin signal detected at all between day 0 and day 7 (figure 2.9). Taken together, these data indicate that the PEG moiety confers substantial protection against enzymatic degradation extracellularly, but following internalisation this protection is lost and the insulin moiety is either sequentially degraded, or metabolically cleaved entirely from PEG, which could result in immunological responses against the liberated protein.

Consequently, subsequent investigation focused on the cellular internalisation of PEG and PEGylated insulin.

Initially, the gel-based platform and ^{1}H NMR were assessed for their ability to monitor the internalisation of ^{40K}PEG-insulin in both HepG2 cells, in order to replicate the *in vivo* findings of the 28 day disposition study in an *in vitro* model, and DCs, in order to begin investigation into the possible effects of PEGylation on processes involved in immune responses. However, these methods proved to be insufficiently sensitive to adequately monitor internalisation of ^{40K}PEG-insulin, and so alternative analytical methods were pursued. These methods were flow cytometry and fluorescence microscopy, which necessitate the use of fluorescent compounds for analysis – consequently, FITC labelled PEGs were utilised. Furthermore, subsequent analysis focussed on internalisation by DC, rather than HepG2 cells, due to their efficient endocytic ability and roles in the immune system. Initial investigation utilised flow cytometry to assess the internalisation of both 5 kDa and 40 kDa PEG-FITC. Internalisation was also assessed in both iDC and mDC, which were employed as an indicator for endocytosis; since mDC have a reduced endocytic capacity in comparison to iDC. When both iDC and mDC were incubated with 5 kDa PEG-FITC, iDC did indeed internalise 5 kDa PEG-FITC at a higher rate than mDC – indicating that the cells were internalising 5 kDa PEG-FITC through endocytosis (figure 4.8). When comparing the internalisation of 5 kDa PEG-FITC and 40 kDa PEG-FITC by iDC, both were internalised to a similar degree; with almost identical rates of acquired fluorescence between the two fluorescent PEGs over two hours (figure 4.9). However, possible concerns over signal saturation led subsequent analysis to focus primarily on fluorescence microscopy. In these analyses, cells were also incubated at 4^{o}C, as well as using mDC, as a negative control for endocytosis, which does not occur at low temperatures as it is an energy-dependent process. Both 5 kDa PEG-FITC and 40 kDa PEG-FITC were internalised over 24 hours by iDC (figures 4.10 and 4.12). When incubated with mDC, both were

internalised to a lesser degree in comparison to iDC (figures 4.13 – 4.14). Furthermore, when incubated at 4^{o}C, no visible fluorescence was observed at 24 hours with either 5 kDa or 40 kDa PEG-FITC; indicating that the cells were internalising PEG-FITC by endocytosis. Again, as found following flow cytometry analysis, both 5 kDa PEG-FITC and 40 kDa PEG-FITC appeared to be internalised by iDC at almost identical rates, over 24 hours (figure 4.12). When comparing the number of iDC that had acquired visible fluorescence between the two probes at 24 hours, the numbers were again remarkably similar, with approximately 83.8% of cells acquiring visible fluorescence following incubation with 5 kDa PEG-FITC compared to 79.4% of cells incubated with 40 kDa PEG-FITC. Furthermore, when comparing the mean pixel intensity of acquired fluorescence by iDC between the two probes at 24 hours, the values were again similar, with mean pixel intensities of 62.8 (arbitrary units) for 5 kDa PEG-FITC compared to 58.5 for 40 kDa PEG-FITC; indicating that iDC internalise both probes equally in terms of the number of PEG-FITC molecules internalised – since both PEGs are coupled to only one FITC molecule – despite the difference in MW. In keeping with the previous work described in this thesis, regarding the disposition and biological fate of ^{40K}PEG-insulin, the internalisation of fluorescently labelled insulin (insulin-rhodamine) was also assessed by fluorescence microscopy, and was shown to be internalised in a time-dependent manner (similar to the internalisation of PEG-FITC) over 24 hours (figure 4.11). These data indicate PEG can be internalised by DC regardless of MW, with remarkably similar rates of internalisation between the two PEG-FITC probes. Whilst neither flow cytometry or fluorescence microscopy can measure the absolute amounts of each probe internalised, the data obtained using fluorescence microscopy revealed that iDC internalise both probes similarly in terms of both the number of cells acquiring visible fluorescence, and the average amount of FITC internalised – as determined by the mean pixel intensity at 24 hours. Given that both probes are conjugated to one FITC molecule it is perhaps feasible that iDC have in fact internalised more PEG

overall when incubated with 40 kDa PEG-FITC, despite the increase in MW compared to 5 kDa PEG-FITC, due to the similarities in mean pixel intensity observed between the two probes; further investigation would be required, however, to resolve this question. In terms of altering the internalisation and biodistribution of a protein by DC however, it is likely that altering PEG MW has little effect, since similar numbers of PEG-FITC molecules were internalised despite the difference in MW; therefore, the overall amount of conjugated protein internalised ought to be similar also. Consequently, subsequent investigation focussed on the effect of PEGylation on events occurring immediately proceeding internalisation.

Internalisation of PEG had been observed both *in vivo* and *in vitro*, and had been shown to occur via endocytosis *in vitro.* The endocytic pathway culminates in the degradation and processing of the internalised substrate by hydrolase enzymes contained in the lumen of the lysosome. Consequently, the intracellular stability of PEGylated insulin to lysosomal degradation was assessed; using an enriched lysosome fraction (L^+ fraction) obtained from human liver. Insulin was conjugated to either 20 kDa or 30 kDa PEG using the same coupling strategy to attach 40 kDa PEG to insulin to synthesise ^{40K}PEG-insulin – used in earlier studies. When non-PEGylated insulin was incubated with L^+ complete degradation was observed by anti-insulin western blotting within 2 hours (figure 5.3). When all three PEGylated insulin conjugates were incubated with L^+, such that each incubation contained equivalent insulin to the non-PEGylated insulin incubation, the insulin moiety was again completely degraded within 2 hours – regardless of the MW of the attached PEG (figure 5.7). Indeed, when incubating each PEGylated insulin with reduced concentrations of L^+, only a very a slight PEG MW-dependent effect was observed; such that only 40 kDa PEG could confer protection against complete degradation over 6 hours when incubated with 4 μg L^+, though degradation had essentially neared completion at this time (figure 5.11). Next, the effect of PEGylation on the peptide repertoires generated

following lysosomal degradation was compared with that of the repertoire generated from non-PEGylated insulin. For non-PEGylated insulin, nearly the entire amino acid sequence was covered in the detected peptides, with only the peptides ICSLY and VEAL not detected from the A and B chains, respectively (table 5.1). In general, there were only minor differences observed in the peptides repertoires between each PEGylated insulin conjugate, with 75% of the detected peptides from the combined PEGylated insulin repertoires found in each repertoire. However, when comparing these repertoires with that of non-PEGylated insulin, there was found to be no peptide sequences originating from the N-terminal of the B chain detected for each conjugate (figure 5.13). The PEGylation chemistry used in this thesis to conjugate PEG to insulin results in the selective coupling of PEG to insulin at the N-terminal α-amine of the B chain. Taken together, these data indicate that PEG, regardless of MW, can provide partial protection against lysosomal degradation at the site of attachment.

The predominant route for exogenous protein degradation proceeds through the lysosome. However, certain APC, primarily DC, possess the capacity to process exogenous proteins through the proteasome also. Consequently, since little is still understood concerning the intracellular disposition of PEGylated proteins, the intracellular stability of PEGylated insulin to proteasomal degradation was also assessed. Whereas no PEG MW-dependent effect was observed following lysosomal degradation, conjugation with either 30 or 40 kDa PEG conferred protection against proteasomal degradation such that ~50% of the insulin moiety had been degraded at 48 hours – a time at which both non-PEGylated insulin and the insulin moiety of ^{20K}PEG-insulin had essentially been completely degraded (figure 6.8). Given that the enzyme-to-substrate ratio in the lysosome *in vivo* favours degradation, as well as containing many different protease enzymes, it is not surprising that differential protection was observed between the lysosomal and proteasomal degradation of PEGylated insulin – under the experimental conditions described in this

thesis – particularly given that the proteasome contains only three proteolytic activities: trypsin-like, chymotrypsin-like and caspase-like. When analysing the peptide repertoires generated following proteasomal degradation, again all three PEGs appeared to selectively protect peptides at the site of attachment. Despite this, much variation was observed in the PEGylated insulin peptide repertoires in terms of the overall numbers of peptides detected in each repertoire. Furthermore, only 18.4% of the detected peptides in the PEGylated insulin repertoires were found in the repertoires of all three conjugates, as opposed to 75% in the repertoires generated following lysosomal degradation. Conjugation with 40 kDa PEG also appeared to confer extra protection to the coupled insulin at the C-terminus of the A chain, which was not observed either in the repertoires of ^{20K}PEG-insulin and ^{30K}PEG-insulin, or any repertoire generated following lysosomal degradation. Taken together, these data indicate that PEG can again, regardless of MW, protect coupled proteins against proteasomal degradation at the site of attachment – suggesting that site-specific PEGylation may represent a viable tool to prevent antigenic peptide formation following proteasomal processing. Furthermore, increased PEG MW appears to confer extra protection, both in terms of overall conjugate stability and in the peptides formed following proteasomal processing. However, much more variation was observed in the proteasomal repertoires in comparison to the lysosomal repertoires. This may reflect differences in the experimental conditions used in these studies and/or differences in the nature of each pathway, as described in more detail in section 6.4. Further investigation is warranted to elucidate the clinical relevance of these findings given that proteasomal degradation and processing of exogenous proteins is not the primary route of antigen generation.

The fact that N-terminal peptides were not detected in either system implies that these peptides remain attached to PEG intact, and are consequently unable to pass through the 3 kDa MWCO filter for MS analysis. However, this does not preclude the

interesting possibility that N-terminal peptides are generated but are still coupled to the linker, or even a small PEG moiety under the MWCO limit, and consequently were not identified. It is more likely that a peptide still coupled to the linker will be formed, rather than a peptide still coupled to a small PEG moiety, since metabolism of PEG is MW-dependent – consequently metabolism of the PEGs used in these studies is unlikely. Furthermore, alcohol dehydrogenase, the enzyme which metabolises PEG, is not a known lysosomal hydrolase enzyme. Nevertheless, the formation of peptides still coupled to the linker/PEG may result in neo-antigens, leading to antibody generation against PEG, the linker, or both. Indeed, the anti-PEG antibody used for western blotting in these studies also recognises the linker – it is, therefore, not unlikely that an immune response could be generated against such neo-antigens.

7.3 PHARMACOLOGICAL AND TOXICOLOGICAL IMPLICATIONS OF THE STUDIES

These studies provide further evidence for the accumulation of PEG in biological tissues, as presented in figure 7.2, which also summarises the pharmacological advantages of PEGylated biologics (using insulin and ^{40K}PEG-insulin as an example), as well as the reported toxicological implications of their use.

As described in the general introduction, the majority of data concerning PEG biodistribution and toxicology has been generated from animal studies. These studies show PEG accumulates in biological matrices such as skin, muscle and bone, as well as liver and kidney, for which the studies described in this thesis provide further evidence. Furthermore, in this thesis, accumulation was shown to occur following a single dose of ^{40K}PEG-insulin, and was measurable up to 28 days post dose, indicating the ease and persistence of PEG accumulation in biological tissues. Whilst the effect of PEGylation on the pharmacology and efficacy of insulin was not assessed in these studies, PEGylation has previously been shown to enhance efficacy through prolonging the coupled therapeutics'

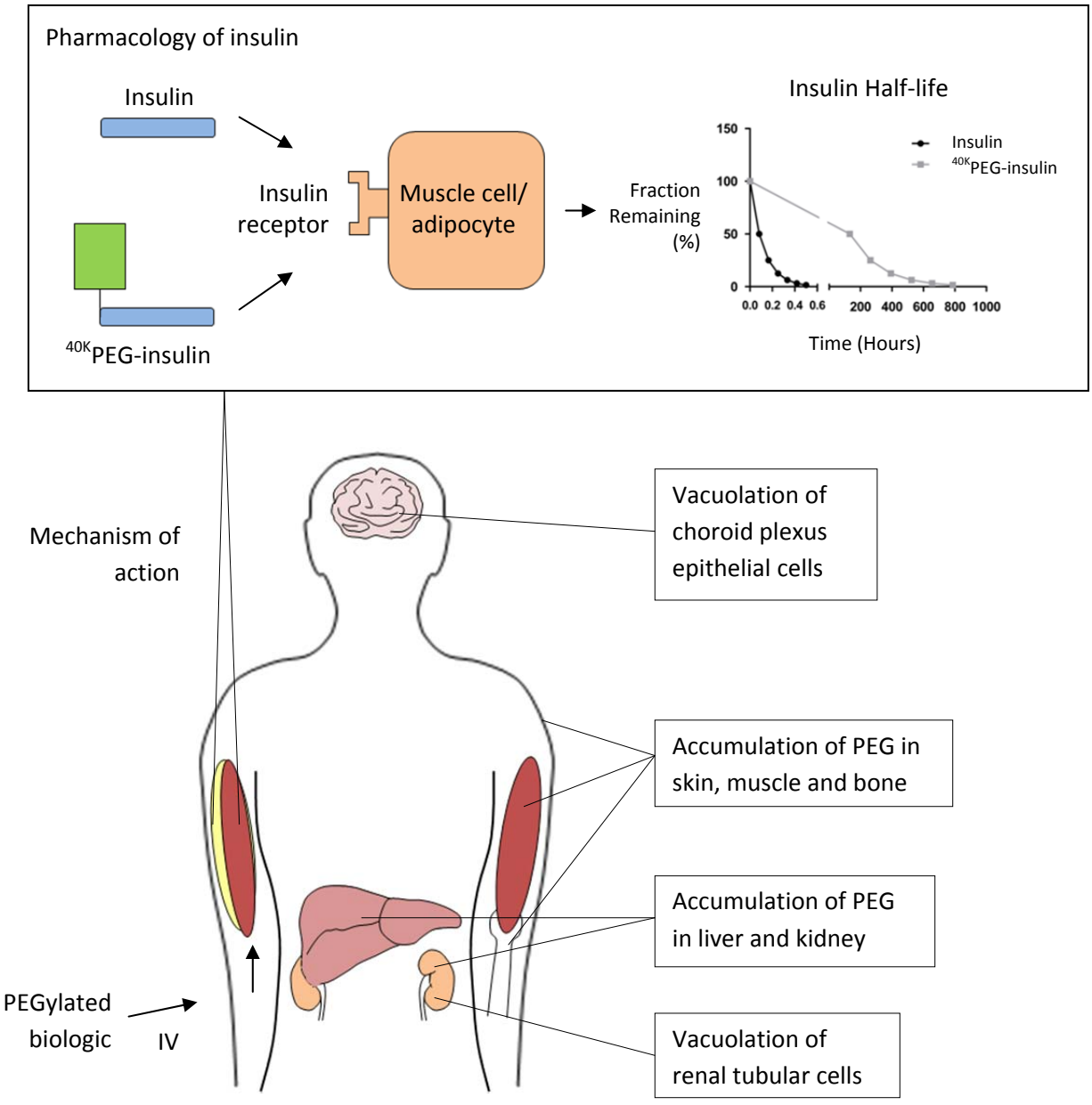

Figure 7.2: Pharmacology and biodistribution of PEGylated biologics and potential toxicological consequences translated to man

Schematic outlining the known biodistribution and toxicological implications of PEGylated biologics. Using ^{40K}PEG-insulin as a model PEGylated biologic, data generated from the 28 day disposition study revealed PEGylation enhanced the circulatory half-life of insulin from ~5 minutes to 131 hours. Furthermore, PEG was shown to accumulate in liver and kidney tissue which was no longer intact PEGylated insulin

half-life – of which PEGylation, in this study, prolonged the half-life of insulin from ~5 minutes to 131 hours, clearly demonstrating the advantage of PEGylation as a strategy to

improve the pharmacokinetics of biologics. Furthermore, ^{40K}PEG-insulin was shown to remain intact in plasma *in vitro* over a period of 7 days, indicating that PEGylation not only prolongs half-life but presumably maintains the activity of coupled biologics through preventing their degradation and consequently still allowing for target receptor binding, though the relevant PD studies must be performed to ascertain this, as described in numerous other reviews. However, this thesis also provides evidence that ^{40K}PEG-insulin did not remain intact throughout the course of the 28 day disposition study, and that it was the PEG moiety of the conjugate which accumulates in liver and kidney tissue. Broadly speaking, the cleavage and/or degradation of a PEGylated biologic has several implications: 1) cleavage of PEG from the biologic leaves the drug vulnerable to proteolytic degradation; 2) cleavage of the conjugate may alter the intracellular disposition of the biologic; 3) loss of PEG may result in the biologic becoming available for immunological processing. These implications have ramifications for the efficacy and safety of PEGylated biologics, as well as the potential toxicological significance of PEG accumulation. Several animal studies provide evidence that accumulation of PEG may lead to vacuolation of renal tubular epithelial cells, whilst these have not as yet been shown to have pathological significance, despite compressing and distorting the nuclei, their existence and toxicological implications in man is currently unknown. Given the propensity of PEG to accumulate in kidney tissue, this may have implications for the chronic dosing of PEGylated biologics, particularly in patients with poor renal function. Interestingly, recent animal studies have shown that cellular vacuolation following administration of PEG or PEGylated proteins may not be restricted to renal tubular epithelial cells, with vacuolation having been shown to also occur in choroid plexus epithelial cells (Rudmann *et al.*, 2013). The choroid plexus is responsible for production of cerebrospinal fluid (CSF), the fluid which bathes the brain and spinal cord, providing a means to supply nutrition and remove waste products, as well as forming the blood-CSF barrier. Consequently, alterations and/or disruption of the choroid plexus

epithelial cells due to vacuolation may have serious repercussions. Vacuolation appears to correlate with PEG MW and has been observed for both unconjugated PEG and PEGylated proteins, including certolizumab pegol (Cimzia®) for the treatment of Crohn's disease. Indeed, a recent scientific guideline from the European Medicines Agency recommends determining whether vacuolation has been observed in non-clinical studies prior to commencing clinical trials (over 4 weeks in duration), as well as determining the biodistribution of the PEG moiety (EMA, 2012).

7.4 IMMUNOLOGICAL SIGNIFICANCE OF THE STUDIES

The potential effects of PEGylation on protein immunogenicity are detailed in figure 7.3, including implications resulting from data generated in this thesis, and potential effects yet to be fully elucidated.

As shown in figure 7.3, the purported mechanism by which PEGylation reduces protein immunogenicity is through reduced recognition of the coupled protein by pre-existing antibody (processes 1 and 2). However, the potential effects of PEGylation on other processes involved in the immune response are yet to be fully elucidated. In this thesis, the internalisation and intracellular disposition of PEGylated proteins was assessed such that insights into the effect of PEGylation on processes 3 to 5 (figure 7.3) could also be made. Furthermore, the data presented in these studies may indirectly provide insight into process 1. ^{40K}PEG-insulin was shown to be stable in plasma over 7 days *in vitro*, indicating that PEG can provide protection against proteolytic degradation in the circulation. It is this same protection that is reported to inhibit the recognition of the coupled protein by B cells, as well as pre-existing antibodies. The stability of the insulin moiety observed in these studies supports these mechanisms and, furthermore, degradation of ^{40K}PEG-insulin was shown to occur intracellularly – suggesting that circulating proteases may not be able to cleave and/or partially degrade the protein moiety to the extent that the required antigenic

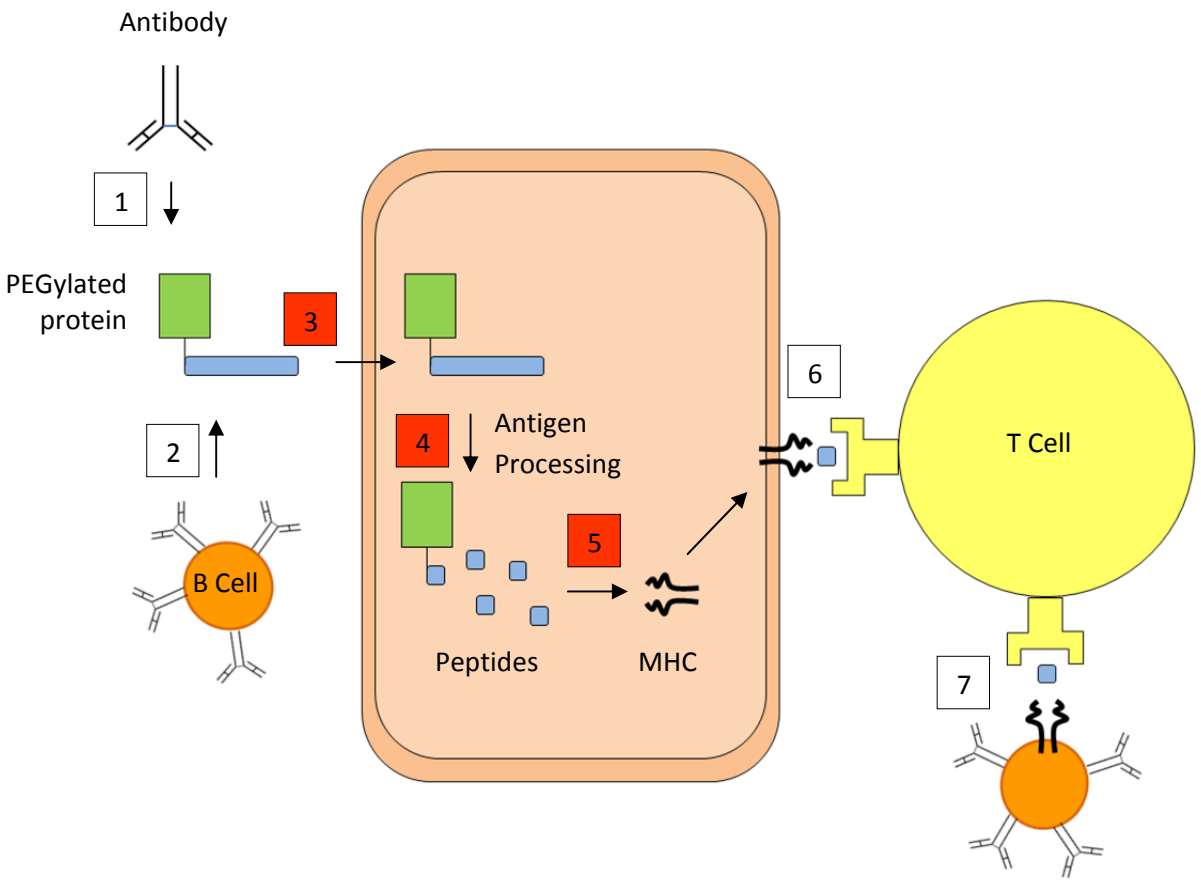

Figure 7.3: Potential effects of PEGylation on protein immunogenicity

Processes potentially affected by PEGylation. 1) Protein recognition by pre-existing antibody. 2) Protein recognition by B cell. 3) Internalisation. 4) Lysosomal/proteasomal antigen processing. 5) Peptide repertoire generation and MHC loading. 6) Presentation to T cell. 7) B cell induction. Highlighted in red are processes addressed in this thesis. Figure adapted from (Pasut *et al.*, 2012)

epitopes for immune recognition become available. In these studies, PEGylation did not appear to be a prohibitive factor in the internalisation of protein of by DC, indicating that PEGylation does not reduce immunogenicity through reduced internalisation of the coupled protein, over the MW ranges used in these studies. Once internalised, exogenous proteins will be degraded and processed into antigens by lysosomal proteases present in the lysosome. In these studies, PEGylation, over a 20 – 40 kDa MW range, was shown to partially protect the coupled protein against lysosomal degradation at the site of attachment, but did not otherwise significantly alter the peptide repertoire in comparison

to non-PEGylated insulin, regardless of MW. These data indicate that site-specific PEGylation may prevent the generation of antigenic peptides and that the methods described in this thesis are suitable for such studies. The effect of PEGylation on proteasomal degradation and processing was also assessed. Again, PEGylation, regardless of MW, conferred partial protection at the site of attachment. However, in contrast to lysosomal processing, proteasomal processing resulted in much more variation in the peptide repertoires generated; with intra-variation between the PEGylated insulin conjugates and with non-PEGylated insulin. Interestingly, a PEG MW-dependent was observed with proteasomal degradation, both in terms of overall degradation of the conjugate and in the peptide repertoires generated. Proteasomal processing of a PEGylated biologic is likely to represent a minor pathway, however, and consequently further investigation is warranted to fully substantiate this PEG protective effect in an immunological setting. Events downstream of antigen processing are currently poorly understood vis-à-vis PEGylated proteins (processes 6 and 7, figure 7.3). Nevertheless, this does not preclude their potential involvement in the role of PEGylation on protein immunogenicity. Further work is required to comprehensively identify the mechanisms by which PEGylation may reduce the immunogenicity of biologics. Furthermore, given the physicochemical differences between biologics and the various PEGylation strategies now in existence, it is likely that one or more processes may be involved and consequently targeted to help further reduce immunogenicity. The methods described herein can be used for such studies, in particular the effect of site-specific PEGylation on preventing the formation of antigenic peptides. Furthermore, these methods may be used to inform and design subsequent evaluation of the processed peptides via T cell assays, such as the lymphocyte transformation test (LTT). Knowledge of the peptides generated forms the basis of such assays. Briefly, T cells, derived from peripheral blood mononuclear cells (PBMC), are incubated with antigen, usually in the form of a peptide, and outcomes such as

proliferation, cytokine secretion and cytotoxic granule release are assessed. These data can also indicate which type of T cell is involved, for example, release of cytotoxic molecules, such as granzyme B, is indicative of $CD8^+$ T cell responses, whereas secretion of cytokines, such as IL-13 and IFNγ, may be indicative of $CD4^+$ T cell responses. Consequently, knowledge of the peptides generated following lysosomal and proteasomal processing combined with their effects on T cells is a powerful tool, which could be exploited for improving the safety of novel and existing PEGylated biologics – particularly if known antigenic epitopes are present in the biologic selected for PEG conjugation.

Whilst PEGylation can reduce the immunogenicity of a protein, PEG itself can also be targeted by the immune system; resulting in a novel immunogenicity. PEG was previously thought to be non-immunogenic, as well as biologically inactive. However, neutralising anti-PEG antibodies and hypersensitivity reactions have been reported for a number of PEGylated proteins, in both animal and human studies, as described in section 1.7. In the studies described in this thesis, antibody generation against the PEG moiety was not investigated. Furthermore, there was no evidence for anti-PEG antibody formation in the 28 day disposition study. Clearly, however, anti-PEG antibodies represent a barrier for the safe and efficacious use of PEGylated biologics, and further investigation into this problem is warranted. Of particular concern is the prevalence of pre-existing anti-PEG antibodies in man, which is reported to have increased to ~25% of the healthy population. This is reportedly a consequence of the increased exposure to PEG in everyday items, such as cosmetics, shampoo and toothpaste, as well as pesticides and fertiliser. Anti-PEG antibodies may, therefore, represent a significant barrier for future PEGylated biologics.

7.5 FUTURE OF PEGYLATION AS A THERAPEUTIC STRATEGY

Since its conception over 40 years ago, PEGylation has been developed and refined into arguably the most successful drug modification strategy to improve the

pharmacokinetics of biologics. Indeed, several PEGylated therapeutics generate annual sales of over $1 billion. Furthermore, PEGylation represents the only viable technology for some biologics to achieve their potential. The pharmacological advantages of PEGylation are undoubted, yet PEGylation does have its limitations. Consequently, there is much interest in improving PEGylation strategies and the methods employed to assess them. It is likely that PEGylation will continue to be a successful drug modification strategy in the near future, reinforcing the need to improve both our understanding of the fundamental mechanics of PEGylation, and the safety of the resulting products – which this thesis has attempted to address. In particular, the advantages of PEGylation on the immunogenicity of biologics have turned out to be more complex than predicted, and the systems developed here provide a platform for investigating this aspect of their safety in more detail.

7.6 CONCLUSIONS AND FUTURE DIRECTIONS

The gel-based methodologies described in chapter 2, provide a facile, inexpensive analytical platform to monitor the disposition and biological fate of PEGylated proteins, as well as being able to measure both the PEG and protein moieties of the conjugate in biological matrices. Where possible, the addition of ^{1}H NMR can provide further bioanalytical power to the assessment of the disposition of PEGylated proteins in biological fluids at the level of absolute quantification. These analytical methodologies allow comprehensive bioanalysis of PEGylated proteins to be achieved – something which had previously been limited; both in terms of what is understood concerning the disposition of PEGylated proteins, and the methods employed for their bioanalysis, as described in the general introduction. These methods may be translated for the bioanalysis of PEGylated agents in other tissues and fluids, as well as for the determination of the pharmacokinetics of novel PEGylated agents under clinical assessment in man.

The gel-based platform revealed that ^{40K}PEG-insulin did not remain intact *in vivo* over 28 days, despite being conjugated using second-generation PEGylation chemistry, and that conjugate cleavage/degradation was occurring intracellularly. Potentially, this could allow for a liberated protein to be immunologically processed. As with the disposition of PEGylated proteins, little is understood concerning definitively how PEGylation can alter the immunogenicity of a protein. Consequently, further investigation focussed on the internalisation and intracellular disposition of PEGylated insulin, processes which are also involved in immunological processing. PEG was shown to be endocytosed by DC regardless of MW, suggesting that PEGylation does not significantly alter the immunogenicity of a protein through preventing their entry into immune cells. Endocytosis culminates in degradation and processing of internalised protein by the lysosome, yet PEG was unable to prevent the lysosomal degradation of insulin over a clinically relevant PEG MW range. Furthermore, when analysing the peptide repertoires generated between PEGylated insulin conjugates, only small differences were found despite the differences in PEG MW. However, PEG could partially protect insulin at the site of attachment, regardless of PEG MW. Taken together, these data indicate that PEG may not be able to alter the immunogenicity of a protein through preventing its degradation and lysosomal processing into peptides suitable for MHC II binding. However, site-specific PEGylation may be able to provide a method to reduce the immunogenicity of a protein should known antigenic peptides present in its amino acid sequence be already known, thereby preventing their formation in the lysosome and subsequent binding to MHC class II molecules and display to $CD4^+$ T cells. Partial protection at the site of attachment was also observed following proteasomal degradation of PEGylated insulin, suggesting that site-specific PEGylation may reduce immunogenicity through this pathway also. Further investigation is warranted to assess the effects of PEGylation on immunological events occurring downstream of processing.

To conclude, the bioanalysis of PEGylated proteins has previously been limited and consequently the biodistribution of PEGylated proteins has been poorly understood. Similarly, the effect of PEGylation on protein immunogenicity is also lacking. This thesis presents methodology to comprehensively bioanalyse PEGylated proteins and determine their pharmacokinetics, as well as methodology to assess the role of PEGylation on processes involved in the immune response. The knowledge generated and the methods developed can be used to inform, design, execute and interpret PK-PD and PK-TD (toxicodynamic) studies of novel PEGylated therapeutics in man; in particular to develop structure-metabolism and structure-immunogenicity relationships, and to individually optimise PEGylation at the molecular level. These methods may also be used to determine the appropriate T cell assay for the further immunological evaluation of epitopes generated from PEGylated biologics.

BIBLIOGRAPHY

Abuchowski A, McCoy JR, Palczuk NC, van Es T, Davis FF (1977a). Effect of covalent attachment of polyethylene glycol on immunogenicity and circulating life of bovine liver catalase. *J Biol Chem* **252**(11)**:** 3582-3586.

Abuchowski A, van Es T, Palczuk NC, Davis FF (1977b). Alteration of immunological properties of bovine serum albumin by covalent attachment of polyethylene glycol. *J Biol Chem* **252**(11)**:** 3578-3581.

Adair F, Ozanne D (2002). The immunogenicity of therapeutic proteins. *Biopharm-Appl T Bio* **15**(2)**:** 30-+.

Aghemo A, Rumi MG, Colombo M (2010). Pegylated interferons alpha2a and alpha2b in the treatment of chronic hepatitis C. *Nat Rev Gastroenterol Hepatol* **7**(9)**:** 485-494.

Aird WC (2007). Phenotypic heterogeneity of the endothelium: I. Structure, function, and mechanisms. *Circ Res* **100**(2)**:** 158-173.

Alcais A, Abel L, Casanova JL (2009). Human genetics of infectious diseases: between proof of principle and paradigm. *J Clin Invest* **119**(9)**:** 2506-2514.

Alter MJ (2007). Epidemiology of hepatitis C virus infection. *World J Gastroenterol* **13**(17)**:** 2436-2441.

Amigorena S, Savina A (2010). Intracellular mechanisms of antigen cross presentation in dendritic cells. *Curr Opin Immunol* **22**(1)**:** 109-117.

Androlewicz MJ (2001). Peptide generation in the major histocompatibility complex class I antigen processing and presentation pathway. *Curr Opin Hematol* **8**(1)**:** 12-16.

Armstrong J, Hempel G, Koling S, Chan LS, Meiselman HJ, Fisher TC*, et al.* (2006). Rapid clearance of PEG-asparaginase in ALL patients by an antibody against poly (ethylene glycol). *Blood* **108**(11)**:** 526a-526a.

Armstrong J, K. (2009). The occurrence, induction, specificity and potential effect of antibodies against poly(ethylene glycol). *PEGylated Protein Drugs: Basic Science and Clinical Applications***:** 147-168.

Armstrong JK, Hempel G, Koling S, Chan LS, Fisher T, Meiselman HJ*, et al.* (2007). Antibody against poly(ethylene glycol) adversely affects PEG-asparaginase therapy in acute lymphoblastic leukemia patients. *Cancer* **110**(1)**:** 103-111.

Bailon P, Palleroni A, Schaffer CA, Spence CL, Fung WJ, Porter JE*, et al.* (2001). Rational design of a potent, long-lasting form of interferon: a 40 kDa branched polyethylene glycol-conjugated interferon alpha-2a for the treatment of hepatitis C. *Bioconjug Chem* **12**(2)**:** 195-202.

Bailon P, Won CY (2009). PEG-modified biopharmaceuticals. *Expert Opin Drug Deliv* **6**(1)**:** 1-16.

Baker MP, Reynolds HM, Lumicisi B, Bryson CJ (2010). Immunogenicity of protein therapeutics: The key causes, consequences and challenges. *Self Nonself* **1**(4)**:** 314-322.

Bardag-Gorce F, Venkatesh R, Li J, French BA, French SW (2004). Hyperphosphorylation of rat liver proteasome subunits: the effects of ethanol and okadaic acid are compared. *Life Sci* **75**(5)**:** 585-597.

Bareford LM, Swaan PW (2007). Endocytic mechanisms for targeted drug delivery. *Adv Drug Deliv Rev* **59**(8)**:** 748-758.

Barsoum N, Kleeman C (2002). Now and then, the history of parenteral fluid administration. *American Journal of Nephrology* **22**(2-3)**:** 284-289.

Bastaki S (2005). Diabetes mellitus and its treatment. *Int J Diabetes & Metabolism*(13)**:** 111-134.

Bax BE, Bain MD, Fairbanks LD, Webster AD, Chalmers RA (2000). In vitro and in vivo studies with human carrier erythrocytes loaded with polyethylene glycol-conjugated and native adenosine deaminase. *Br J Haematol* **109**(3)**:** 549-554.

Baxby D (1999). Edward Jenner's inquiry; a bicentenary analysis. *Vaccine* **17**(4)**:** 301-307.

Bazin H (2003). A brief history of the prevention of infectious diseases by immunisations. *Comp Immunol Microbiol Infect Dis* **26**(5-6)**:** 293-308.

Bendele A, Seely J, Richey C, Sennello G, Shopp G (1998). Short communication: renal tubular vacuolation in animals treated with polyethylene-glycol-conjugated proteins. *Toxicol Sci* **42**(2)**:** 152-157.

Beyette JR, Hubbell T, Monaco JJ (2001). Purification of 20S proteasomes. *Methods Mol Biol* **156:** 1-16.

Bliss M (1993a). The history of insulin. *Diabetes Care* **16 Suppl 3:** 4-7.

Bliss M (1993b). Rewriting medical history: Charles Best and the Banting and Best myth. *J Hist Med Allied Sci* **48**(3)**:** 253-274.

Blundell TL, Cutfield JF, Cutfield SM, Dodson EJ, Dodson GG, Hodgkin DC*, et al.* (1972). Three-Dimensional Atomic Structure of Insulin and Its Relationship to Activity. *Diabetes* **21**(Supplement 2)**:** 492-505.

Bocci V (1989). Catabolism of therapeutic proteins and peptides with implications for drug delivery. *Adv Drug Deliver Rev* **4**(2)**:** 149-169.

Boo I, Fischer AE, Johnson D, Chin R, Giourouki M, Bharadwaj M*, et al.* (2007). Neutralizing antibodies in patients with chronic hepatitis C infection treated with (Peg)-interferon/ribavirin. *J Clin Virol* **39**(4)**:** 288-294.

Booth C, Gaspar HB (2009). Pegademase bovine (PEG-ADA) for the treatment of infants and children with severe combined immunodeficiency (SCID). *Biologics* **3:** 349-358.

Brown LR (2005). Commercial challenges of protein drug delivery. *Expert Opin Drug Deliv* **2**(1)**:** 29-42.

Bruns DE, Herold DA, Rodeheaver GT, Edlich RF (1982). Polyethylene glycol intoxication in burn patients. *Burns Incl Therm Inj* **9**(1)**:** 49-52.

Bukowski RM, Tendler C, Cutler D, Rose E, Laughlin MM, Statkevich P (2002). Treating cancer with PEG Intron: pharmacokinetic profile and dosing guidelines for an improved interferon-alpha-2b formulation. *Cancer* **95**(2)**:** 389-396.

Burlet-Schiltz O, Claverol S, Gairin JE, Monsarrat B (2005). The use of mass spectrometry to identify antigens from proteasome processing. *Method Enzymol* **405:** 264-300.

Burnham NL (1994). Polymers for delivering peptides and proteins. *Am J Hosp Pharm* **51**(2)**:** 210-218; quiz 228-219.

Busnardo AC, DiDio LJ, Tidrick RT, Thomford NR (1983). History of the pancreas. *Am J Surg* **146**(5)**:** 539-550.

Caliceti P, Veronese FM (2003). Pharmacokinetic and biodistribution properties of poly(ethylene glycol)-protein conjugates. *Adv Drug Deliv Rev* **55**(10)**:** 1261-1277.

Campbell JL, Le Blanc JC (2011). Peptide and protein drug analysis by MS: challenges and opportunities for the discovery environment. *Bioanalysis* **3**(6)**:** 645-657.

Campbell MK, Farrell SO (2010). *Biochemistry*. Seventh Edition edn.

Carpenter CP, Woodside MD, Kinkead ER, King JM, Sullivan LJ (1971). Response of dogs to repeated intravenous injection of polyethylene glycol 4000 with notes on excretion and sensitization. *Toxicology and Applied Pharmacology* **18**(1)**:** 35-40.

Chan KW (2002). Acute lymphoblastic leukemia. *Curr Probl Pediatr Adolesc Health Care* **32**(2)**:** 40-49.

Chance RE, Frank BH (1993). Research, development, production, and safety of biosynthetic human insulin. *Diabetes Care* **16 Suppl 3:** 133-142.

Chessells JM (2001). Acute Lymphoblastic Leukaemia. In: (ed)^(eds). *eLS*, edn: John Wiley & Sons, Ltd. p^pp.

Chilukuri N, Sun W, Parikh K, Naik RS, Tang L, Doctor BP*, et al.* (2008). A repeated injection of polyethyleneglycol-conjugated recombinant human butyrylcholinesterase elicits immune response in mice. *Toxicol Appl Pharmacol* **231**(3)**:** 423-429.

Chirino AJ, Ary ML, Marshall SA (2004). Minimizing the immunogenicity of protein therapeutics. *Drug Discov Today* **9**(2)**:** 82-90.

Chung RT, Gale M, Jr., Polyak SJ, Lemon SM, Liang TJ, Hoofnagle JH (2008). Mechanisms of action of interferon and ribavirin in chronic hepatitis C: Summary of a workshop. *Hepatology* **47**(1)**:** 306-320.

Cohen A, Hirschhorn R, Horowitz SD, Rubinstein A, Polmar SH, Hong R*, et al.* (1978). Deoxyadenosine triphosphate as a potentially toxic metabolite in adenosine deaminase deficiency. *Proc Natl Acad Sci U S A* **75**(1)**:** 472-476.

Colbert JD, Matthews SP, Miller G, Watts C (2009). Diverse regulatory roles for lysosomal proteases in the immune response. *Eur J Immunol* **39**(11)**:** 2955-2965.

Conconi M, Petropoulos I, Emod I, Turlin E, Biville F, Friguet B (1998). Protection from oxidative inactivation of the 20S proteasome by heat-shock protein 90. *Biochem J* **333 (Pt 2):** 407-415.

Conconi M, Szweda LI, Levine RL, Stadtman ER, Friguet B (1996). Age-related decline of rat liver multicatalytic proteinase activity and protection from oxidative inactivation by heat-shock protein 90. *Arch Biochem Biophys* **331**(2)**:** 232-240.

Conover C, Lejeune L, Linberg R, Shum K, Shorr RG (1996). Transitional vacuole formation following a bolus infusion of PEG-hemoglobin in the rat. *Artif Cells Blood Substit Immobil Biotechnol* **24**(6)**:** 599-611.

Cristalli G, Costanzi S, Lambertucci C, Lupidi G, Vittori S, Volpini R*, et al.* (2001). Adenosine deaminase: functional implications and different classes of inhibitors. *Med Res Rev* **21**(2)**:** 105-128.

Croft M, Dubey C (1997). Accessory molecule and costimulation requirements for CD4 T cell response. *Crit Rev Immunol* **17**(1)**:** 89-118.

Curtsinger JM, Johnson CM, Mescher MF (2003). CD8 T cell clonal expansion and development of effector function require prolonged exposure to antigen, costimulation, and signal 3 cytokine. *J Immunol* **171**(10)**:** 5165-5171.

Dams ET, Laverman P, Oyen WJ, Storm G, Scherphof GL, van Der Meer JW*, et al.* (2000). Accelerated blood clearance and altered biodistribution of repeated injections of sterically stabilized liposomes. *J Pharmacol Exp Ther* **292**(3)**:** 1071-1079.

Davis FF (2002). The origin of pegnology. *Adv Drug Deliv Rev* **54**(4)**:** 457-458.

De Graaf R (2008). *In Vivo NMR Spectroscopy: Principles and Techniques*. edn.

Delamarre L, Couture R, Mellman I, Trombetta ES (2006). Enhancing immunogenicity by limiting susceptibility to lysosomal proteolysis. *J Exp Med* **203**(9)**:** 2049-2055.

Di Noto L, Whitson LJ, Cao X, Hart PJ, Levine RL (2005). Proteasomal degradation of mutant superoxide dismutases linked to amyotrophic lateral sclerosis. *J Biol Chem* **280**(48)**:** 39907-39913.

Dinndorf PA, Gootenberg J, Cohen MH, Keegan P, Pazdur R (2007). FDA drug approval summary: pegaspargase (oncaspar) for the first-line treatment of children with acute lymphoblastic leukemia (ALL). *Oncologist* **12**(8)**:** 991-998.

Dou H, Zhang M, Zhang Y, Yin C (2007). Synthesis and purification of mono-PEGylated insulin. *Chem Biol Drug Des* **69**(2)**:** 132-138.

Duncan R (2003). The dawning era of polymer therapeutics. *Nat Rev Drug Discov* **2**(5)**:** 347-360.

Duncan R (2006). Polymer conjugates as anticancer nanomedicines. *Nat Rev Cancer* **6**(9)**:** 688-701.

Eckardt KU (2013). Anaemia: The safety and efficacy of peginesatide in patients with CKD. *Nat Rev Nephrol* **9**(4)**:** 192-193.

Egger M, Jurets A, Wallner M, Briza P, Ruzek S, Hainzl S*, et al.* (2011). Assessing protein immunogenicity with a dendritic cell line-derived endolysosomal degradome. *PLoS One* **6**(2)**:** e17278.

EMA (2012). *CHMP Safety Working Party's Response to the PDCO regarding the use of PEGylated drug products in the paediatric population*.

Emmerich NP, Nussbaum AK, Stevanovic S, Priemer M, Toes RE, Rammensee HG*, et al.* (2000). The human 26 S and 20 S proteasomes generate overlapping but different sets of peptide fragments from a model protein substrate. *J Biol Chem* **275**(28)**:** 21140-21148.

Engel BC, Podsakoff GM, Ireland JL, Smogorzewska EM, Carbonaro DA, Wilson K*, et al.* (2007). Prolonged pancytopenia in a gene therapy patient with ADA-deficient SCID and trisomy 8 mosaicism: a case report. *Blood* **109**(2)**:** 503-506.

Ewles M, Goodwin L (2011). Bioanalytical approaches to analyzing peptides and proteins by LC--MS/MS. *Bioanalysis* **3**(12)**:** 1379-1397.

Ezan E, Bitsch F (2009). Critical comparison of MS and immunoassays for the bioanalysis of therapeutic antibodies. *Bioanalysis* **1**(8)**:** 1375-1388.

Farout L, Mary J, Vinh J, Szweda LI, Friguet B (2006). Inactivation of the proteasome by 4-hydroxy-2-nonenal is site specific and dependant on 20S proteasome subtypes. *Arch Biochem Biophys* **453**(1)**:** 135-142.

Farr AD (1979). Blood group serology--the first four decades (1900--1939). *Med Hist* **23**(2)**:** 215-226.

Fasano M, Curry S, Terreno E, Galliano M, Fanali G, Narciso P*, et al.* (2005). The extraordinary ligand binding properties of human serum albumin. *IUBMB Life* **57**(12)**:** 787-796.

Feasby WR (1958). The discovery of insulin. *J Hist Med Allied Sci* **13**(1)**:** 68-84.

Fee CJ (2007). Size comparison between proteins PEGylated with branched and linear poly(ethylene glycol) molecules. *Biotechnol Bioeng* **98**(4)**:** 725-731.

Findlay JW, Smith WC, Lee JW, Nordblom GD, Das I, DeSilva BS*, et al.* (2000). Validation of immunoassays for bioanalysis: a pharmaceutical industry perspective. *J Pharm Biomed Anal* **21**(6)**:** 1249-1273.

Fishbane S, Shah HH (2013). Choice of erythropoiesis stimulating agent in ESRD. *Nephrol News Issues* **27**(7)**:** Supp 10-12.

Fishburn CS (2008). The pharmacology of PEGylation: balancing PD with PK to generate novel therapeutics. *J Pharm Sci* **97**(10)**:** 4167-4183.

Fleckman AM (1993). Diabetic ketoacidosis. *Endocrinol Metab Clin North Am* **22**(2)**:** 181-207.

Friguet B, Bulteau AL, Conconi M, Petropoulos I (2002). Redox control of 20S proteasome. *Methods Enzymol* **353:** 253-262.

Friman S, Egestad B, Sjovall J, Svanvik J (1993). Hepatic excretion and metabolism of polyethylene glycols and mannitol in the cat. *J Hepatol* **17**(1)**:** 48-55.

Fruijtier-Polloth C (2005). Safety assessment on polyethylene glycols (PEGs) and their derivatives as used in cosmetic products. *Toxicology* **214**(1-2)**:** 1-38.

Gaberc-Porekar V, Zore I, Podobnik B, Menart V (2008). Obstacles and pitfalls in the PEGylation of therapeutic proteins. *Curr Opin Drug Discov Devel* **11**(2)**:** 242-250.

Gabizon A, Shmeeda H, Barenholz Y (2003). Pharmacokinetics of pegylated liposomal Doxorubicin: review of animal and human studies. *Clin Pharmacokinet* **42**(5)**:** 419-436.

Ganson NJ, Kelly SJ, Scarlett E, Sundy JS, Hershfield MS (2006). Control of hyperuricemia in subjects with refractory gout, and induction of antibody against poly(ethylene glycol) (PEG), in a phase I trial of subcutaneous PEGylated urate oxidase. *Arthritis Res Ther* **8**(1)**:** R12.

Giangrande PL (2000). The history of blood transfusion. *Br J Haematol* **110**(4)**:** 758-767.

Glickman MH (2000). Getting in and out of the proteasome. *Semin Cell Dev Biol* **11**(3)**:** 149-158.

Graham ML (2003). Pegaspargase: a review of clinical studies. *Adv Drug Deliv Rev* **55**(10)**:** 1293-1302.

Greish K, Fang J, Inutsuka T, Nagamitsu A, Maeda H (2003). Macromolecular therapeutics: advantages and prospects with special emphasis on solid tumour targeting. *Clin Pharmacokinet* **42**(13)**:** 1089-1105.

Gursahani H, Riggs-Sauthier J, Pfeiffer J, Lechuga-Ballesteros D, Fishburn CS (2009). Absorption of polyethylene glycol (PEG) polymers: the effect of PEG size on permeability. *J Pharm Sci* **98**(8)**:** 2847-2856.

Halfon P, Perusat S, Bourliere M, Bronowicki JP, Trimoulet P, Benhamou Y*, et al.* (2010). Neutralizing antibodies to interferon-alpha and circulating interferon in patients with chronic hepatitis C non-responding to pegylated interferon plus ribavirin re-treated by pegylated interferon-alpha-2a and ribavirin (ANRS HC16 GAMMATRI substudy). *J Med Virol* **82**(12)**:** 2027-2031.

Hamad I, Hunter AC, Szebeni J, Moghimi SM (2008). Poly(ethylene glycol)s generate complement activation products in human serum through increased alternative pathway turnover and a MASP-2-dependent process. *Mol Immunol* **46**(2)**:** 225-232.

Harris JM, Chess RB (2003). Effect of pegylation on pharmaceuticals. *Nat Rev Drug Discov* **2**(3)**:** 214-221.

Harris JM, Martin NE, Modi M (2001). Pegylation: a novel process for modifying pharmacokinetics. *Clin Pharmacokinet* **40**(7)**:** 539-551.

Hashida M, Mahato RI, Kawabata K, Miyao T, Nishikawa M, Takakura Y (1996). Pharmacokinetics and targeted delivery of proteins and genes. *Journal of Controlled Release* **41**(1–2)**:** 91-97.

Heinemann L, Richter B (1993). Clinical pharmacology of human insulin. *Diabetes Care* **16 Suppl 3:** 90-100.

Hendriksen CFM (2008). Vaccine Development: Past, Present and Future. In: (ed)^(eds). *Fighting Infection in the 21st Century*, edn: Blackwell Science Ltd. p^pp 61-71.

Herold DA, Keil K, Bruns DE (1989). Oxidation of polyethylene glycols by alcohol dehydrogenase. *Biochem Pharmacol* **38**(1)**:** 73-76.

Herold DA, Rodeheaver GT, Bellamy WT, Fitton LA, Bruns DE, Edlich RF (1982). Toxicity of topical polyethylene glycol. *Toxicol Appl Pharmacol* **65**(2)**:** 329-335.

Hilleman MR (2000). Vaccines in historic evolution and perspective: a narrative of vaccine discoveries. *J Hum Virol* **3**(2)**:** 63-76.

Hirschhorn R, Martiniuk F, Roegner-Maniscalco V, Ellenbogen A, Perignon JL, Jenkins T (1983). Genetic heterogeneity in partial adenosine deaminase deficiency. *J Clin Invest* **71**(6)**:** 1887-1892.

Hoofnagle JH, Seeff LB (2006). Peginterferon and ribavirin for chronic hepatitis C. *N Engl J Med* **355**(23)**:** 2444-2451.

Immordino ML, Dosio F, Cattel L (2006). Stealth liposomes: review of the basic science, rationale, and clinical applications, existing and potential. *Int J Nanomedicine* **1**(3)**:** 297-315.

Inward CD, Chambers TL (2002). Fluid management in diabetic ketoacidosis. *Arch Dis Child* **86**(6)**:** 443-444.

Ishida T, Atobe K, Wang X, Kiwada H (2006a). Accelerated blood clearance of PEGylated liposomes upon repeated injections: effect of doxorubicin-encapsulation and high-dose first injection. *J Control Release* **115**(3)**:** 251-258.

Ishida T, Harada M, Wang XY, Ichihara M, Irimura K, Kiwada H (2005). Accelerated blood clearance of PEGylated liposomes following preceding liposome injection: effects of lipid dose and PEG surface-density and chain length of the first-dose liposomes. *J Control Release* **105**(3)**:** 305-317.

Ishida T, Ichihara M, Wang X, Kiwada H (2006b). Spleen plays an important role in the induction of accelerated blood clearance of PEGylated liposomes. *J Control Release* **115**(3)**:** 243-250.

Ishida T, Ichihara M, Wang X, Yamamoto K, Kimura J, Majima E*, et al.* (2006c). Injection of PEGylated liposomes in rats elicits PEG-specific IgM, which is responsible for rapid elimination of a second dose of PEGylated liposomes. *J Control Release* **112**(1)**:** 15-25.

Ishida T, Kashima S, Kiwada H (2008a). The contribution of phagocytic activity of liver macrophages to the accelerated blood clearance (ABC) phenomenon of PEGylated liposomes in rats. *J Control Release* **126**(2)**:** 162-165.

Ishida T, Kiwada H (2008b). Accelerated blood clearance (ABC) phenomenon upon repeated injection of PEGylated liposomes. *Int J Pharm* **354**(1-2)**:** 56-62.

Ishida T, Maeda R, Ichihara M, Irimura K, Kiwada H (2003). Accelerated clearance of PEGylated liposomes in rats after repeated injections. *J Control Release* **88**(1)**:** 35-42.

Jelley-Gibbs DM, Lepak NM, Yen M, Swain SL (2000). Two distinct stages in the transition from naive CD4 T cells to effectors, early antigen-dependent and late cytokine-driven expansion and differentiation. *J Immunol* **165**(9)**:** 5017-5026.

Jenkins MK, Khoruts A, Ingulli E, Mueller DL, McSorley SJ, Reinhardt RL*, et al.* (2001). In vivo activation of antigen-specific CD4 T cells. *Annu Rev Immunol* **19:** 23-45.

Jennings GT, Bachmann MF (2009). Immunodrugs: therapeutic VLP-based vaccines for chronic diseases. *Annu Rev Pharmacol Toxicol* **49:** 303-326.

Jensen PE (2007). Recent advances in antigen processing and presentation. *Nat Immunol* **8**(10)**:** 1041-1048.

Jevsevar S, Kunstelj M, Porekar VG (2010). PEGylation of therapeutic proteins. *Biotechnol J* **5**(1)**:** 113-128.

Johnson IS (1983). Human insulin from recombinant DNA technology. *Science* **219**(4585)**:** 632-637.

Joralemon MJ, McRae S, Emrick T (2010). PEGylated polymers for medicine: from conjugation to self-assembled systems. *Chem Commun (Camb)* **46**(9)**:** 1377-1393.

Joshi SK, Shrestha S (2010). Diabetes mellitus: a review of its associations with different environmental factors. *Kathmandu Univ Med J (KUMJ)* **8**(29)**:** 109-115.

Joshi SR, Parikh RM, Das AK (2007). Insulin--history, biochemistry, physiology and pharmacology. *J Assoc Physicians India* **55 Suppl:** 19-25.

Judge A, McClintock K, Phelps JR, Maclachlan I (2006). Hypersensitivity and loss of disease site targeting caused by antibody responses to PEGylated liposomes. *Mol Ther* **13**(2)**:** 328-337.

Kaech SM, Wherry EJ, Ahmed R (2002). Effector and memory T-cell differentiation: implications for vaccine development. *Nat Rev Immunol* **2**(4)**:** 251-262.

Kalish RS, Askenase PW (1999). Molecular mechanisms of CD8+ T cell-mediated delayed hypersensitivity: implications for allergies, asthma, and autoimmunity. *J Allergy Clin Immunol* **103**(2 Pt 1)**:** 192-199.

Kang JS, Deluca PP, Lee KC (2009). Emerging PEGylated drugs. *Expert Opin Emerg Drugs* **14**(2)**:** 363-380.

Keating GM (2009). Peginterferon-alpha-2a (40 kD): A review of its use in chronic hepatitis B. *Drugs* **69**(18)**:** 2633-2660.

Khan S, van den Broek M, Schwarz K, de Giuli R, Diener PA, Groettrup M (2001). Immunoproteasomes largely replace constitutive proteasomes during an antiviral and antibacterial immune response in the liver. *J Immunol* **167**(12)**:** 6859-6868.

King KM, Rubin G (2003). A history of diabetes: from antiquity to discovering insulin. *Br J Nurs* **12**(18)**:** 1091-1095.

Knop K, Hoogenboom R, Fischer D, Schubert US (2010). Poly(ethylene glycol) in drug delivery: pros and cons as well as potential alternatives. *Angew Chem Int Ed Engl* **49**(36)**:** 6288-6308.

Koch KL (1999). Diabetic gastropathy: gastric neuromuscular dysfunction in diabetes mellitus: a review of symptoms, pathophysiology, and treatment. *Dig Dis Sci* **44**(6)**:** 1061-1075.

Koide H, Asai T, Hatanaka K, Akai S, Ishii T, Kenjo E*, et al.* (2010). T cell-independent B cell response is responsible for ABC phenomenon induced by repeated injection of PEGylated liposomes. *Int J Pharm* **392**(1-2)**:** 218-223.

Kozlowski A, Harris JM (2001). Improvements in protein PEGylation: pegylated interferons for treatment of hepatitis C. *J Control Release* **72**(1-3)**:** 217-224.

Krippendorff BF, Kuester K, Kloft C, Huisinga W (2009). Nonlinear pharmacokinetics of therapeutic proteins resulting from receptor mediated endocytosis. *J Pharmacokinet Pharmacodyn* **36**(3)**:** 239-260.

Kurfurst MM (1992). Detection and molecular weight determination of polyethylene glycol-modified hirudin by staining after sodium dodecyl sulfate-polyacrylamide gel electrophoresis. *Anal Biochem* **200**(2)**:** 244-248.

Lallemand C, Meritet JF, Blanchard B, Lebon P, Tovey MG (2010). One-step assay for quantification of neutralizing antibodies to biopharmaceuticals. *J Immunol Methods* **356**(1-2)**:** 18-28.

Laverman P, Carstens MG, Boerman OC, Dams ET, Oyen WJ, van Rooijen N*, et al.* (2001). Factors affecting the accelerated blood clearance of polyethylene glycol-liposomes upon repeated injection. *J Pharmacol Exp Ther* **298**(2)**:** 607-612.

Leader B, Baca QJ, Golan DE (2008). Protein therapeutics: a summary and pharmacological classification. *Nat Rev Drug Discov* **7**(1)**:** 21-39.

Lian T, Ho RJ (2001). Trends and developments in liposome drug delivery systems. *J Pharm Sci* **90**(6)**:** 667-680.

Linsley PS, Ledbetter JA (1993). The role of the CD28 receptor during T cell responses to antigen. *Annu Rev Immunol* **11:** 191-212.

Locatelli F, Del Vecchio L (2013). Peginesatide as a new approach for treating anemia of CKD patient: is it like a falling star? *Expert Opin Pharmacother* **14**(10)**:** 1277-1280.

Lombard M, Pastoret PP, Moulin AM (2007). A brief history of vaccines and vaccination. *Rev Sci Tech* **26**(1)**:** 29-48.

Maeda H, Seymour LW, Miyamoto Y (1992). Conjugates of anticancer agents and polymers: advantages of macromolecular therapeutics in vivo. *Bioconjug Chem* **3**(5)**:** 351-362.

Mahmood I, Green MD (2007). Drug Interaction Studies of Therapeutic Proteins or Monoclonal Antibodies. *The Journal of Clinical Pharmacology* **47**(12)**:** 1540-1554.

Mahmood I, Green MD (2005). Pharmacokinetic and pharmacodynamic considerations in the development of therapeutic proteins. *Clin Pharmacokinet* **44**(4)**:** 331-347.

Masetti R, Pession A (2009). First-line treatment of acute lymphoblastic leukemia with pegasparaginase. *Biologics* **3:** 359-368.

Materi W, Gombos Z, Wishart DS (2007). Proteins: Hormones, enzymes, and monoclonal antibodies - background. In: *Handbook of Pharmaceutical Biotechnology*, pp 773-822.

Mero A, Spolaore B, Veronese FM, Fontana A (2009). Transglutaminase-mediated PEGylation of proteins: direct identification of the sites of protein modification by mass spectrometry using a novel monodisperse PEG. *Bioconjug Chem* **20**(2)**:** 384-389.

Michel CC (1996). Transport of macromolecules through microvascular walls. *Cardiovasc Res* **32**(4)**:** 644-653.

Mikhail A (2012). Profile of peginesatide and its potential for the treatment of anemia in adults with chronic kidney disease who are on dialysis. *J Blood Med* **3:** 25-31.

Miller WL, Baxter JD (1980). Recombinant DNA--a new source of insulin. *Diabetologia* **18**(6)**:** 431-436.

Molineux G (2003). Pegylation: engineering improved biopharmaceuticals for oncology. *Pharmacotherapy* **23**(8 Pt 2)**:** 3S-8S.

Moran N (2012). Affymax poised to challenge Amgen. *Nat Biotechnol* **30**(5)**:** 377-379.

Narta UK, Kanwar SS, Azmi W (2007). Pharmacological and clinical evaluation of L-asparaginase in the treatment of leukemia. *Crit Rev Oncol Hematol* **61**(3)**:** 208-221.

Newton CA, Raskin P (2004). Diabetic ketoacidosis in type 1 and type 2 diabetes mellitus: clinical and biochemical differences. *Arch Intern Med* **164**(17)**:** 1925-1931.

Niedermann G, Geier E, Lucchiari-Hartz M, Hitziger N, Ramsperger A, Eichmann K (1999). The specificity of proteasomes: impact on MHC class I processing and presentation of antigens. *Immunol Rev* **172:** 29-48.

Niedermann G, King G, Butz S, Birsner U, Grimm R, Shabanowitz J*, et al.* (1996). The proteolytic fragments generated by vertebrate proteasomes: structural relationships to major histocompatibility complex class I binding peptides. *Proc Natl Acad Sci U S A* **93**(16)**:** 8572-8577.

Nowatzke WL, Rogers K, Wells E, Bowsher RR, Ray C, Unger S (2011). Unique challenges of providing bioanalytical support for biological therapeutic pharmacokinetic programs. *Bioanalysis* **3**(5)**:** 509-521.

Pai SS, Hammouda B, Hong K, Pozzo DC, Przybycien TM, Tilton RD (2011). The conformation of the poly(ethylene glycol) chain in mono-PEGylated lysozyme and mono-PEGylated human growth hormone. *Bioconjug Chem* **22**(11)**:** 2317-2323.

Pardigon N, Bercovici N, Calbo S, Santos-Lima EC, Liblau R, Kourilsky P*, et al.* (1998). Role of co-stimulation in CD8+ T cell activation. *Int Immunol* **10**(5)**:** 619-630.

Pasut G, Veronese FM (2009). PEG conjugates in clinical development or use as anticancer agents: an overview. *Adv Drug Deliv Rev* **61**(13)**:** 1177-1188.

Pasut G, Veronese FM (2007). Polymer-drug conjugation, recent achievements and general strategies. *Progress in Polymer Science* **32**(8-9)**:** 933-961.

Pasut G, Veronese FM (2012). State of the art in PEGylation: the great versatility achieved after forty years of research. *J Control Release* **161**(2)**:** 461-472.

Pavlou AK, Reichert JM (2004). Recombinant protein therapeutics--success rates, market trends and values to 2010. *Nat Biotechnol* **22**(12)**:** 1513-1519.

Payne RW, Murphy BM, Manning MC (2010). Product development issues for PEGylated proteins. *Pharm Dev Technol*.

Perz JF, Armstrong GL, Farrington LA, Hutin YJ, Bell BP (2006). The contributions of hepatitis B virus and hepatitis C virus infections to cirrhosis and primary liver cancer worldwide. *J Hepatol* **45**(4)**:** 529-538.

Pickup J (1986). Human insulin. *Br Med J (Clin Res Ed)* **292**(6514)**:** 155-157.

Pillay CS, Elliott E, Dennison C (2002). Endolysosomal proteolysis and its regulation. *Biochem J* **363**(Pt 3)**:** 417-429.

Pisal DS, Kosloski MP, Balu-Iyer SV (2010). Delivery of therapeutic proteins. *J Pharm Sci* **99**(6)**:** 2557-2575.

Plotkin SA (2005). Vaccines: past, present and future. *Nat Med* **11**(4 Suppl)**:** S5-11.

Reddy KR, Modi MW, Pedder S (2002). Use of peginterferon a1fa-2a (40 KD) (Pegasys (R)) for the treatment of hepatitis C. *Adv Drug Deliver Rev* **54**(4)**:** 571-586.

Reinders MK, Jansen TL (2010). New advances in the treatment of gout: review of pegloticase. *Ther Clin Risk Manag* **6:** 543-550.

Richter AW, Akerblom E (1983). Antibodies against polyethylene glycol produced in animals by immunization with monomethoxy polyethylene glycol modified proteins. *Int Arch Allergy Appl Immunol* **70**(2)**:** 124-131.

Richter AW, Akerblom E (1984). Polyethylene glycol reactive antibodies in man: titer distribution in allergic patients treated with monomethoxy polyethylene glycol modified allergens or placebo, and in healthy blood donors. *Int Arch Allergy Appl Immunol* **74**(1)**:** 36-39.

Riedel S (2005). Edward Jenner and the history of smallpox and vaccination. *Proc (Bayl Univ Med Cent)* **18**(1)**:** 21-25.

Rivett AJ, Savory PJ, Djaballah H (1994). Multicatalytic endopeptidase complex: proteasome. *Methods Enzymol* **244:** 331-350.

Roberts MJ, Bentley MD, Harris JM (2002). Chemistry for peptide and protein PEGylation. *Adv Drug Deliv Rev* **54**(4)**:** 459-476.

Rosenfeld L (2002). Insulin: discovery and controversy. *Clin Chem* **48**(12)**:** 2270-2288.

Rudmann DG, Alston JT, Hanson JC, Heidel S (2013). High molecular weight polyethylene glycol cellular distribution and PEG-associated cytoplasmic vacuolation is molecular weight dependent and does not require conjugation to proteins. *Toxicol Pathol* **41**(7)**:** 970-983.

Ryan SM, Mantovani G, Wang X, Haddleton DM, Brayden DJ (2008). Advances in PEGylation of important biotech molecules: delivery aspects. *Expert Opin Drug Deliv* **5**(4)**:** 371-383.

Sanger F (1988). Sequences, sequences, and sequences. *Annu Rev Biochem* **57:** 1-28.

Sasayama M, Deng L, Kim SR, Ide Y, Shoji I, Hotta H (2010). Analysis of neutralizing antibodies against hepatitis C virus in patients who were treated with pegylated-interferon plus ribavirin. *Kobe J Med Sci* **56**(2)**:** E60-66.

Schellekens H (2005). Factors influencing the immunogenicity of therapeutic proteins. *Nephrol Dial Transplant* **20 Suppl 6:** vi3-9.

Schellekens H (2003). Immunogenicity of therapeutic proteins. *Nephrol Dial Transplant* **18**(7)**:** 1257-1259.

Schernthaner G (1993). Immunogenicity and allergenic potential of animal and human insulins. *Diabetes Care* **16 Suppl 3:** 155-165.

Schmidt PJ, Leacock AG (2002). Forgotten transfusion history: John Leacock of Barbados. *BMJ* **325**(7378)**:** 1485-1487.

Schroder BA, Wrocklage C, Hasilik A, Saftig P (2010). The proteome of lysosomes. *Proteomics* **10**(22)**:** 4053-4076.

Schwartz M (2001). The life and works of Louis Pasteur. *J Appl Microbiol* **91**(4)**:** 597-601.

Seder RA, Ahmed R (2003). Similarities and differences in CD4+ and CD8+ effector and memory T cell generation. *Nat Immunol* **4**(9)**:** 835-842.

Shaffer CB, Critchfield FH (1947). The absorption and excretion of the solid polyethylene glycols; (carbowax compounds). *J Am Pharm Assoc Am Pharm Assoc* **36**(5)**:** 152-157.

Shaffer CB, Critchfield FH, Carpenter CP (1948). Renal excretion and volume distribution of some polyethylene glycols in the dog. *Am J Physiol* **152**(1)**:** 93-99.

Shaffer CB, Critchfield FH, Nair JH, 3rd (1950). The absorption and excretion of a liquid polyethylene glycol. *J Am Pharm Assoc Am Pharm Assoc* **39**(6)**:** 340-344.

Shepard CW, Finelli L, Alter MJ (2005). Global epidemiology of hepatitis C virus infection. *Lancet Infect Dis* **5**(9)**:** 558-567.

Shilov IV, Seymour SL, Patel AA, Loboda A, Tang WH, Keating SP*, et al.* (2007). The Paragon Algorithm, a next generation search engine that uses sequence temperature values and feature probabilities to identify peptides from tandem mass spectra. *Mol Cell Proteomics* **6**(9)**:** 1638-1655.

Siperstein MD (1992). Diabetic ketoacidosis and hyperosmolar coma. *Endocrinol Metab Clin North Am* **21**(2)**:** 415-432.

Stern AM, Markel H (2005). The history of vaccines and immunization: familiar patterns, new challenges. *Health Aff (Millwood)* **24**(3)**:** 611-621.

Strader DB, Wright T, Thomas DL, Seeff LB (2004). Diagnosis, management, and treatment of hepatitis C. *Hepatology* **39**(4)**:** 1147-1171.

Sturgis CC (1942). The History of Blood Transfusion. *Bull Med Libr Assoc* **30**(2)**:** 105-112.

Sundy JS, Becker MA, Baraf HS, Barkhuizen A, Moreland LW, Huang W*, et al.* (2008). Reduction of plasma urate levels following treatment with multiple doses of pegloticase (polyethylene glycol-conjugated uricase) in patients with treatment-failure gout: results of a phase II randomized study. *Arthritis Rheum* **58**(9)**:** 2882-2891.

Takakura Y, Mahato RI, Hashida M (1998). Extravasation of macromolecules. *Adv Drug Deliv Rev* **34**(1)**:** 93-108.

Takakura Y, Mihara K, Hashida M (1994). Control of the Disposition Profiles of Proteins in the Kidney Via Chemical Modification. *Journal of Controlled Release* **28**(1-3)**:** 111-119.

Tamiya T, Kashiwagi I, Takahashi R, Yasukawa H, Yoshimura A (2011). Suppressors of cytokine signaling (SOCS) proteins and JAK/STAT pathways: regulation of T-cell inflammation by SOCS1 and SOCS3. *Arterioscler Thromb Vasc Biol* **31**(5)**:** 980-985.

Taylor R, Agius L (1988). The biochemistry of diabetes. *Biochem J* **250**(3)**:** 625-640.

Tenzer S, Schild H (2005). Assays of proteasome-dependent cleavage products. *Methods Mol Biol* **301:** 97-115.

Thompson MD, Dar MJ, Monga SP (2011). Pegylated interferon alpha targets Wnt signaling by inducing nuclear export of beta-catenin. *J Hepatol* **54**(3)**:** 506-512.

Torchilin VP, Lukyanov AN (2003). Peptide and protein drug delivery to and into tumors: challenges and solutions. *Drug Discovery Today* **8**(6)**:** 259-266.

Torresi J, Johnson D, Wedemeyer H (2011). Progress in the development of preventive and therapeutic vaccines for hepatitis C virus. *Journal of Hepatology* **54**(6)**:** 1273-1285.

Tsai JC, Shen LC, Sheu HM, Lu CC (2003). Tape stripping and sodium dodecyl sulfate treatment increase the molecular weight cutoff of polyethylene glycol penetration across murine skin. *Arch Dermatol Res* **295**(4)**:** 169-174.

Tsuji J, Hirose K, Kasahara E, Naitoh M, Yamamoto I (1985). Studies on antigenicity of the polyethylene glycol (PEG)-modified uricase. *Int J Immunopharmacol* **7**(5)**:** 725-730.

Valliant A, Hofmann RM (2013). Managing dialysis patients who develop anemia caused by chronic kidney disease: focus on peginesatide. *Int J Nanomedicine* **8:** 3297-3307.

van der Eijk AA, Vrolijk JM, Haagmans BL (2006). Antibodies Neutralizing Peginterferon Alfa during Retreatment of Hepatitis C. *New England Journal of Medicine* **354**(12)**:** 1323-1324.

Vellard M (2003). The enzyme as drug: application of enzymes as pharmaceuticals. *Current Opinion in Biotechnology* **14**(4)**:** 444-450.

Veronese FM, Mero A, Pasut G (2009). Protein PEGylation, basic science and biological applications. In: Veronese FM (ed)^(eds). *PEGylated Protein Drugs: Basic Science and Clinical Applications*, edn: Birkhäuser Basel. pp 11-31.

Veronese FM, Pasut G (2005). PEGylation, successful approach to drug delivery. *Drug Discov Today* **10**(21)**:** 1451-1458.

Veronese FM, Pasut G (2008). PEGylation: Posttranslational bioengineering of protein biotherapeutics. *Drug Discovery Today: Technologies* **5**(2–3)**:** e57-e64.

Vickery HB (1950). The origin of the word protein. *Yale J Biol Med* **22**(5)**:** 387-393.

Voeten JT, Rimmelzwaan GF, Nieuwkoop NJ, Fouchier RA, Osterhaus AD (2001). Antigen processing for MHC class I restricted presentation of exogenous influenza A virus nucleoprotein by B-lymphoblastoid cells. *Clin Exp Immunol* **125**(3)**:** 423-431.

Wadhwa M, Thorpe R (2010). Unwanted immunogenicity: lessons learned and future challenges. *Bioanalysis* **2**(6)**:** 1073-1084.

Wang X, Ishida T, Kiwada H (2007). Anti-PEG IgM elicited by injection of liposomes is involved in the enhanced blood clearance of a subsequent dose of PEGylated liposomes. *J Control Release* **119**(2)**:** 236-244.

Watts C (2004). The exogenous pathway for antigen presentation on major histocompatibility complex class II and CD1 molecules. *Nat Immunol* **5**(7)**:** 685-692.

Webster R, Didier E, Harris P, Siegel N, Stadler J, Tilbury L*, et al.* (2007). PEGylated proteins: evaluation of their safety in the absence of definitive metabolism studies. *Drug Metab Dispos* **35**(1)**:** 9-16.

Webster R, Elliott V, Park BK, Walker D, Hankin M, Taupin P (2009). PEG and PEG conjugates toxicity: towards an understanding of the toxicity of PEG and its relevance to PEGylated biologicals. In: Veronese FM (ed)^(eds). *PEGylated Protein Drugs: Basic Science and Clinical Applications*, edn: Birkhäuser Basel. p^pp 127-146.

Wooten JM (2011). Adverse drug effects and pegylation. *South Med J* **104**(2)**:** 83-84.

(1997). Safety of poly (ethylene glycol) and poly (ethylene glycol) derivatives. *ACS Symposium Series*. ACS Publications. pp 45-59.

Wozniak KL, Levitz SM (2008). Cryptococcus neoformans enters the endolysosomal pathway of dendritic cells and is killed by lysosomal components. *Infect Immun* **76**(10)**:** 4764-4771.

Yamaoka T, Tabata Y, Ikada Y (1994). Distribution and tissue uptake of poly(ethylene glycol) with different molecular weights after intravenous administration to mice. *J Pharm Sci* **83**(4)**:** 601-606.

Yang Z, Hayes M, Fang X, Daley MP, Ettenberg S, Tse FL (2007). LC-MS/MS approach for quantification of therapeutic proteins in plasma using a protein internal standard and 2D-solid-phase extraction cleanup. *Anal Chem* **79**(24)**:** 9294-9301.

Yewdell JW (2005). Immunoproteasomes: regulating the regulator. *Proc Natl Acad Sci U S A* **102**(26)**:** 9089-9090.

Zeidan A, Wang ES, Wetzler M (2009). Pegasparaginase: where do we stand? *Expert Opin Biol Ther* **9**(1)**:** 111-119.

Zhang S, Rozell M, Verma RK, Albu DI, Califano D, VanValkenburgh J*, et al.* (2010). Antigen-specific clonal expansion and cytolytic effector function of CD8+ T lymphocytes depend on the transcription factor Bcl11b. *J Exp Med* **207**(8)**:** 1687-1699.